



**University of  
Sunderland**

Salmon, Andrew B (2006) Application of Natural and Modified Biomacromolecules in Miniaturised Separative Analytical Techniques. Doctoral thesis, University of Sunderland.

Downloaded from: <http://sure.sunderland.ac.uk/id/eprint/3783/>

**Usage guidelines**

Please refer to the usage guidelines at <http://sure.sunderland.ac.uk/policies.html> or alternatively contact [sure@sunderland.ac.uk](mailto:sure@sunderland.ac.uk).

**Application of Natural and Modified  
Biomacromolecules in Miniaturised Separative  
Analytical Techniques**

**Andrew B Salmon**

**A thesis submitted in partial fulfilment of the requirements of the  
University of Sunderland for the degree of Doctor of Philosophy**

December 2006

## Abstract

In pharmaceutical R & D, drug stereochemistry, and consequently the resolution of enantiomers, is very important. Because they act as chiral selectors *in vivo*, biomacromolecules have been extensively used as chiral selectors for the liquid chromatographic (LC) resolution of enantiomers and more latterly have also been employed in the newer separative technique, capillary electrophoresis (CE). However, at the outset of this research programme, this had generally been restricted to common easily accessible biomacromolecules such as plasma-binding proteins. It was clear that it would be useful therefore to adapt LC and CE in such a way as would allow the use of a much wider range of biomacromolecules. Accordingly the general aim of this study was to develop LC and CE protocols involving biomacromolecules that would give rise to minimum consumption of the biomacromolecule.

To study biomacromolecules in free solution CE, a number of experimental variables had to be established for both optimum chiral discrimination and for investigating biomacromolecule-ligand interactions. The typical and widely used biomacromolecule for chiral discrimination, bovine serum albumin (BSA) was used to study the variables of pH from pH 5.4 to 8.4, concentration of BSA from 0 to 60  $\mu\text{M}$  and concentration of organic modifiers in the range 0 – 20 % v/v for chiral selectivity. This involved an investigation into some unusual artefacts such as ghost peaks and stepped baselines, but ultimately the outcome was a successful free solution CE protocol suitable for the rapid evaluation of chiral discrimination of other biomacromolecules. The conditions were: run buffer (30  $\mu\text{M}$  protein, 67 mM phosphate (pH 7.4) – methanol (97.5 : 2.5, v/v)), capillary CElect p150, 40 cm (35 cm to detector) x 50  $\mu\text{m}$  i.d., temperature of ambient or 25 °C and an applied voltage of 10 kV. The ability of other biomacromolecules, such as human serum albumin (HSA), lactoferrin and protamine, to resolve enantiomers was studied using this protocol including looking at the effect of the addition of modifiers to the buffer such as metal ions like manganese and zinc, competing ligands, e.g. warfarin and ibuprofen, and  $\beta$ -cyclodextrin.

As well as using CE, miniaturisation of LC was also studied in view of the success of biomacromolecule-affinity chiral LC. Two different, but similar, microbore LC protocols were employed, i.e. using the protein in free solution or as a pseudo stationary phase. For the former, a Lichrosorb DIOL stationary phase, based on hydroxyl groups immobilised on silica, was chosen in order to minimise the adsorption of protein to the stationary phase. Using this protocol it was demonstrated that free solution microbore LC could be easily be carried out, therefore used to evaluate chiral discrimination and that the use of the system to study *in vivo* interactions was feasible.

The creation of a biomacromolecule pseudo stationary phase, as opposed to conventional chiral stationary phases where the protein is permanently bonded to the stationary phases, involves the biomacromolecule being adsorbed within the pores of the stationary phase. In this way the overall biomacromolecule structure should not be grossly distorted. Three stationary phases were evaluated, *viz* wide-pore Nucleosil silica, Nucleosil C<sub>8</sub> and Lichrosorb DIOL, for optimum biomacromolecule loading and minimal biomacromolecule leakage when mobile phase was pumped through the column. The Nucleosil silica with adsorbed BSA proved the most successful, e.g.  $\alpha$  of 3.6 and 4.0 for tryptophan and kynurenine respectively, and robust of the stationary phases with respect to demonstrating the chiral discrimination potential for this system.

All the miniaturised systems evaluated were successful, to a greater or lesser degree, for the demonstration of chiral selectivity of biomacromolecules. While CE was better for minimisation of the consumption of the biomacromolecule, it was also important that the biomacromolecule LC systems could be operated in reduced dimensions since these systems have perhaps greater potential for exhibiting enantioselectivity and are more appropriate for the ever increasing need for the study of the interaction of ligands with the biomacromolecule in its 'natural' form. With the knowledge gained from this research programme it will now be possible to more easily carry out such studies with much smaller amounts of biomacromolecule, and, accordingly be able to work with biomacromolecules which hitherto it has not been possible to study because of limited availability.

While some of the protocols have now been superseded by recent developments the system developed still has potential. The use of such small scale systems offers the potential to study chiral selectivity and drug-biomacromolecule binding of rare or expensive biomacromolecules.

## Acknowledgements

I would like to thank the following: -

My supervisor Dr. John Lough for his assistance throughout this project.

My parents for their support.

Louise for sharing the anguish and always being positive.

Bill and Chris for providing wonderful food and accommodation.

Dr. Malcolm Mills for useful discussion.

Anyone else who would listen to me rambling on about chiral separations...

For George and Emma

## Table of Contents

Abstract	i
Acknowledgements	iii
Table of Contents	iv
List of Figures	ix
1 Introduction	1
1.1 Preface	1
1.2 Chirality	1
1.2.1 Overview of chirality	1
1.2.2 Stereoisomers	2
1.2.3 Asymmetric carbon	3
1.2.4 Properties of chiral molecules	5
1.2.4.1 Achiral properties	5
1.2.4.2 Optical properties	5
1.2.4.3 Chemical properties	6
1.2.5 Three point interaction rule	6
1.2.6 Nomenclature of chiral molecules	6
1.2.6.1 Cahn-Ingold R,S notational system	7
1.2.6.2 Nomenclature assigned by the rotation of polarised light	8
1.2.6.3 Fisher convention	8
1.2.6.4 Determination of the absolute configuration of enantiomers	9
1.2.7 Chirality and pharmaceuticals	9
1.2.8 Chiral agrochemicals	10
1.3 The use of biomacromolecules as chiral selectors	11
1.3.1 Proteins	11
1.3.1.1 Amino acids	11
1.3.1.2 The peptide bond	12
1.3.1.3 Structure of proteins	13
1.3.2 Serum albumins	14
1.3.2.1 Structure of albumins	14
1.3.3 Binding sites	15
1.4 Capillary electrophoresis	15

1.4.1	Basic instrumentation for capillary electrophoresis	16
1.4.2	Theory of capillary electrophoresis	17
1.4.2.1	Electroosmotic flow	17
1.4.2.2	Separation of molecules using capillary electrophoresis	19
1.4.3	The role of CE in separating enantiomers	20
1.4.4	Chiral Selectors employed in capillary electrophoresis	22
1.4.4.1	Cyclodextrins	22
1.4.4.2	Chiral micellar electrokinetic capillary chromatography	25
1.4.4.3	Biomacromolecules	25
1.4.4.4	Proteins	26
1.4.5	The measurement of drug-protein binding constants by chromatographic techniques	30
1.4.5.1	Drug-protein binding studies using high-performance liquid chromatography (HPLC)	30
1.4.5.2	Drug-protein binding studies using capillary electrophoresis	32
1.5	Aims and Objectives	34
2	Experimental	36
2.1	Equipment for capillary electrophoresis	36
2.2	Equipment for liquid chromatography	36
2.3	Materials	37
2.3.1	Chemical structures of the analytes	38
2.4	Experimental for capillary electrophoresis	40
2.4.1	Capillary Electrophoresis Instrument Set-up	40
2.4.1.1	Dionex CES I	40
2.4.1.2	Beckman PACE 2050	41
2.4.2	Investigation of the experimental variables	42
2.4.2.1	Concentration of bovine serum albumin (BSA)	42
2.4.2.2	The effect of pH of the run buffer	42
2.4.2.3	Investigation of increasing the concentration of organic solvents to the run buffer	43
2.4.3	Enantioselectivity using a BSA coated capillary	43

2.4.4	Enantioselectivity of a range of compounds using BSA as the chiral selector and standard conditions	44
2.4.5	Enantioselectivity of a range of compounds using standard conditions to screen other biomacromolecules	44
2.4.6	Investigation of enantioselectivity by adding modifiers to the run buffer	45
2.4.6.1	$\beta$ -Cyclodextrin	45
2.4.6.2	Allosteric Interactions	46
2.4.6.3	Metal salts	46
2.5	Experimental for liquid chromatography	47
2.5.1	BSA as a mobile phase additive in microbore LC	47
2.5.2	BSA as a mobile phase additive in capillary LC	48
2.5.3	Adsorption of BSA	48
2.5.3.1	Preparation of the pseudo-stationary phase	49
3	Optimisation of experimental variables using BSA in free-solution CE	50
3.1	Introduction	50
3.2	Variables available for BSA affinity CE	50
3.3	Optimisation of the pH	52
3.4	Optimisation of the concentration of BSA	53
3.5	Addition of organic solvent	59
3.6	Enantioselectivity of a BSA coated capillary	62
3.7	Conclusions	67
4	Evaluation of biomacromolecules for chiral discrimination in free solution capillary electrophoresis	69
4.1	Introduction	69
4.2	Results and discussion	69



4.3	Results for the separation of a range of compounds with BSA with the protein affinity CE protocol	70
4.4	Results for the separation of a range of compounds with HSA with the protein affinity CE protocol	84
4.5	Results for the separation of a range of compounds with protamine and lactoferrin the protein affinity CE protocol	84
4.6	Discussion	93
4.6.1	Evaluation of protein affinity CE	93
4.6.2	Features of the electropherograms	96
5	Addition of modifiers to the CE run buffer	97
5.1	Introduction	97
5.2	Addition of metal ions to protein affinity CE	98
5.3	Addition of $\beta$ -cyclodextrin to a protein affinity CE buffer	108
5.3.1	Analysis of tryptophan enantiomers	108
5.3.2	Analysis of ibuprofen enantiomers	118
5.4	Allosteric interactions	127
5.4.1	Introduction	127
5.4.2	Discussion	128
5.5	Conclusions	133
6	Practical issues associated with protein affinity CE	135
6.1	Artefacts associated with the Dionex CES I	135
6.1.1	Capillary fill method	135
6.1.2	Reduction of the overall run time	139
6.1.3	Baseline anomalies	141
6.1.4	Ibuprofen ghost peaks	144
6.2	Artefacts associated with the PACE 2050	149
6.2.1	The stepped baseline	149
6.2.2	Buffer depletion	149
6.2.3	Siphoning	151
6.2.4	Overload of BSA in the outlet vial	151

6.3	Conclusions	152
7	BSA as a mobile phase additive in microbore HPLC	153
7.1	Introduction	153
7.2	Results and discussion	154
7.2.1	Mechanism of separation	154
7.2.2	Enantioselectivity of the method	155
7.2.3	Method practicalities	159
7.3	BSA as a mobile phase additive in capillary LC	161
7.4	Conclusions	161
8	BSA as pseudo stationary phase in microbore HPLC	163
8.1	Introduction	163
8.2	Results and discussion	164
8.2.1	Mechanism of separation	164
8.2.2	BSA as a pseudo stationary phase on a C <sub>8</sub> stationary phase	165
8.3.3	BSA as a pseudo stationary phase on a DIOL stationary phase	169
8.3.4	BSA as a pseudo stationary phase on Nucleosil silica	169
8.4	Conclusions	177
9	Conclusions	178
	References	189

## List of Figures

Fig. 1	Hands to give an easily recognisable representation of chirality in nature	2
Fig. 2	Diastereoisomers of 1,1-dichloropentane	3
Fig. 3	Representation of enantiomers where a, b, c and d are different substituents	4
Fig. 4	Steric overcrowding leading to chiral molecules	4
Equation 5	Specific Rotation	5
Fig. 6	Orientation of chiral molecules to determine the Cahn-Ingold notation	7
Fig. 7	Glyceraldehyde enantiomers	8
Fig. 8	R-2-[4-(trifluoromethyl-2-pyridyloxy)phenoxy]propionate	10
Fig. 9	Chemical Structure of an $\alpha$ -amino acid	11
Table 10	Structure of six common amino acid side chains	12
Fig. 11	Proline	13
Fig. 12	The structure of human serum albumin and the possible location of drug binding sites	14
Fig. 13	Basic capillary electrophoresis instrument	17
Equation 14	Dissociation equilibrium of silanol groups at the capillary surface.	17
Fig. 15	Schematic representation of the electroosmotic flow	18
Fig. 16	Difference of the flow profiles in CE (plug-like) and HPLC (parabolic)	18
Fig. 17	Graphical representation for the separation of molecules under an applied electric field	19
Equation 18	Electrophoretic mobility	20
Equation 19	Association equilibria	21
Equation 20	Apparent electrophoretic mobility	22
Equation 21	Difference in electrophoretic mobilities of enantiomers in the presence of a chiral selector	22
Fig. 22	Three dimensional structure of the Cyclodextrin ring	23

Fig. 23	Chemical structure of cyclodextrins	24
Fig. 24	Chemical structure of leucovorin	27
Fig. 25	Chemical structure of quinolone bactericidal reagents Ofloxacin and DR-3862	27
Fig. 26	Representation of protein pseudo-stationary phase	28
Fig. 27	Stylised chromatogram depicting high-performance frontal analysis chromatography	32
Fig. 28	Stylised electropherogram depicting the vacancy peak method	33
Fig. 29	Stylised electropherogram depicting frontal analysis capillary electrophoresis	34
Fig. 30	Representation of the relative migration of BSA at different pH values	53
Fig. 31	Resolution of tryptophan enantiomers with increasing concentration of BSA in the run buffer	55
Fig. 32	Migration times of tryptophan enantiomers with increasing concentration of of BSA in the run buffer	56
Fig. 33	CE of tryptophan enantiomers with 30 $\mu$ M BSA	57
Fig. 34	CE of tryptophan enantiomers with 60 $\mu$ M BSA	58
Fig. 35	Resolution of tryptophan enantiomers with increasing organic additives	60
Fig. 36	Resolution of benzoin enantiomers with increasing organic additives	61
Fig. 37	The capillary fill method showing the BSA breakthrough	63
Fig. 38	CE of tryptophan enantiomers with the immobilised BSA capillary	65
Fig. 39	Theoretical calculation for the surface area ratio of a packed capillary to an open tubular capillary	67
Table 40	Resolution of enantiomers using BSA as the chiral selector and standard conditions	70
Fig. 41	CE of benzoin enantiomers	72
Fig. 42	CE of thioridazine enantiomers	73
Fig. 43	CE of bepridil enantiomers	74

Fig. 44	CE of kynurenine enantiomers	75
Fig. 45	CE of leucovorin enantiomers	76
Fig. 46	CE of ibuprofen enantiomers	77
Fig. 47	CE of 2-(4-methylphenyl) propionic acid enantiomers	78
Fig. 48	CE of tryptophan amide enantiomers	79
Fig. 49	CE of hexobarbitone enantiomers	80
Fig. 50	CE of N-acetyl-DL-tryptophan enantiomers	81
Fig. 51	CE of warfarin enantiomers	82
Fig. 52	CE of tyrosine enantiomers	83
Table 53	Resolution of enantiomers using HSA as the chiral selector and standard conditions	84
Fig. 54	CE of bepridil enantiomers	86
Fig. 55	CE of promethazine enantiomers	87
Fig. 56	CE of tryptophan enantiomers	88
Fig. 57	CE of thioridazine enantiomers	89
Fig. 58	CE of kynurenine enantiomers	90
Fig. 59	CE of tryptophan enantiomers	91
Fig. 60	CE of leucovorin enantiomers	92
Table 61	Review of chiral separations with proteins in free-solution CE	94
Table 62	Selectivity of tryptophan enantiomers with the addition of metal ions	99
Fig. 63	CE of tryptophan enantiomers using 67mM Borate buffer	100
Fig. 64	CE of tryptophan enantiomers in the presence of manganese	101
Fig. 65	CE of tryptophan enantiomers in the presence of zinc	102
Table 66	Selectivity of kynurenine enantiomers with the addition of metal ions	103
Fig. 67	CE of kynurenine enantiomers using 67mM Borate buffer	105
Fig. 68	CE of kynurenine enantiomers in the presence of manganese	106
Fig. 69	CE of kynurenine enantiomers in the presence of zinc	107
Fig. 70	Migration times of tryptophan enantiomers with the addition of $\beta$ -cyclodextrin	110

Fig. 71	Resolution of tryptophan enantiomers with the addition of $\beta$ -cyclodextrin	111
Fig. 72	Resolution of tryptophan enantiomers	112
Fig. 73	Resolution of tryptophan enantiomers with 6 $\mu$ M $\beta$ -cyclodextrin	113
Fig. 74	Resolution of tryptophan enantiomers with 12 $\mu$ M $\beta$ -cyclodextrin	114
Fig. 75	Resolution of tryptophan enantiomers with 18 $\mu$ M $\beta$ -cyclodextrin	115
Fig. 76	Resolution of tryptophan enantiomers with 24 $\mu$ M $\beta$ -cyclodextrin	116
Fig. 77	Resolution of tryptophan enantiomers with 30 $\mu$ M $\beta$ -cyclodextrin	117
Fig. 78	Migration times of tryptophan enantiomers with the addition of $\beta$ -cyclodextrin	120
Fig. 79	Resolution of ibuprofen enantiomers with the addition of $\beta$ -cyclodextrin	121
Fig. 80	CE of ibuprofen with 12 mM $\beta$ -cyclodextrin	122
Fig. 81	CE of ibuprofen with 18 $\mu$ M $\beta$ -cyclodextrin	123
Fig. 82	CE of ibuprofen with 24 $\mu$ M $\beta$ -cyclodextrin	124
Fig. 83	CE of ibuprofen with 30 $\mu$ M $\beta$ -cyclodextrin	125
Fig. 84	Area of the ibuprofen-BSA void	126
Table 85	Summary of molecules which bind to specific sites on HSA	127
Table 86	Selectivity of tryptophan enantiomers with the addition of competing ligands	128
Fig. 87	Resolution of tryptophan enantiomers with addition of lorazepam	129
Fig. 88	Resolution of tryptophan enantiomers with addition of digitoxin	130
Fig. 89	Resolution of tryptophan enantiomers with addition of warfarin	131

Fig. 90	Resolution of tryptophan enantiomers with addition of ibuprofen	132
Fig. 91	CE of tryptophan using a three minute pressure injection to load BSA onto the capillary	136
Fig. 92	The capillary fill method showing the BSA breakthrough	137
Fig. 93	CE of tryptophan enantiomers following the BSA breakthrough	140
Fig. 94	CE of hexobarbitone enantiomers showing a spontaneous peak marker	142
Fig. 95	CE of N-acetyl-DL-tryptophan enantiomers showing both a spontaneous peak marker and a baseline shift	143
Fig. 96	CE of ibuprofen enantiomers showing the dip in the baseline	145
Fig. 97	Separation of ibuprofen enantiomers as they migrate towards the detector	146
Fig. 98	CE of ibuprofen enantiomers injected with 60 $\mu$ M BSA	148
Fig. 99	CE of ibuprofen enantiomers showing the stepped baseline	150
Fig. 100	Graphical representation between the stationary phase, the protein and the analytes	154
Table 101	<i>k</i> values of analytes with BSA as a mobile phase additive	156
Fig. 102	Resolution of tryptophan using free-solution BSA and microbore HPLC	157
Fig. 103	Resolution of kynurenine using free-solution BSA and microbore HPLC	158
Fig. 104	Selectivity of tryptophan enantiomers with the amount of mobile phase pumped through the column	160
Fig. 105	Simplified graphical representation of the equilibrium of the pseudo protein stationary phase and the analytes	164
Fig. 106	Absorption of BSA onto the wide pore C <sub>8</sub> stationary phase	166
Fig. 107	Resolution of tryptophan enantiomers with a BSA pseudo stationary phase	167
Fig. 108	Resolution of kynurenine enantiomers with a BSA pseudo stationary phase	168

Fig. 109	Absorption of BSA onto the wide pore Lichrosorb DIOL stationary phase	170
Fig. 110	Absorption of BSA onto the wide pore Nucleosil silica stationary phase	171
Table 111	<i>k</i> values of analytes with BSA adsorbed on the Nucleosil silica	172
Fig. 112	Resolution of tryptophan enantiomers with a BSA pseudo stationary phase	173
Fig. 113	Resolution of kynurenine enantiomers with a BSA pseudo stationary phase	174
Fig. 114	Resolution of benzoin enantiomers with a BSA pseudo stationary phase	175
Fig. 115	Resolution of warfarin enantiomers with a BSA pseudo stationary phase	176
Fig. 116	Advantages and disadvantages of each system	179
Fig. 117	A double loop HPLC system	182



## **Chapter 1 Introduction**

### **1.1 Preface**

The research programme described in this thesis involves the general area of the study of the interaction of analytes, usually drug molecules, with biopolymers in separative systems. Such systems have potential value in providing the basis for understanding of separative methods based on bioaffinity, particularly those involving the resolution of enantiomers. Also they might prove useful in assessing, at least qualitatively, the ability of drugs to bind to biopolymers. It ought to be instructive then to consider the over-arching principles and key issues in areas such as chirality in order to set the scene for the rationale for the aims and objectives at the outset of the research programme.

### **1.2 Chirality**

#### **1.2.1 Overview of chirality**

Chirality is the property of molecules or objects whereby their respective mirror images cannot be superimposed. It is not necessary to go very far to find an excellent example of chirality. The hands of a human being are chiral. As shown in Fig. 1, even though they appear identical they are non-superimposable.

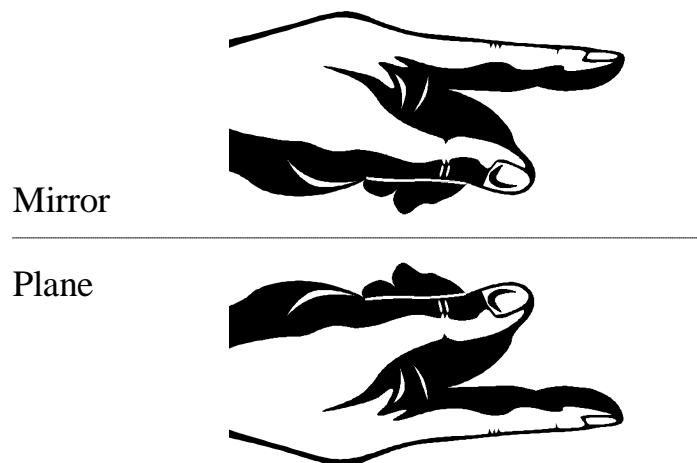


Fig. 1 Hands to give an easily recognisable representation of chirality in nature. No matter which way the lower mirror image hand is translated or rotated, it cannot be superimposed on the upper original hand

Importantly, chirality such as this exists at the molecular level.

### 1.2.2 Stereoisomers

Stereoisomers are molecules which have atoms bonded in the same order or 'connectivities' but do not have the same arrangement in space. Stereoisomers that have non-superimposable mirror images are termed enantiomers.

Diastereoisomers are molecules which contain more than one chiral centre. For such molecules a number of stereoisomers are possible, for example, 2,3-dichloropentane has four stereoisomers, Fig. 2.

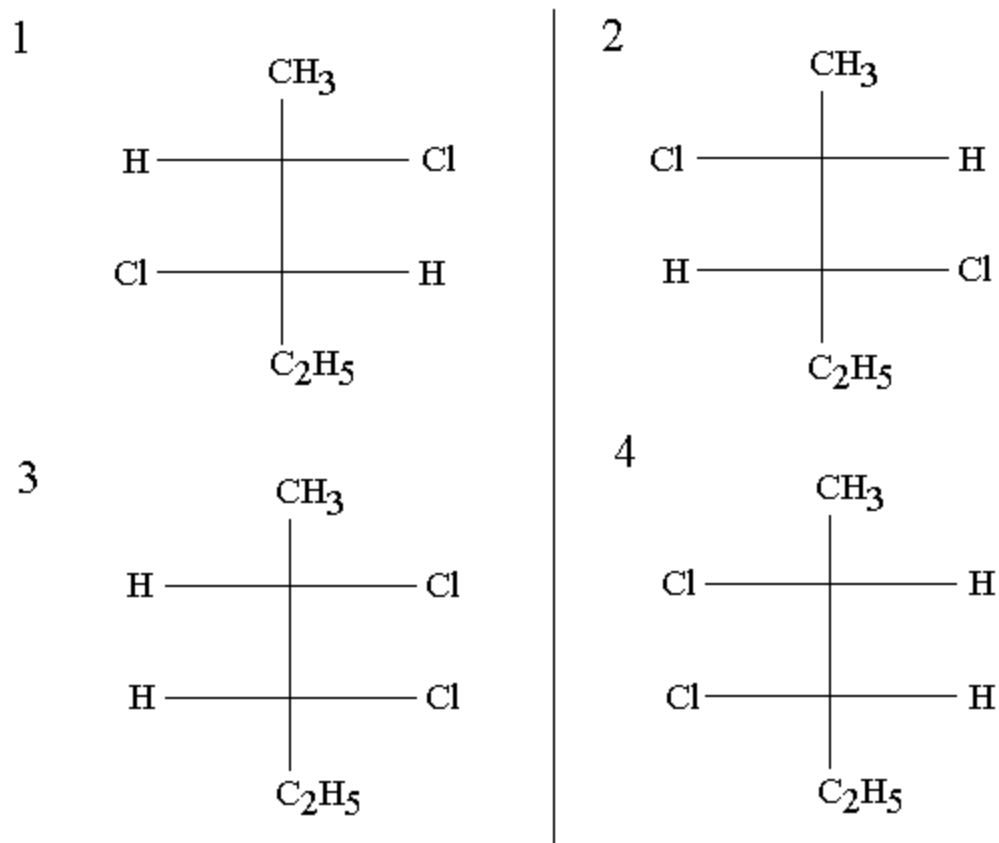


Fig. 2 Diastereoisomers of 1,1-dichloropentane

From Fig. 2, 1 + 2 and 3 + 4 are enantiomers. However, 1 + 3 and 2 + 4 are not enantiomers, as they do not have non-superimposable mirror images. Diastereoisomers have similar chemical properties although not identical chemical properties of enantiomers. They have different physical properties and can be separated by fractional crystallisation and fractional distillation. From Fig 2, 1 + 2 can be separated from 3 + 4 using these methods.

### 1.2.3 Asymmetric carbon

The most common source of chirality, especially in drug molecules, is the tetrahedral carbon centre. When there are four different groups attached then it is chiral and has two enantiomers, Fig. 3. Other terms used include stereogenic centre and chiral centre.

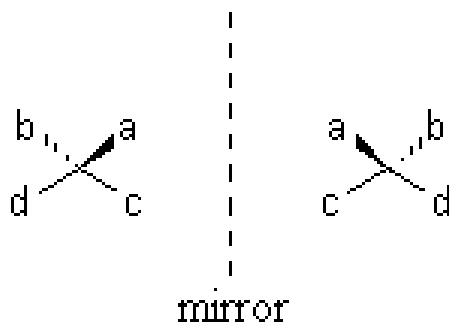


Fig. 3 Representation of enantiomers where a, b, c and d are different substituents.

However, it is worth noting that chirality may also arise from steric overcrowding, as is the case for hexahelicene. From Fig 4, there is overcrowding indicated by the R and R' groups. This will form two different chiral molecules depending on the orientation of the R and R' and the plane of the molecule.

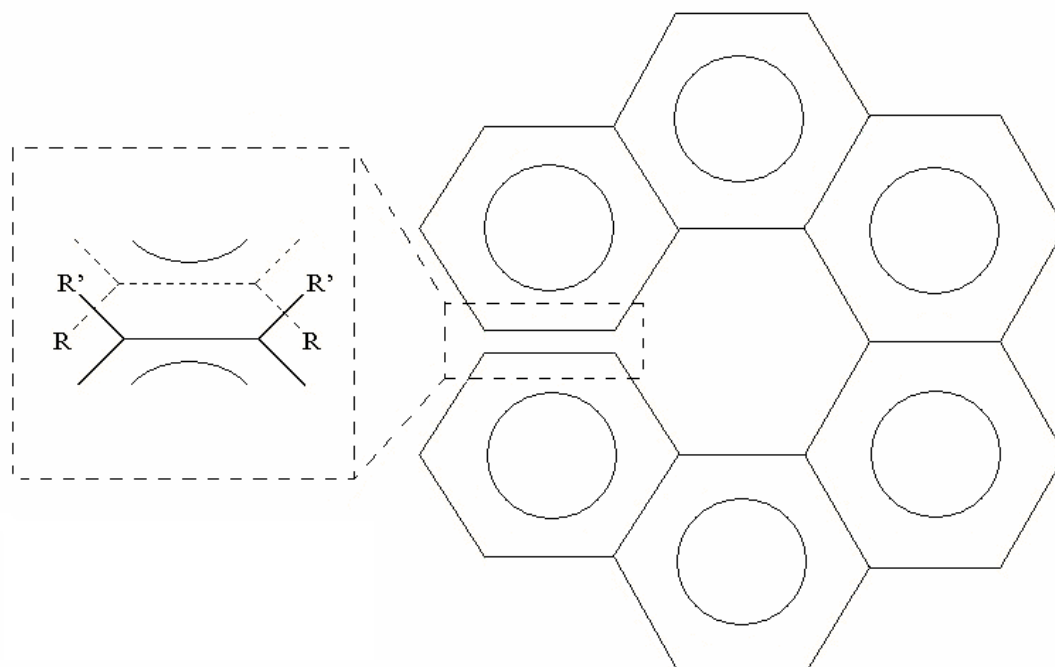


Fig.4. Steric overcrowding leading to chiral molecules. The plane of the hexahelicene molecule will be conformationally locked if the R and R' substituents are sterically too bulky to allow the ends of the molecule to slip past each other.

## 1.2.4 Properties of chiral compounds

### 1.2.4.1 Achiral properties

The physical properties, e.g. density, boiling point and melting point, are identical for both enantiomers. Where there are no interactions from chiral molecules during chemical reactions then both enantiomers will have the same reaction kinetics and thermodynamic profiles.

### 1.2.4.2 Optical properties

When chiral compounds contain an excess of one enantiomer [Mason 2002], a solution of the compound will rotate a plane of polarised light through an angle  $\alpha$ , which is the observed rotation. When the amounts of each compound are equal, a racemate, then there is no rotation of polarised light. The specific rotation,  $[\alpha]$ , of a compound is shown in the following equation 5: -

$$[\alpha] = \frac{100\alpha}{cl}$$

Equation 5 Specific rotation

where

$[\alpha]$	=	specific rotation
$\alpha$	=	angle of rotation of the polarised light
$c$	=	concentration, g 100 ml <sup>-1</sup>
$l$	=	path length, dm

### **1.2.4.3 Chemical properties**

When reactions occur in chiral environments the enantiomers have different reaction kinetics and thermodynamic profiles. Where a reagent only interacts effectively with one of the enantiomers then it has chiral recognition properties. This is important in nature, which has many such chiral recognition reactions. The three-point interaction rule is an attempt to describe the nature of chiral recognition.

### **1.2.5 Three point interaction rule**

The rule was proposed by Dalgliesh [Dalgliesh 1952] after studying optical resolution of aromatic amino acids using cellulose. He proposed that if an  $\alpha$ -amino group and carboxyl group were simultaneously bonded, by hydrogen bonding, to cellulose then resolution could not occur. However when another part of the molecule was bonded to the cellulose, e.g. an aromatic group, then there will be a three-point attachment of the molecule, which is required for stereochemical specificity. The interactions between different groups can be from covalent bonding, ion-ion interactions, hydrogen bonding, steric repulsion and dipole-dipole interactions.

### **1.2.6 Nomenclature of chiral molecules**

To differentiate between enantiomers three naming conventions have been adopted [Carey 1992]. These are Cahn-Ingold R,S [Cahn 1966] notational system, nomenclature assigned by the rotation of polarised light and the Fischer convention [Fischer 1891].

### 1.2.6.1 Cahn-Ingold R,S notational system

This system [Cahn 1966] allows the specific structure of each enantiomer to be determined. The substituents of the stereogenic centre have to be identified. The substituents are then assigned a rank based on the molecular mass of the bonded atoms from the lowest to the highest, e.g. carbon will have a higher rank compared to hydrogen. The molecule is orientated such that the lowest rank is pointing away from the viewer, Fig. 6. Of the remaining three substituents if the order of decreasing rank is clockwise then it is assigned as R otherwise it will be assigned as S for anti-clockwise.

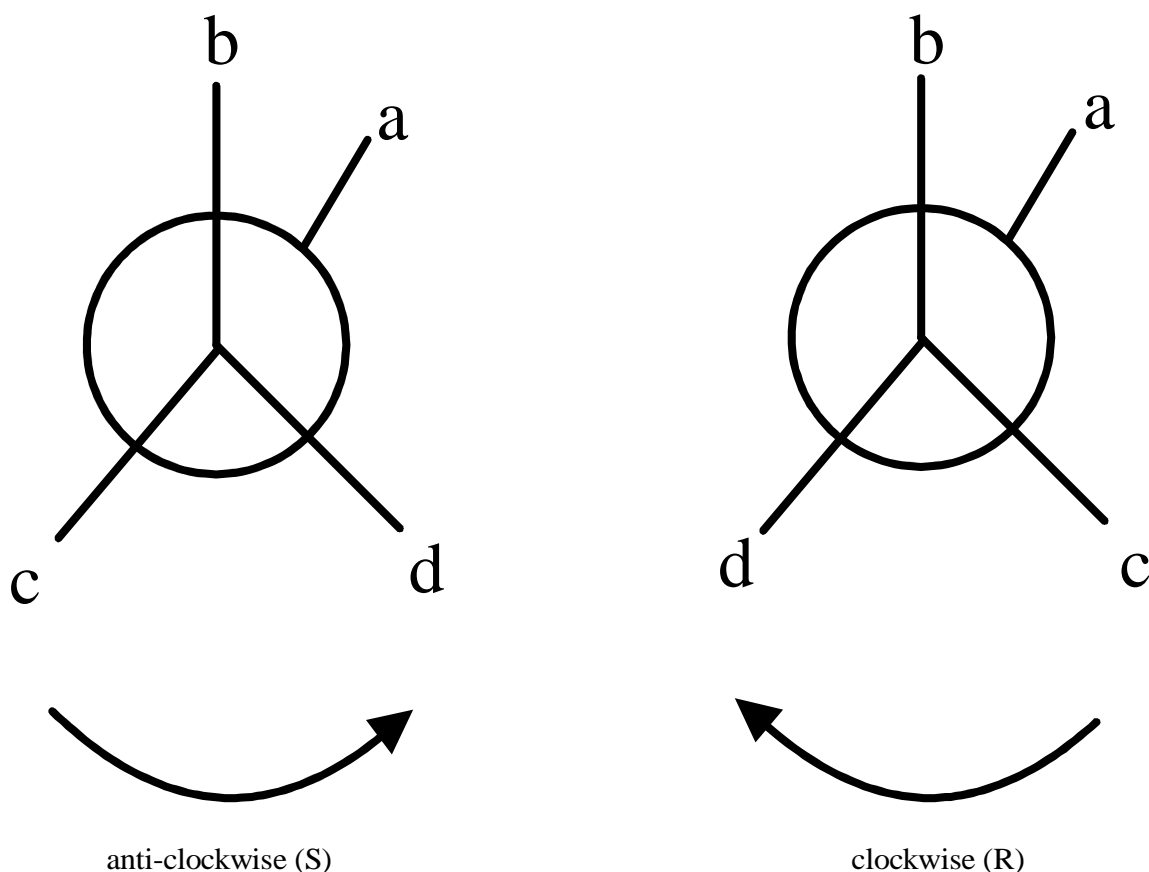


Fig. 6 Orientation of chiral molecules to determine the Cahn-Ingold notation, with a the lowest ranking group being furthest away from the viewer above the plane of the page.

### 1.2.6.2 Nomenclature assigned by the rotation of polarised light

When chiral molecules rotate polarised light, the light is a single wavelength and is typically 589 nm based on the sodium D-line standard, in a clockwise direction then they are assigned as (d) or (+) molecules. Similarly for anti-clockwise rotation they are assigned as (l) or (-) molecules. This notational system does not give structural information about the molecule, unlike the Cahn-Ingold notation.

### 1.2.6.3 Fischer convention

Emil Fischer introduced the convention in 1891 [Fischer 1891]. Configurations of chiral molecules could be related by reactions of known stereochemistry. Fischer projections are used for sugars and other carbohydrates. The simplest carbohydrate, glyceraldehydes, was chosen as the standard by which all others could be related. From their rotation of polarised light (+)-glyceraldehyde was designated D-glyceraldehyde and (-)-glyceraldehyde was designated L-glyceraldehyde [Carey 1992]. The configuration of the glyceraldehyde molecules is shown in Fig. 7.

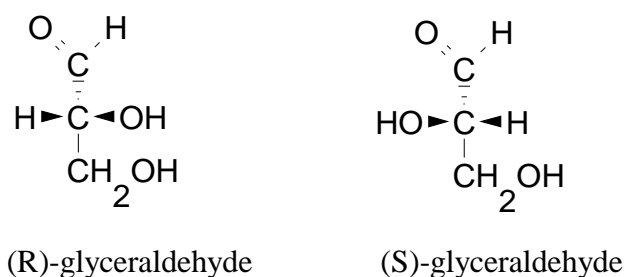


Fig. 7 Glyceraldehyde enantiomers, set out with the most oxidised C atom at the top.



From the absolute configurations in Fig 7, D-glyceraldehyde has the R configuration and conversely L-glyceraldehyde has the S configuration. As it transpired from the studies of Bijvoet in 1951 [Bijvoet 1951 & Bijvoet 1955] the configurations were indeed as Fischer postulated.

#### **1.2.6.4 Determination of the absolute configuration of enantiomers**

The absolute configuration of enantiomers was not determined until 1951 by J.M. Bijvoet at the University of Utrecht. By using the x-ray analysis method of anomalous scattering he studied the salt of (+)-tartaric acid to determine the configuration. Once the configuration of (+)-tartaric acid was known then this was then related to glyceraldehyde so the configuration of many enantiomers could then be determined.

#### **1.2.7 Chirality and pharmaceuticals**

As biological systems are chiral in nature and since many drugs contain enantiomers so it is important to understand the pharmacokinetics and pharmacological profile of all the enantiomeric forms. Both enantiomers can exhibit several different effects ranging from beneficial activity to inactivity or even extreme toxicity. The case of the enantiomers of thalidomide has been well documented [The Insight Team 1979]. Thalidomide was employed as a sedative and anti-nausea drug between 1959 and 1962. The R enantiomer was beneficial but the S enantiomer was held responsible for over 2000 cases of serious birth defects in children born to women who took thalidomide during pregnancy. It has since been established that the *in vitro* racemisation of thalidomide is far more complex [Agranat 2002, Knoche<sup>1</sup> 1994 & Knoche<sup>2</sup> 1994] than had originally been thought.

Where chiral compounds are used then it is important to know the amounts of enantiomers present. As enantiomers have the same physical properties then normal analytical techniques cannot be used. However in chiral environments enantiomers react differently, so in order to separate them a chiral recognition step has to be incorporated into the analytical procedure. With increased understanding of separating and the pharmacokinetics of enantiomers by the mid-90s many states were issuing regulations for chiral medicinal products [Rauws 1994].

### 1.2.8 Chiral agrochemicals

Another area where single enantiomers are used is pest control. Previous generations of pesticides have not been species specific and have caused wider problems in the environment. Such pesticides include organochlorine compounds and organophosphates. It has been suggested that future agrochemicals could be single enantiomers and target a particular crop or pest through their stereochemistry [Massey 1994] and one such agrochemichemical which they studied was R-2-[4-(trifluoromethyl-2-pyridyloxy)phenoxy]propionate, Fig. 8.

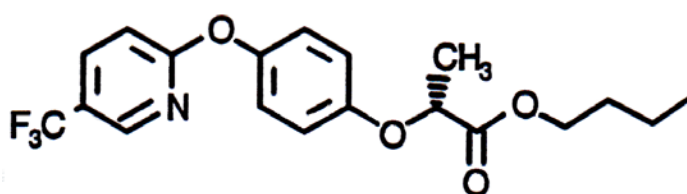


Fig.8 R-2-[4-(trifluoromethyl-2-pyridyloxy)phenoxy]propionate, a novel chiral agrochemical.

Therefore, as is the case for pharmaceuticals, the separation and quantitation of enantiomers are important. Chiral HPLC has been the analytical technique of choice to resolve enantiomers of such compounds including hexobarbital and chlorothalidone [Riering 1996], homologous malathion derivatives [Chilmonczyk

1998], organophosphorus pesticides [Ellington 2001] and fungicidal triazolyl alcohols [Spitzer 1999].

### 1.3 The use of biomacromolecules as chiral selectors

Biomacromolecules such as proteins and polysaccharides are large biological molecules which are colloidal in nature. In general, they have complex structures with many points for interaction and so a broad spectrum of drug classes may bind to them while, at the same time, the binding can be quite selective.

#### 1.3.1 Proteins

##### 1.3.1.1 Amino acids

Proteins are straight chain polymers of amino acids, Fig. 9, that perform a wide a wide variety of cellular functions ranging from the structure of cells to the controlling elements in living systems. The protein polymers fold into unique three dimensional structures. The shape of proteins can be defined into four distinct areas.

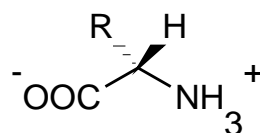


Fig. 9 Chemical structure of an  $\alpha$ -amino acid, showing the 'zwitterionic form' with both the amino- and carboxylic acid groups ionised but with no net charge. Only the L form (shown) is found in higher organisms.

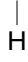
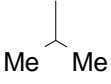
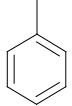
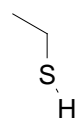
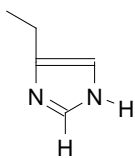
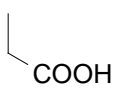
There are several theories as to why amino acids only appear as the L enantiomer in nature [Dickerson 1969]. The L enantiomer is thermodynamically more stable in magnetic fields and UV light, so over a period there would be more of the L enantiomer compared to the D enantiomer. It could have been thermodynamically

favourable for the L enantiomers to react in the early stages of life thus leading to a gradual, but, over time, very marked enrichment [MacDermott 2002].

### 1.3.1.2 The peptide bond

The peptide bond is formed by a condensation reaction between amine and carboxylic acid groups with the loss of a molecule of water. The amino acid monomer can have any number of side chains. Some amino acid side chains are shown in Table 10. With twenty different side chains for each monomer then there are a huge number of different possible polypeptides. The side chains have the most effect on the properties of the protein; for example, in regions where the side chains are hydrophobic they will adopt a structure to minimise water interactions and so form hydrophobic pockets. This arises from the change in entropy around a hydrophobic molecule. The water molecules form an ordered lattice so when the hydrophobic molecule is removed, the ordered lattice breaks down so there is an increase in entropy. Hydrophilic side chains are found on the surface of the protein [Kaliszan 1992].

Table 10 Structure of six common amino acid side chains

Amino Acid Residues		
		
Glycine Gly	Leucine Leu	Phenylalanine Phe
		
Cysteine Cys	Histidine His	Aspartic Acid Asp

### 1.3.1.3 Structure of proteins

The primary structure is the amino acid sequence of the protein. The secondary structures are locally defined and can be patterned sub-structures of  $\alpha$ -helices and  $\beta$ -sheets or segments of the chain that have no discernable shape. Each turn of an  $\alpha$ -helix requires 3.6 amino acid subunits. Proline is unique in the side chain bonded to the  $\alpha$ -carbon and the nitrogen to form a secondary rather than a primary amino group, Fig. 11. As a result the helical chain is slightly distorted around this amino acid. There can be many such secondary structures on a single protein. The tertiary structure is the overall shape of the single protein molecule and is defined by the interactions of the secondary structures to one another. The quaternary structure is the result of the formation of a protein complex from more than one protein molecule.

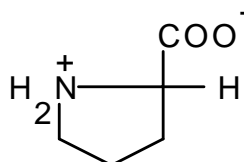


Fig. 11 Proline, the only secondary amine containing natural amino acid

The four structures of the protein molecule are held together by a wide range of bonds and chemical interactions. The primary amino acid sequence is formed by peptide bonds. The secondary structure is formed by hydrogen bonding. The tertiary structure is formed by a variety of different bonds including hydrophobic interactions, hydrogen bonds, ionic interactions and disulphide bridges. A process called protein folding forms the quaternary structure. The mechanism of the protein folding remains essentially unresolved because there are too many conformations that can occur to be evaluated [Peters 1977].

### 1.3.2 Serum albumins

Albumins are the main circulatory proteins in the blood plasma [Peters 1977]. A variety of ligands are reversibly bound to albumins so they can be transported around the body. This is especially important for hydrophobic molecules like fatty acids where solubility in aqueous plasma would be problematic.

#### 1.3.2.1 Structure of albumins

Albumins contain approximately 580 residues with a number loops, usually between eight and ten, formed by disulphide bridges. The structure of Human Serum Albumin with possible drug binding sites has been suggested by Fehske [Fehske 1981]. This is shown in Fig. 12.

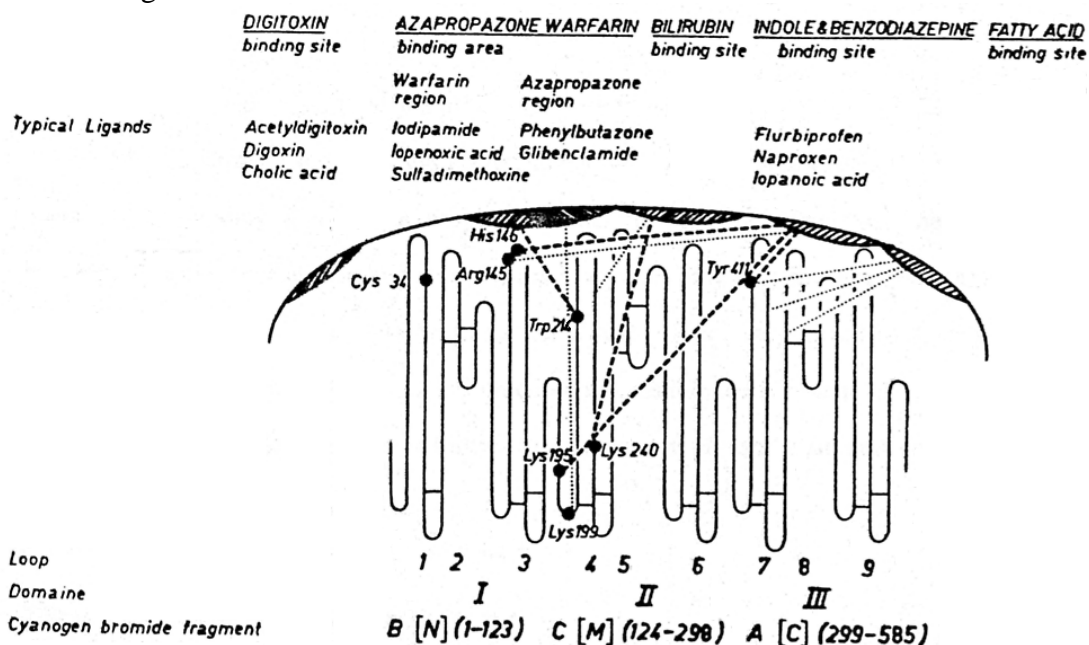


Fig. 12 The structure of human serum albumin and the possible location of drug binding sites [Fehske 1981].

The amino acid sequence of bovine serum albumin (BSA) used in this study has been solved [Peters 1977] and it has 576 residues and nine loops. BSA has a molecular

weight of 66000. Models have been used to predict the general structure of albumin based on physical and chemical measurements. The proposed structures are that of a prolate ellipsoid with dimensions 141 Å x 42 Å and a three-domain structure of spheres with approximate diameters of 38, 53 and 38 Å respectively.

### **1.3.3 Binding sites**

As noted previously, a number of low molecular weight compounds can be reversibly bound to albumins. There are many potential sites of interaction for ligands on albumins, for example, there are areas of hydrophobic character, which would favour fatty acid binding, and there are hydrophilic areas on the surface of the albumin, which favour polar molecules. Where ligands favour a particular area then this is commonly referred to as a binding site. As albumins contain only L-amino acids then the binding sites will exhibit one stereoscopic orientation. Assuming that there are three points of interaction [Dalglish 1952] at the binding site then enantiomers will exhibit different binding properties. The basis of the different pharmacological and toxicological profiles of proteins and in particular albumins is used to separate enantiomers.

## **1.4 Capillary electrophoresis**

Capillary electrophoresis (CE) is still a relatively new analytical technique and in the early 1990s was rapidly gaining acceptance as a mainstream separating technique. Electroosmosis has been known for a number of years in thin-layer chromatographic systems. Columns with an internal diameter of less than 100 µm, have only been used experimentally since the early 1980s. These columns are generally referred to as capillaries. The first experiments were carried by Jorgensen [Jorgensen 1981] to resolve mixtures of fluorescamine labelled peptides and since then there has been an exponential growth in the number of publications including books [Camilleri 1993,

Grossman 1992 & Landers 1994] and a launch of a new journal in 1994, Journal of Capillary Electrophoresis, dedicated to CE. There is also a dedicated capillary electrophoresis website at [www.ceandcec.com](http://www.ceandcec.com). By the end of the 1990s there were several commercial instruments from different manufacturers (Beckman, Dionex, Hewlett Packard, BioRad, Spectraphysics and Unicam) which allow full automation and the use of different detectors including UV, diode-array, conductivity and mass spectrometry.

#### **1.4.1 Basic instrumentation for capillary electrophoresis**

The instrumentation of CE is straightforward requiring a capillary, a high voltage power supply, detector and two buffer vials in which the capillary is placed. Most instruments have a safety feature to protect users from the high voltages used. A schematic diagram is shown in Fig. 13. The capillary used is made from fused silica and has typical dimensions of 20 - 100 cm length and 25 - 75  $\mu\text{m}$  internal diameter. The capillary is coated with polyimide which provides flexibility and strength. Normally a small portion of the polyimide coating is removed, typically 5mm, to provide a window, this is typically 5 mm. The window part of the capillary provides a path, the internal diameter of the capillary, for UV light to pass through the capillary to the detector. The power supplies a typical voltage between 0 and 30 kV. With the high voltages used all instruments have a safety-locking device when the instrument is in use. Commercial instruments typically have an autosampler which allows many samples to be analysed during a single analytical run.



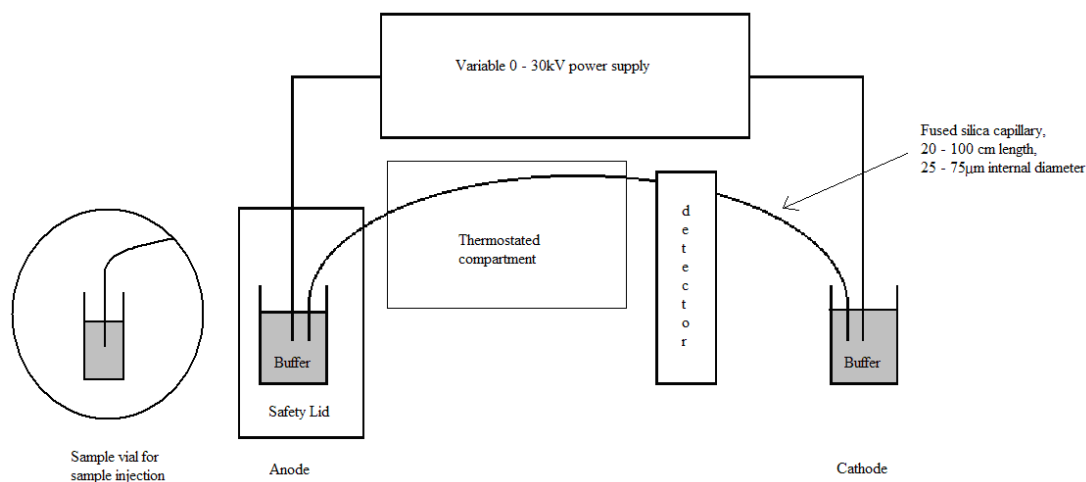
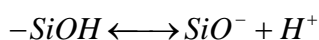


Fig. 13. Basic capillary electrophoresis instrument. Samples are usually injected onto the capillary by either applying positive pressure or by the use of an electric field.

## 1.4.2 Theory of capillary electrophoresis

### 1.4.2.1 Electroosmotic flow

The electroosmotic flow (EOF) is the bulk flow of the buffer through a capillary when a voltage is applied and is only associated with CE. The EOF is pH dependent and is governed by the dissociation of the silanol groups as shown by equation 14.



Equation 14. Dissociation equilibrium of silanol groups at the capillary surface.

The  $\text{pK}_a$  of the silanol groups at the surface of the capillary wall is between 4 and 5 so at pH 7 and above the silanol groups will be fully ionised. The cations within the buffer will then form a double layer to neutralise the excess negative charge, Fig. 15.

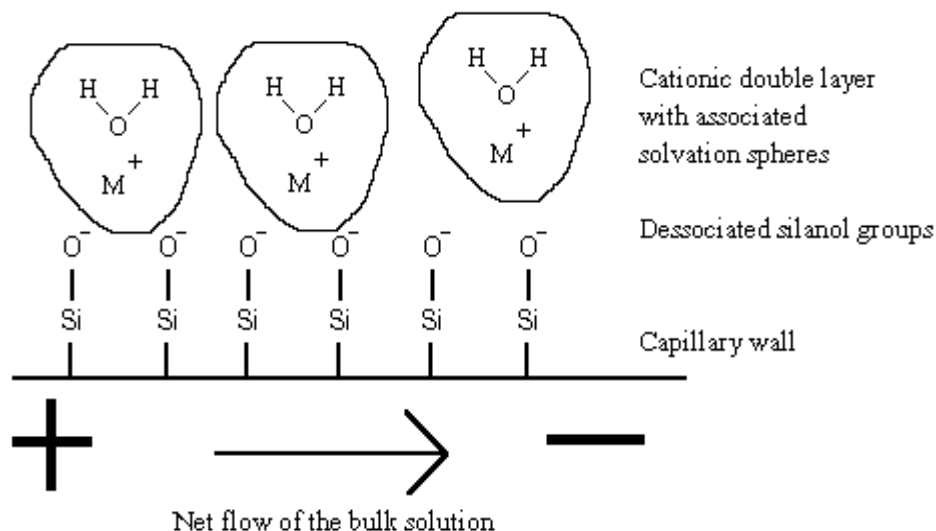


Fig. 15. Schematic representation of the electroosmotic flow. The electric double layer is formed by the negatively charged surface and nearby cations. The net flow of the bulk solution is produced by the predominance of cations in the double layer forming a net electroosmotic flow towards the cathode when an external field is applied.

When the voltage is applied cations migrate with their solvation spheres towards the cathode and this results in the plug-like flow associated with CE. The benefit of a plug-like flow is that it reduces band broadening unlike the parabolic flow profile found in HPLC, Fig. 16.



Fig. 16. Difference of the flow profiles in CE (plug-like) and HPLC (parabolic) with the force being applied all along the capillary and from one end of the capillary respectively.

To have reproducibility for the migration times of analytes the EOF needs to be constant. This is best achieved when the silanol groups are either completely ionised or completely unionised. To be fully ionised the pH has to be greater than 7 and unionised the pH has to be less than 2 so it is not practical to use buffers of pH between 2 and 7 as a slight difference in the pH can have dramatic effects on the silanol ionisation and hence on the EOF. Another method to prevent ionisation of the silanol groups is to react them with protecting groups like small alkyl groups. It is then possible to reduce the EOF when using buffers greater than pH 7.

#### 1.4.2.2 Separation of molecules using capillary electrophoresis

The separation of molecules using CE is based on their mobility in an applied electric field and is proportional to the charge and inversely proportional to the size of the molecules and the viscosity of the buffer, Fig. 17.

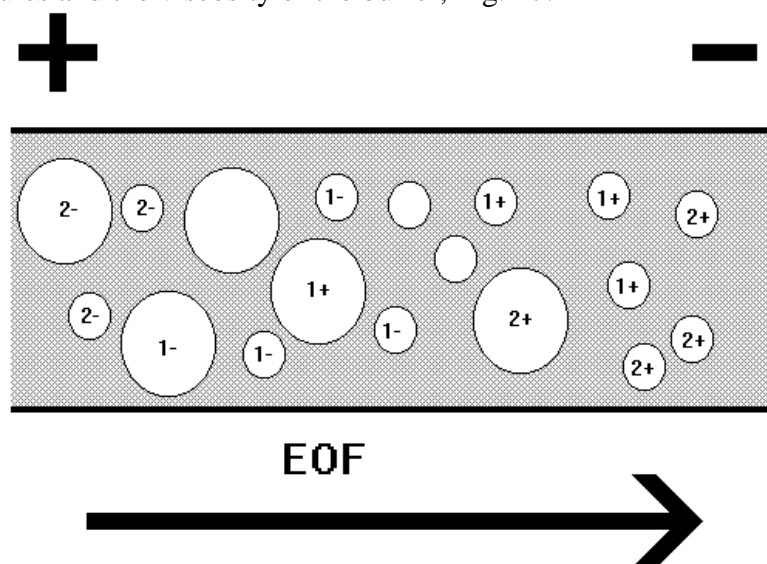


Fig. 17. Graphical representation for the separation of molecules under an applied electric field; with the EOF in the direction of the cathode being the overriding force and mobility of the ions being dependent on charge/mass the order of migration to the cathode is small positive ions > large positive ions > neutral molecules > large negative ions > small negative ions.

The electrophoretic mobility, the effective velocity of molecules, can be expressed as follows: -

$$\bar{\mu} = \frac{\bar{v}}{\bar{E}} = \frac{q}{6\pi\eta r}$$

Equation 18 Electrophoretic mobility

where

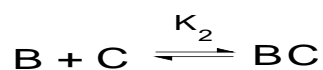
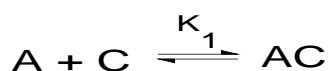
$\bar{\mu}$	=	electrophoretic mobility
$\bar{v}$	=	electrophoretic velocity
$\bar{E}$	=	electric field strength
$q$	=	charge of the ion
$\eta$	=	viscosity of the buffer
$r$	=	radius of the molecules.

The EOF is generally sufficient to elute negatively charged ions towards the cathode where the detector is situated. Therefore, CE can be used to separate a variety of charged species with all components of the sample passing the detector at the cathode end of the capillary. Accordingly CE is a very versatile technique which has been used for a very wide range of analytes ranging from aromatic sulfonic-acids [Brumley 1992] to unsaturated fatty acids [Schmitz 1997] to enantiomeric acidic herbicides [Desiderio 1997] to DNA restriction fragments [Baba 1993].

### 1.4.3 The role of CE in separating enantiomers

A number of techniques have been successfully used to separate a range of enantiomers and a great deal of experience has been gained, for example in HPLC, and there are books solely for chiral HPLC [Lough 1989 & Krstulovic 1989]. Some of the classes of chiral selector have been applied to use with CE and have shown reproducible results in the separation of enantiomers.

In the early 1990s, chiral CE is becoming widely used with reviews already being published [Snopeck 1992, Novotny 1994, Ward 1994 & Nishi 1995]. The most common form of chiral CE is to add chiral compounds to the run buffer. As the enantiomers complex with the additives at different rates and the resulting complexes will have different electrophoretic mobilities compared to the enantiomers then the effective mobilities of the enantiomers will be different and hence there will be a separation. Wren [Wren 1992] suggested the following equations for the enantiomers in free solution CE.



Equation 19 Association equilibria

where

- A = enantiomer 1
- B = enantiomer 2
- C = chiral selector
- K<sub>1</sub> = equilibrium constant for enantiomer 1 and the chiral selector
- K<sub>2</sub> = equilibrium constant for enantiomer 2 and the chiral selector
- AC = complex with enantiomer 1
- BC = complex with enantiomer 2.

Assuming that the exchange of A between the free form and the complex is rapidly reversible then the apparent electrophoretic mobility of A,  $\mu_a$  can be expressed as follows:-

$$\bar{\mu}_a = \frac{[A]}{[A]+[AC]} \mu_1 + \frac{[AC]}{[A]+[AC]} \mu_2$$

Equation 20 Apparent electrophoretic mobility

where

$\mu_1$  = electrophoretic mobility of the enantiomer

$\mu_2$  = electrophoretic mobility of the complex.

A similar equation can be given for enantiomer 2. Manipulating the equations for both enantiomers gives the apparent mobility between them:-

$$\mu = \frac{[C](\mu_1 - \mu_2)(K_2 - K_1)}{1 + [C](K_1 + K_2) + K_1 K_2 [C]^2}$$

Equation 21 Difference in electrophoretic mobilities of enantiomers in the presence of a chiral selector

As the equation shows there will be an optimum concentration for the concentration of the chiral selector as at low concentrations and high concentrations  $\mu$  will tend to zero. Thinking of this in qualitative terms, there will be very little scope for chiral discrimination if there is so little selector that both enantiomers are principally in their free form or so much selector that they are both very highly complexed.

## 1.4.4 Chiral selectors employed in capillary electrophoresis

### 1.4.4.1 Cyclodextrins

These are the most popular choice of chiral selector used. Cyclodextrins (CDs) are cyclic oligosaccharides which form 'bucket' shaped molecules; a graphical representation of the three dimensional structure and the hydrophobic cavity is shown in Fig. 22. When cyclodextrins are used under reverse-phase conditions the hydrophobic cavity can form inclusion complexes with the non-polar moieties of the enantiomers. The difference between competing enantiomers is determined by the interaction of the secondary hydroxyls on the edge of the cyclodextrin ring and the remaining ligands of the enantiomers.

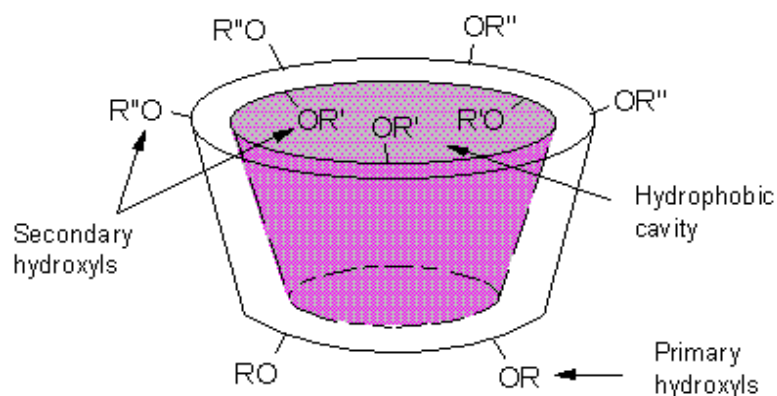


Fig. 22 Three dimensional structure of the cyclodextrin ring. Cyclodextrins (CDs) are cyclic oligosaccharides which form 'bucket' shaped molecules with a hydrophobic cavity

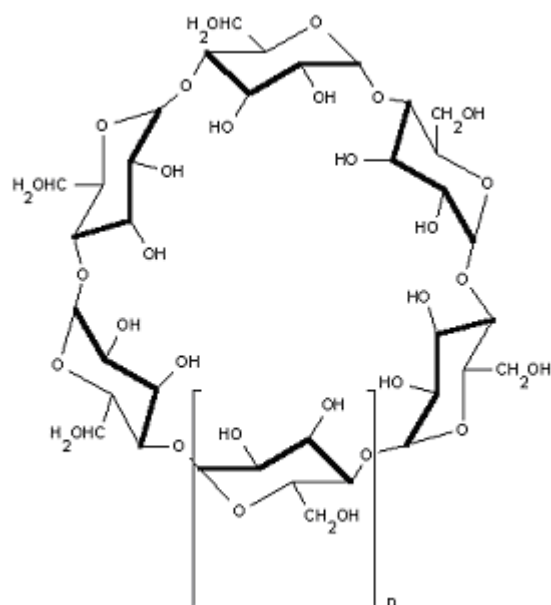


Fig. 23 Chemical structure of cyclodextrins. The cyclodextrins encountered for chiral separation  $n=1$ , 2 and 3. These represent  $\alpha$ -,  $\beta$ -, and  $\gamma$ -cyclodextrins and are 6-, 7- and 8- ring structures respectively

The cyclodextrin structure is shown in Fig. 23. They contain six, seven and eight glucopyranose units which give rise to  $\alpha$ -,  $\beta$ - and  $\gamma$ -CDs, where  $n=1$ , 2 and 3 respectively.

The separation of enantiomers arises from complexation within the hydrophobic cavity of the CDs. Compounds separated in early work in this field included terbutaline and propranolol by  $\beta$ -CD [Fanali 1991] and mandelic acid enantiomers by  $\gamma$ -CD [Valko 1994].

Work has been carried out to alter the size of the CD by derivatisation and in some cases has led to increased separation compared to the underivatized CDs. There have been several types of derivatised CDs with examples such as heptakis (2,6-di-O-



methyl)- $\beta$ -CD to separate terbutaline and propranolol [Fanali 1991] and sulfobutyl ether  $\beta$ -CD in the separation of ephedrine, pseudoephedrine and related compounds [Tait 1994]. In the former case the nature of the interaction on the 'rim' of the cyclodextrin 'bucket' is modified while in the latter case the charge on the 'base' of the 'bucket' serves to open up a 'window' of migration between, say, a neutral free analyte and its charged complexed form.

#### **1.4.4.2 Chiral micellar electrokinetic capillary chromatography**

Instead of using sodium dodecyl sulphate (SDS) as the surfactant in micellar electrokinetic capillary chromatography (MECC), chiral surfactants have been utilised to form a chiral micellar pseudo stationary phase. There are many naturally occurring chiral surfactants from which analysts may choose. One example of a family of natural surfactants are bile salts such as sodium cholate, which along with sodium deoxycholate, has been used to separate the enantiomers of 3-hydroxy-1,4-benzodiazepines [Michotte, 1995]. Another approach was used by Warner *et al* [Ward 1994] who used a chiral micelle polymer, poly(sodium N-undecylenyl-L-valinate), as the chiral stationary phase. There were some advantages over conventional chiral MECC such as improved mass transfer rate and the elimination of the equilibrium between the monomer and micelle so there is no CMC and so the methodology can be used at lower concentrations.

#### **1.4.4.3 Biomacromolecules**

Biomacromolecules are another source of chiral selectors. With the amount of chiral selectors needed for CE being very small, expensive and exotic biomacromolecules can be tested and subsequently used successfully. Typical biomacromolecules include macrocyclic antibiotics, carbohydrates and proteins. The use of macrocyclic antibiotics was pioneered by Armstrong *et al* [Armstrong 1994 & Armstrong 1995]

who were able to separate a range of compounds with vancomycin and ristocetin A. These chiral selectors were particularly effective in that, as recognised by Armstrong, they had the structural complexity of proteins without the potential band-broadening problems that might arise from the large molecular mass and structural heterogeneity associated with proteins.

As well as the cyclodextrins, non-cyclic oligosaccharides have also been used as buffer additives in chiral CE. Current research has been limited compared to the CDs but there are still some examples. Heparin is a naturally, polydisperse, polyionic glycosaminoglycan and has been used to achieve baseline separations of oxamniquine [Clark 1995], antimalarial and antihistamine drugs [Stalcup 1994]. Other carbohydrates used are maltooligosaccharides [Novotny 1994 & Verbeke 1994] and linear dextrans [Kano 1995].

Other examples of buffer additives are copper-histidine complexes in the separation of Dansyl-amino acids [Gozel 1987] and the use of chiral crown ethers [Kuhn 1994].

#### **1.4.4.4 Proteins**

Commercial protein chiral stationary phases for HPLC were first introduced into the UK in 1985 and by the early 1990s, proteins had been extensively used in chiral LC separations; examples of proteins used were bovine serum albumin (BSA) [Wainer 1998], human serum albumin (HSA) [Loun 1994] and  $\alpha_1$ -acid glycoprotein ( $\alpha_1$ -AGP) [Hermansson 1995]. However, their use as chiral selectors in CE has been modest with only a few papers having been published by the beginning of 1992.

The separation of leucovorin enantiomers, Fig 24, to measure thermodynamic variables using BSA as a buffer additive was reported by Barker *et al* [Barker 1992]. They concluded that coating the capillary surface with poly(ethylene) glycol (PEG)

improved run time reproducibility because the PEG coating prevented the BSA adhering to the capillary wall. Ligands, run buffer modifiers, or both, needed to be charged for acceptable analysis times. They found the optimum pH to use for run time, peak shape and resolution to be 7.2.

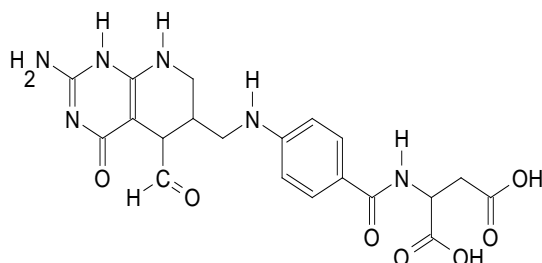


Fig. 24 Chemical structure of Leucovorin

Vespalec [Vespalec 1993] used a 10 mg ml<sup>-1</sup> HSA in 10 mM acetic acid-TRIS buffer, pH 8, to separate enantiomers of kynurenine, tryptophan and 3-indole lactic acid. Arai [Arai 1994] investigated the experimental variables to separate the enantiomers of quinolone bactericidal reagents Ofloxacin and DR-3862 with BSA and HSA as the chiral selectors, Fig. 25.

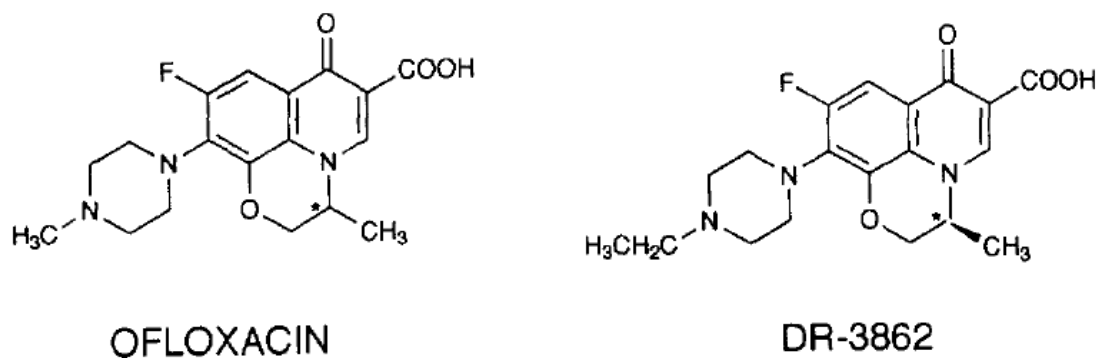


Fig. 25 Chemical structure of quinolone bactericidal reagents Ofloxacin and DR-3862.

A modification of proteins as buffer additives is to have a protein pseudo-stationary phase. A solution of the run buffer and protein is injected onto the capillary to a point close to, but not beyond, the detection window. The pH is adjusted such that when the voltage is applied the protein remains stationary or migrates towards the anode, that is away from the detector at the cathode. The advantage is the increased sensitivity as the high UV adsorbing proteins do not pass the detection window to interfere with the detection of analytes. While this is clearly an advantage, it introduces an extra element of complexity in that the pH must be optimal for both enantioselectivity and for keeping the protein band in position. Such “partial filling” strategies were pioneered by Tanaka and Terabe [Tanaka 1995, Tanaka 1997, Muijselaar 1998, Tanaka 1998 & Tanaka 2000] who used this type of system to concentrate up analyte bands as well as to allow higher concentrations of selector.

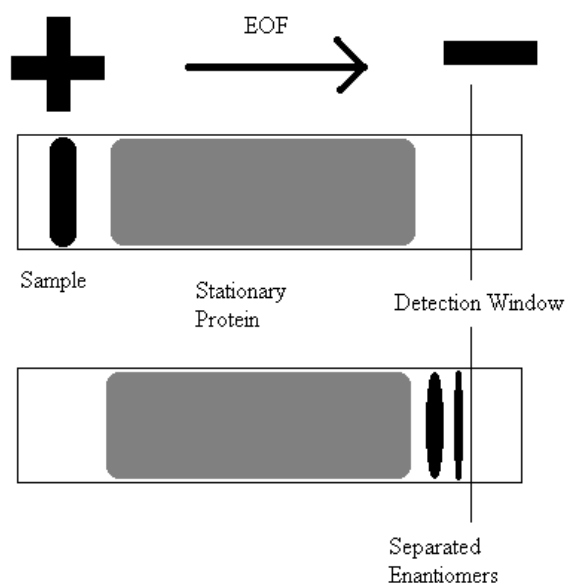


Fig. 26 A representation of protein pseudo-stationary phases with the capillary almost “complete filled” with protein; also a higher protein concentration may be used in a narrower band.

This method was successfully applied by Fanali [Fanali 1995] to separate derivatised tryptophan enantiomers using iron-free human transferrin. Tanaka [Tanaka 1995]

also applied the same technique to separate enantiomers with four different proteins, BSA, ovomucoid,  $\alpha_1$ -AGP and conalbumin.

Ishihama [Ishihama 1994] studied ovomucoid with effects of changing the experimental variables of concentration of the run buffer, uncoated and coated capillaries, concentration of the chiral selector and organic modifiers. Successful separations occurred in the pH range of 4, but the peaks were severely tailed and it was suggested that the protein was binding to the capillary wall. Reproducibility was improved with coated capillaries as the binding of protein to the capillary wall was reduced. With increasing protein concentration the resolution was enhanced and the apparent mobilities of the enantiomers were decreased. The enhanced resolution can be explained by equation 21. With increasing concentration of protein there was enhanced resolution. However, the amount of chiral selector added was not sufficient to give the maximum resolution or to give a decrease in resolution. The addition of organic modifiers improved the peak shape but there was a decrease on the separation factor.

Another application used to prevent proteins passing through the detection window was to use an immobilised protein (on spherical silica microparticles) chiral stationary phase in protein capillary electrochromatography (CEC). Lloyd *et al* [Lloyd 1995] immobilised HSA onto 7  $\mu\text{m}$  silica and then compared the HSA stationary phase with HSA in free solution. A number of enantiomers were separated with both techniques. Organic modifiers were added to both systems and it was observed that the greatest enantioselectivity was shown by 2-propanol and acetonitrile compared to 1-propanol. As there was a similarity between the electrically driven system of protein CEC and the pressure driven system of HPLC it was suggested that the electric field had a negligible effect on the immobilised protein. The separation efficiencies in protein CEC were found to be similar to protein chiral stationary phases (CSPs) used in HPLC. However, they were found to

be poor when compared to  $\beta$ -cyclodextrins and other chiral selectors used in free solution CE. While CEC seemed like an attractive technique in principle at the time, especially with analysts raised with a thorough understanding of packed beds as used in HPLC, it has since fallen out of favour because of some of the practical difficulties involved (frit preparation, organic solvents dissolving polyimide coating at the ends of the capillary, inconsistent chromatography of basic compounds, L Frame, PhD, University of Sunderland).

#### **1.4.5 The measurement of drug-protein binding constants by chromatographic techniques**

As noted earlier, blood plasma proteins play a significant role in the transport and release of drugs around the body [Peters 1977]. As such, many studies have been undertaken to ascertain drug-protein binding and the affects of competing ligands on drug-protein binding. Such studies now play a very important part in screening strategies for pre-Development drug candidates and in safety studies with respect to co-administration with highly bound drugs and chromatographic techniques offer a practical way of obtaining such very important data in a very rapid, efficient and accurate manner.

##### **1.4.5.1 Drug-protein binding studies using high-performance liquid chromatography (HPLC)**

Ashton *et al* [Ashton 1996] used HPLC to study the binding of indolocarbazole derivatives, which show anti-viral properties, to immobilised human serum albumin (HSA). They calculated the percentage of drug-protein binding from the retention times of the analytes when injected onto an immobilised HSA column. They found that all of the analytes were strongly bound to HSA and required a mobile phase containing 30% 2-propanol to obtain reasonable retention times. HPLC was also

used by Thaud *et al* [Thaud 1983] to study diazepam-HSA binding. The first HPLC method they used was the Hummel-Dreyer method [Thaud 1983] which required several eluents to cover a range of diazepam concentrations from 0.3  $\mu\text{M}$  to 100  $\mu\text{M}$ . The second method they described was the equilibrium saturation method. Like the previous method this required a combination of eluents to include mixtures of 0.4 and 2.0  $\text{g l}^{-1}$  HSA with 10  $\mu\text{M}$  to 100  $\mu\text{M}$  diazepam. A volume of buffer was injected and the resulting negative peak corresponded to the free-drug concentration of the mixture studied. They found that lower molar binding ratios could be determined with the Hummel-Dreyer method than the equilibrium saturation method.

The technique of high performance frontal analysis has proved successful for the determination of binding constants of warfarin to HSA [Shibukawa 1996 & He 1997]. The technique utilises columns which have stationary phases of small pore sizes. These columns effectively restrict large protein molecules to the mobile phase. When a drug-protein mixture is injected onto the column, the drug concentration in the pore becomes equal to the unbound drug concentration in the sample solution. The authors stated that the protein eluted first followed by the drug which was characterised by a trapezoidal peak having a plateau region, Fig. 27. The unbound drug concentration could then be determined by measuring the drug concentration in the plateau region.

This method offers some advantages over conventional chromatography such as it allows a direct sample injection analysis using a simple procedure and the protein does not form a constituent part of the mobile phase.

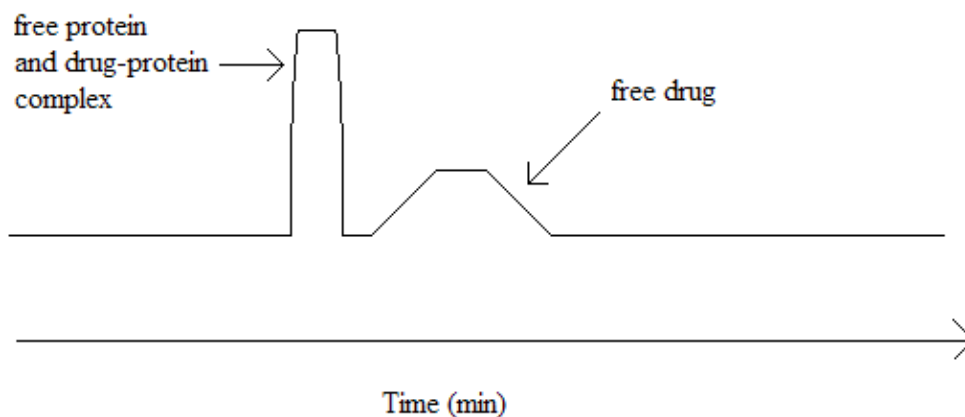


Fig. 27. Stylised chromatogram depicting high-performance frontal analysis chromatography. The protein and protein-drug complex is eluted ahead of the free drug.

#### 1.4.5.2 Drug-protein binding studies using capillary electrophoresis

In the early to mid-1990s, Capillary Electrophoresis was also being employed to measure drug-protein binding. Kraak [Kraak 1992] and Busch [Busch 1997] have compared different methods in order to study drug-protein binding in CE.

The Hummel-Dreyer method utilises a run buffer containing the drug to be studied. An array of samples are then injected. The samples contain a fixed concentration of protein and variable concentrations of the drug. By comparing the peaks of the drug the binding constant of the drug to the protein can be calculated.

The affinity capillary electrophoresis method uses the same procedure as the Hummel-Dreyer method. However, the binding constants are calculated in a different manner. Instead of comparing the peaks of the drug in the Hummel-Dreyer method the binding constants are calculated from the electrophoretic mobility of the protein when injected with the different concentrations of drug.



Rather than using only the drug as the buffer additive the vacancy peak method uses both the protein and drug as the buffer additives. A series of buffers are prepared with one of the additive concentrations being varied while the other buffer additive remains fixed. The capillary is filled with the run buffer. The sample in this method is run buffer without any drug or protein additives. A small amount of the sample is injected. The corresponding electropherogram, Fig. 28, will show two negative peaks. The second negative peak will be directly proportional to the free drug.

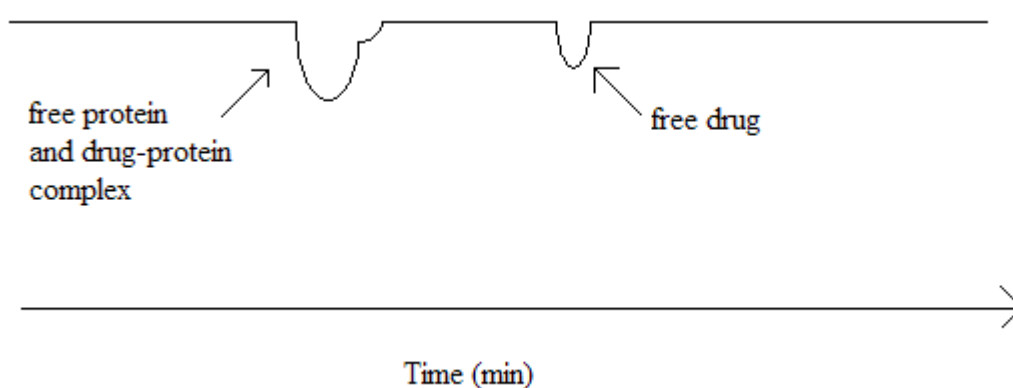


Fig. 28 Stylised electropherogram showing the vacancy peak method. In this example the peaks are negative since the buffer contains the UV absorbing drug and protein and the sample is run buffer without any additives.

Frontal analysis capillary electrophoresis uses analogous methodology as described for high performance frontal analysis in HPLC. In this method the capillary is filled with plain buffer, i.e. the buffer does not contain any protein or analytes of interest. The sample comprises of the protein, free-drug and protein-drug complex. After the sample has been injected an electropherogram will be produced which will have two visible plateaus, providing that the mobility of the free-drug differs significantly from the protein-drug complex. The first plateau region will be the protein and protein-drug complex. The second plateau region will be the free drug. A representation of

the electropherogram is shown in Fig. 29. The free drug concentration can then be calculated by comparison to an injection of a sample of the drug substance.

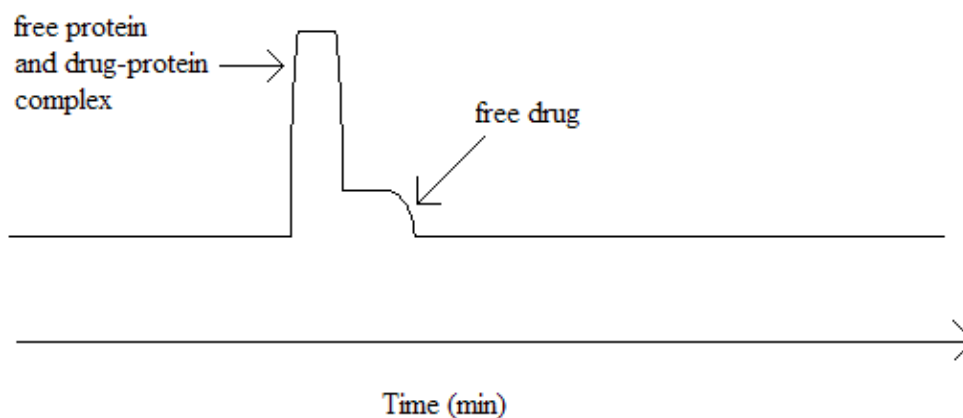


Fig. 29 Stylised electropherogram depicting frontal analysis capillary electrophoresis. The protein and protein-drug complex is eluted ahead of the free drug.

The vacancy affinity capillary electrophoresis method. This method uses the same procedure as described in the vacancy peak method. That is, the capillary is filled with both protein and drug, the concentration of one compound remains fixed while the other is varied, an injection of plain run buffer is then injected. This method uses the shift in migration time of the negative peaks as a measure of drug-protein binding.

### 1.5 Aims and Objectives

Given that, at the outset of this research programme, the use of biomacromolecules as chiral selectors in LC and CE had been restricted to common easily accessible biomacromolecules such as plasma-binding proteins. It was clear that it would be useful therefore to adapt LC and CE in such a way as would allow the use of a much wider range of biomacromolecules. Accordingly the general aim of this study was to

develop LC and CE protocols involving biomacromolecules that would give rise to minimum consumption of the biomacromolecule.

The strategy was to fulfil this general aim by addressing some specific objectives which in the main, for CE, involved optimising conditions to allow screening of biomacromolecules as potential chiral selectors, and, for LC, involved attempting to prove the concept that chiral resolutions could be achieved on down-sized systems. For both LC and CE, a secondary consideration was to bear in mind the likely suitability of the systems being developed as vehicles for the *in vitro* evaluation of drug-biomacromolecule binding.

## **Chapter 2 Experimental**

### **2.1 Equipment for capillary electrophoresis**

Two capillary electrophoresis instruments were employed during this study. They were the CES I from Dionex (UK) Ltd. (Camberley, Surrey, UK) and the PACE 2050 from Beckman Instruments Ltd. (Fullerton, CA, USA). The capillaries of 50  $\mu\text{m}$  i.d. (363  $\mu\text{m}$  o.d.) were CElect P150 from Supelco, (Poole, Dorset, UK) and were cut to appropriate lengths.

### **2.2 Equipment for liquid chromatography**

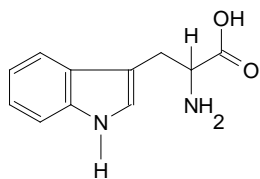
The HPLC system consisted of a Shimadzu LC-10AD pump from Dyson Instruments Ltd. (Hetton-le-Hole, UK), a Rheodyne 7520 microsample injector with 0.5  $\mu\text{l}$  sample rotor from Supelco (Poole, UK), a Valco 0.5  $\mu\text{l}$  4 port injector from LC-Packings (Amsterdam, Holland) and a model 200 detector from Linear Instruments (Freemont, CA, USA) with a UZ-LI-Mic flow cell from LC-Packings (Amsterdam, Holland). The detector was connected to a Shimadzu C-R5A Chromatopac integrator from Dyson Instruments Ltd. (Hetton-le-Hole, UK).

The pH of the mobile phase buffers was adjusted using a model HI8417 Microprocessor pH meter supplied by Hanna Instruments (Leighton Buzzard, UK). The packing materials were (1) Lichrosorb DIOL (5  $\mu\text{m}$ , 60  $\text{\AA}$ ) and (2) Lichrosorb Diol (5  $\mu\text{m}$ , 300  $\text{\AA}$ ) supplied by Merck (Darmstadt, Germany) and (3) Nucleosil C<sub>8</sub> (5  $\mu\text{m}$ , 300  $\text{\AA}$ ) and (4) Nucleosil silica (5  $\mu\text{m}$ , 300  $\text{\AA}$ ) from Macherey Nagel (Duerren, Germany).

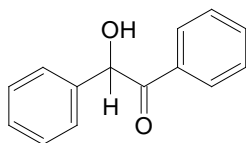
### 2.3 Materials

Acetonitrile, tetrahydrofuran, methanol and propan-1-ol were of HPLC grade and were obtained from BDH (Lutterworth, Leics., UK). BDH were also the suppliers of orthophosphoric acid, disodium hydrogen phosphate and disodium tetraborate. Aldrich (Gillingham, Dorset, UK) was the source of digitoxin, N,N-dimethyloctylamine, DL- $\beta$ -indolelactic acid, tyrosine, DL-3-( $\alpha$ -acetyly-4-chlorobenzyl)-4-hydroxycoumarin, and octanoic acid. Bovine serum albumin (BSA), kynurenine, tryptophan amide, suprofen, carprofen, protamine, nicardipine, lormetazepam, bepridil, 2-(4-chlorophenoxy)propionic acid, 2-(3-chlorophenoxy)propionic acid, 2-(2-chlorophenoxy)propionic acid and warfarin were purchased from Sigma (Poole, Dorset, UK). May & Baker Ltd. (Dagenham, London, UK) were the suppliers of promethazine, pentobarbitone, hexobarbitone and quinalbarbitone. Fluka (Gillingham, Dorset, UK) supplied 4-chloro-DL-mandelic acid, 4-hydroxy-3-methoxymandelic acid and 3-hydroxymandelic acid. Leucovorin was from Acros (Hyde, Cheshire, UK), DL-4-hydroxymandelic acid from Lancaster Synthesis (Morecambe, UK), bupivocaine from Duncan Flockhart & Co. Ltd. (London, UK), thioridazine from Sandoz Products Ltd. (Horsforth, Leeds, UK) and naproxen from Secifarma (Milan, Italy). Lorazepam, oxazepam and temazepam were from Wyeth Laboratories (Maidenhead, Berkshire, UK). The three  $\alpha$ -aryl alkanolic acids, 2-(4-methoxyphenyl) propionic acid, 2-(4-methylphenyl) propionic acid and 2-(4-phenyl-3-fluorophenyl) propionic acid were gifts from Dr. Wang (University of Sunderland). Recombinant lactoferrin was a gift from Dr. David Small (Zeneca Biological). All deionised water was obtained from an Elgastat UHQPS system supplied by Elga Water Systems Equipment (High Wycombe, UK). All solutions were filtered through 0.2  $\mu$ m HV filters from Millipore (Bedford, MA, USA) and degassed by sonication for 15 min using a model V300H ultrasonic bath supplied by Ultrawave Limited (Cardiff, UK).

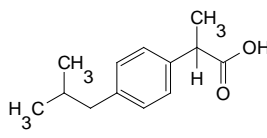
### 2.3.1 Chemical structures of the analytes



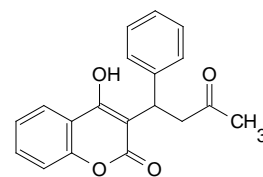
Tryptophan



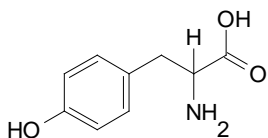
Benzoin



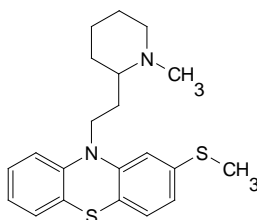
Ibuprofen



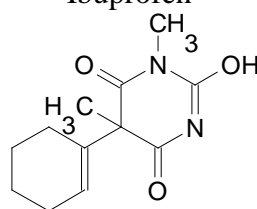
Warfarin



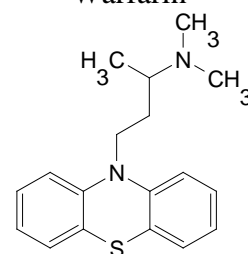
Tyrosine



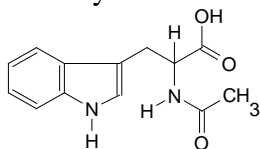
Thioridazine



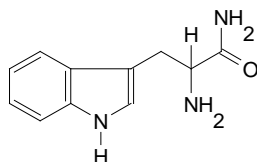
Hexobarbital



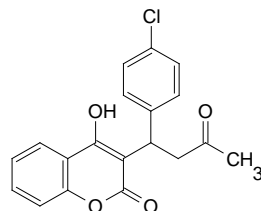
Promethazine



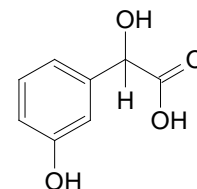
N-acetyl-DL-tryptophan



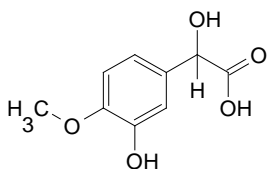
Tryptophanamide



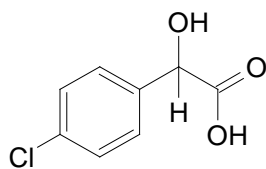
DL-3-( $\alpha$ -acetyl-4-chlorobenzyl)-4-hydroxycoumarin



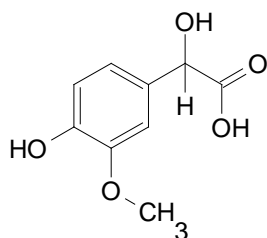
3-hydroxymandelic acid



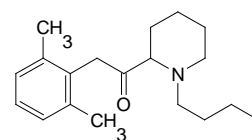
3-hydroxy-4-methoxymandelic acid



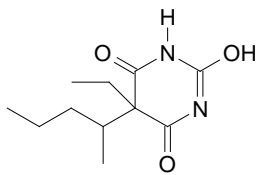
4-chloromandelic acid



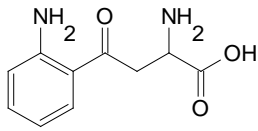
4-hydroxy-3-methoxymandelic acid



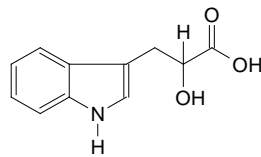
Bupivacaine



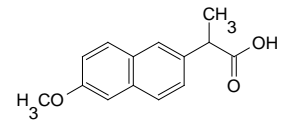
Pentobarbitone



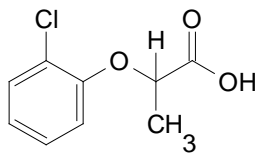
Kynurenine



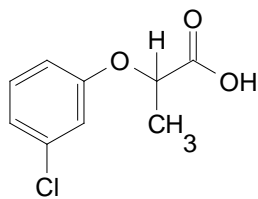
DL-indole lactic  
acid



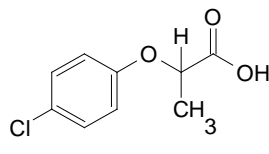
Naproxen



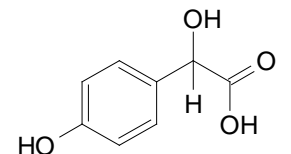
2-(2-chlorophenoxy)  
propionic acid



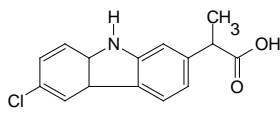
2-(3-chlorophenoxy)  
propionic acid



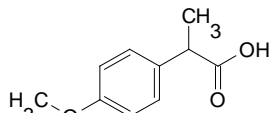
2-(4-chlorophenoxy)  
propionic acid



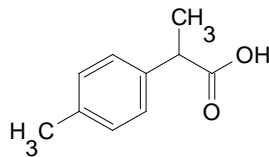
4-hydroxymandelic  
acid



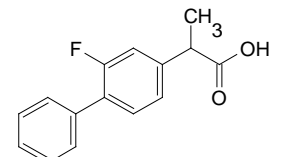
Carprofen



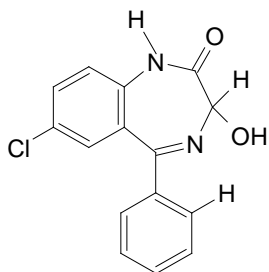
2-(4-  
methoxyphenyl)  
propionic acid



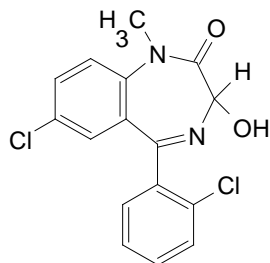
2-(4-methylphenyl)  
propionic acid



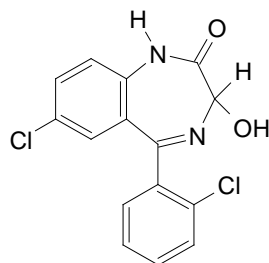
2-(4-hydroxy-3-  
fluorophenyl)  
propionic acid



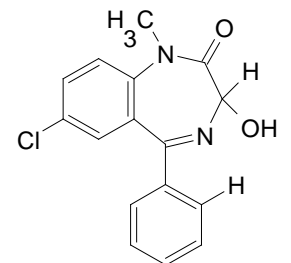
Oxazepam



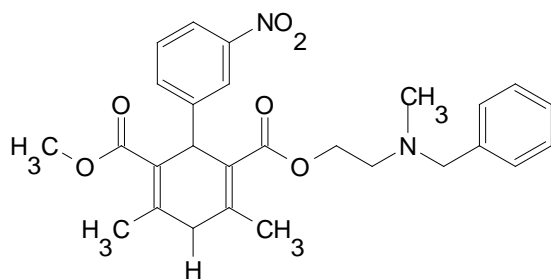
Lormetazepam



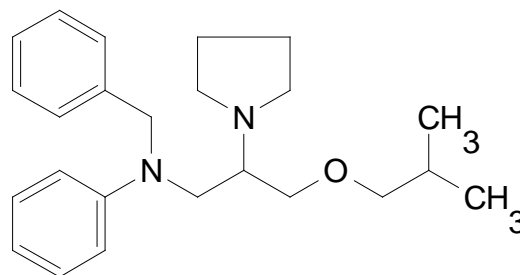
Lorazepam



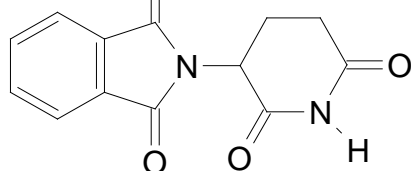
Temazepam



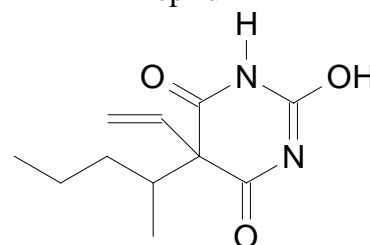
Nicardipine



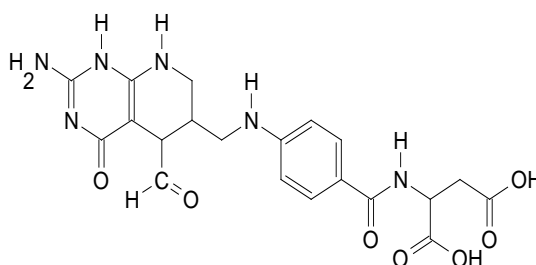
Bepridil



Thalidomide



Quinalbarbitone



Leucovorin

## 2.4 Experimental for capillary electrophoresis

### 2.4.1 Capillary electrophoresis instrument set-up

#### 2.4.1.1 Dionex CES I

The Dionex CES I required three wash solutions in order to condition the capillary prior to analysis. The solutions were located in three 250 ml Duran flasks towards the back of the instrument. The three wash solutions were 0.05 M sodium hydroxide,



water and run buffer. The run buffer was 67 mM disodium hydrogen phosphate adjusted to pH 7.4 by orthophosphoric acid and sodium hydroxide as described in the literature [Kraak 1992]. All solutions were filtered and sonicated prior to use to minimise the possibility of any particulate matter blocking the capillary. There was no adequate method of controlling the capillary temperature.

Samples were dissolved in run buffer and were placed in small 0.8 ml plastic vials. The vials were then lightly tapped to remove any air bubbles. The vials were then placed in the CES I carousel. The analysis schedule was programmed via the keypad on the CES I. The parameters that were set-up included capillary rinse times, voltage, injection mode (hydrodynamic pressure, gravity and electrokinetic), injection time and the run time for each analysis. Before the start of each analysis the interlocked guard had to be put in place. This was a safety feature to protect the user against the high voltages used in capillary electrophoresis. All the data was collected and analysed using the Dionex AI-450 software.

#### **2.4.1.2 Beckman PACE 2050**

The wash solutions and buffers were prepared as previously described. All samples, wash solutions and run buffers were placed in specific 3.5 ml glass vials. The vials were then covered with a rubber stopper. The vials were placed into two carousels on the PACE 2050. The outer carousel contained all the samples, wash solutions and run buffers while the inner carousel contained the run buffer and the waste vials. Unlike the Dionex CES I, the capillaries used with the Beckman PACE 2050 were housed in a cartridge. Coolant could then be circulated within the cartridge and control the capillary temperature. The operation and control was via a PC operating Beckman System Gold software. The software was also used to collect and analyse the data.

## **2.4.2 Investigation of the experimental variables**

### **2.4.2.1 Concentration of bovine serum albumin (BSA)**

The wash solutions and the disodium hydrogen phosphate buffer adjusted to pH 7.4 were prepared as described previously. BSA was dissolved in the run buffer to give concentrations of 0, 15, 30, 45 and 60  $\mu\text{M}$  BSA. The test compound was tryptophan dissolved in the BSA-run buffers. The capillary was conditioned with 0.05 M sodium hydroxide for 3 minutes, water for 3 minutes and run buffer for 3 minutes. A blank run was performed from the vial containing the BSA-run buffer for 20 minutes. The samples were injected by applying hydrodynamic pressure (0.5 psi) for 2 s. The separation voltage was 10 kV at ambient temperature using the Dionex CES I.

### **2.4.2.2 The effect of pH of the run buffer**

The wash solutions and the disodium hydrogen phosphate buffers adjusted to pH 4.4, 5.4, 6.4, 7.4 and 8.4 were prepared as described previously. BSA was dissolved in each of the run buffers at a concentration of 30  $\mu\text{M}$ . The test compound was tryptophan dissolved in the BSA-run buffers. The capillary was conditioned with 0.05 M sodium hydroxide for 3 minutes, water for 3 minutes and run buffer for 3 minutes. A blank run was performed from the vial containing the BSA-run buffer for 25 minutes. The samples were injected by applying hydrodynamic pressure (0.5 psi) for 2 s. The separation voltage was 10 kV at ambient temperature using the Dionex CES I.

#### **2.4.2.3 Investigation of increasing the concentration of organic solvents to the run buffer**

The run buffer consisted of 67 mM disodium hydrogen phosphate adjusted to pH 7.4 using orthophosphoric acid, 30  $\mu$ M BSA, 0 – 20 %v/v organic solvent. The four organic solvents used for this study were methanol, propan-1-ol, tetrahydrofuran and acetonitrile. All solutions were filtered and sonicated as before. The separation voltage using the CES I was 10 kV at ambient temperature. The capillary was conditioned with 0.05 M sodium hydroxide for 3 minutes, water for 3 minutes and run buffer for 3 minutes. A blank run was performed from the vial containing the BSA-run buffer for 25 minutes. The samples were tryptophan and benzoin at a concentration of 1 mg ml<sup>-1</sup>. The samples were injected as solutions in the run buffer by applying hydrodynamic pressure (0.5 psi) for 2 s. The samples were monitored by UV at 254 for benzoin and 280 nm for tryptophan. Migration and peak areas were measured using the Dionex AI-450 software. Each sample was run in duplicate.

The separations using the PACE 2050 were as the CES I except the temperature was constant at 25 °C, the separation voltage was 8 kV and samples were injected by hydrodynamic pressure (0.5 psi) for 2 s. Migration times and peak areas were measured using the Beckman System Gold software.

#### **2.4.3 Enantioselectivity using a BSA coated capillary**

The BSA coated capillary was kindly supplied by H.Burt from the University of Leeds. The dimensions of the capillary were 50 cm  $\times$  75  $\mu$ m. To maintain the polyamide-BSA coating the capillary was rinsed with distilled water and run buffer only.

The run buffer was 67 mM disodium hydrogen phosphate adjusted to pH 7.4 using orthophosphoric acid. The sample was tryptophan at a concentration of 1 mg ml<sup>-1</sup> dissolved in run buffer. The sample was injected by applying hydrodynamic pressure (0.5 psi) for 2 s.

The PACE 2050 was used throughout this study. The separation voltage was 7 kV and the temperature was maintained at 25°C. Migration times and peak areas were measured using the Beckman System Gold software.

#### **2.4.4 Enantioselectivity of a range of compounds using BSA as the chiral selector and standard conditions**

The run buffer consisted of 67 mM disodium hydrogen phosphate adjusted to pH 7.4 using orthophosphoric acid, 30 µM BSA and 2.5 %v/v organic solvent. A range of analytes were dissolved in the run buffer at a concentration of 1 mg ml<sup>-1</sup> and injected by hydrodynamic pressure (0.5 psi) for 2 s. The capillary was conditioned with 0.05 M sodium hydroxide for 3 minutes, water for 3 minutes and run buffer for 3 minutes. The final step was a 1 minute high pressure rinse of the protein-run buffer.

The PACE 2050 was used throughout this study. The separation voltage was 8 kV and the temperature was maintained at 25°C. Migration times and peak areas were measured using the Beckman System Gold software.

#### **2.4.5 Enantioselectivity of a range of compounds using standard conditions to screen other biomacromolecules**

The wash solutions of 0.05 M sodium hydroxide, water and 67 mM disodium hydrogen phosphate buffer adjusted to pH 7.4 were prepared as described previously. The run buffers were prepared by adding the test biomacromolecule to the 67 mM

disodium hydrogen phosphate, pH 7.4, with 2.5% v/v methanol. The biomacromolecules screened were human serum albumin (HSA), protamine and recombinant lactoferrin. The concentration used for the biomacromolecules was 2 mg ml<sup>-1</sup>.

A range of analytes were dissolved in the run buffer at a concentrations of 1 mg ml<sup>-1</sup> and injected by hydrodynamic pressure (0.5 psi) for 2 s. The capillary was conditioned with 0.05 M sodium hydroxide for 3 minutes, water for 3 minutes and run buffer for 3 minutes. The final step was a 1 minute high pressure rinse of the protein-run buffer.

The PACE 2050 was used throughout this study. The separation voltage was 8 kV and the temperature was maintained at 25°C. Migration times and peak areas were measured using the Beckman System Gold software.

#### **2.4.6 Investigation of enantioselectivity by adding modifiers to the run buffer**

##### **2.4.6.1 $\beta$ -Cyclodextrin**

The wash solutions of 0.05 M sodium hydroxide, water and 67 mM disodium hydrogen phosphate buffer adjusted to pH 7.4 were prepared as described previously. The run buffers were made up as follows, 67 mM disodium hydrogen phosphate, pH 7.4, 30  $\mu$ M HSA and  $\beta$ -cyclodextrin. The amounts of  $\beta$ -cyclodextrin added to the run buffers were 6, 12, 18, 24 and 30  $\mu$ M. Samples were dissolved in the run buffer at a concentration of 0.5 mg ml<sup>-1</sup> and injected by hydrodynamic pressure (0.5 psi) for 2 s. The capillary was conditioned with 0.05 M sodium hydroxide for 3 minutes, water for 3 minutes and run buffer for 3 minutes. The final step was a 1 minute high pressure rinse of the protein/ $\beta$ -cyclodextrin-run buffer.

The PACE 2050 was used throughout this study. The separation voltage was 8 kV and the temperature was maintained at 25°C. Migration times and peak areas were measured using the Beckman System Gold software.

#### **2.4.6.2 Allosteric interactions**

The wash solutions of 0.05 M sodium hydroxide, water and 67 mM disodium hydrogen phosphate buffer adjusted to pH 7.4 were prepared as described previously. The run buffers were made up as follows, 67 mM phosphate, pH 7.4, 30 µM HSA and 3 µM modifier. The concentration of the modifiers were 3 µM so the ratio between HSA and modifier was 10 : 1. The modifiers were digitoxin, ibuprofen, warfarin, and lorazepam. Samples were dissolved in the run buffer at a concentration of 0.5 mg ml<sup>-1</sup> and injected by hydrodynamic pressure (0.5 psi) for 2 s. The capillary was conditioned with 0.05 M sodium hydroxide for 3 minutes, water for 3 minutes and run buffer for 3 minutes. The final step was a 1 minute high pressure rinse of the protein/modifier-run buffer.

The PACE 2050 was used throughout this study. The separation voltage was 8 kV and the temperature was maintained at 25°C. Migration times and peak areas were measured using the Beckman System Gold software.

#### **2.4.6.3 Metal salts**

The wash solutions of 0.05 M sodium hydroxide, water and 67 mM sodium borate adjusted to pH 7.4 were prepared as described previously. All the metal salts were insoluble in 67 mM disodium hydrogen phosphate buffer so the run buffer was changed to 67 mM sodium borate. The run buffers were made up as follows, 67 mM sodium borate, pH 7.4, 30 µM HSA and metal salt. The ratios of the metal salt to the protein were 1 : 1, 2 : 1 and 3 : 1. The metal salts were manganese phosphate, zinc

sulphate, manganese carbonate and nickel phosphate. Samples were dissolved in the run buffer at a concentration of 0.5 mg ml<sup>-1</sup> and injected by hydrodynamic pressure (0.5 psi) for 2 s. The capillary was conditioned with 0.05 M sodium hydroxide for 3 minutes, water for 3 minutes and run buffer for 3 minutes. The final step was a 1 minute high pressure rinse of the protein/modifier-run buffer.

The PACE 2050 was used throughout this study. The separation voltage was 8 kV and the temperature was maintained at 25°C. Migration times and peak areas were measured using the Beckman System Gold software.

## **2.5 Experimental for liquid chromatography**

### **2.5.1 BSA as a mobile phase additive in microbore LC**

Mobile phase buffers were made up by first preparing a stock solution of 67 mM disodium hydrogen phosphate which was adjusted to pH 7.4 using orthophosphoric acid. The 30 µM and 60 µM BSA mobile phases were prepared by dissolving 100 mg and 200 mg BSA in 100ml of 67 mM disodium hydrogen phosphate, pH 7.4. Test analytes were dissolved in mobile phase. All solutions were filtered and sonicated prior to use.

The column used for this study was 15 cm x 1 mm i.d. with a stationary phase of Lichrosorb DIOL with a 5 µm particle diameter and 60 pore size. Several steps were undertaken to condition the column prior to analysis. The column was supplied with a mobile phase of 50:50 acetonitrile – water and was flushed with propan-2-ol, water and 67 mM disodium hydrogen phosphate, pH 7.4, prior to the introduction of the BSA containing mobile phase. Analysis was undertaken after the BSA containing mobile phase had been detected. This was observed as an increase in absorbance followed by an absorbance plateau.

### 2.5.2 BSA as a mobile phase additive in capillary LC

Mobile phase buffers were made up by first preparing a stock solution of 67 mM disodium hydrogen phosphate which was adjusted to pH 7.4 using orthophosphoric acid. The 60  $\mu\text{M}$  BSA mobile phases were prepared by dissolving 200 mg BSA in 100ml of 67 mM disodium hydrogen phosphate, pH 7.4. Test analytes were dissolved in mobile phase. All solutions were filtered and sonicated prior to use.

The column used for this study was 15 cm x 320  $\mu\text{m}$  i.d. with a stationary phase of Lichrosorb DIOL with a 5  $\mu\text{m}$  particle diameter and 60 pore size. Several steps were undertaken to condition the column prior to analysis. The column was supplied with a mobile phase of 50:50 acetonitrile – water and was flushed with propan-2-ol, water and 67 mM disodium hydrogen phosphate, pH 7.4, prior to the introduction of the BSA containing mobile phase. The flow rate was set at 3  $\mu\text{l min}^{-1}$ .

### 2.5.3 Adsorption of BSA

Adsorption of BSA was carried out according to the method of Erlandsson *et al* [Erlandsson 1986]. Mobile phase buffers were 67 mM disodium hydrogen phosphate adjusted to pH 5.0 and 7.4 by orthophosphoric acid. The BSA containing mobile phase was 15  $\mu\text{M}$  BSA dissolved in 67 mM disodium hydrogen phosphate pH 5.0. The test analytes were tryptophan and kynurenine. The test analytes were dissolved in 67 mM disodium hydrogen phosphate pH 7.4. All solutions were filtered and sonicated prior to use.

The columns used in this study were 15 cm x 1 mm i.d. The three stationary phases were Lichrosorb DIOL, Nucleosil silica and Nucleosil C<sub>8</sub>. All three stationary phases were of 5  $\mu\text{m}$  diameter and pore size of 300 Å.



### **2.5.3.1 Preparation of the pseudo-stationary phase**

The columns were equilibrated with propan-2-ol for 2 h, then equilibrated with water for 2 h and finally equilibrated with 67 mM disodium hydrogen phosphate, pH 5.0, for 2 h. A mobile phase of 15  $\mu\text{M}$  BSA and 67 mM disodium hydrogen phosphate, pH 5.0, was pumped through the columns at a flow rate of  $50 \mu\text{l min}^{-1}$  until BSA was detected at 280 nm. At this stage the pseudo-stationary phase was deemed to have formed. The columns were then equilibrated with 67 mM phosphate, pH 7.4, until a stable baseline was obtained. The test analytes were then injected.

## **Chapter 3    Optimisation of experimental variables using BSA in free-solution CE**

### **3.1    Introduction**

To make the most of protein affinity CE as a means of resolving enantiomers it would clearly be necessary to have a good understanding of the effect of experimental variables on enantioselectivity and migration times so that they could best be manipulated to get the optimum performance out of each protein that might be used. The optimum conditions would be expected to vary from protein to protein but at the same time it was thought that it might be useful to attempt to arrive at a set of standard conditions, employing as little as possible protein since some might be in short supply, that could be used to screen a range of proteins. These standard conditions would probably be non-optimal for most proteins but the reasoning was that if any given protein was going to be very useful as a broad spectrum chiral selector, then it would hopefully show good enantioselectivity even under non-optimal conditions. The general aim then of this initial study was to explore the effect of experimental variables on protein affinity CE using bovine serum albumin (BSA) a protein the properties of which were relatively well known. The intention was that the information gained would serve as a useful platform from which to move on to study other proteins.

### **3.2 Variables available for BSA affinity CE**

To use BSA for chiral discrimination as a buffer additive a number of experimental conditions had to be determined. The pH of the buffer would be expected to have a dramatic effect on the electrophoretic mobility of the BSA. Therefore, the pH would have to be adjusted so that the electrophoretic mobility of the BSA and BSA-complex would be significantly different to the electrophoretic mobility of the

uncomplexed analyte, thereby opening up a large enough 'window' in which to obtain the chiral separation of the pair of enantiomers in the analyte.

As a consequence of Equation 21 [Wren 1992] the concentration of BSA would be critical to achieve optimum chiral separations. The aim was to minimise the amount of BSA required for chiral separations. This would be critical for other chiral selectors that were only available in limited quantities or were prohibitively expensive.

$$\mu = \frac{[C](\mu_1 - \mu_2)(K_2 - K_1)}{1 + [C](K_1 + K_2) + K_1 K_2 [C]^2}$$

Equation 21      Difference in electrophoretic mobilities,  $\mu$ , of enantiomers in the presence of a chiral selector.

where

$\mu$	=	difference in electrophoretic mobilities of enantiomers in the presence of a chiral selector
$\mu_1$	=	electrophoretic mobility of the enantiomer
$\mu_2$	=	electrophoretic mobility of the complex
C	=	chiral selector
$K_1$	=	equilibrium constant for enantiomer 1 and the chiral selector
$K_2$	=	equilibrium constant for enantiomer 2 and the chiral selector

There will be an optimum concentration of chiral selector; at high and low concentrations  $\mu$  will tend to zero. Also, the greater the difference between the equilibrium constants  $K_1$  and  $K_2$  will lead to an increase in  $\mu$ .

Another variable that needed to be considered was the nature and amount of organic solvent to be added to the run buffer. Organic solvents denature proteins and alter their overall structure [Peters 1977]. Altering the structure of the protein could improve, or otherwise, the chiral discrimination properties. Another issue was that

many analytes of interest are hydrophobic and are very likely to precipitate in typical aqueous buffer solutions used in CE. Increasing proportion of the organic phase would improve the solubility of hydrophobic analytes and prevent their precipitation. Organic solvents could also influence migration times in other ways such as competing for the analyte and could even affect any loss of protein through any adsorption on the capillary walls that might be taking place. A systematic study of organic modifiers such as methanol, propan-1-ol, acetonitrile and tetrahydrofuran in the concentration range 0 – 20 % v/v on chiral selectivity would therefore need to be undertaken.

From the range of variables that could be altered then, it was decided to focus on the buffer pH, the chiral selector concentration and the concentration of organic solvent. At least initially the objective would be to study these individually changing one variable at a time. From these studies a set of standard conditions would then be employed to test a range of biomacromolecules for chiral discrimination.

### **3.3 Optimisation of pH**

The separation of tryptophan enantiomers by BSA has been characterised by many researchers using different chromatographic techniques. Allenmark *et al* [Allenmark 1982] used tryptophan to study the effects of pH on resolution using BSA in liquid affinity chromatography. Tryptophan was also used to study resolution using BSA adsorbed silica stationary phase by Erlandsson *et al* [Erlandsson 1986]. Recently tryptophan been used to ascertain the applicability of BSA for the separation of enantiomers using capillary affinity gel electrophoresis [Birnbbaum 1992]. Therefore tryptophan was an ideal test compound.

From the range of pH in this study chiral separations were only observed at pH 7.4 and 8.4. There were no chiral separations observed for pH 4.4, 5.4 and 6.4. This was

in agreement with literature results [Barker 1992 & Arai 1994]. The isoelectric point, pI, of BSA is between 4.7 and 4.9 [Tanaka 1995]. Below the pI BSA is positively charged, at around the pI value it is neutral and above the pI it is negatively charged. This is illustrated in Fig. 30.

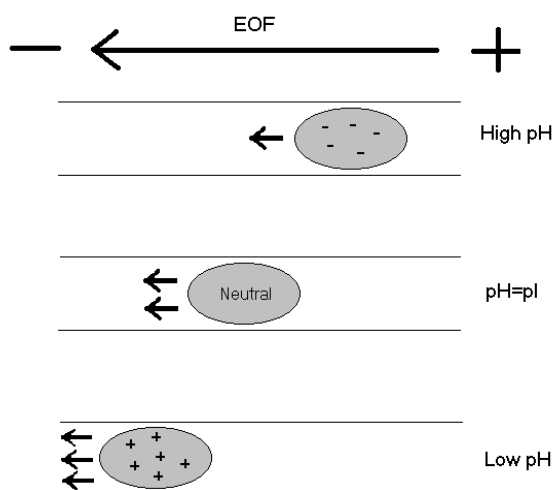


Fig. 30 Representation of the relative migration of BSA at different pH values. The window of separation can be maximised by changing the pH. For example, the window for the separation of cationic drugs would be greatest at a high pH.

### 3.4 Optimisation of the concentration of BSA

The effects of increasing the concentration of BSA on the resolution and the migration times of tryptophan enantiomers are illustrated in Figs. 31 and 32. The minimum concentration of BSA required for a baseline separation of the enantiomers was 30  $\mu\text{M}$ , unfortunately this is difficult to visualise from the corresponding electropherogram, Fig. 33. By further increasing the concentration there was an increase in resolution, Fig 31. There was a loss in peak shape of the second eluting enantiomer as illustrated in Figs 33 and 34 with concentrations of BSA of 30  $\mu\text{M}$  and 60  $\mu\text{M}$ .

There are a number of reasons for the increase in resolution and migration times. As the concentration of the BSA is increased then this will affect the viscosity of the buffer. The electrophoretic mobility of a sample is inversely proportional to the viscosity of the run buffer, equation 18.

$$\bar{\mu} = \frac{\bar{v}}{\bar{E}} = \frac{q}{6\pi\eta r}$$

Equation 18 Electrophoretic mobility

where

$\bar{\mu}$	=	electrophoretic mobility
$\bar{v}$	=	electrophoretic velocity
$\bar{E}$	=	electric field strength
$q$	=	charge of the ion
$\eta$	=	viscosity of the buffer
$r$	=	radius of the molecules.

Another explanation for the increased resolution and migration times is the binding of the sample to the protein. In the case of tryptophan it is known that the L enantiomer [McMenamy 1958] forms highly bound complexes with albumin compared to the D enantiomer. In this experiment the amount of tryptophan injected into the capillary remained constant so as the concentration of BSA increased there would be more BSA available to complex with the L enantiomer. Hence the migration time of the highly bound enantiomer would tend towards the migration time of the BSA, assuming that the contribution to the migration time of tryptophan was negligible compared to BSA when in the complexed form. Another consequence of increasing the concentration of BSA on the highly bound enantiomer was to increase the degree of tailing of the peak.

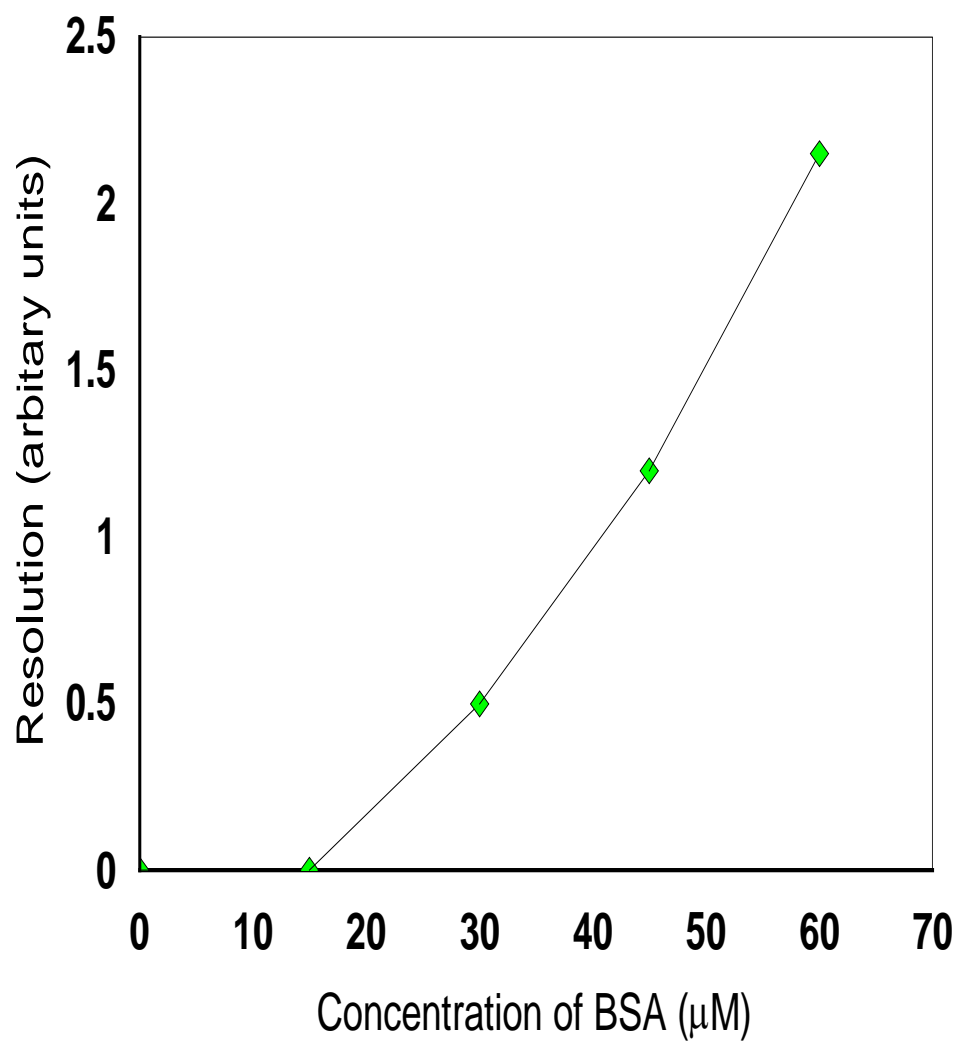


Fig. 31 Resolution of tryptophan enantiomers with increasing concentration of BSA in the run buffer. Conditions: run buffer, 67 mM phosphate (pH 7.4); capillary, CElect P150, 40 cm (35 cm to detector) x 50 μm i.d.; instrument, CES I; temperature, ambient; voltage 10 kV; detection wavelength, 280 nm.

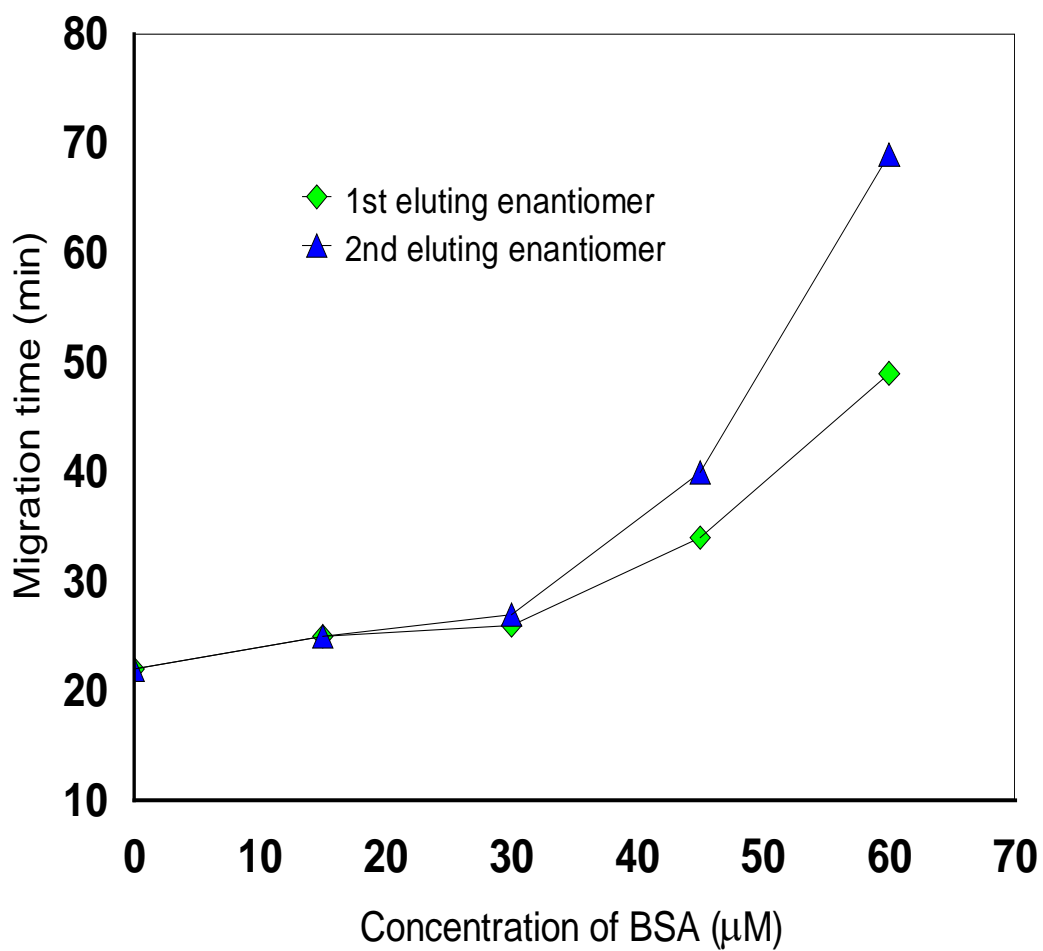


Fig. 32 Migration times of tryptophan enantiomers with increasing concentration of BSA in the run buffer. Conditions: run buffer, 67 mM phosphate (pH 7.4); capillary, CElect P150, 40 cm (35 cm to detector) x 50  $\mu\text{m}$  i.d.; instrument, CES I; temperature, ambient; voltage 10 kV; detection wavelength, 280 nm.



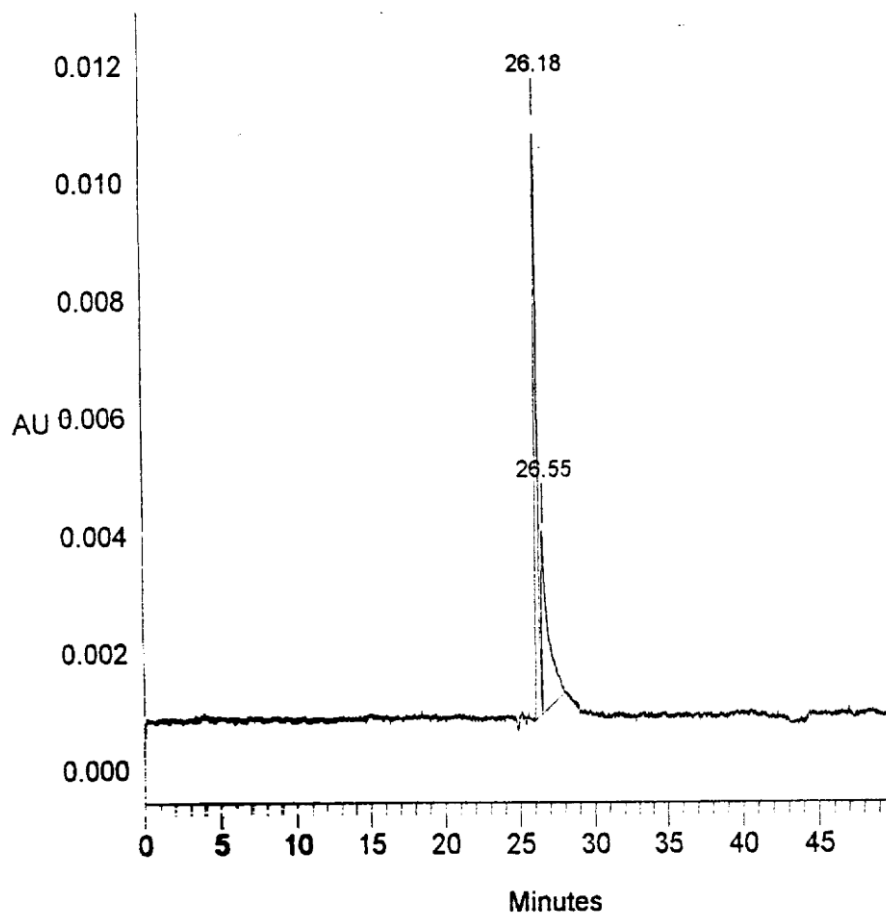


Fig. 33 CE of tryptophan enantiomers with 30  $\mu$ M BSA. Conditions: run buffer, 67 mM phosphate (pH 7.4); capillary, CElect P150, 40 cm (35 cm to detector) x 50  $\mu$ m i.d.; instrument, CES I; temperature, ambient; voltage 10 kV; detection wavelength, 280 nm. Baseline resolution of tryptophan enantiomers, unfortunately this is difficult to visualise from the electropherogram.

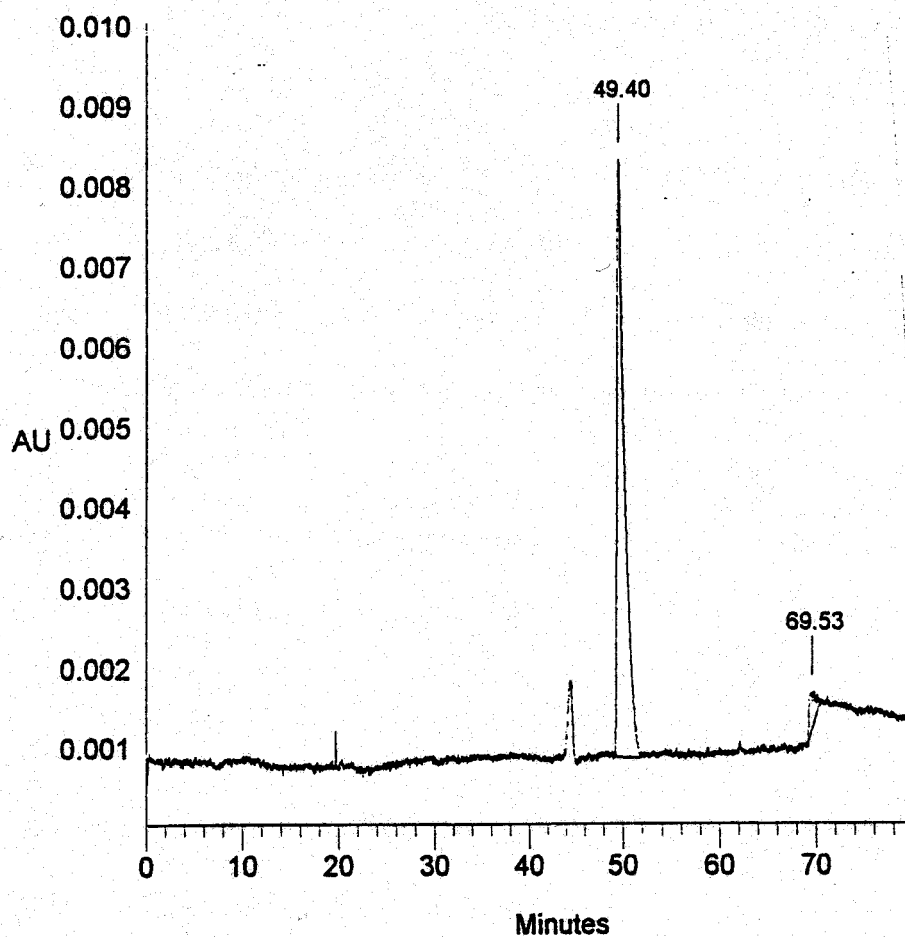


Fig. 34 CE of tryptophan enantiomers with 60  $\mu$ M BSA. Conditions: run buffer, 67 mM phosphate (pH 7.4); capillary, CElect P150, 40 cm (35 cm to detector) x 50  $\mu$ m i.d.; instrument, CES I; temperature, ambient; voltage 10 kV; detection wavelength, 280 nm. Baseline resolution of tryptophan enantiomers. The migration times of the

enantiomers were longer and the tailing of the second peak was increased compared to using a concentration of 30  $\mu$ M BSA.

### **3.5 Addition of organic solvent**

Albumins are resistant to relatively high concentrations of organic solvents and this is used commercially to precipitate albumins with 40 % ethanol [Peters 1977]. Therefore using small amounts of solvents should not denature BSA or decrease the degree of chiral discrimination. The test analytes have been separated using BSA before. Tryptophan and benzoin have been separated using BSA as a chiral selector in CE, Lloyd *et al* [Lloyd 1995].

The resolution of tryptophan and benzoin enantiomers significantly decreased with addition of the organic solvents. The decrease in resolution is illustrated graphically in Fig. 35 and Fig. 36. The decrease in resolution is known from LC, [Krstulovic 1989] where the addition of 1 – 4 % propanol resulted in a decrease in selectivity.

The loss of enantioselectivity can be explained by the organic solvents reducing the hydrophobic interactions between the protein and the analyte. The addition of the organic solvents would distort the structure of protein including the binding sites which would disrupt the three point interaction between the analyte and protein and so decrease the overall selectivity.

The separation of tryptophan enantiomers showed a dramatic loss of resolution at the addition of small amounts of organic solvents, 2.5 % v/v and there was no baseline separation with 5 % v/v organic solvents. The effectiveness of eliminating enantioselectivity of tryptophan is propan-1-ol, tetrahydrofuran, acetonitrile and methanol.

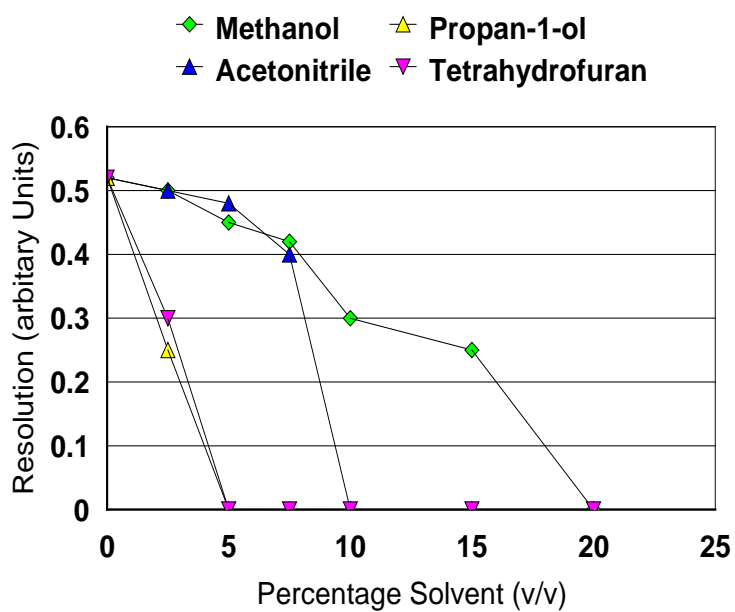


Fig. 35 Resolution of tryptophan enantiomers with increasing organic additives. Conditions: run buffer, 30  $\mu$ M BSA, 67 mM phosphate (pH 7.4) – organic additive (100-x : x, v/v); capillary, CElect P150, 40 cm (35 cm to detector) x 50  $\mu$ m i.d.;

instrument, CES I; temperature, ambient; voltage 10 kV; detection wavelength, 280 nm.

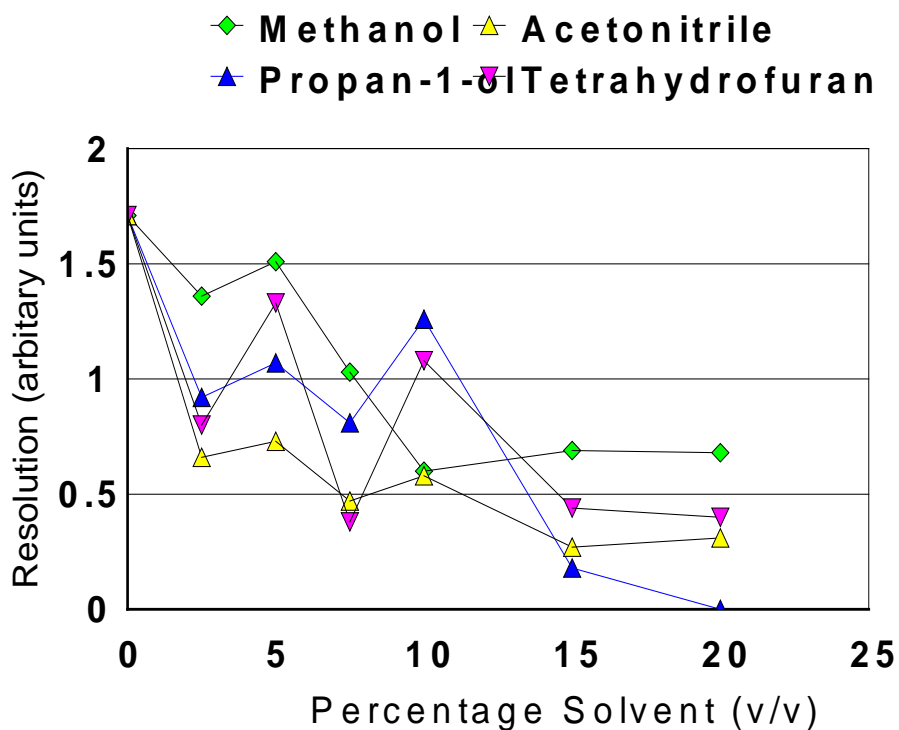


Fig. 36 Resolution of benzoin enantiomers with increasing organic additives. Conditions: run buffer, 30  $\mu$ M BSA, 67 mM phosphate (pH 7.4) – organic additive (100-x : x, v/v); capillary, CElect P150, 40 cm (35 cm to detector) x 50  $\mu$ m i.d.;

instrument, CES I; temperature, ambient; voltage 10 kV; detection wavelength, 254 nm.

The graph for benzoin shows a general decrease in resolution but the observed peaks were relatively small so any errors were magnified hence the results appear erratic. Some chiral selectivity was observed at relatively high concentrations, 15 % v/v, of organic solvent when compared to the tryptophan graph.

Lloyd *et al* [Lloyd 1997] reported similar findings with the addition of organic solvents to a human serum albumin (HSA) containing run buffer. They studied the effects on the enantiomeric separation of benzoin and promethazine enantiomers with methanol, 2-propanol, 1-propanol and acetonitrile. They noted that more organic modifier was required to eliminate enantioselectivity of promethazine compared to benzoin because promethazine had a binding constant to HSA of approximately an order of magnitude greater than benzoin.

### **3.6 Enantioselectivity of a BSA coated capillary**

The main drawback of using proteins as chiral selectors in free solution CE had proved to be the significant adsorption at the detection window which masked the UV absorption of the analytes, Chapter 6. This is illustrated in Fig. 37 where a solution of a typical 30  $\mu\text{M}$  concentration of BSA is flushed through a capillary to give an absorption of 0.12 AU. When the tryptophan enantiomers are injected into the BSA run buffer and the detector re-zeroed the corresponding adsorption of the enantiomer is 0.01, Fig. 32. Therefore the adsorption of the protein is approximately 100 times greater than the adsorbance of tryptophan. To improve the overall sensitivity of the method then the detection window had ideally to remain free of the high UV absorbing protein.

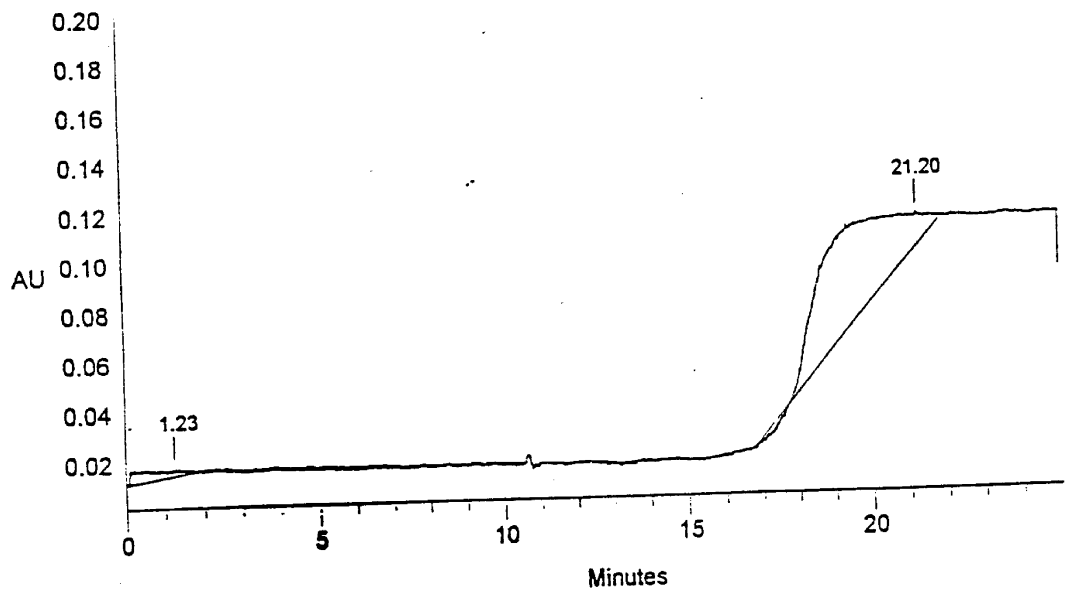


Fig.37. The capillary fill method showing the BSA breakthrough Conditions: run buffer, 30  $\mu$ M BSA, 67 mM phosphate (pH 7.4); capillary, CElect p150, 40 cm (35

cm to detector) x 50  $\mu\text{m}$  i.d.; instrument, CES I; temperature, ambient; voltage 10 kV; detection wavelength, 254 nm.

One approach to circumvent this problem was to immobilise or coat the protein onto the capillary wall. A BSA coated capillary was donated by the University of Leeds for the evaluation of chiral selectivity. The BSA coated capillary would potentially offer two major benefits. The first would be to ensure that the detection window would remain free of the protein while the second was that the method would also significantly decrease the amount of BSA required providing that the amount used to coat the capillary was small and that the coated capillary could be extensively re-used.

The chiral analyte used to test the BSA-coated capillary was tryptophan. This has been resolved using BSA as a buffer additive in CE from earlier studies. Unfortunately, no enantiomer separations were observed, Fig. 38. It was thought that the typical amount of tryptophan injected in free solution CE was overloading the BSA at the capillary wall. Consequently the concentration of tryptophan was decreased such that it was just at the limits of detection where the signal to noise ratio was 5 : 1. However, still no chiral separations were observed for tryptophan using the immobilised BSA capillary. Decreasing the concentration of tryptophan did not change the migration of the tryptophan which proved that sample overload was not the reason for the lack of chiral selectivity of this method.

There are a number of possible reasons why the BSA coated capillary did not resolve the tryptophan enantiomers. As described earlier BSA is a prolate ellipsoid with dimensions of 141  $\text{\AA}$  by 42  $\text{\AA}$ , so when compared to the capillary internal diameter of 75  $\mu\text{m}$  the BSA would not extend more than 0.2  $\mu\text{m}$  from the capillary surface. Providing the tryptophan enantiomers were distributed evenly throughout the buffer solution then only a fraction would be available to interact with the coated BSA



phase. Another reason could be that the structure of the BSA was grossly distorted during the coating process thereby reducing the chiral selectivity. However, this was

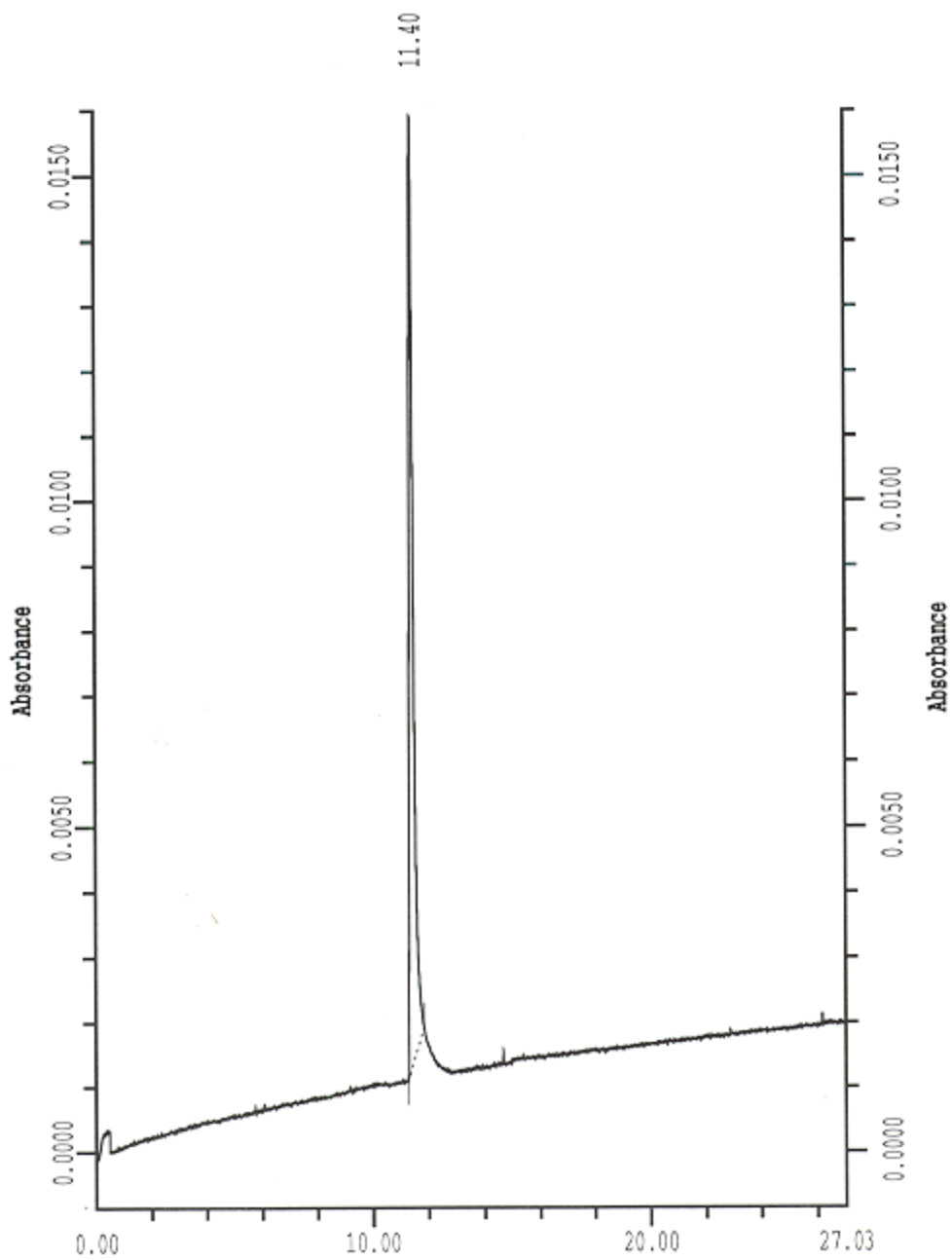


Fig.38 CE of tryptophan enantiomers with the immobilised BSA capillary. Conditions: run buffer, 67mM phosphate (pH 7.4); capillary, BSA immobilised capillary, 37 cm (30 cm to detector) x 75 µm i.d.; instrument, PACE 2050; temperature, 25 °C; voltage 7 kV; detection wavelength, 254 nm.

thought unlikely as BSA has been used successfully as a chiral stationary phase (CSP) in HPLC [Krstulovic 1989]. One final reason could be the overall stability of the BSA phase. As noted in the Experimental, Chapter 2, flushing the capillary with sodium hydroxide could lead to the disassociation of the BSA from the capillary wall. During the analysis undertaken at pH 7.4 there would be hydroxide ions in solution which would cause the BSA to dissociate from the capillary wall therefore decreasing the concentration of BSA available for chiral selectivity.

This method did not offer any practical benefits for use as a CSP in CE. Studies using more conventional CSPs in capillary electrochromatography would be more suitable. The amount of chiral selector available using a conventional CSP would be far greater than a chiral selector coated on the capillary wall. For a theoretical example of a 75 µm i.d. capillary packed with spheres of diameter 5 µm the surface area is approximately 12 times greater than for an open tubular 75 µm i.d. capillary, Fig. 39.

The surface area of a 5 µm length of 75 µm i.d. capillary: -

$$\begin{aligned}\text{Surface area} &= 2\pi rh \\ &= 2\pi \times 37.5 \times 5 \\ &= 1178.3 \mu\text{m}^2\end{aligned}$$

The surface area the same capillary packed with 5 µm particles, assuming that the particles are cubic packed such that their effective volume approximates to a cube, can be calculated as: -

$$\begin{aligned}
\text{Number of particles} &= \text{volume of the capillary} / \text{volume of the sphere} \\
&= (\pi r^2 h) / (\text{diameter of sphere})^3 \\
&= (\pi \times 37.5^2 \times 5) / 5^3 \\
&= 176.7
\end{aligned}$$

$$\begin{aligned}
\text{Surface area of a} &= 4\pi r^2 \\
\text{particle} & \\
&= 4\pi \times 2.5^2 \\
&= 78.6 \mu\text{m}^2
\end{aligned}$$

$$\begin{aligned}
\text{Total surface area} &= \text{surface area of capillary} + \text{total surface area of} \\
\text{of packed capillary} & \qquad \qquad \qquad \text{all particles} \\
&= 1178.3 \mu\text{m}^2 + (176.7 \times 78.6 \mu\text{m}^2) \\
&= 15066.9 \mu\text{m}^2
\end{aligned}$$

Therefore the ratio between the surface area of a packed capillary to an open tubular capillary is: -

$$\begin{aligned}
\text{Ratio of areas} &= (15066.9 / 1178.3) \\
&= 12.7
\end{aligned}$$

Fig.39. Theoretical calculation for the surface area ratio of a packed capillary to an open tubular capillary

### 3.7 Conclusions

As discussed, the findings of the adventure into the use of a BSA immobilised capillary did not suggest that there would be any significant benefit to be had from switching to this format; quite the contrary in fact. Of course, it would also have introduced the undesirable additional complication of having to perfect

immobilisation chemistry for every new protein tested. Similarly, protein affinity CEC was discounted on the grounds of the extra complication of not only having to address bonding chemistry but also having to perfect packing procedures and frit formation (L Frame, PhD, University of Sunderland).

The work on the bonded capillary had done nothing to change the impression at the outset that the use of the protein as a buffer additive would be the most simple, versatile and easily accessible way of conducting electrophoretic protein affinity enantioseparations and certainly the most facile way of testing out a range of proteins, or even protein mixtures, for potential as chiral selectors. From the work on BSA and tryptophan it appeared that the best combination of variables for the run buffer to test BSA with a wide range of racemates were 67 mM phosphate (pH 7.4) – methanol (97.5 : 2.5, v/v) and a chiral selector concentration of 2 mg ml<sup>-1</sup>. The length of the capillary was instrument dependent, they were 40 cm for the Dionex CES I and 37 cm for the Beckman PACE 2050. The voltage was set to 10 kV.

## **Chapter 4 Evaluation of biomacromolecules for chiral discrimination in free solution capillary electrophoresis**

### **4.1 Introduction**

Protein affinity CE has been successfully applied to separate the enantiomers of tryptophan and benzoin, as described in Chapter 3. The protocol developed in Chapter 3 was designed such that it would easily lend itself to screen many chiral compounds against biomacromolecules of the analyst's choice. At the time of the outset of this element of the practical work only a few enantiomers had been separated by protein affinity CE using BSA as the chiral selector. However, many more had been separated using BSA as a chiral stationary phase in HPLC [Barker 1992]. Accordingly it was thought that it would be appropriate to use the CE protocol for a broader range of enantiomers than had previously been studied by CE. Similarly, another obvious aim was to apply the protocol to study chiral resolution by protein affinity CE for a range of other proteins. The use of proteins that had been used for chiral LC would allow an LC to CE comparison and those not studied by LC would hopefully illustrate the easier accessibility of CE.

### **4.2 Results and discussion**

The enantiomers selected had already been successfully separated using a BSA-CSP e.g. leucovorin [Barker 1992], or were structurally related to enantiomers separated previously with this protocol, e.g. promethazine and the propionic acids.

Following on from studying protein affinity CE with BSA to screen a range of compounds for chiral selectivity, the protocol was easily modified to study chiral selectivity of other biomacromolecules. Human serum albumin (HSA) is structurally similar to BSA and performs identical functions in humans as BSA does in cattle. Consequently, it has been successfully used as a chiral stationary phase in HPLC so HSA ought to lend itself as a chiral selector in protein affinity CE. Two other biomacromolecules were used to test the applicability of protein affinity CE to ascertain chiral discrimination of potentially rare or novel biomacromolecules. These were human lactoferrin and protamine.

#### **4.3 Results for the separation of a range of compounds with BSA with the protein affinity CE protocol**

A summary of the results for resolving a range of enantiomers is shown in Table 40.

Table 40 Resolution of enantiomers using BSA as the chiral selector and standard conditions

Compound	Migration time 1 (min)	Migration time 2 (min)	Resolution (arbitrary units)	Electrophero- gram
Benzoin	21.3	21.6	1.2	41
Thioridazine	15.8	16.5	0.67	42
Bepidil	7.9	8.0	0.61	43
Kynurenine	26.8	27.5	0.51	44

Table 40 Resolution of enantiomers using BSA as the chiral selector and standard conditions

Compound	Migration time 1 (min)	Migration time 2 (min)	Resolution (arbitrary units)	Electrophero- gram
Leucovorin	36.1	37.5	1.12	45
Ibuprofen	59.0	61.3	0.57	46
2-(4-methylphenyl) propionic acid	13.8	14.1	0.52	47
Tryptophan amide	12.5	-	-	48
Hexabarbitalone	19.0	-	-	49
N-acetyl-DL- tryptophan	52.0	-	-	50
Warfarin	49.0	-	-	51
Tyrosine	22.1	-	-	52
Suprofen	∞	-	-	Not shown
Carprofen	∞	-	-	Not shown
Quinalbarbitone	∞	-	-	Not shown
Temazepam	∞	-	-	Not shown
Oxazepam	∞	-	-	Not shown
Lorazepam	∞	-	-	Not shown

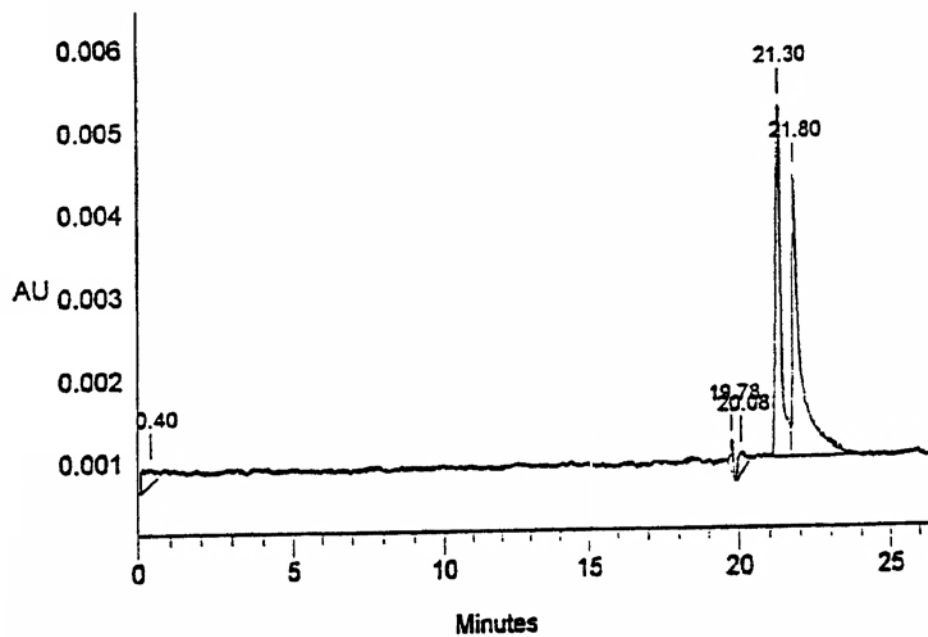


Fig. 41 CE of benzoin enantiomers showing good selectivity but failure to obtain baseline resolution because of peak tailing. Conditions: run buffer, 30  $\mu$ M BSA, 67 mM phosphate (pH 7.4) – methanol (97.5 : 2.5,v/v); capillary, CElect p150, 40 cm (35 cm to detector) x 50  $\mu$ m i.d.; instrument, CES I; temperature, ambient; voltage 10 kV; detection wavelength, 254 nm.



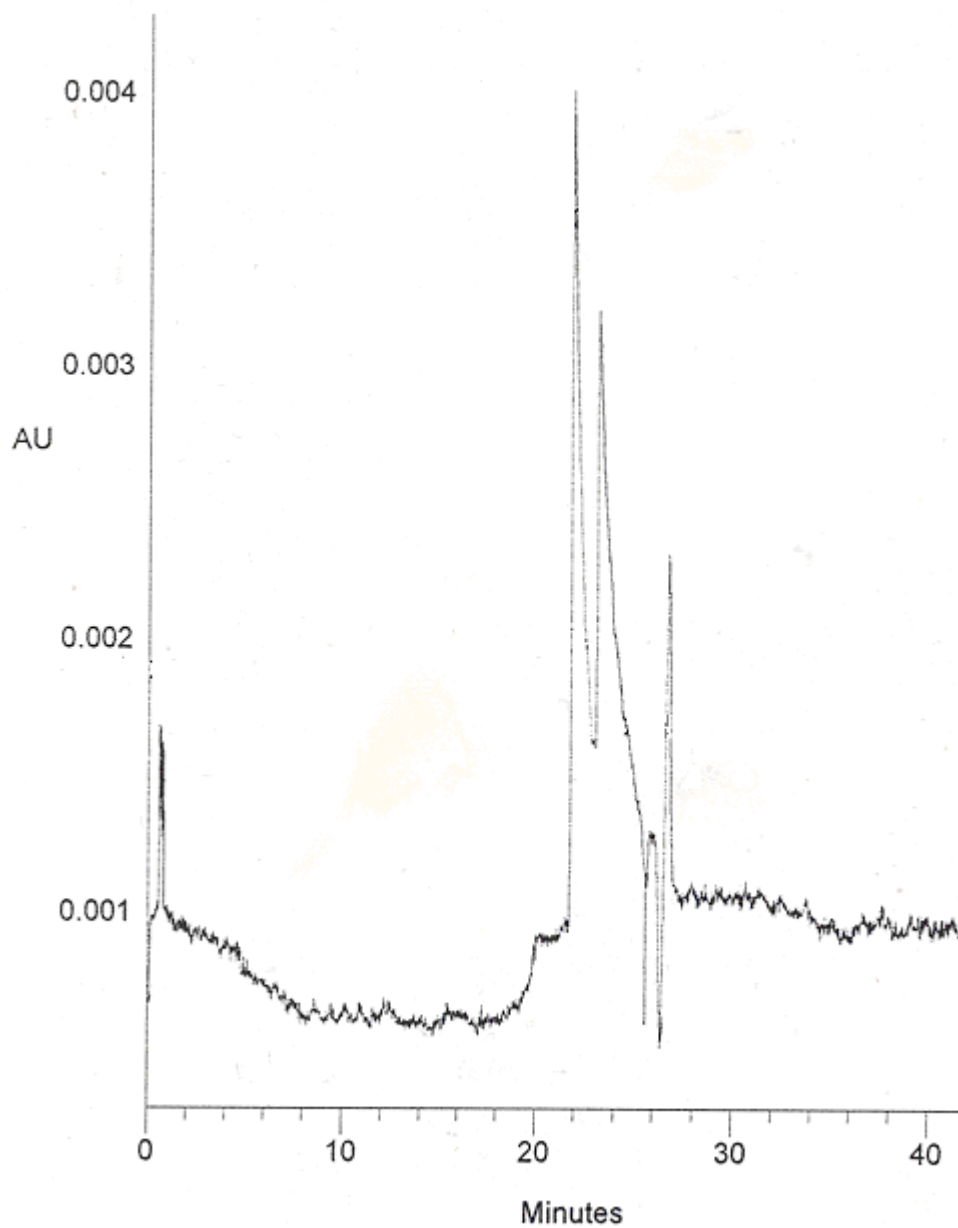


Fig. 42 CE of thioridazine enantiomers; an example of resolution for a basic analyte.

Conditions: run buffer, 30  $\mu$ M BSA, 67 mM phosphate (pH 7.4) – methanol (97.5 : 2.5, v/v); capillary, CElect p150, 40 cm (35 cm to detector) x 50  $\mu$ m i.d.; instrument, CES I; temperature, ambient; voltage 10 kV; detection wavelength, 254 nm.

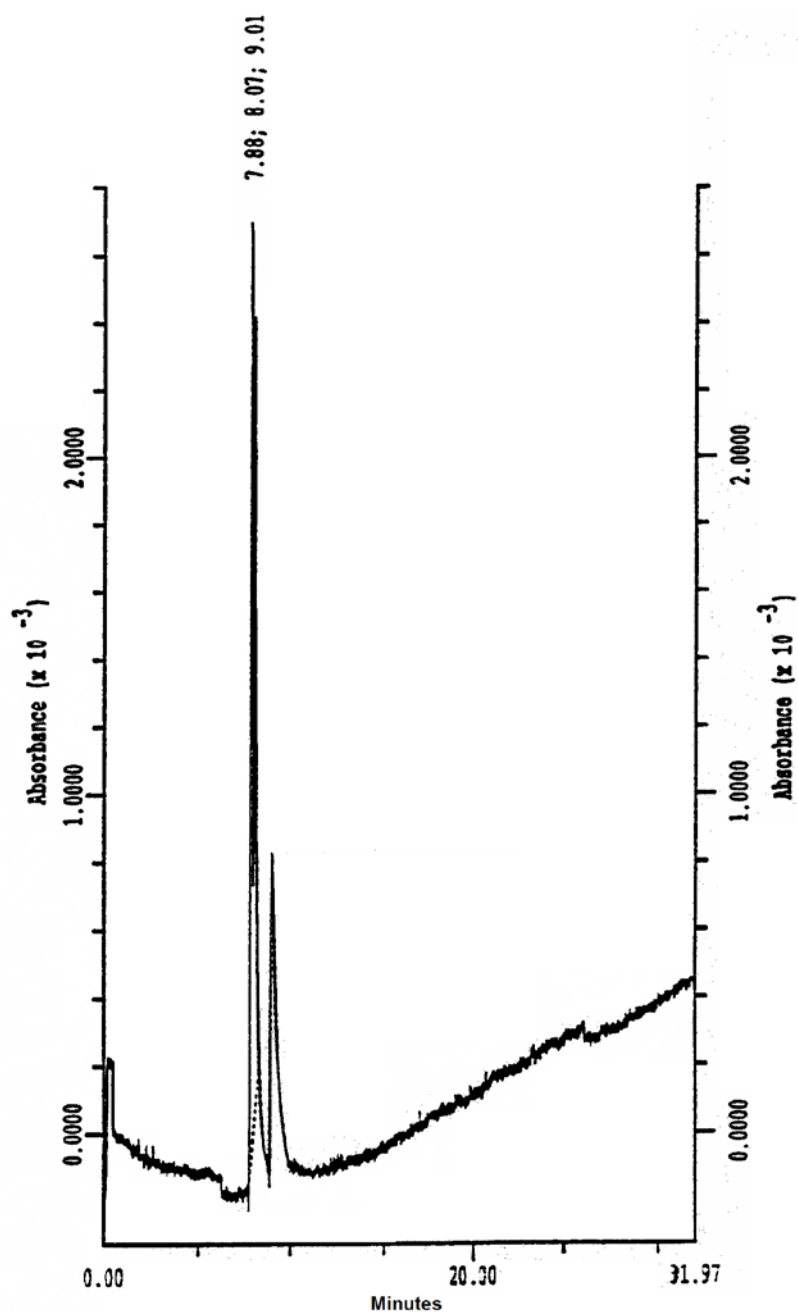


Fig. 43 CE of bepridil enantiomers showing good resolution inside 10 min; spiking on the apex of the first peak is the likely reason that the peak areas are not in a 50:50 ratio Conditions: run buffer, 30  $\mu$ M BSA, 67mM phosphate (pH 7.4) – methanol (97.5 : 2.5, v/v); capillary, CElect p150, 37 cm (30 cm to detector) x 50  $\mu$ m i.d.; instrument, PACE 2050; temperature, 25  $^{\circ}$ C; voltage 10 kV; detection wavelength, 254 nm.

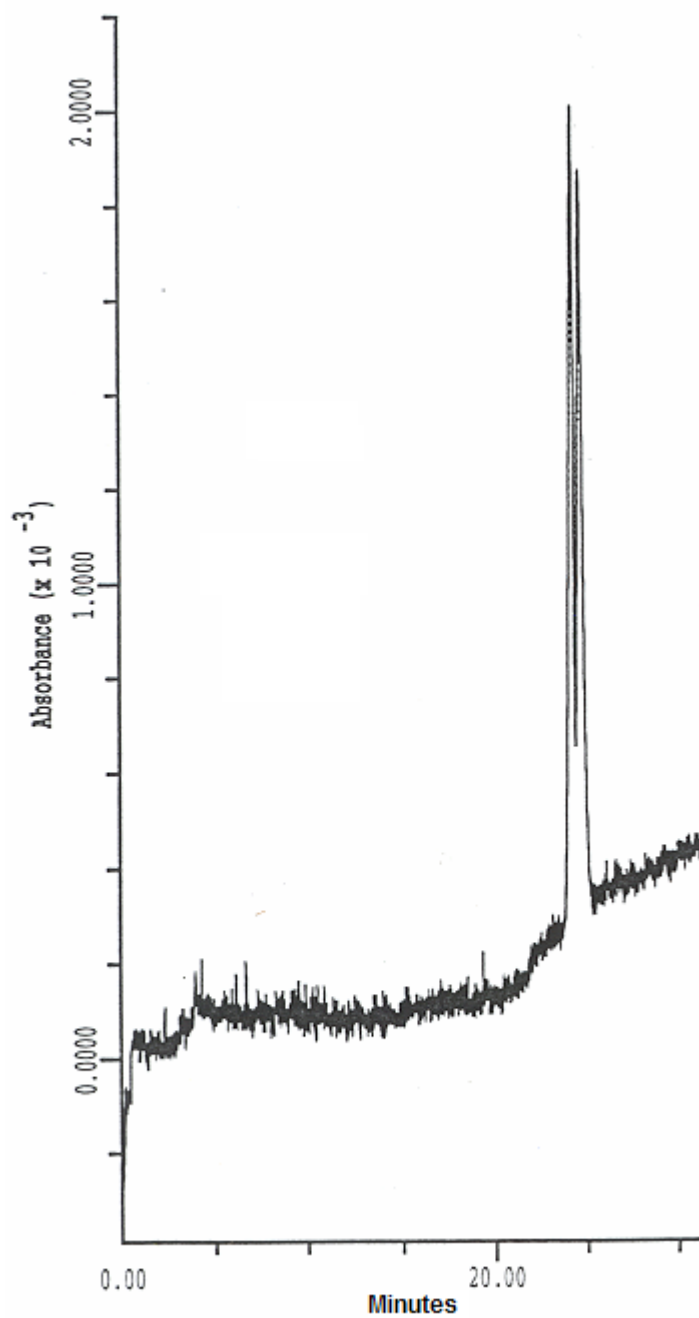


Fig. 44 CE of kynurenine enantiomers showing limited selectivity but good resolution because of the high efficiency and absence of peak tailing. Conditions: run buffer, 30  $\mu$ M BSA, 67 mM phosphate (pH 7.4) – methanol (97.5 : 2.5,v/v); capillary, CElect p150, 37 cm (30 cm to detector) x 50  $\mu$ m i.d.; instrument, PACE 2050; temperature, 25  $^{\circ}$ C; voltage 10 kV; detection wavelength, 254 nm.

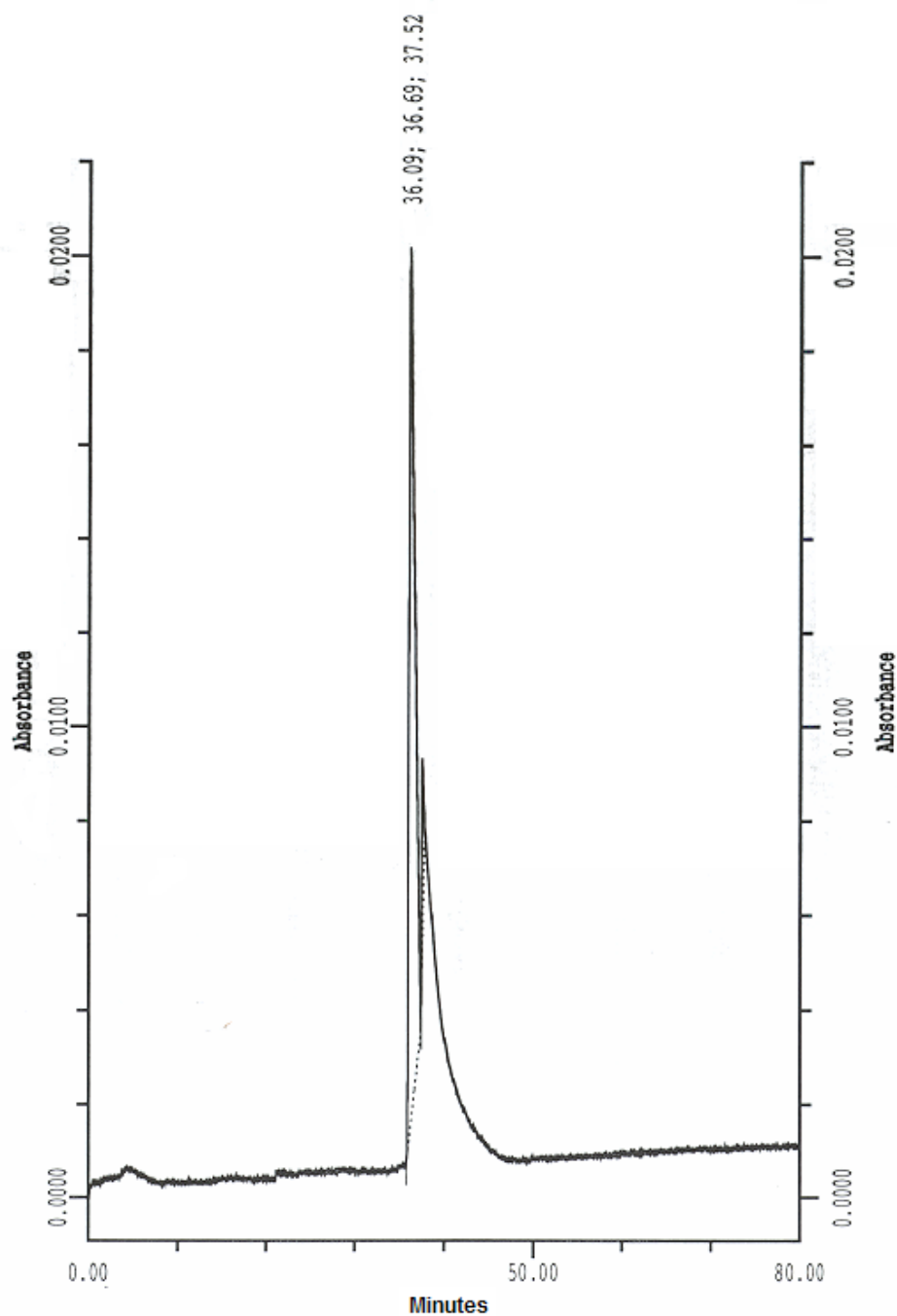


Fig. 45 CE of leucovorin enantiomers showing peak tailing for the second peak (similarly to tryptophan). Conditions: run buffer, 30  $\mu$ M BSA, 67 mM phosphate (pH 7.4) – methanol (97.5 : 2.5,v/v); capillary, CElect p150, 37 cm (30 cm to detector) x 50  $\mu$ m i.d.; instrument, PACE 2050; temperature, 25  $^{\circ}$ C; voltage 10 kV; detection wavelength, 254 nm.

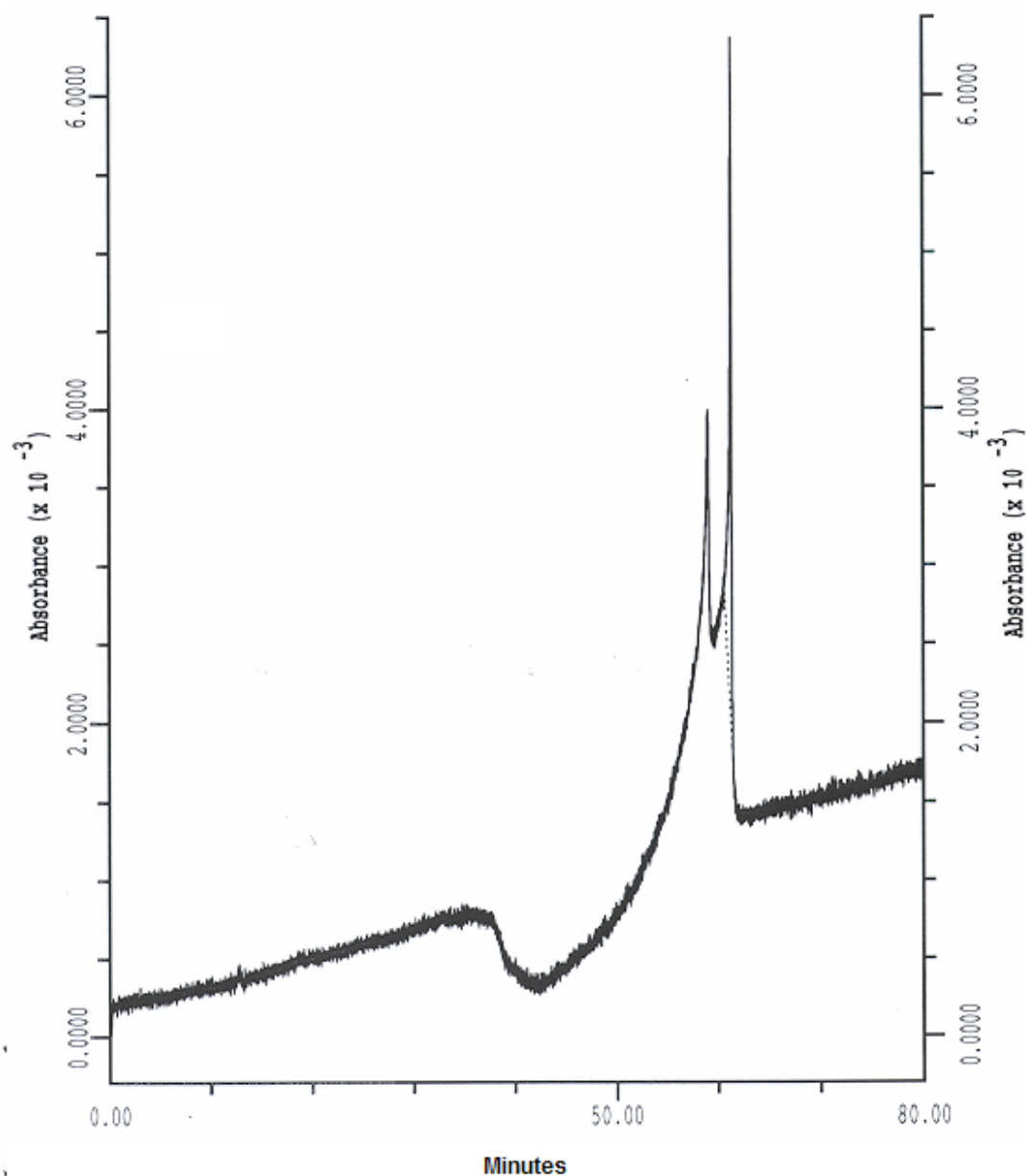


Fig. 46 CE of ibuprofen enantiomers showing the very characteristic trough before the resolved enantiomers. Conditions: run buffer, 30  $\mu$ M BSA, 67 mM phosphate (pH 7.4) – methanol (97.5 : 2.5,v/v); capillary, CElect p150, 37 cm (30 cm to detector) x 50  $\mu$ m i.d.; instrument, PACE 2050; temperature, 25  $^{\circ}$ C; voltage 10 kV; detection wavelength, 254 nm.

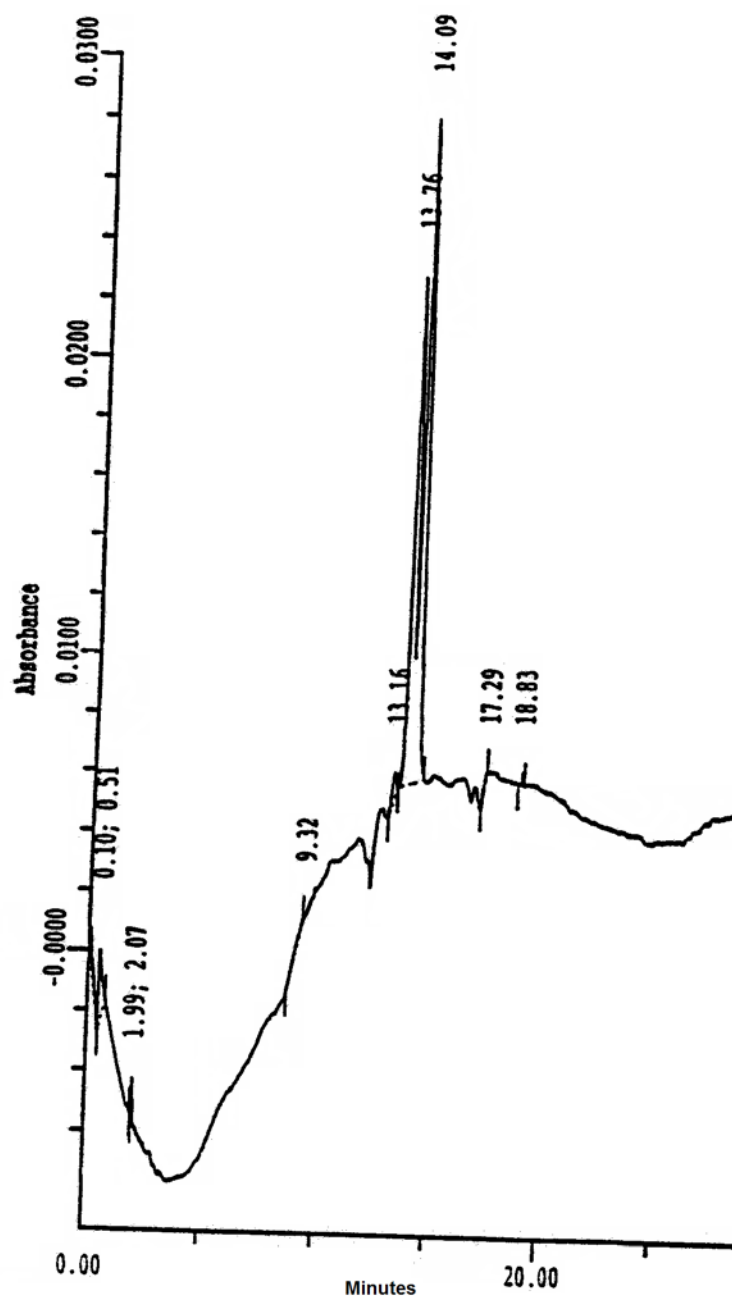


Fig. 47 CE of 2-(4-methylphenyl) propionic acid enantiomers showing a similar trough as for ibuprofen and good resolution with limited selectivity because of the high efficiency and absence of tailing. Conditions: run buffer, 30  $\mu$ M BSA, 67 mM phosphate (pH 7.4) – methanol (97.5 : 2.5,v/v); capillary, CElect p150, 37 cm (30 cm to detector) x 50  $\mu$ m i.d.; instrument, PACE 2050; temperature, 25  $^{\circ}$ C; voltage 10 kV; detection wavelength, 254 nm.

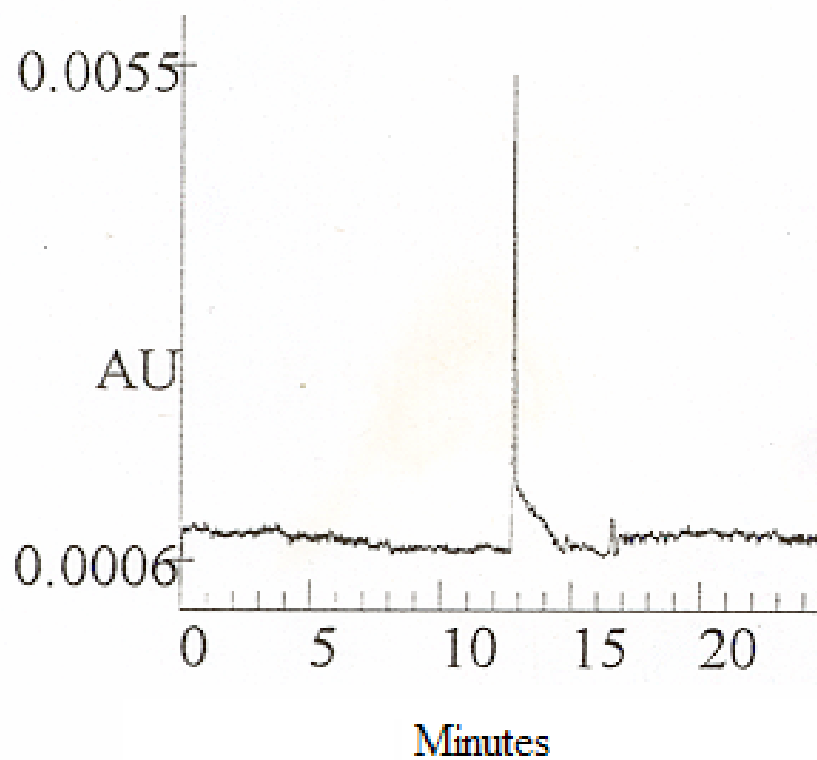


Fig. 48 CE of tryptophan amide enantiomers, suggesting that the tryptophan resolution is dependent on the presence of the free carboxylic acid (similarly the failure to resolve N-acetyltryptophan enantiomers suggests that the free amine is also needed). Conditions: run buffer, 30  $\mu$ M BSA, 67 mM phosphate (pH 7.4) – methanol (97.5 : 2.5, v/v); capillary, CElect p150, 40 cm (35 cm to detector) x 50  $\mu$ m i.d.; instrument, CES I; temperature, ambient; voltage 10 kV; detection wavelength, 254 nm.

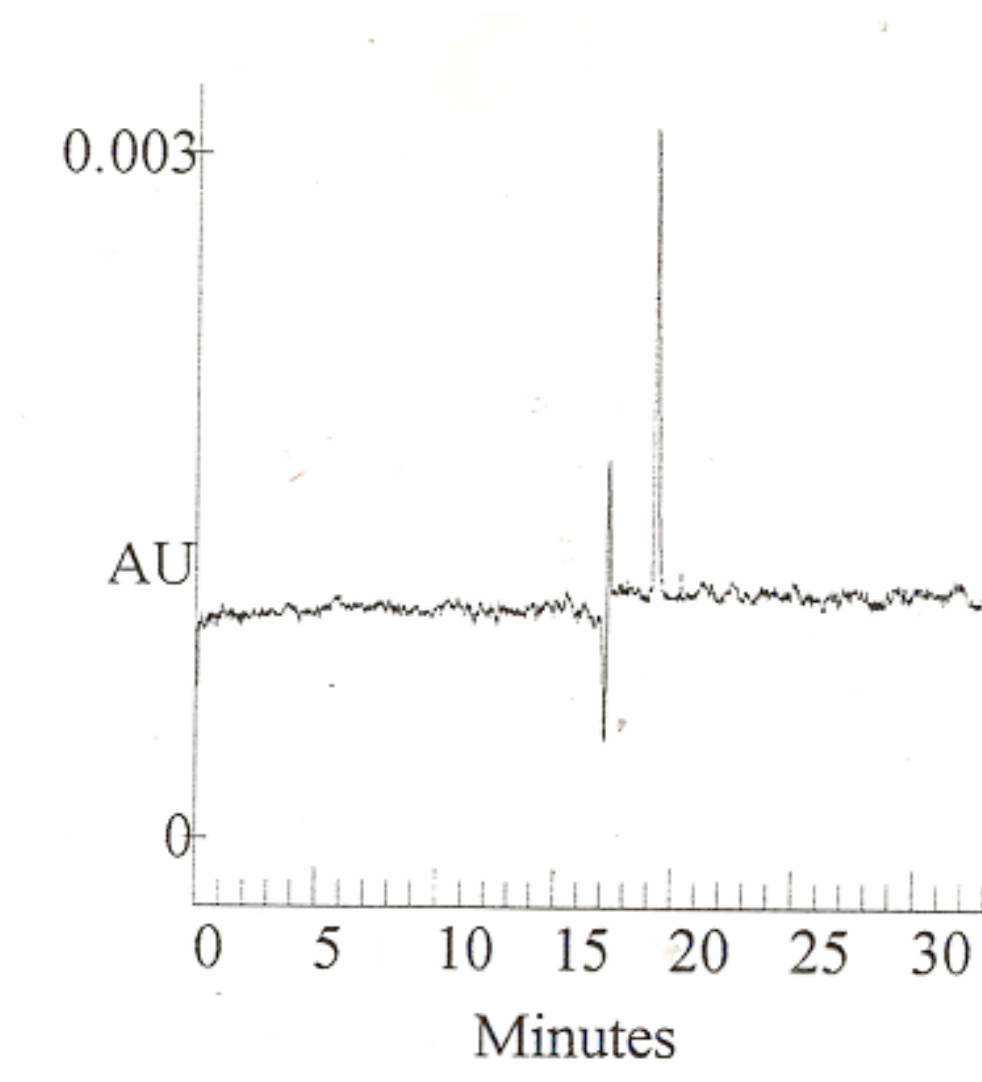


Fig. 49 CE of hexobarbitone enantiomers showing lack of resolution. Conditions: run buffer, 30  $\mu$ M BSA, 67 mM phosphate (pH 7.4) – methanol (97.5 : 2.5, v/v); capillary, CElect p150, 40 cm (35 cm to detector) x 50  $\mu$ m i.d.; instrument, CES I; temperature, ambient; voltage 10 kV; detection wavelength, 254 nm.



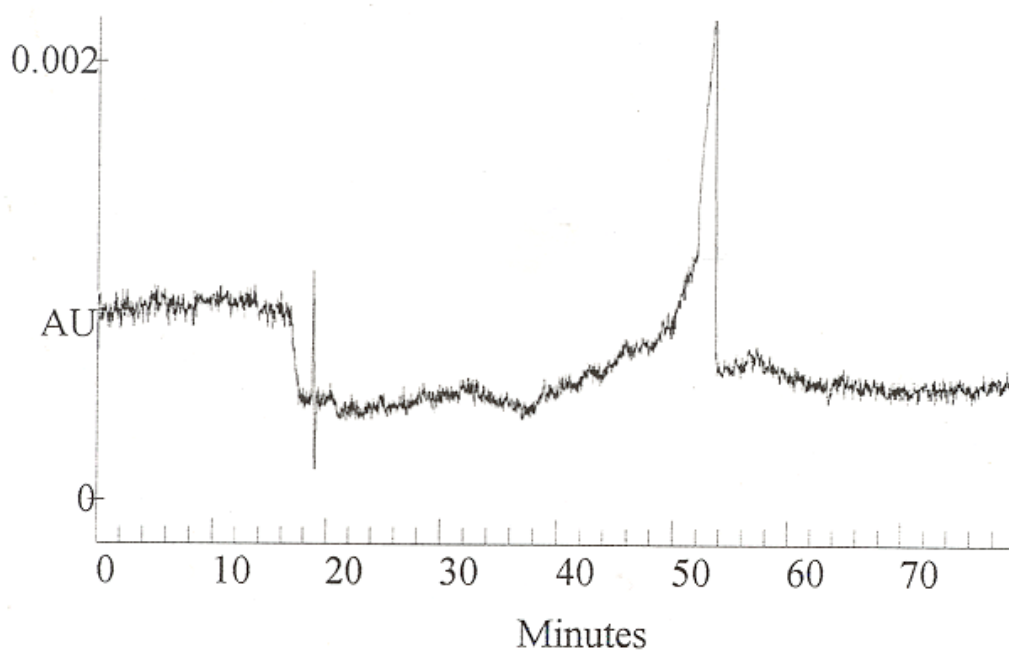


Fig. 50 CE of N-acetyl-DL-tryptophan enantiomers showing longer migration time than DL-tryptophanamide but still no resolution. Conditions: run buffer, 30  $\mu$ M BSA, 67 mM phosphate (pH 7.4) – methanol (97.5 : 2.5, v/v); capillary, CElect p150, 40 cm (35 cm to detector) x 50  $\mu$ m i.d.; instrument, CES I; temperature, ambient; voltage 10 kV; detection wavelength, 254 nm.

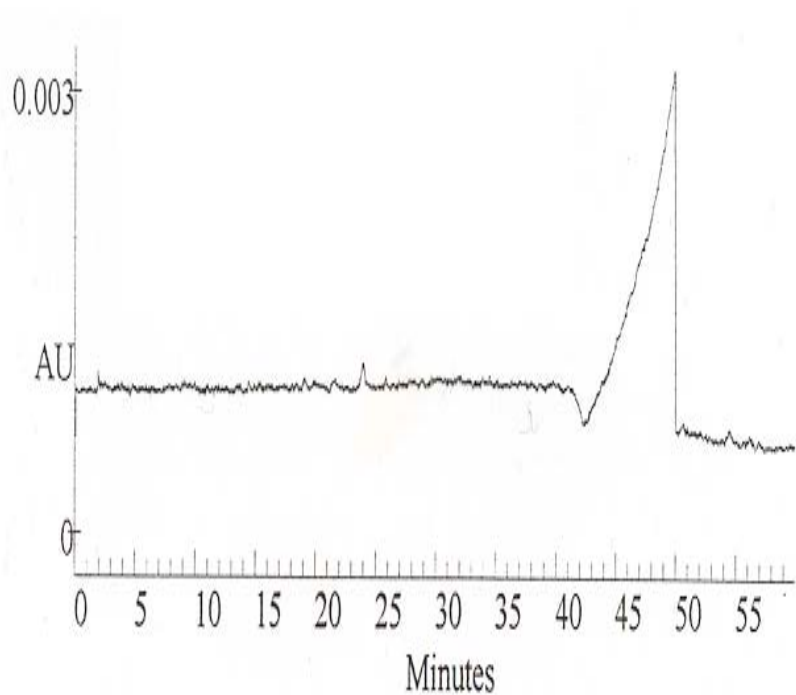


Fig. 51 CE of warfarin enantiomers showing a small (compared to ibuprofen) trough ahead of the relatively wide peak. Conditions: run buffer, 30  $\mu$ M BSA, 67 mM phosphate (pH 7.4) – methanol (97.5 : 2.5, v/v); capillary, CElect p150, 40 cm (35 cm to detector) x 50  $\mu$ m i.d.; instrument, CES I; temperature, ambient; voltage 10 kV; detection wavelength, 254 nm.

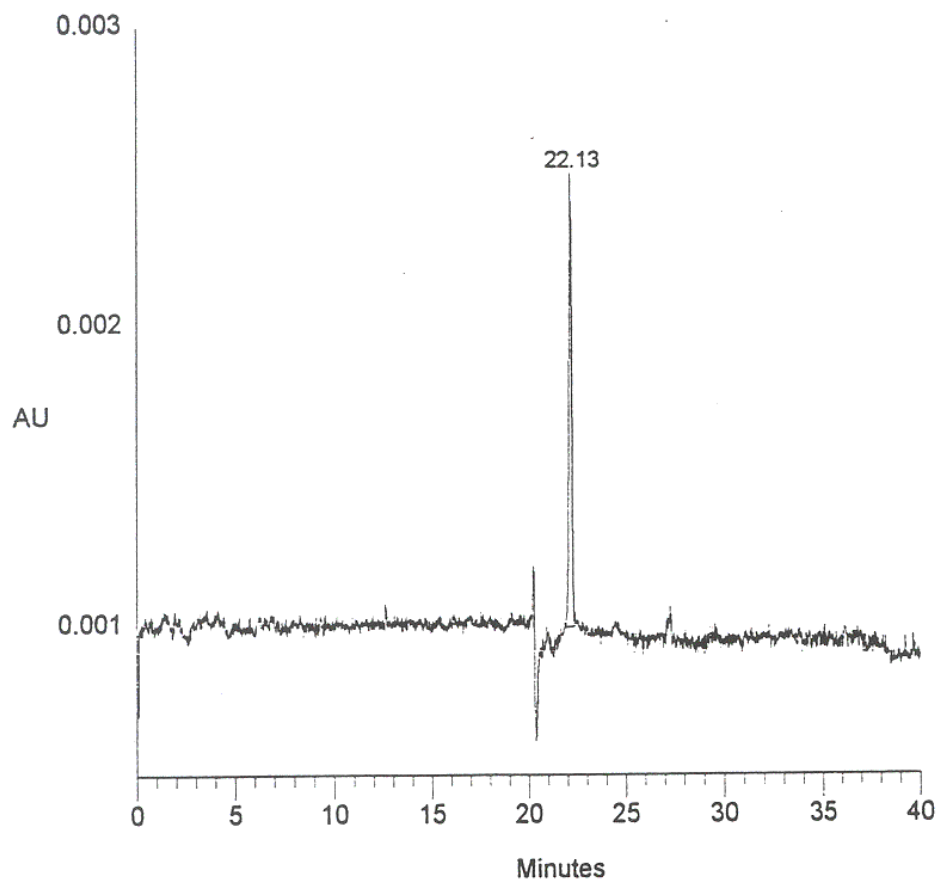


Fig. 52 CE of tyrosine enantiomers; the very good efficiency perhaps indicating a lack of interaction with the protein. Conditions: run buffer, 30  $\mu$ M BSA, 67 mM phosphate (pH 7.4) – methanol (97.5 : 2.5, v/v); capillary, CElect p150, 40 cm (35 cm to detector) x 50  $\mu$ m I.D.; instrument, CES I; temperature, ambient; voltage 10 kV; detection wavelength, 254 nm.

#### 4.4 Results for the separation of a range of compounds with HSA with the protein affinity CE protocol

A summary of the enantiomers resolved by HSA by protein affinity CE is shown in Table 53.

Table 53 Resolution of enantiomers using HSA as the chiral selector and standard conditions

Compound	Migration time 1 (min)	Migration time 2 (min)	Resolution (arbitrary units)	Electropherogram
Bepiridil	19.0	21.0	0.61	54
Promethazine	13.2	14.2	0.51	55
Tryptophan	12.2	14.0	0.42	56
Thioridazine	20.8	23.2	0.26	57
Kynurenine	23.8	24.2	0.30	58

#### 4.5 Results for the separation of a range of compounds with protamine and lactoferrin with the protein affinity CE protocol

There was no chiral resolution of any of the enantiomers with the protein affinity CE protocol. Example electropherograms are shown for tryptophan with lactoferrin, Fig. 59 and leucovorin with protamine, Fig. 60. It could not be determined whether there was any interaction between the protein and the enantiomers. The migration times of the enantiomers were longer in the presence of the protein although a more plausible explanation for this increase is due to the increased viscosity of the run buffer, equation 18.

$$\bar{\mu} = \frac{\bar{v}}{\bar{E}} = \frac{q}{6\pi\eta r}$$

Equation 18 Electrophoretic Mobility

where

$\bar{\mu}$	=	electrophoretic mobility
$\bar{v}$	=	electrophoretic velocity
$\bar{E}$	=	electric field strength
$q$	=	charge of the ion
$\eta$	=	viscosity of the buffer
$r$	=	radius of the molecules.

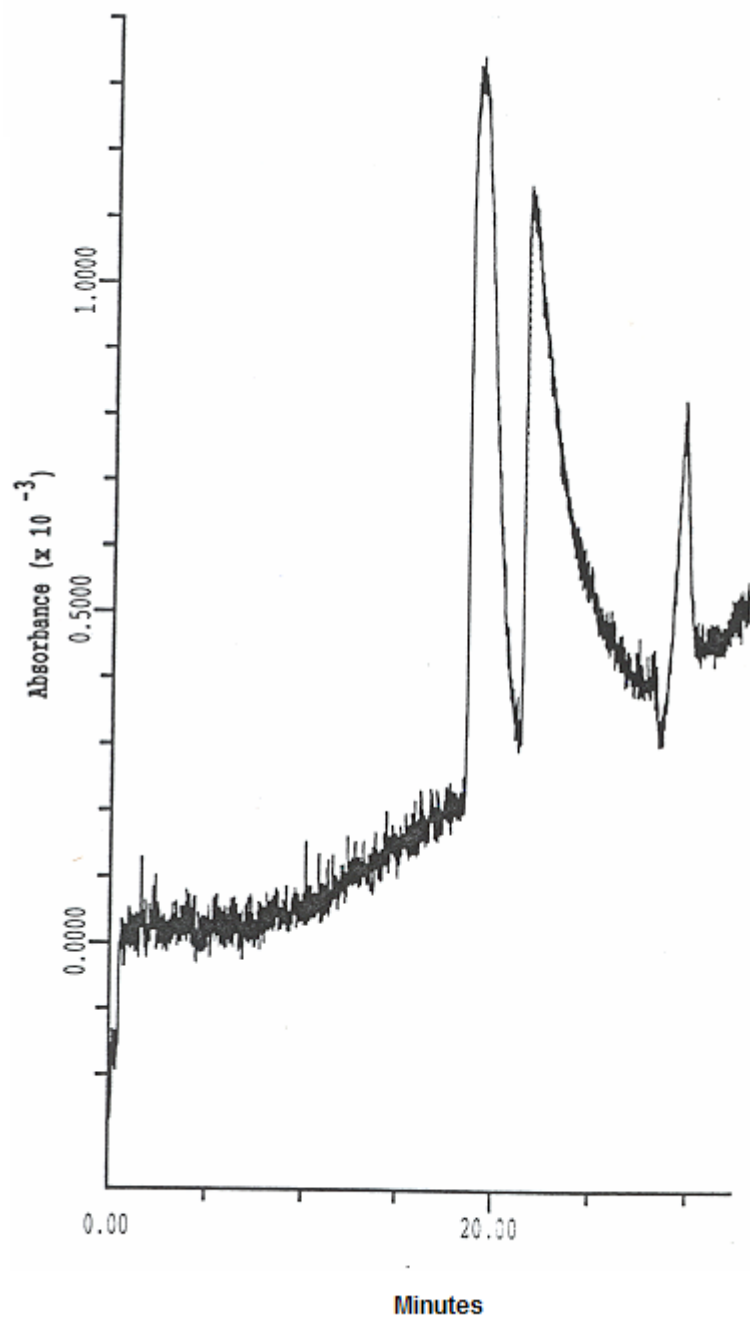


Fig. 54 CE of bepridil enantiomers, showing considerably more retardation and greater resolution than with BSA. Conditions: run buffer, 30  $\mu$ M HSA, 67 mM phosphate (pH 7.4) – methanol (97.5 : 2.5, v/v); capillary, CElect p150, 37 cm (30 cm to detector) x 50  $\mu$ m i.d.; instrument, PACE 2050; temperature, 25  $^{\circ}$ C; voltage 10 kV; detection wavelength, 254 nm.

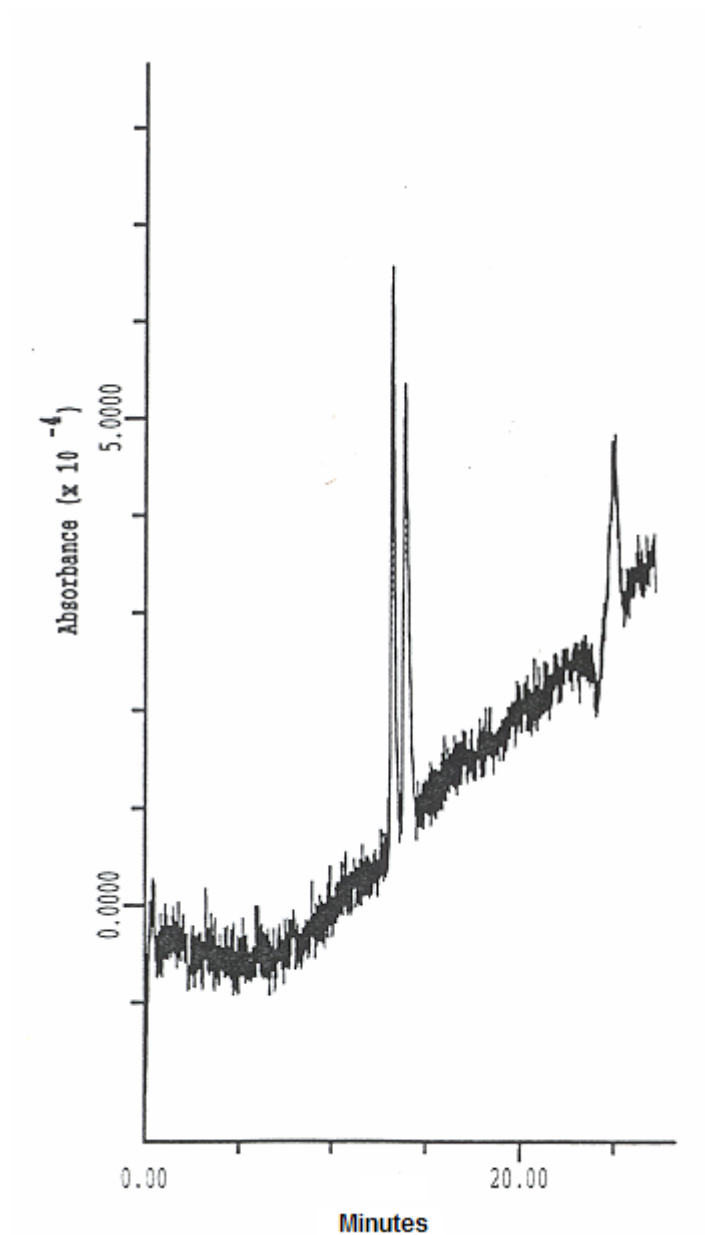


Fig. 55 CE of promethazine enantiomers, showing good resolution and efficiency. The system peak at about 30 min is the EOF. Conditions: run buffer, 30  $\mu$ M HSA, 67 mM phosphate (pH 7.4) – methanol (97.5 : 2.5, v/v; capillary, CElect p150, 37 cm (30 cm to detector) x 50  $\mu$ m i.d.; instrument, PACE 2050; temperature, 25  $^{\circ}$ C; voltage 10 kV; detection wavelength, 254 nm.

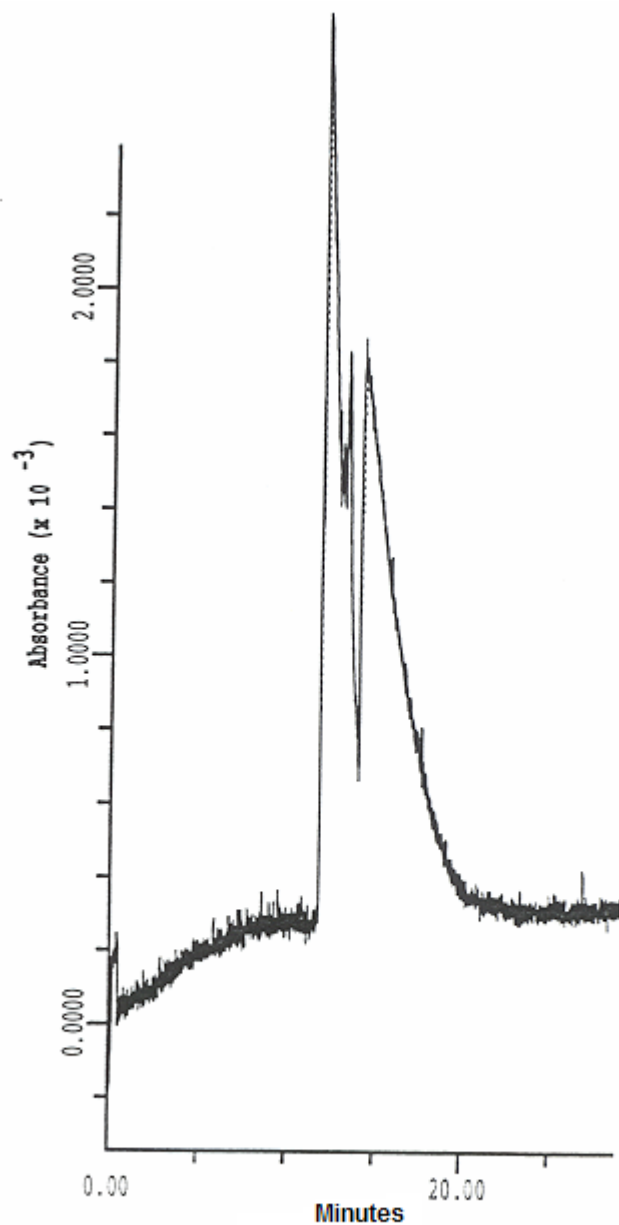


Fig. 56 CE of tryptophan enantiomers, showing resolution but with both peaks fairly broad. Conditions: run buffer, 30  $\mu$ M HSA, 67 mM phosphate (pH 7.4) – methanol (97.5 : 2.5, v/v); capillary, CElect p150, 37 cm (30 cm to detector) x 50  $\mu$ m i.d.; instrument, PACE 2050; temperature, 25  $^{\circ}$ C; voltage 10 kV; detection wavelength, 280nm.



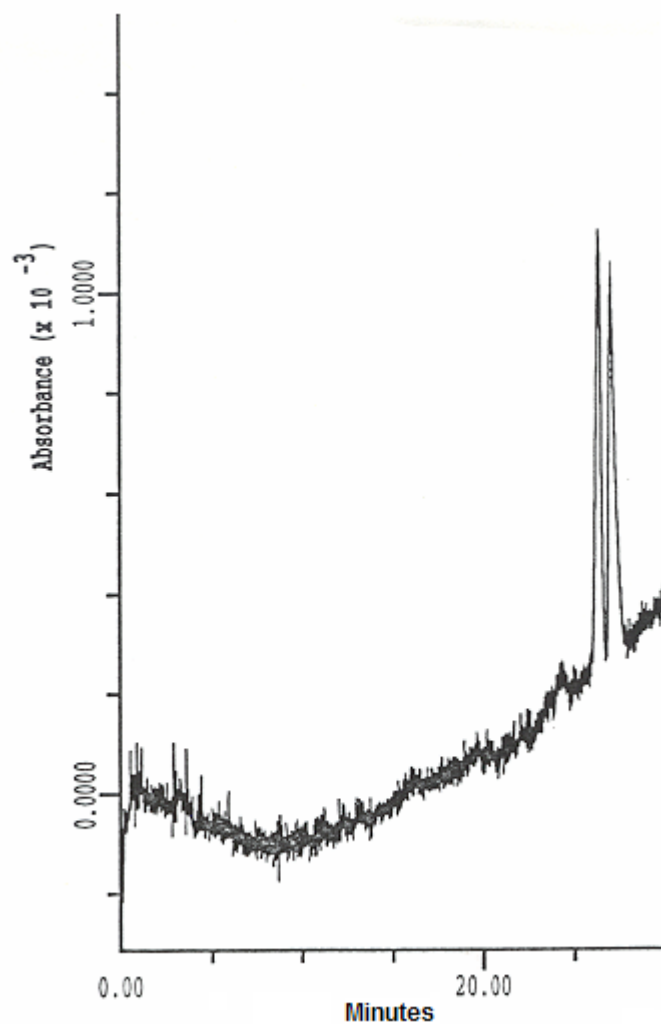


Fig. 57 CE of thioridazine enantiomers, showing good resolution with better peak shape than with BSA. Conditions: run buffer, 30  $\mu$ M HSA, 67 mM phosphate (pH 7.4) – methanol (97.5 : 2.5, v/v); capillary, CElect p150, 37 cm (30 cm to detector) x 50  $\mu$ m i.d.; instrument, PACE 2050; temperature, 25  $^{\circ}$ C; voltage 10 kV; detection wavelength, 254 nm.

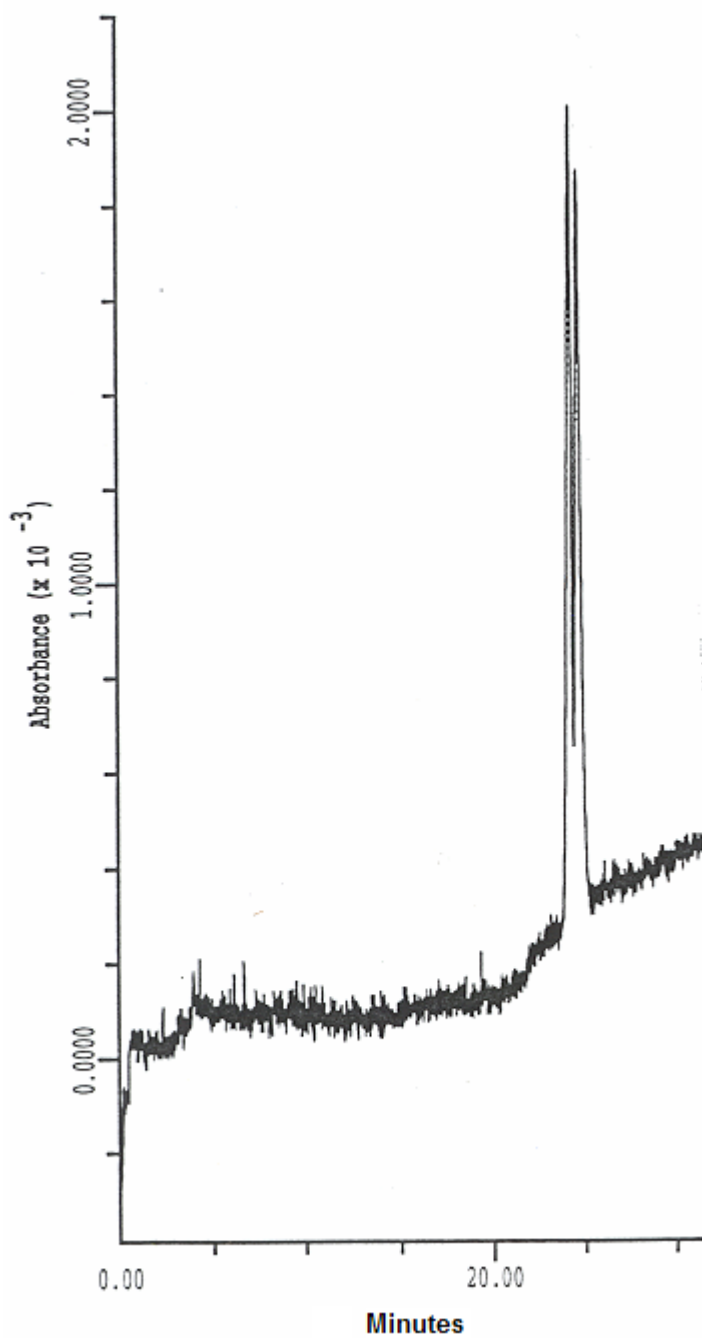


Fig. 58 CE of kynurenine enantiomers, showing limited selectivity but good resolution because of the high efficiency and absence of peak tailing as for with BSA and with very similar migration time to the BSA case. Conditions: run buffer, 30  $\mu$ M HSA, 67 mM phosphate (pH 7.4) – methanol (97.5 : 2.5, v/v); capillary, CElect p150, 37 cm (30 cm to detector) x 50  $\mu$ m i.d.; instrument, PACE 2050; temperature, 25 °C; voltage 10 kV; detection wavelength, 254 nm.

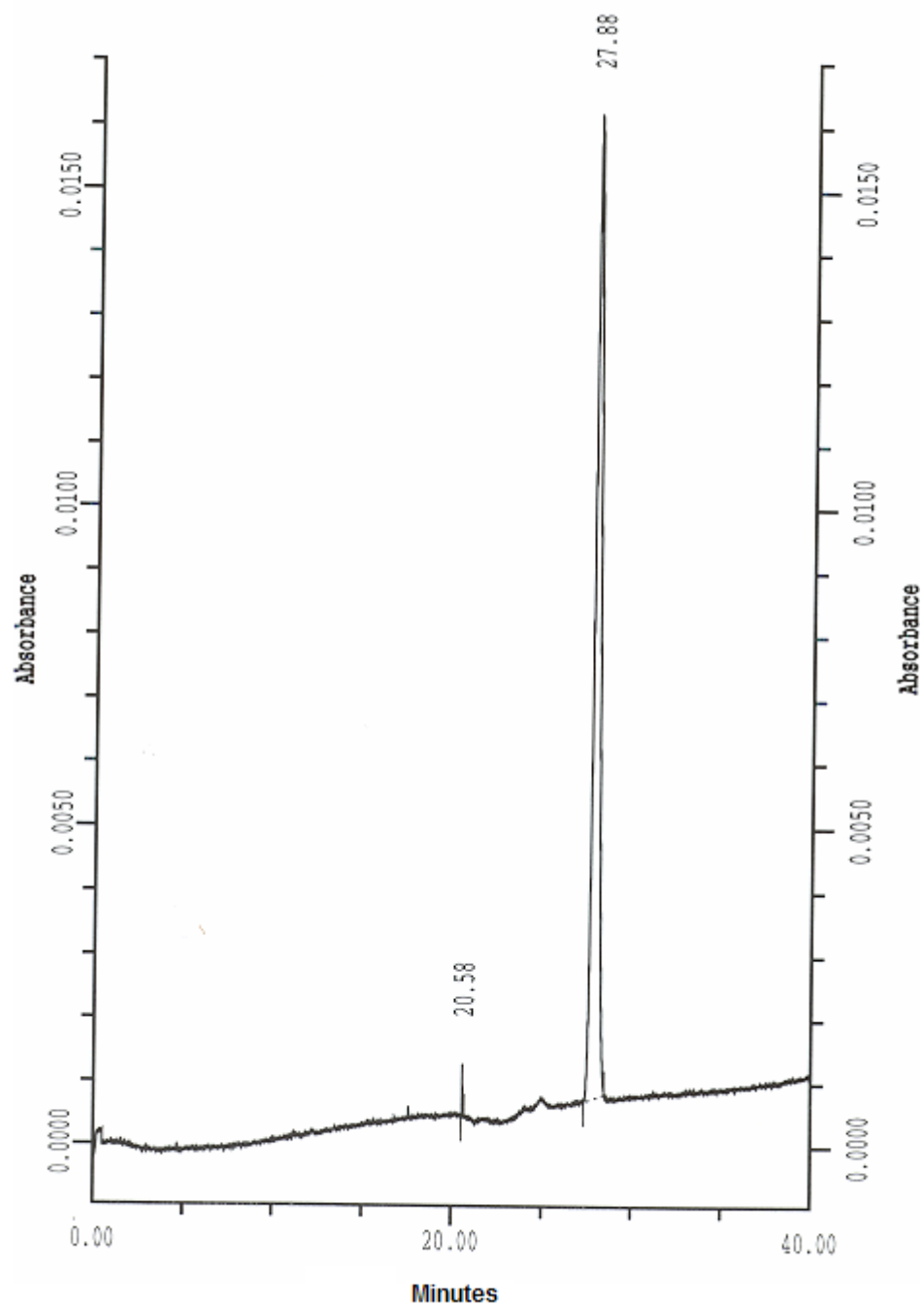


Fig. 59 CE of tryptophan enantiomers showing good peak shape but no resolution. Conditions: run buffer, 30  $\mu$ M lactoferrin, 67 mM phosphate (pH 7.4) – methanol (97.5 : 2.5, v/v); capillary, CElect p150, 37 cm (30 cm to detector) x 50  $\mu$ m i.d.; instrument, PACE 2050; temperature, 25  $^{\circ}$ C; voltage 10 kV; detection wavelength, 280 nm.

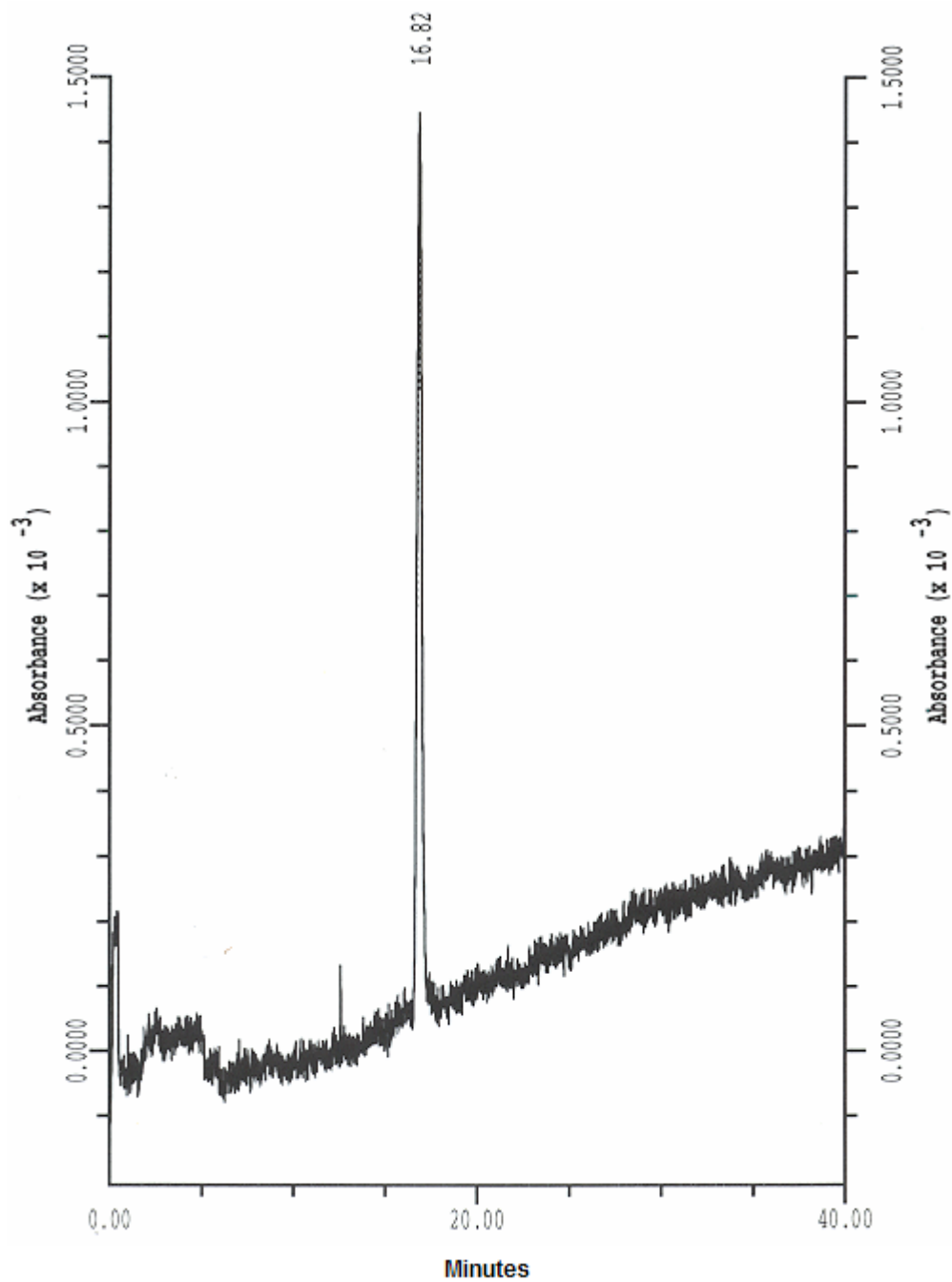


Fig. 60 CE of leucovorin enantiomers showing good peak shape but with no resolution. Conditions: run buffer, 30  $\mu$ M protamine, 67 mM phosphate (pH 7.4) – methanol (97.5 : 2.5, v/v); capillary, CElect p150, 37 cm (30 cm to detector) x 50  $\mu$ m i.d.; instrument, PACE 2050; temperature, 25  $^{\circ}$ C; voltage 10 kV; detection wavelength, 254 nm.

## 4.6 Discussion

### 4.6.1 Evaluation of protein affinity CE

The protocol developed in Chapter 3 was successfully applied to study the range of enantiomers with different biomacromolecules. Disappointingly, only a few enantiomers were resolved with HSA and BSA compared to comparable LC methods [Lloyd 1995] and none were resolved with either lactoferrin or protamine. In some cases, no peaks were observed at all e.g. temazepam and suprofen. On the whole, BSA was more successful as a chiral selector than HSA although in some cases when using HSA there were significant differences in migration times, e.g. Bepridil. While peak tailing seemed to be less of a problem when using HSA, in the case of tryptophan it was found that both peaks were broad, as opposed to the BSA case where only the second peak, L-tryptophan, was broad and tailed. Broadly speaking the situation in LC is that, because HSA does not offer striking advantages over the cheaper, first-used BSA as a chiral selector, HSA CSP tend now to be used more as tools for studying drug – protein binding [Wainer 1993] rather than for resolving enantiomers. In CE a similar situation would apply. BSA would be used for resolving enantiomers and, obviously, there would be more interest in studying binding to HSA than to BSA.

By the time this study was complete and, more so, subsequent to this, other researchers had also reported limited success in separating enantiomers with proteins in free-solution CE, Table 61. Massolini [Massolini 1998] reported a surprising lack of chiral selectivity of  $\beta$ -lactoglobulin. An explanation for the lack of chiral selectivity is the concentration of biomacromolecule in the run buffer. The

concentration of BSA as a chiral stationary phase is in the region of millimolar [Ahmed 1997] compared to the micromolar range used with the protocol.

Table 61 Review of chiral separations with proteins in free-solution CE

Author	Chiral selector	Enantiomers
Kilar [1995]	iron-free human serum transferrin	DL-Tryptophan methyl ester, DL-Tryptophan ethyl ester, DL-Tryptophan butyl ester
Amini [1997]	$\alpha_1$ -acid glycoprotein	Dispyramide
Massolini [1998]	$\beta$ -lactoglobulin	No observed selectivity
Beck [1996]	Lamda-Carrageenan	Tryptophanol, Propranolol
Valtcheva [1993]	Cellobiohydrolase I	Propranolol, alprenolol, metaprolol, pindolol, labetolol
Ferguson [1998]	HSA	Benzoin
Lloyd [1997]	HSA	Benzoin
Tanaka [1994]	Avidin	Vanilmandelic acid, Warfarin, Ibuprofen, Ketoprofen, Flurbiprofen, Folinic acid (leucovorin)
Ohara [1995]	HSA	Verapamil
Tanaka [1997]	$\alpha_1$ -acid glycoprotein	Acebutolol, Arotinolol, Atropine, Bupivocaine, Chlorprenaline, Denopamine, Eperisone, Epinastine, Etilefrin, Fenoterol, Homatropine, Ketamine, Metanephrine, Metoprolol, Mexiletine, Nicardipine, Verapamil Oxyphencyclimine, Phenylephrine, Pindolol, Primaquine, Promethazine, Sulpiride, Terbutaline, Tolperisone, Trihexyphenidyl, Trimebutine, Trimetoquinol, Trimipramine
Ahmed [1997]	HSA	Benzoin

Table 61 Review of chiral separations with proteins in free-solution CE

Author	Chiral selector	Enantiomers
Ishihama [1994]	Ovomucoid	Tolperisone, Benzoin, Eperisone, Chlorpheniramine
Tanaka [1995]	BSA	Homochlorcyclizine, Oxyphencyclimine, Propranolol, Trimebutine, Epinastine
	Ovomucoid	Butitrolol, Pindolol, Arotinolol, Oxyphencyclimine, Tolperisone, Verapamil, Chlopheniramine, Primaquine, Trimebutine
	$\alpha_1$ -acid glycoprotein	Chloprenaline
	Conalbumin	Trimetoquinol

Tellingly, the most successful of the protein affinity CE chiral resolutions shown in Table 54 are those in which high protein concentrations were used. Concentrated solutions of proteins were in the capillary partial filling application, detailed in Chapter 1, for the resolution of a few enantiomers. These include  $\alpha_1$ -AGP in the range 100-1000  $\mu\text{M}$  [Tanaka 1997] and Kilar [1995] who used 100-200  $\text{mg ml}^{-1}$  solution of iron-free human serum transferrin to separate tryptophan ester enantiomers. While increasing the concentration of the biomacromolecule would be beneficial there are associated difficulties such as increased migration as discussed in Chapter 3, an increased concentration of UV absorbing species in the run buffer and a greater amount of biomacromolecule required.

The lack of chiral resolution using this protocol could be used advantageously to screen rare or novel biomacromolecules for chiral selectivity. As already demonstrated with the four biomacromolecules tested, only the ones which exhibit excellent chiral selectivity successfully resolved enantiomers. Therefore, the protocol

could be used initially to discriminate for highly promising chiral selectors before pursuing in-depth investigations which may be potentially be unrewarding.

Similarly, the use of low protein concentrations as used in the protocol here could also be advantageous with respect to the study of drug – protein binding by CE. In studying strongly binding species (which would be being sought if looking at drug – receptor protein binding), the use of a high concentration of protein with partial filling would almost certainly lead to the situation where the highly bound drug did not migrate past the detector. Also it has been found that when using partial filling with a smaller proportion of the capillary filled in order to reduce the total mass of selector in the capillary that the reproducibility was not so good as when using larger filled zones with lower concentrations of selector (Williams, University of Sunderland, B.Sc. Chemical & Pharmaceutical Science, final year project, 2001).

#### **4.6.2 Features of the electropherograms**

There were a number of features on some electropherograms observed during these studies. In cases where no peaks were observed at all could have been caused by the biomacromolecule masking the UV absorbance of the analyte or that the analyte had a long migration such that it did not pass the detector during the analytical run. Other features will be discussed in detail in Chapter 6. These are spontaneous peak markers and baselines shifts, e.g. Figs. 42, 49 and 50, and the electropherograms of ibuprofen which exhibit a dip in the baseline prior to a partial resolution of the enantiomers, Fig. 46.



## Chapter 5    Addition of modifiers to the CE run buffer

### 5.1    Introduction

Using CE, protein affinity chiral separations may be obtained using small amounts of protein. Another aspect of the use of CE for protein affinity separations is that the method protocol can easily be modified to include the addition of other chemical entities to the run buffer. This readily provides a vehicle for the study of a wide range of variables on protein ligand interactions. Such studies could be used to probe the very nature of the drug-protein interactions and importantly might in principle provide a means of improving chiral selectivity.

The addition of certain modifiers to the run buffer may improve the overall chiral selectivity of the system by slightly altering the tertiary structure of the protein so that the difference between the three-point interactions of the enantiomers [Dalglish 1952] with the protein would be more pronounced. The modifiers used need not be restricted to those that might occur in nature. For example, the modifier  $\beta$ -cyclodextrin, could improve the solubility of hydrophobic analytes to give an obvious practical benefit but also would give rise to a mixed chiral selector system. If the chiral selectors are complementary with respect to their breadth of spectrum then it is possible that the mixed system might give chiral separations for a wider range of compounds and in rare cases it might even be possible to observe synergistic effects.

The addition of competing ligands to the system can be used to probe the different binding sites of the protein [Hage 1995, Noctor 1993 & Wainer 1993]. Such information can be used to ascertain, for example, the interaction of different drugs on the protein and to observe any potential preferential displacement of one enantiomer over the other. In this way the concentration of an unbound drug could be predicted in the presence of a competing ligand.

To use CE in this way almost as a model of *in vivo* behaviour would require extensive development and validation work to be carried out. The aim here was to only investigate the extent to which selected modifiers affected migration, selectivity, resolution and establish the levels of modifiers required to observe the effects.

## 5.2 Addition of metal ions to protein affinity CE

Metal<sup>2+</sup> ions offer interesting possibilities when used to study protein affinity CE. They are known to bind to proteins and can therefore change the tertiary structure of the protein [Peters 1977]. This in turn can lead to a change in the chiral selectivity of the protein and potentially give improved separations. However, the addition of metal<sup>2+</sup> ions to the normal buffer of 67 mM phosphate was not possible since this caused the precipitation of the inorganic salt. Consequently the make-up of the run buffer was changed to 67 mM borate which did not cause any inorganic salt precipitation.

As already demonstrated, only small amounts of protein are consumed in protein affinity CE. It was therefore possible to study HSA, which was available in more limited quantities, rather than BSA. The test analytes, tryptophan and kynurenine enantiomers, had both been separated using HSA (Chapter 4). Since the buffer had been changed, injections of the test analytes were made without any metal ions present for comparison.

The results for the addition of metal ions on the resolution of tryptophan enantiomers are shown in Table 62 and the corresponding electropherograms in Figures 63 – 65.

Table 62 Selectivity of tryptophan enantiomers with the addition of metal ions.

Metal Ion	t <sub>1</sub>	t <sub>2</sub>	Resolution
None	16.00	16.25	1.5
Manganese	15.94	16.08	0.33
Zinc	16.09	16.22	0.13

The addition of the metal ions had only a small effect on the overall migration times of the tryptophan. Despite this, the resolution of the tryptophan enantiomers by HSA was reduced by the presence of the metal ions, the slight drop in selectivity being sufficient to bring about a loss of resolution. There was no significant change in efficiency. However, it would have been difficult to observe any improvement in efficiency, given that using borate buffer the efficiency was already good, the characteristic broadness of the peak of the second migrating enantiomer as seen with phosphate buffer not being observed.

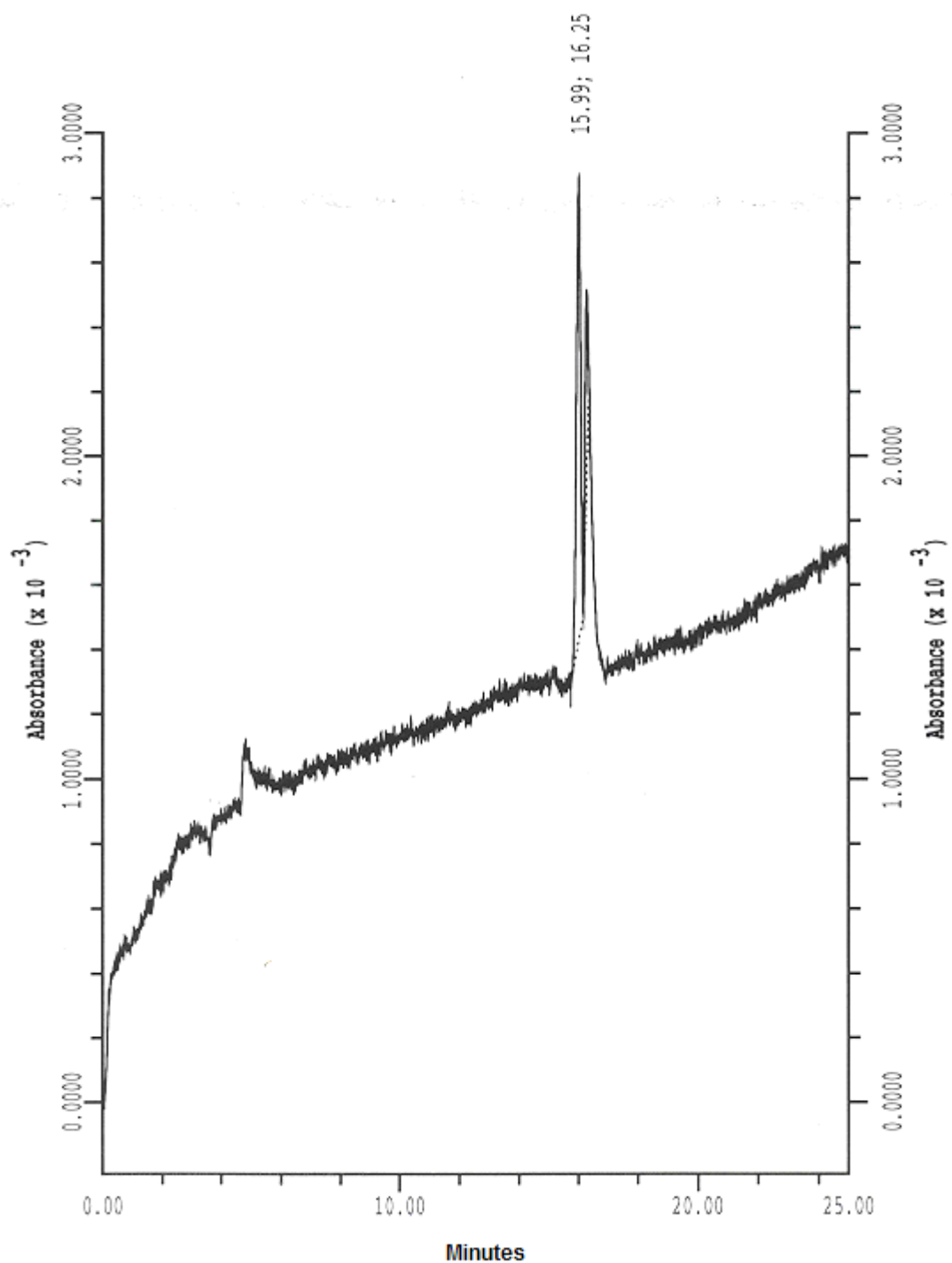


Fig. 63 CE of tryptophan enantiomers using 67mM borate buffer. Conditions: run buffer. 30  $\mu$ M HSA, 67 mM sodium borate (pH 7.4); capillary, CElect P150, 37 cm (30 cm to detector)  $\times$  50  $\mu$ m i.d.; instrument, PACE 2050; temperature, 25  $^{\circ}$ C; voltage 8 kV; detection wavelength, 280 nm.

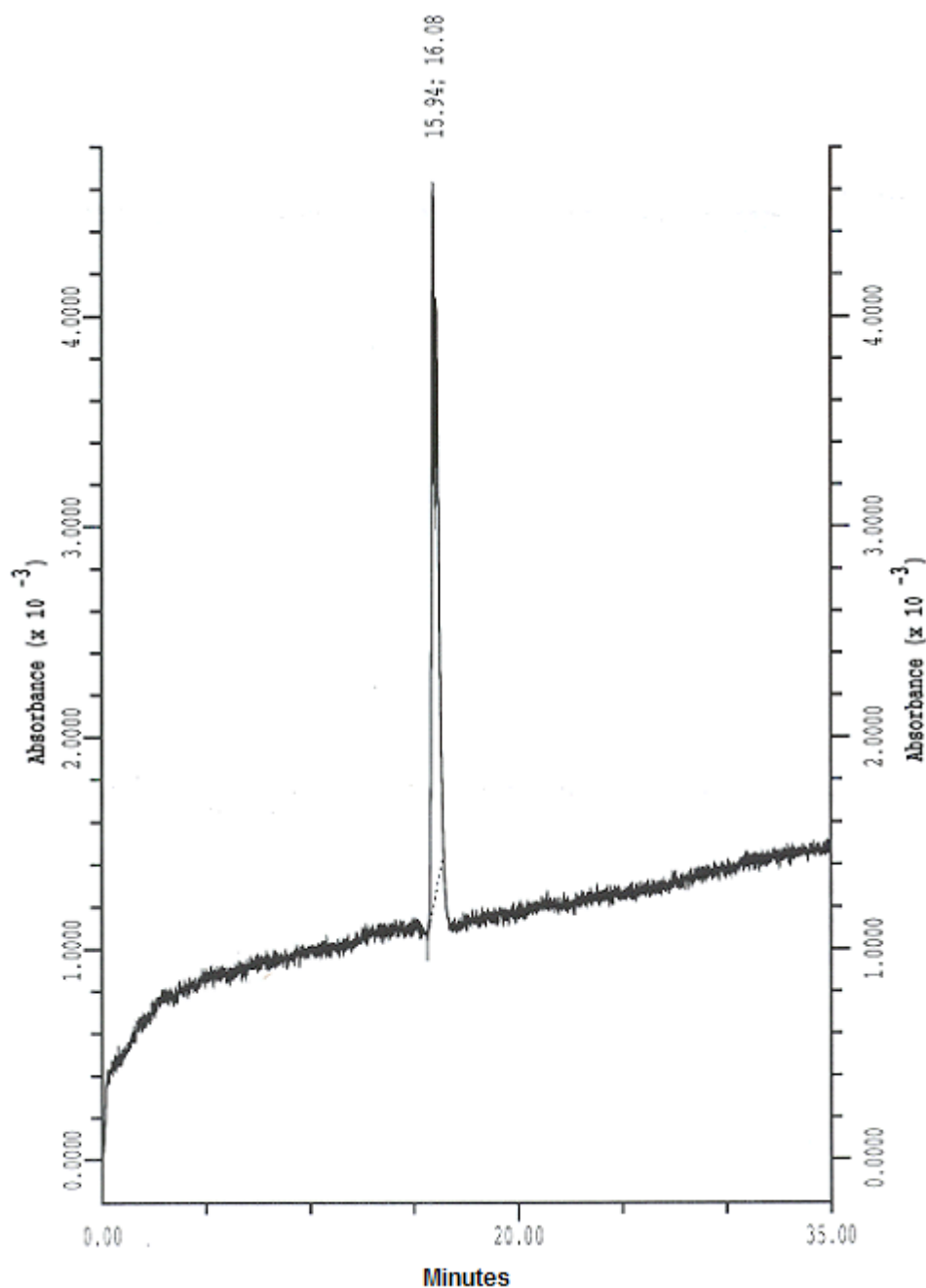


Fig. 64 CE of tryptophan enantiomers in the presence of manganese. Conditions: run buffer, 30  $\mu\text{M}$  HSA, 30  $\mu\text{M}$   $\text{Mn}^{2+}$ , 67 mM sodium borate (pH 7.4); capillary, CElect P150, 37 cm (30 cm to detector)  $\times$  50  $\mu\text{m}$  i.d.; instrument, PACE 2050; temperature, 25  $^{\circ}\text{C}$ ; voltage 8 kV; detection wavelength, 280 nm.

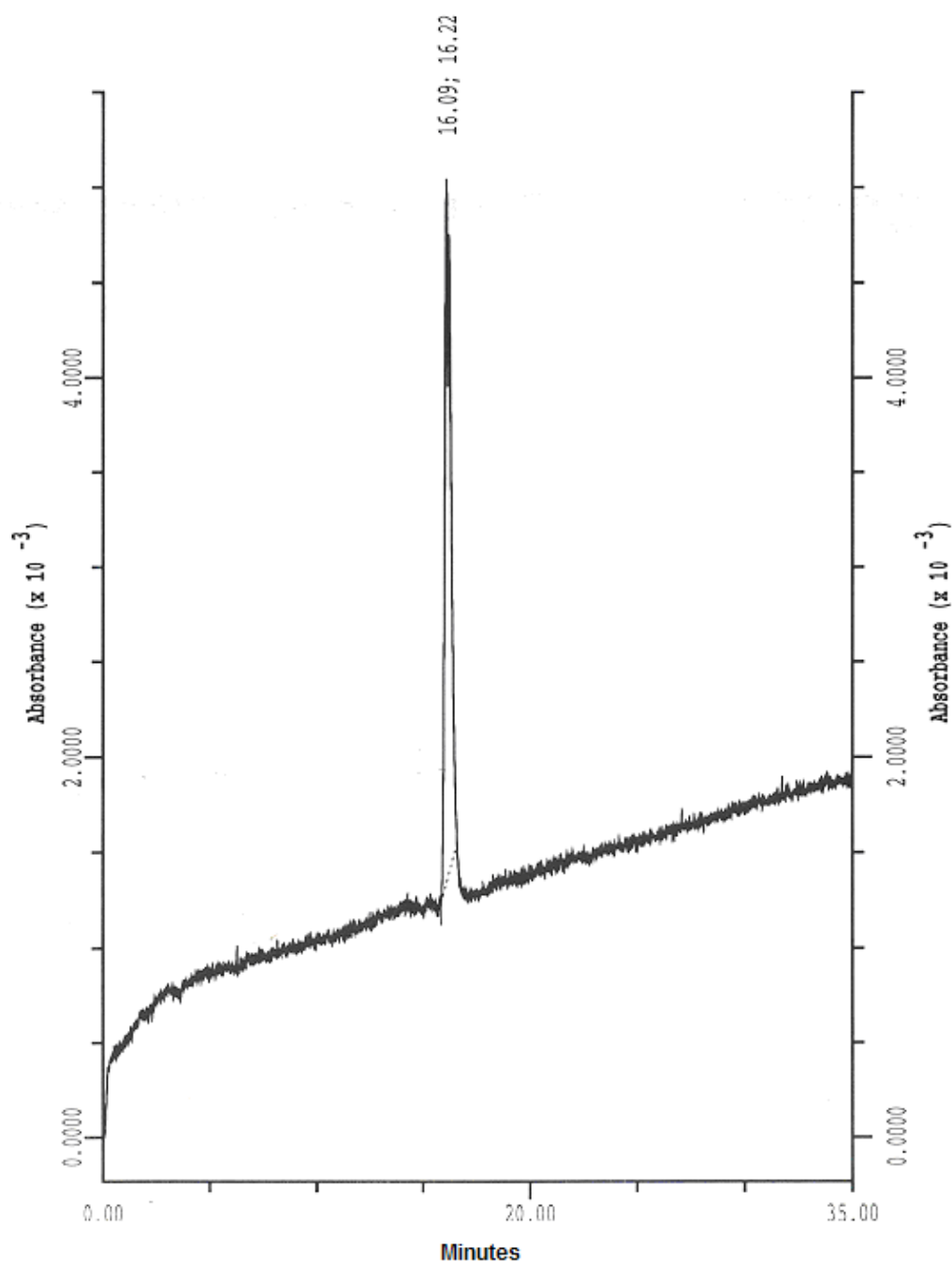


Fig. 65 CE of tryptophan enantiomers in the presence of zinc . Conditions: run buffer. 30  $\mu\text{M}$  HSA, 30  $\mu\text{M}$   $\text{Zn}^{2+}$ , 67 mM sodium borate (pH 7.4); capillary, CElect P150, 37 cm (30 cm to detector)  $\times$  50  $\mu\text{m}$  i.d.; instrument, PACE 2050; temperature, 25  $^{\circ}\text{C}$ ; voltage 8 kV; detection wavelength, 280 nm.

The results for the addition of metal ions on the resolution of kynurenine enantiomers are shown in Table 66 and the corresponding electropherograms Figures 67 – 69.

Table 66 Selectivity of kynurenine enantiomers with the addition of metal ions.

Metal Ion	t <sub>1</sub>	t <sub>2</sub>	Resolution
None	15.93	16.20	1.6
Manganese	16.18	16.44	1.0
Zinc	16.20	16.32	0.1

The results for kynurenine enantiomers were very similar to those for tryptophan in that there was little overall change in the migration times of the kynurenine enantiomers and there was a reduction in the resolution with the addition of both manganese and zinc. However, there was a clear difference in that there was a distinction between the effects of the two metals. Zinc caused the greatest decrease in resolution, perhaps because the zinc was bound more to the binding site of the protein compared to the manganese so preventing the kynurenine enantiomers from binding to the protein. When metal ions bind to HSA they do so to one major binding site [Peters 1977] so perhaps this is also the binding site for tryptophan and kynurenine. The migration data is not inconsistent with the original resolution being generated by the second migrating enantiomer being bound to the protein but this generating only a small increase in migration time compared the unbound first migrating enantiomer. In this way, when the second enantiomer cannot bind to the

protein because of the metal ions, resolution is lost by reduction of its migration time. The fact that the migration data was not exactly consistent with this scenario was probably down to the precision of the migration times relative to the minor changes in relative migration taking place. This could have been calculated by the relative migration of the EOF peak. Unfortunately, there were no such peaks in the electropherograms.

Any direct interaction of the analytes with the metal ion would have been more likely to manifest itself in a significant change in migration time. Similarly the interaction of the metal with the specific binding site for the L-tryptophan while, being enough to reduce or eliminate enantioselectivity, was not so strong as to affect the electrophoretic mobility of the HSA. Different levels of metal ions could have been applied but lower levels might well have had a smaller effect that would have been difficult to measure and higher levels might simply have reduced the resolution to zero. It was possible that at different levels something very different might have been observed because of a change of mechanism. However it was thought that the chances of this were slim and so it was decided to proceed to other options which it was thought would have a greater chance of success. Also it was difficult to envisage any possible useful analytical application of the reduced resolution. It could be used to control situations where a method is not useful because of excessive chiral resolution leading to an excessive run time but this was not the case with HSA and there are simpler ways of doing this such as reducing the protein concentration.



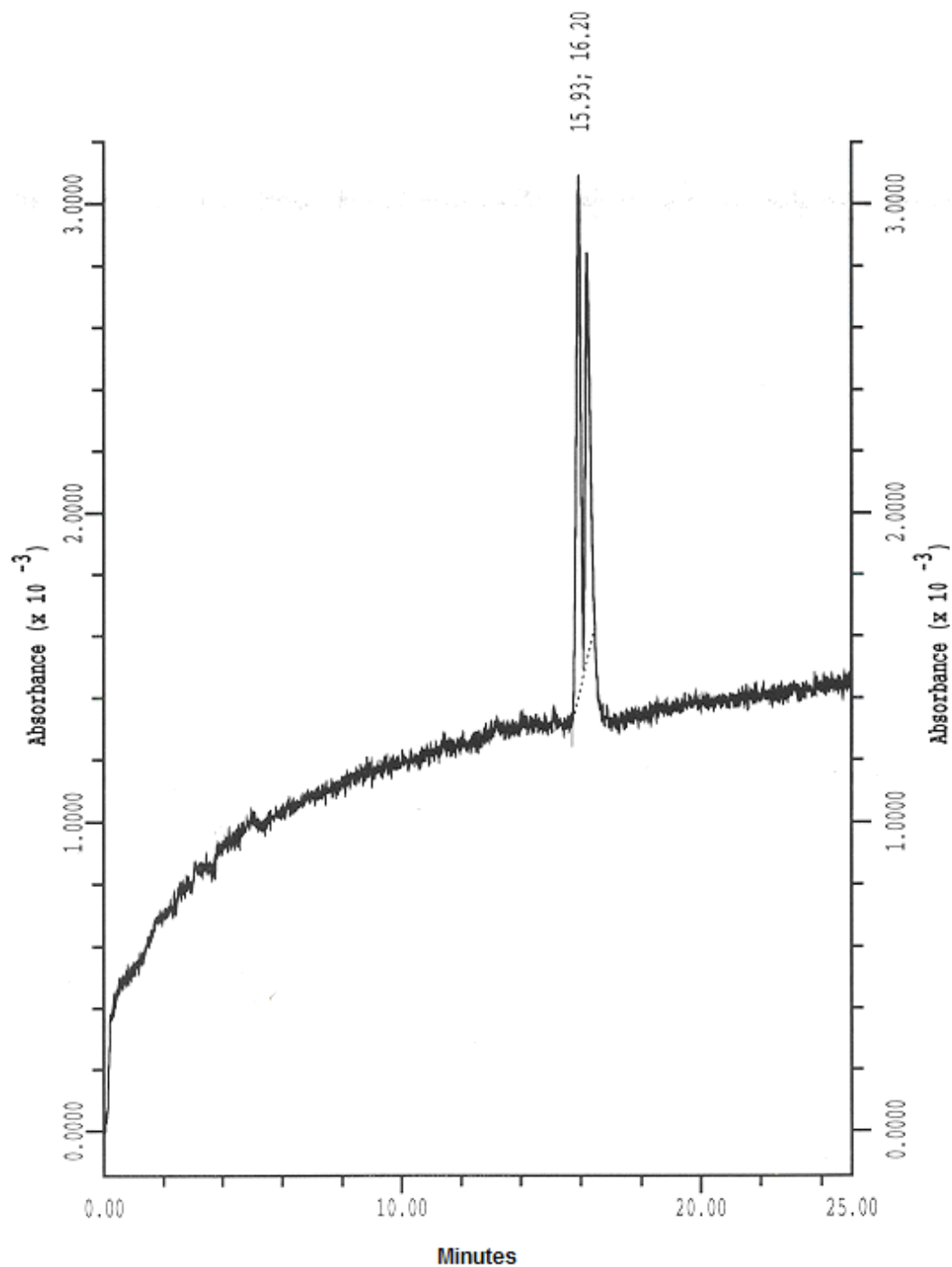


Fig. 67 CE of kynurenine enantiomers using 67mM borate buffer. Conditions: run buffer. 30  $\mu$ M HSA, 67 mM sodium borate (pH 7.4); capillary, CElect P150, 37 cm (30 cm to detector)  $\times$  50  $\mu$ m i.d.; instrument, PACE 2050; temperature, 25  $^{\circ}$ C; voltage 8 kV; detection wavelength, 254 nm.

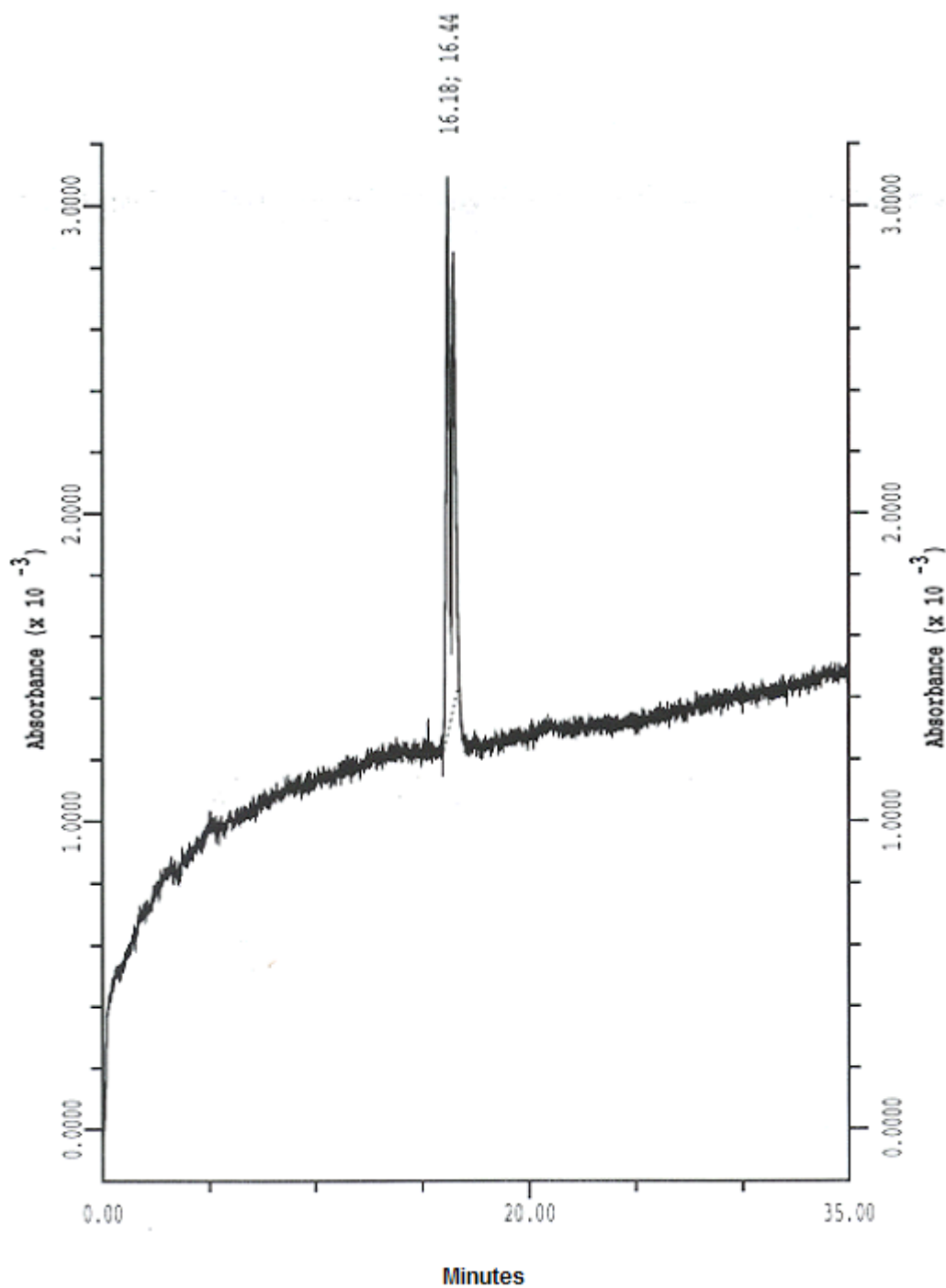


Fig. 68 CE of kynurenine enantiomers in the presence of manganese . Conditions: run buffer. 30  $\mu\text{M}$  HSA, 30  $\mu\text{M}$   $\text{Mn}^{2+}$ , 67 mM sodium borate (pH 7.4); capillary, CElect P150, 37 cm (30 cm to detector)  $\times$  50  $\mu\text{m}$  i.d.; instrument, PACE 2050; temperature, 25  $^{\circ}\text{C}$ ; voltage 8 kV; detection wavelength, 254 nm.

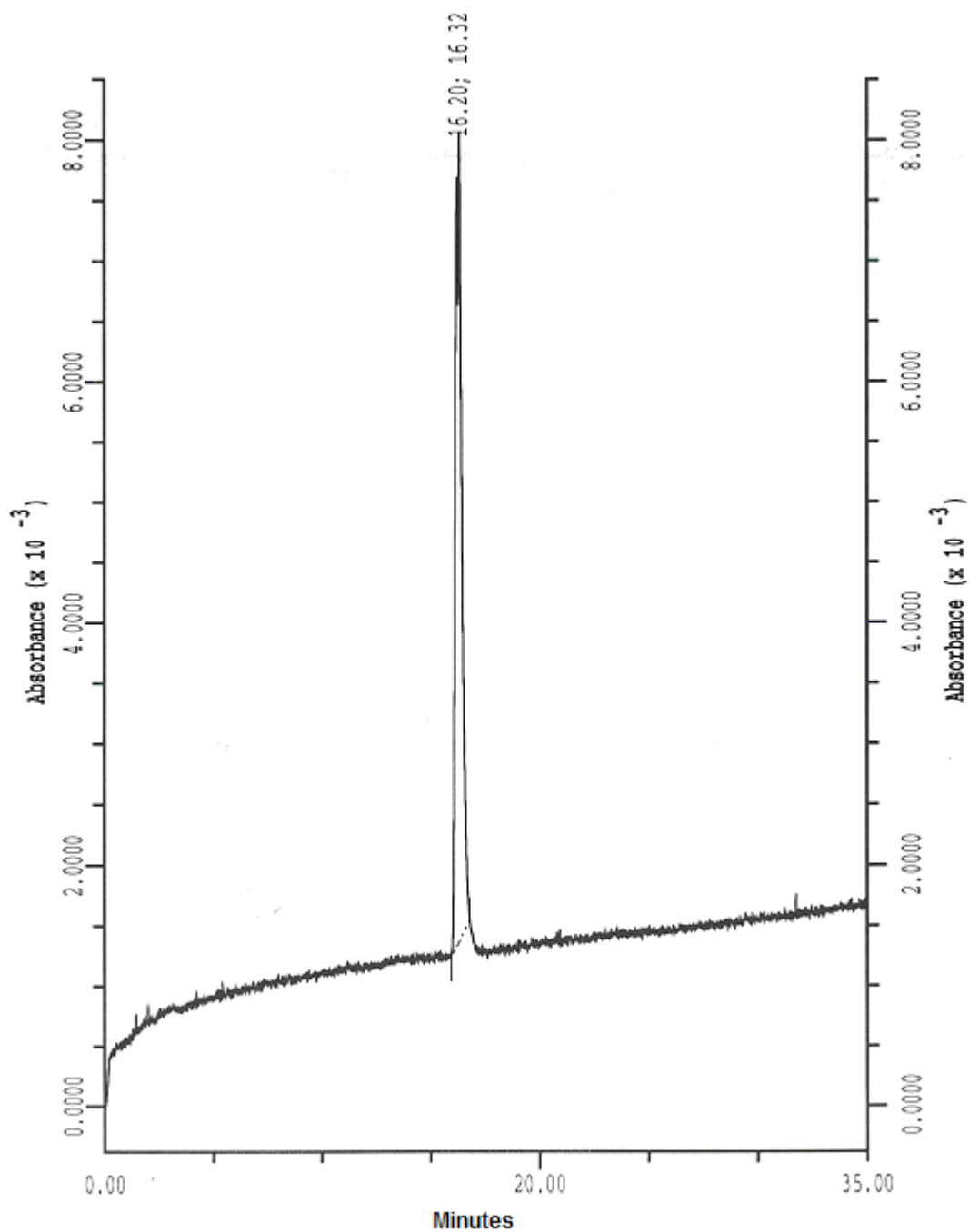


Fig. 69 CE of kynurenine enantiomers in the presence of zinc. Conditions: run buffer. 30  $\mu\text{M}$  HSA, 30  $\mu\text{M}$   $\text{Zn}^{2+}$ , 67 mM sodium borate (pH 7.4); capillary, CElect P150, 37 cm (30 cm to detector)  $\times$  50  $\mu\text{m}$  i.d.; instrument, PACE 2050; temperature, 25  $^{\circ}\text{C}$ ; voltage 8 kV; detection wavelength, 254 nm.

### **5.3 Addition of $\beta$ -cyclodextrin to a protein affinity CE buffer**

#### **5.3.1 Analysis of tryptophan enantiomers**

The protein affinity CE protocol for the resolution of tryptophan enantiomers had proved to be successful and was the obvious choice to use for studying the addition of  $\beta$ -cyclodextrin to the run buffer in an attempt to assess the possibilities for complementary or even synergistic chiral resolution. Interestingly there has been no mention of using  $\beta$ -cyclodextrins to separate tryptophan or tryptophan derivatives in the literature. The results are shown graphically in Fig. 70 for the effect on the migration times of the enantiomers and Fig. 71 for the effect on the resolution. The corresponding electropherograms are shown in Figs. 72-77.

The addition of  $\beta$ -cyclodextrin to the run buffer gave rise to significant variation of the resolution and the overall migration times of the tryptophan enantiomers. Certainly the changes were significant enough to suggest that the cyclodextrin was having an influence, albeit not necessarily directly. However, there was no specific trend in either the migration times or the resolution. In all cases the tryptophan enantiomers were baseline resolved. Therefore it was concluded that the  $\beta$ -cyclodextrin did not change the binding of the tryptophan to the BSA as was indicated by the peak shape of the second migrating enantiomer which was consistent throughout the range of  $\beta$ -cyclodextrin concentrations even though there was variability in resolution and migration times. Given this and the almost erratic nature of the changes in resolution, the results were considered to be not sufficiently encouraging to proceed to a full-scale optimisation exercise. With the benefit of hindsight gained from the increasing use of sulphated cyclodextrins in CE [Iwata 2002, Aumatell 1994 & Christians 2000], it might have been better to have used a  $\gamma$ -sulphated (or amino) cyclodextrin, the  $\gamma$  to obtain a better interaction with the tryptophan and the charged cyclodextrin to obtain a better separation window.

One observation from Figs. 73, 74 and 76 was that there was a stepped baseline. However, the stepped baseline always occurred after the two enantiomers had eluted and did not interfere with the experiment. Another feature of the stepped baseline was the apparently random nature of when it occurred. This can be seen in the electropherograms in Figures 72, 75 and 77, which were run using similar conditions, but where no such stepped baseline was observed. The drop in baseline could have been caused by BSA depletion but importantly the level of BSA in the capillary, at least at the point of the detector was constant at the time of the elution of the enantiomers.

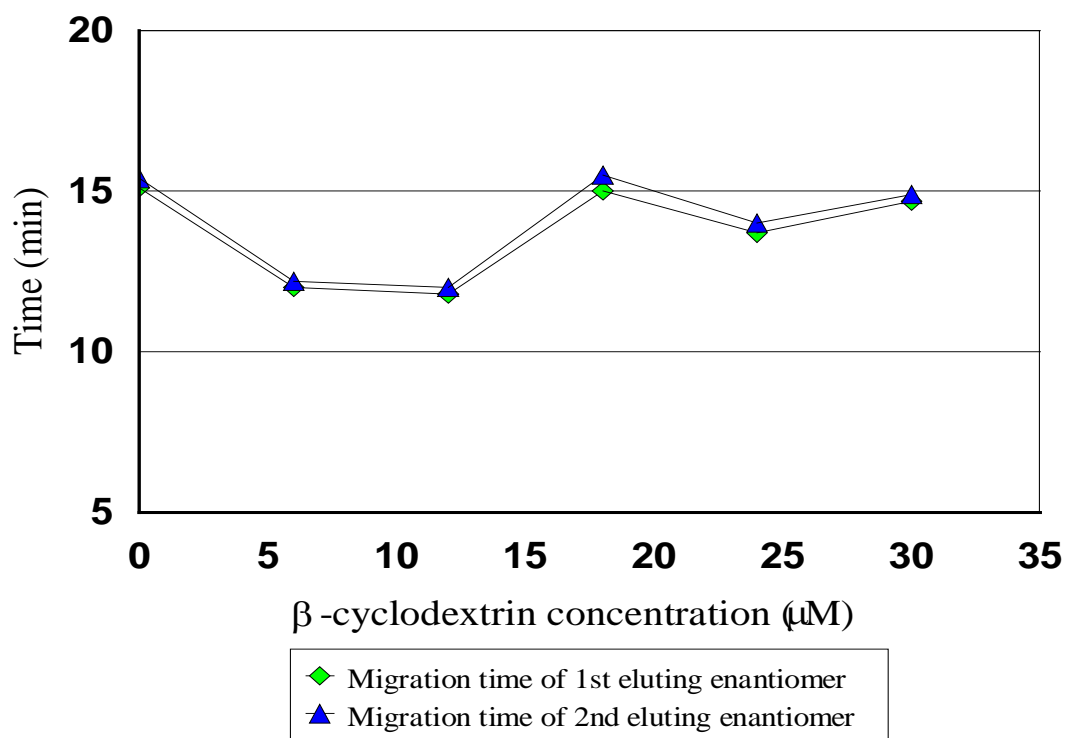


Fig. 70 Migration times of tryptophan enantiomers with the addition of  $\beta$ -cyclodextrin. Conditions: run buffer, 30  $\mu\text{M}$  BSA, 67 mM phosphate (pH7.4); capillary, CElect P150, 37 cm (30 cm to detector)  $\times$  50  $\mu\text{m}$  i.d.; instrument, PACE 2050; temperature, 25  $^{\circ}\text{C}$ ; voltage 8 kV; detection wavelength, 280 nm.

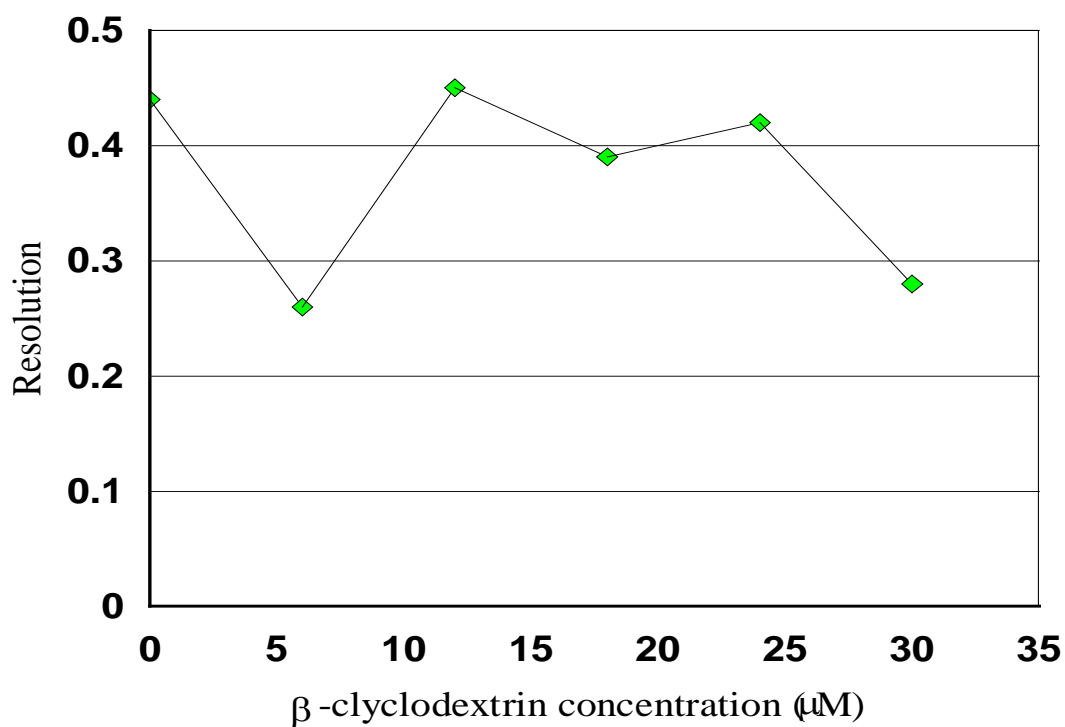


Fig. 71 Resolution of tryptophan enantiomers with the addition of  $\beta$ -cyclodextrin. Conditions: run buffer, 30  $\mu\text{M}$  BSA, 67 mM phosphate (pH7.4); capillary, CElect P150, 37 cm (30 cm to detector)  $\times$  50  $\mu\text{m}$  i.d.; instrument, PACE 2050; temperature, 25  $^{\circ}\text{C}$ ; voltage 8 kV; detection wavelength, 280 nm.

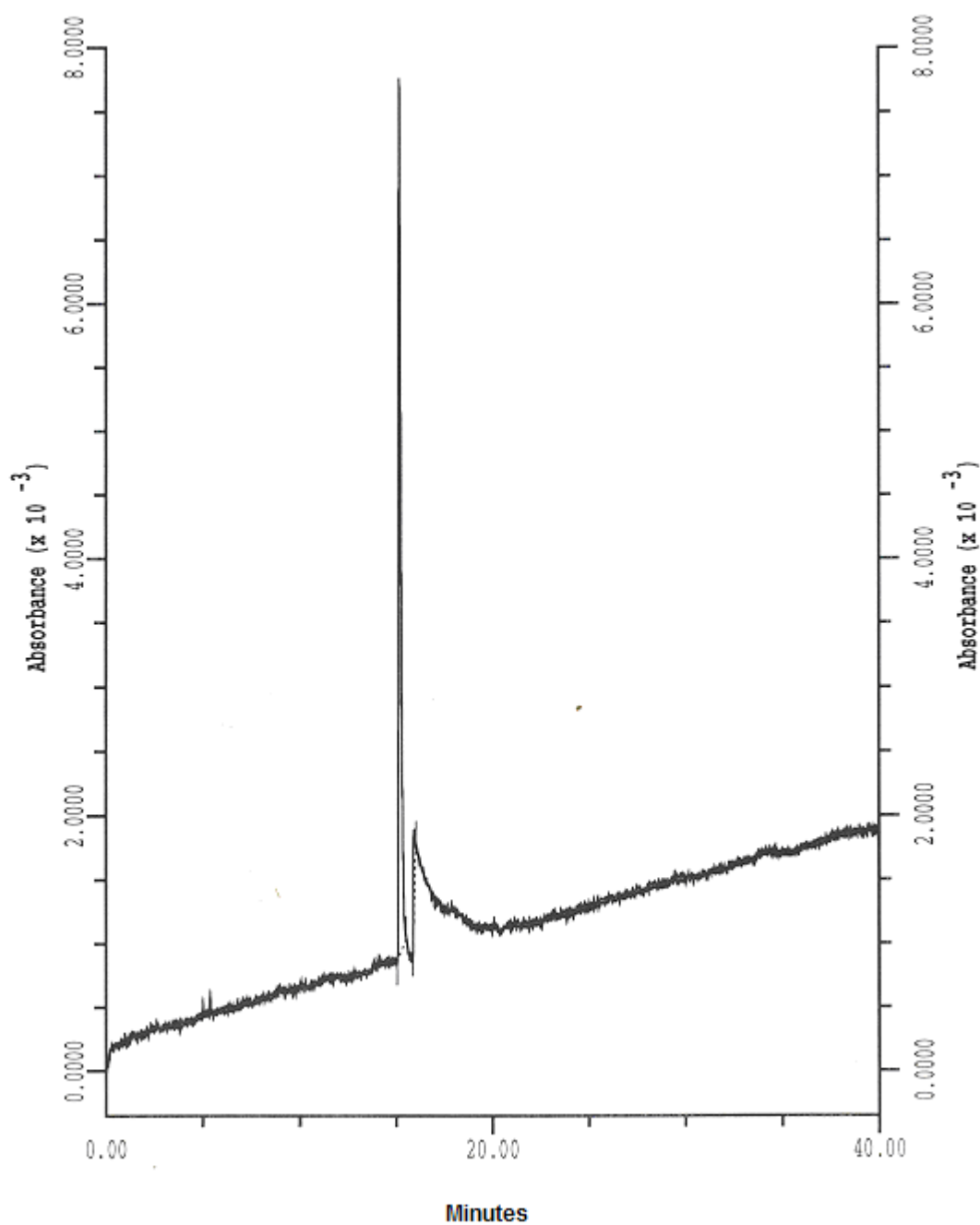


Fig. 72 Resolution of tryptophan enantiomers. Conditions: run buffer, 30  $\mu\text{M}$  BSA, 67 mM phosphate (pH7.4); capillary, CElect P150, 37 cm (30 cm to detector)  $\times$  50  $\mu\text{m}$  i.d.; instrument, PACE 2050; temperature, 25  $^{\circ}\text{C}$ ; voltage 8 kV; detection wavelength, 280 nm.



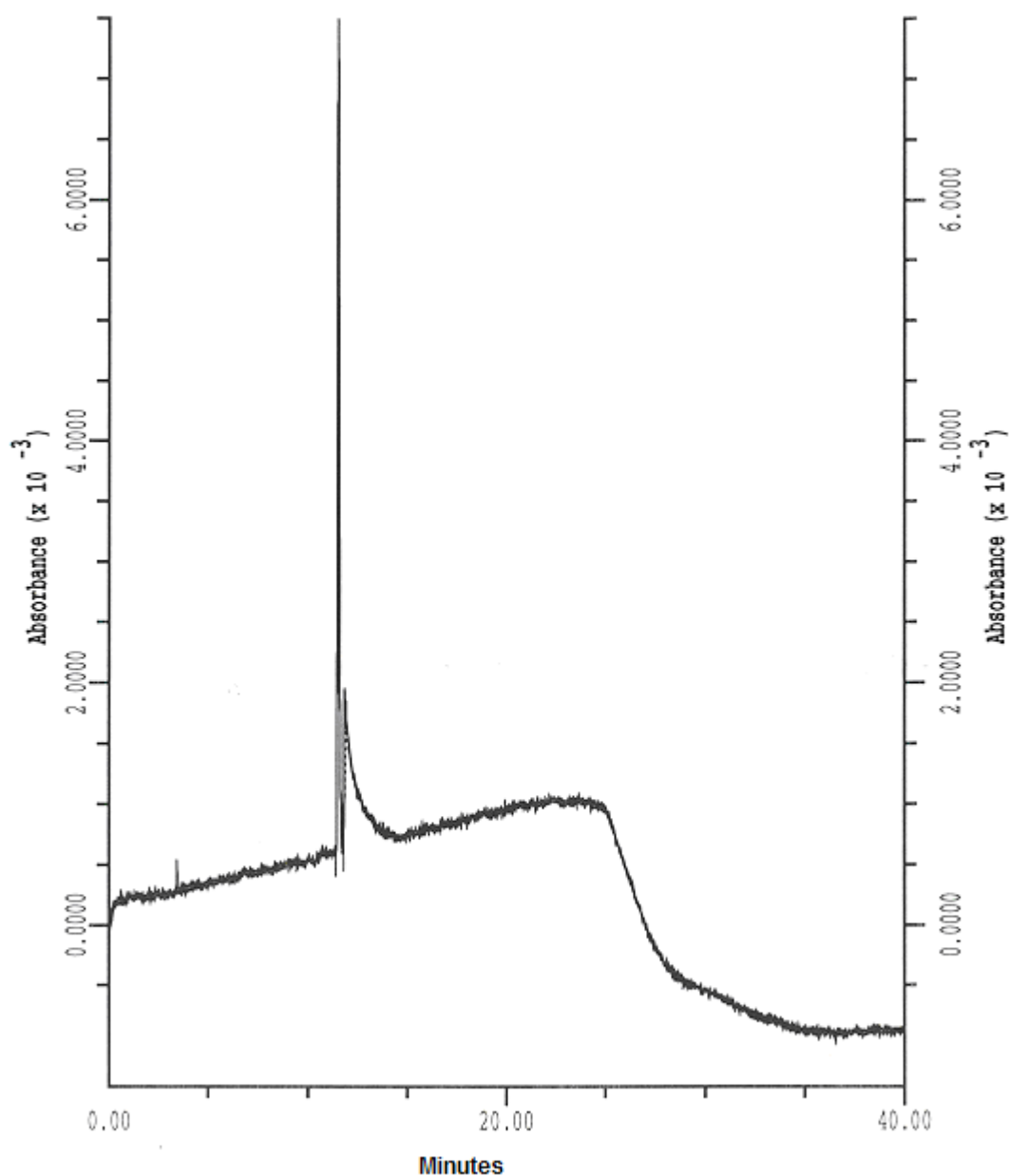


Fig. 73 Resolution of tryptophan enantiomers with 6  $\mu\text{M}$   $\beta$ -cyclodextrin. Conditions: run buffer, 30  $\mu\text{M}$  BSA, 67 mM phosphate (pH7.4), 6  $\mu\text{M}$   $\beta$ -cyclodextrin; capillary, CElect P150, 37 cm (30 cm to detector)  $\times$  50  $\mu\text{m}$  i.d.; instrument, PACE 2050; temperature, 25  $^{\circ}\text{C}$ ; voltage 8 kV; detection wavelength, 280 nm.

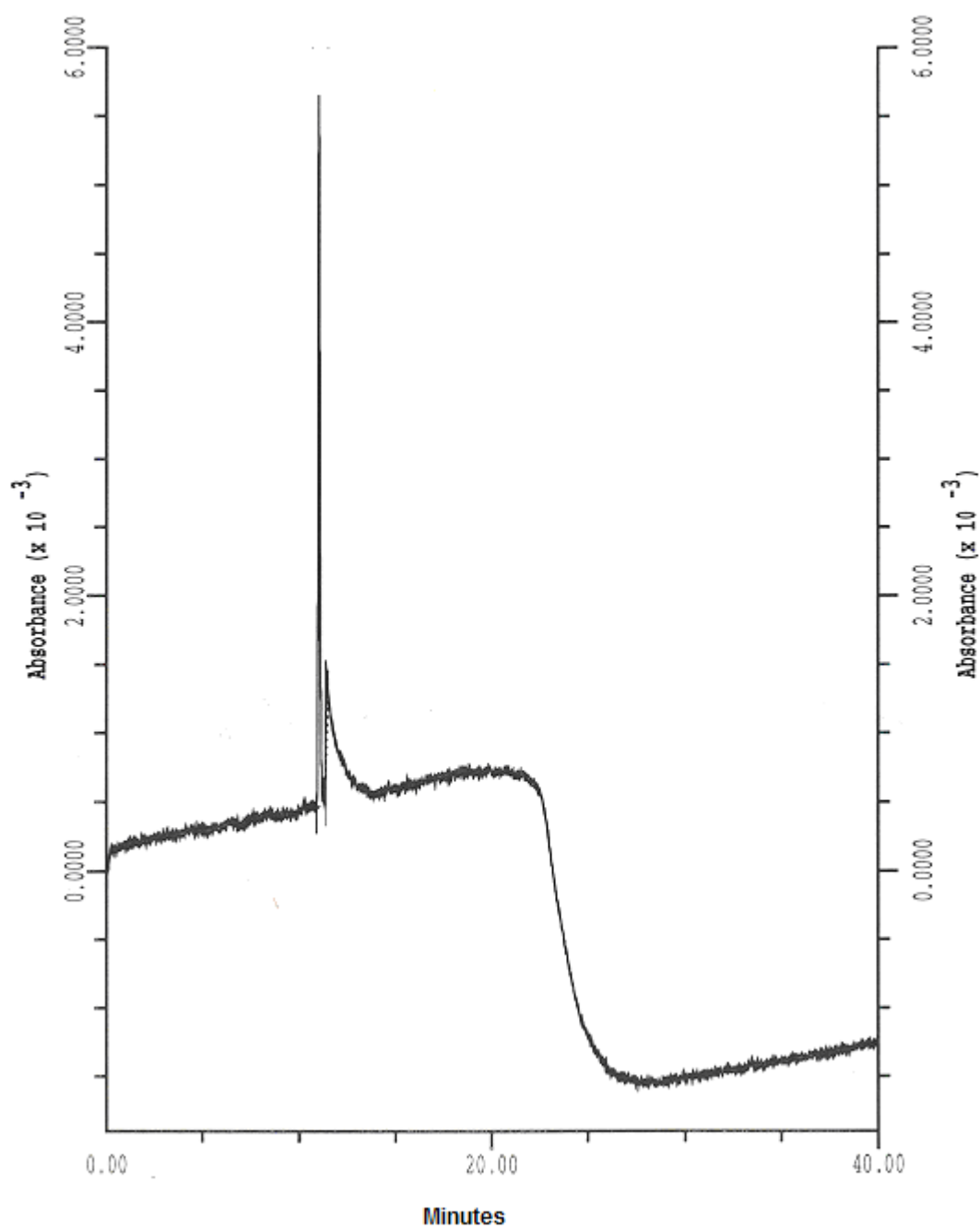


Fig. 74 Resolution of tryptophan enantiomers with 12  $\mu\text{M}$   $\beta$ -cyclodextrin. Conditions: run buffer, 30  $\mu\text{M}$  BSA, 67 mM phosphate (pH7.4), 12  $\mu\text{M}$   $\beta$ -cyclodextrin; capillary, CElect P150, 37 cm (30 cm to detector)  $\times$  50  $\mu\text{m}$  i.d.; instrument, PACE 2050; temperature, 25  $^{\circ}\text{C}$ ; voltage 8 kV; detection wavelength, 280 nm.

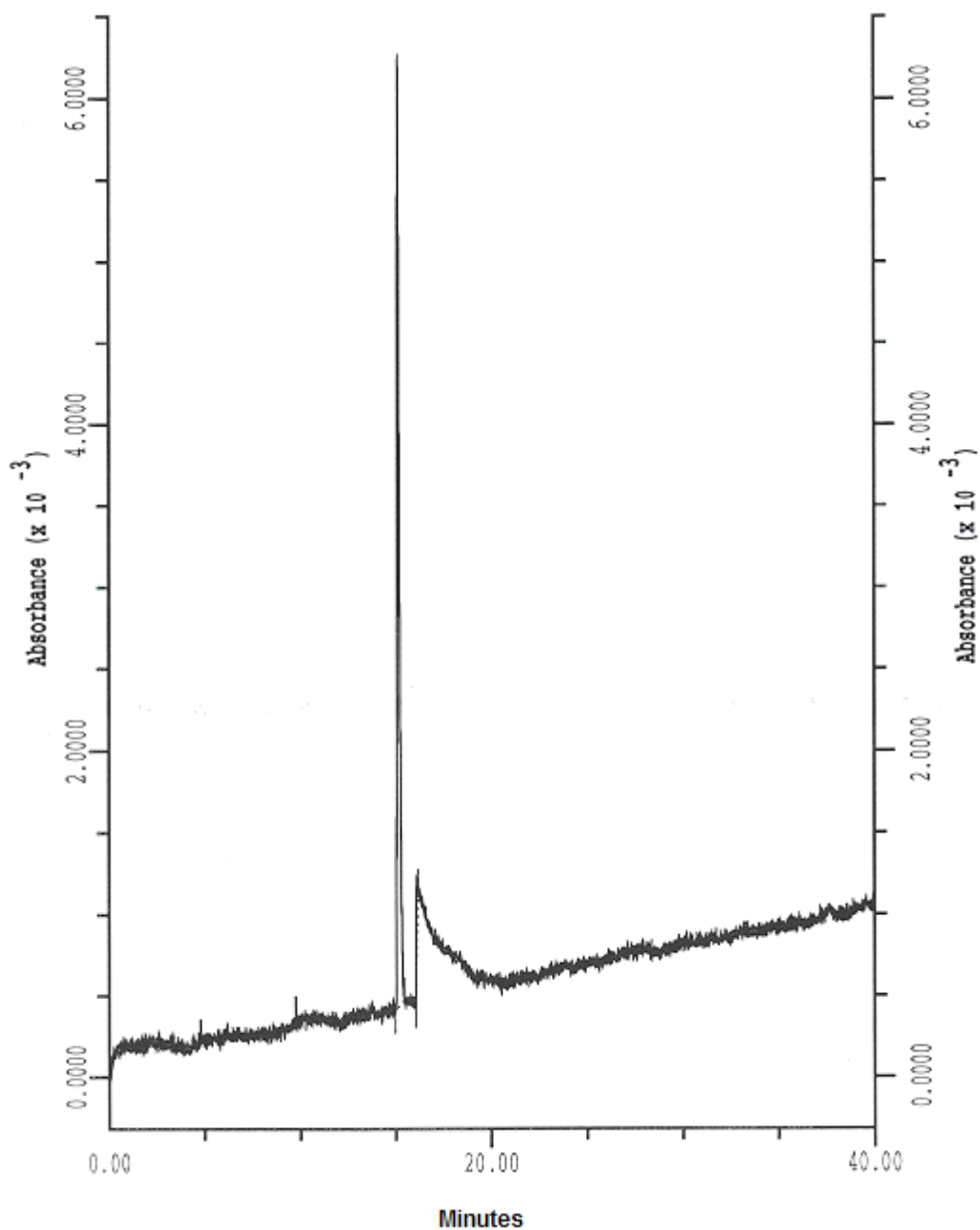


Fig. 75 Resolution of tryptophan enantiomers with 18  $\mu\text{M}$   $\beta$ -cyclodextrin. Conditions: run buffer, 30  $\mu\text{M}$  BSA, 67 mM phosphate (pH7.4), 18  $\mu\text{M}$   $\beta$ -cyclodextrin; capillary, CElect P150, 37 cm (30 cm to detector)  $\times$  50  $\mu\text{m}$  i.d.; instrument, PACE 2050; temperature, 25  $^{\circ}\text{C}$ ; voltage 8 kV; detection wavelength, 280 nm.

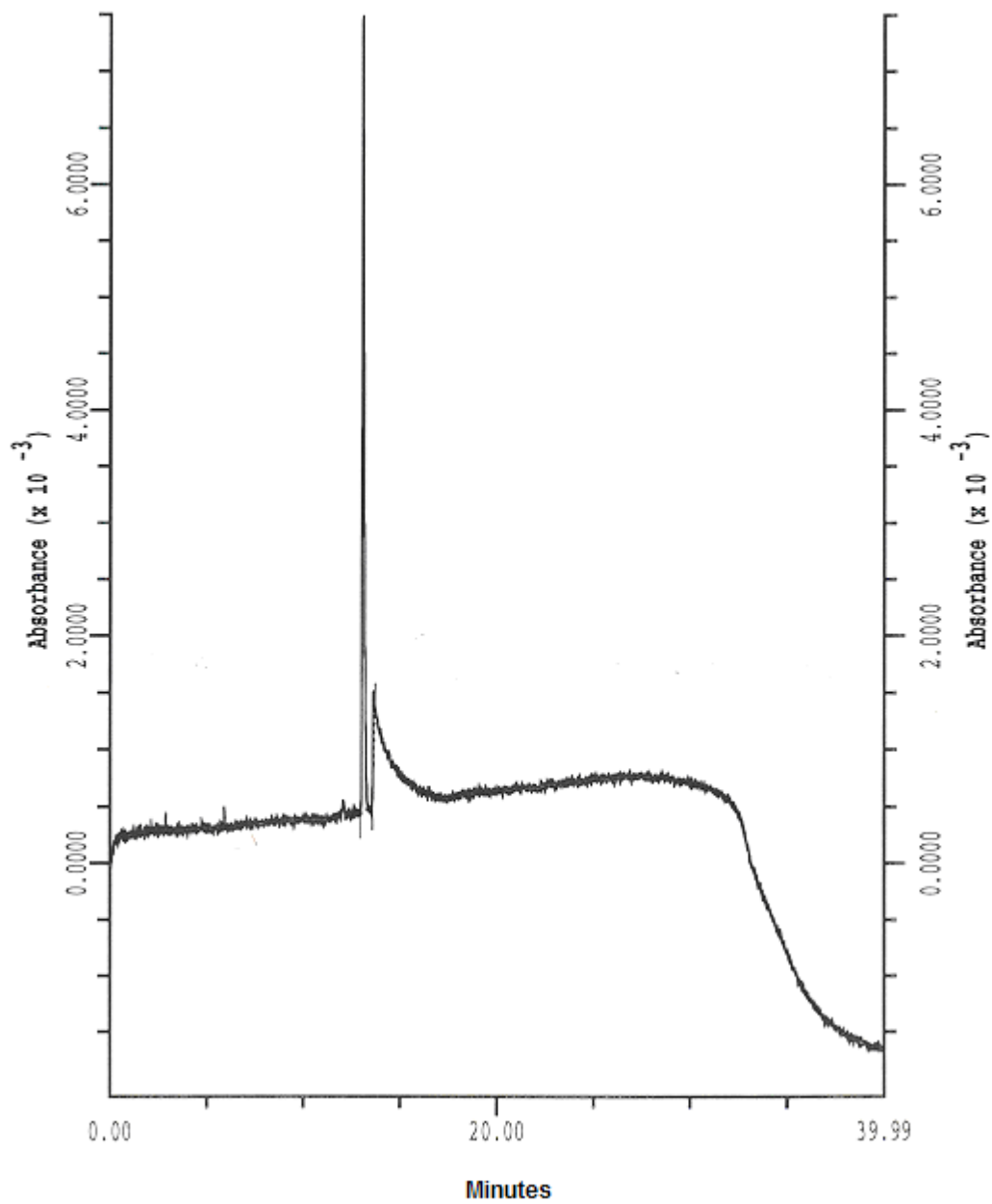


Fig. 76 Resolution of tryptophan enantiomers with 24  $\mu\text{M}$   $\beta$ -cyclodextrin. Conditions: run buffer, 30  $\mu\text{M}$  BSA, 67 mM phosphate (pH7.4), 24  $\mu\text{M}$   $\beta$ -cyclodextrin; capillary, CElect P150, 37 cm (30 cm to detector)  $\times$  50  $\mu\text{m}$  i.d.; instrument, PACE 2050; temperature, 25  $^{\circ}\text{C}$ ; voltage 8 kV; detection wavelength, 280 nm.

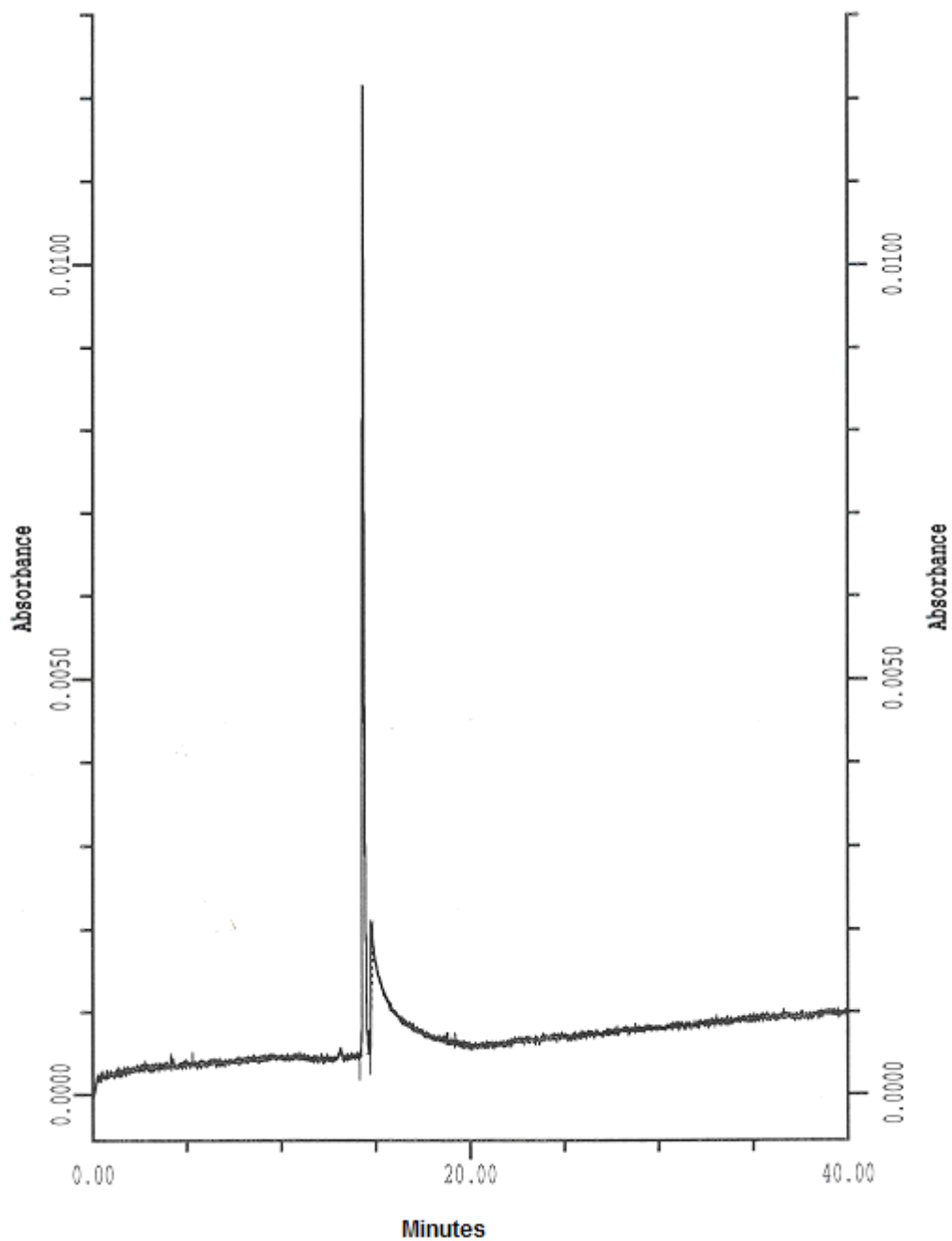


Fig. 77 Resolution of tryptophan enantiomers with 30  $\mu$ M  $\beta$ -cyclodextrin. Conditions: run buffer, 30  $\mu$ M BSA, 67 mM phosphate (pH7.4), 30  $\mu$ M  $\beta$ -cyclodextrin; capillary, CElect P150, 37 cm (30 cm to detector)  $\times$  50  $\mu$ m i.d.; instrument, PACE 2050; temperature, 25  $^{\circ}$ C; voltage 8 kV; detection wavelength, 280 nm.

### 5.3.2 Analysis of ibuprofen enantiomers

The same protocol was used to study ibuprofen enantiomers. The results are shown graphically in Fig. 78 for the effect on the migration times of the enantiomers and Fig. 79 for the effect on the resolution. The corresponding electropherograms are shown in Figs. 80-83.

The addition of  $\beta$ -cyclodextrin to the run buffer for the study of ibuprofen enantiomers did have a dramatic effect on both the migration times and resolution of the enantiomers. As the concentration of the  $\beta$ -cyclodextrin increased to 30  $\mu\text{M}$  the migration time was decreased by 50 % and the resolution decreased until no separations were observed at 30  $\mu\text{M}$   $\beta$ -cyclodextrin.

Electropherograms of ibuprofen exhibited a void immediately before the main peaks. It was thought that the electrophoretic mobility of the ibuprofen-BSA complex was less than BSA and the rate of association and dissociation of the ibuprofen and BSA was high compared to the length of the experiment, therefore a void of BSA would develop in the run buffer; a fuller discussion is presented in Chapter 6. As illustrated from the electropherograms in Figs. 80 to 83 the void was still present. However, as illustrated by Fig. 84 the area of the void decreased with increasing concentration of  $\beta$ -cyclodextrin.

Assuming that  $\beta$ -cyclodextrin does not alter the electrophoretic mobilities of either the BSA-ibuprofen complex or BSA then the area of the void can only be decreased by the changing of the rate of association and dissociation between ibuprofen and BSA. This would be the case where the ibuprofen would interact preferentially with  $\beta$ -cyclodextrin compared to BSA and this was observed as the  $\beta$ -cyclodextrin concentration increased.

However, the void was still present at a  $\beta$ -cyclodextrin concentration of 30  $\mu\text{M}$  when no chiral separations were observed. This indicated that there was still binding between the ibuprofen and BSA so a degree of chiral selectivity could be expected. It can be hypothesised that there was no separation, even though there was still some ibuprofen-BSA interaction, because the decrease in the overall migration times allowed insufficient time for the differences in electrophoretic mobilities to be observed.

The apparent increase in significance of an ibuprofen -  $\beta$ -cyclodextrin complex did not give rise to an alternative ibuprofen enantiomer resolution based on the  $\beta$ -cyclodextrin association. Again hindsight with the benefit of the knowledge of more recent work suggests that a charged cyclodextrin known to resolve ibuprofen enantiomers might have been a better option to look for competition or enhancement of resolution. An amino cyclodextrin would probably have been suitable in this case to create a greater separation window given the relatively long retention time of the BSA-bound ibuprofen.

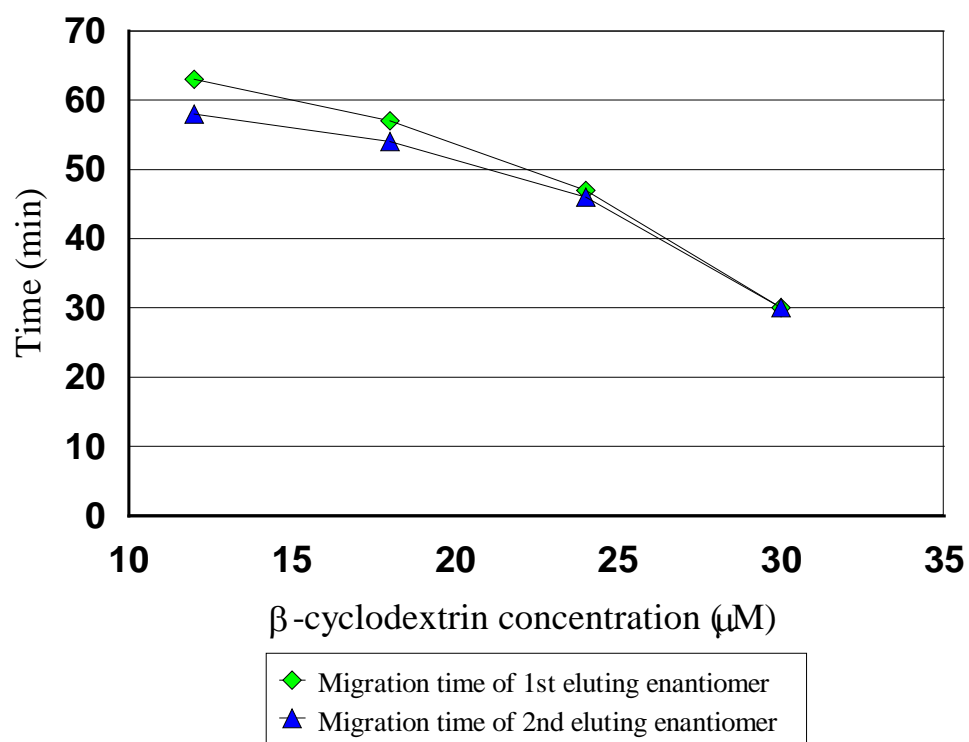


Fig. 78 Migration times of ibuprofen enantiomers with the addition of  $\beta$ -cyclodextrin. Conditions: run buffer, 30  $\mu\text{M}$  BSA, 67 mM phosphate (pH7.4); capillary, CElect P150, 37 cm (30 cm to detector)  $\times$  50  $\mu\text{m}$  i.d.; instrument, PACE 2050; temperature, 25  $^{\circ}\text{C}$ ; voltage 8 kV; detection wavelength, 254 nm.



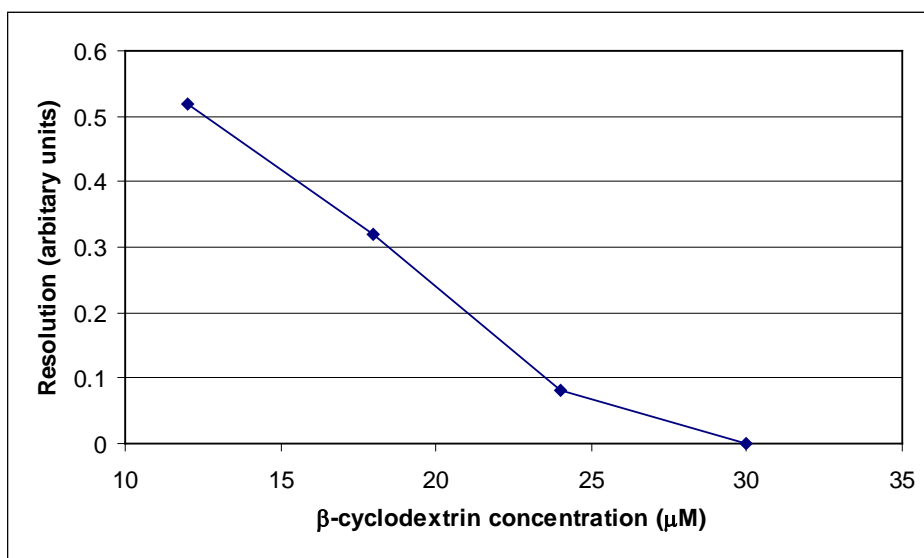


Fig. 79 Resolution of ibuprofen enantiomers with the addition of  $\beta$ -cyclodextrin. Conditions: run buffer, 30  $\mu\text{M}$  BSA, 67 mM phosphate (pH7.4); capillary, CElect P150, 37 cm (30 cm to detector)  $\times$  50  $\mu\text{m}$  i.d.; instrument, PACE 2050; temperature, 25  $^{\circ}\text{C}$ ; voltage 8 kV; detection wavelength, 254 nm.

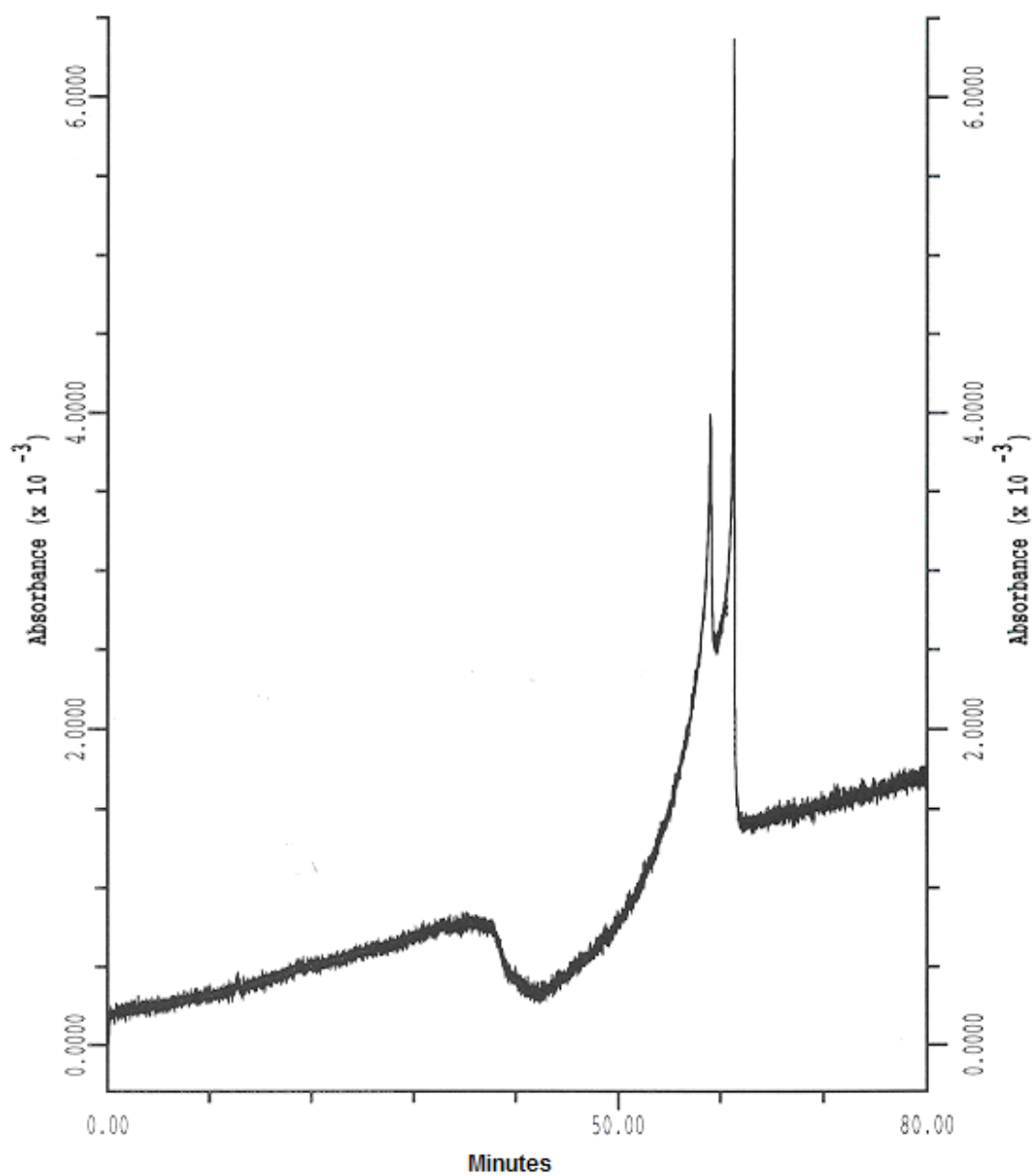


Fig. 80 CE of ibuprofen with 12  $\mu\text{M}$   $\beta$ -cyclodextrin. Conditions: run buffer, 30  $\mu\text{M}$  BSA, 67 mM phosphate (pH7.4), 12  $\mu\text{M}$   $\beta$ -cyclodextrin; capillary, CElect P150, 37 cm (30 cm to detector)  $\times$  50  $\mu\text{m}$  i.d.; instrument, PACE 2050; temperature, 25  $^{\circ}\text{C}$ ; voltage 8 kV; detection wavelength, 254 nm.

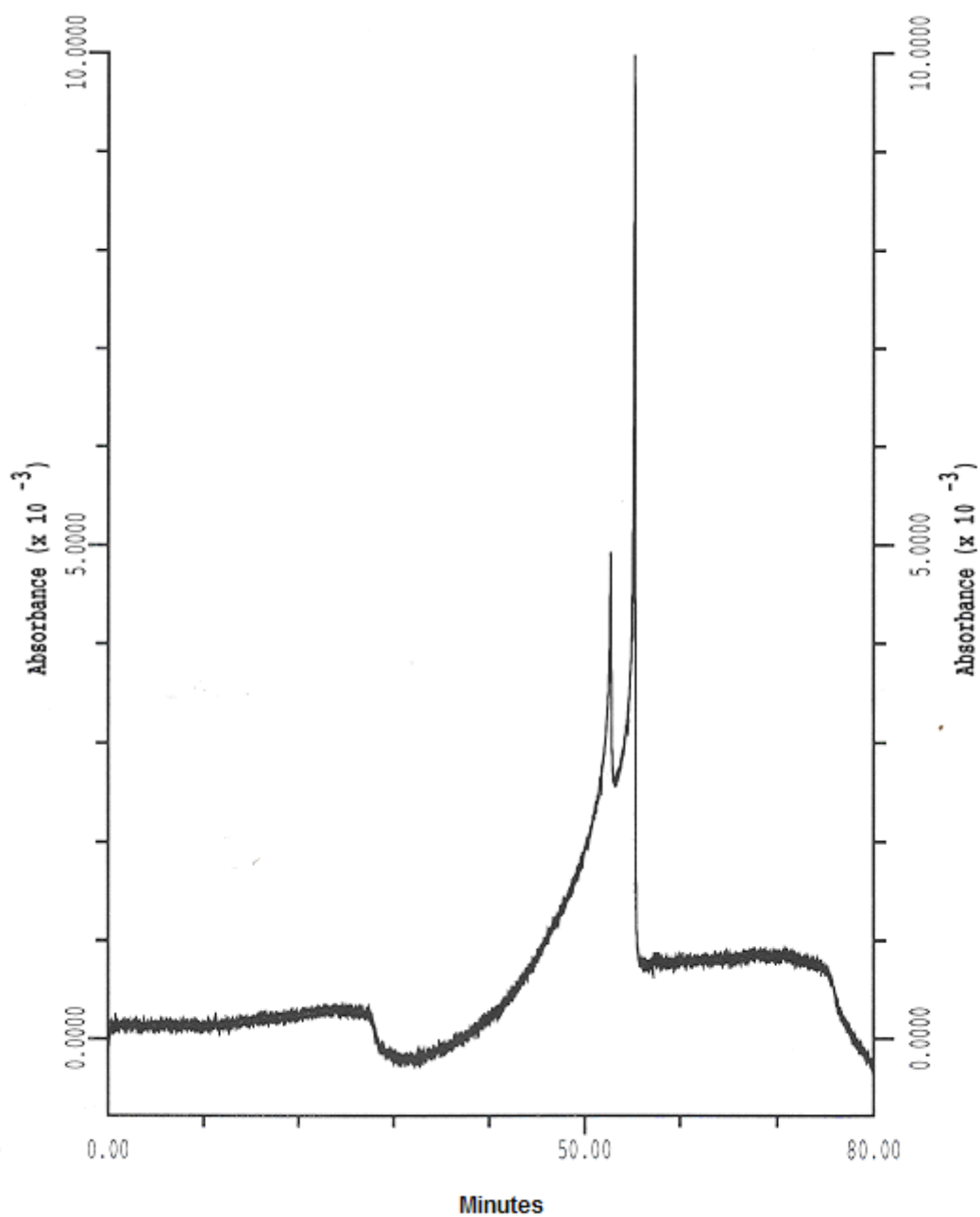


Fig. 81 CE of ibuprofen with 18  $\mu\text{M}$   $\beta$ -cyclodextrin. Conditions: run buffer, 30  $\mu\text{M}$  BSA, 67 mM phosphate (pH7.4), 18  $\mu\text{M}$   $\beta$ -cyclodextrin; capillary, CElect P150, 37 cm (30 cm to detector)  $\times$  50  $\mu\text{m}$  i.d.; instrument, PACE 2050; temperature, 25  $^{\circ}\text{C}$ ; voltage 8 kV; detection wavelength, 254 nm.

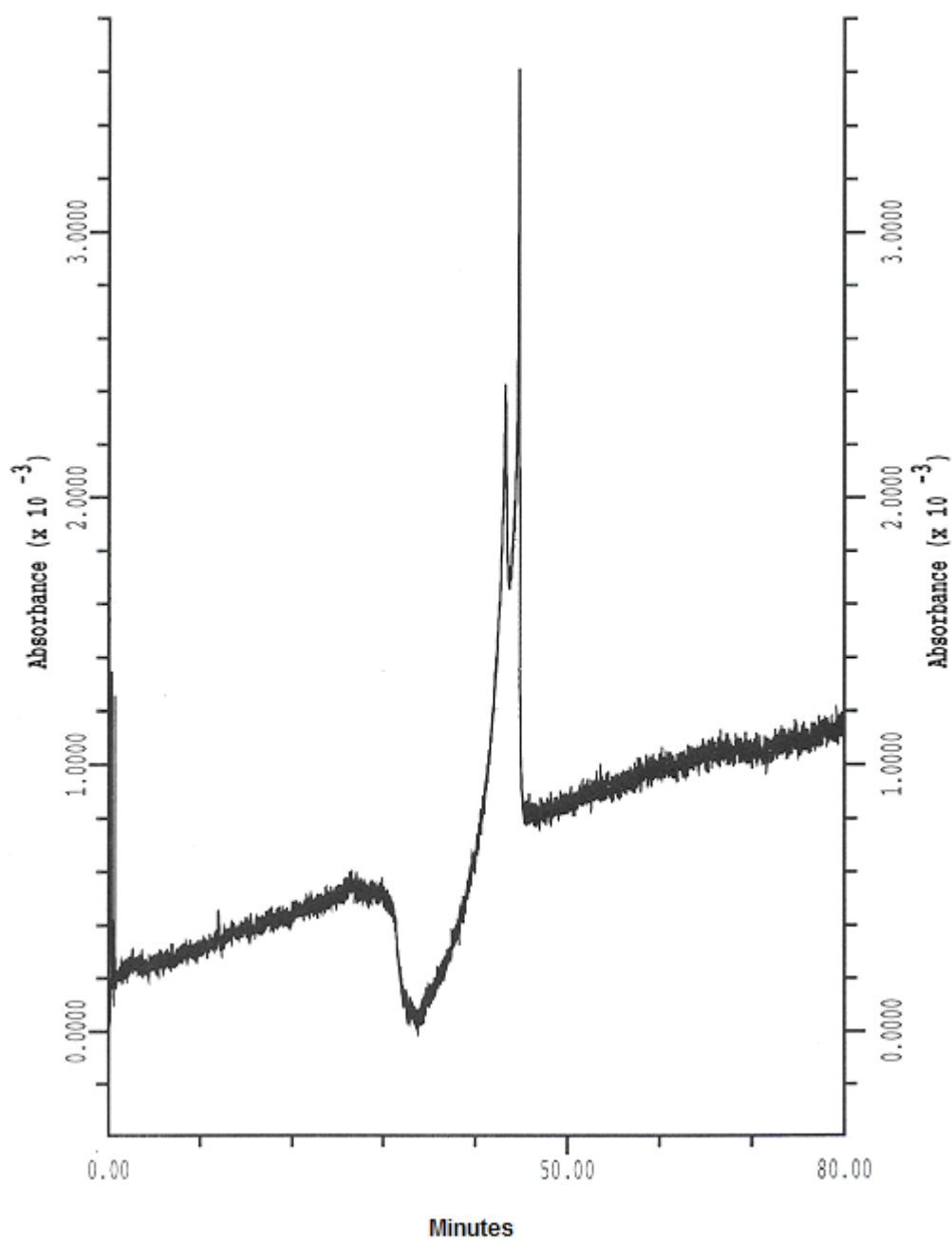


Fig. 82 CE of ibuprofen with 24  $\mu\text{M}$   $\beta$ -cyclodextrin. Conditions: run buffer, 30  $\mu\text{M}$  BSA, 67 mM phosphate (pH7.4), 24  $\mu\text{M}$   $\beta$ -cyclodextrin; capillary, CElect P150, 37 cm (30 cm to detector)  $\times$  50  $\mu\text{m}$  i.d.; instrument, PACE 2050; temperature, 25  $^{\circ}\text{C}$ ; voltage 8 kV; detection wavelength, 254 nm.

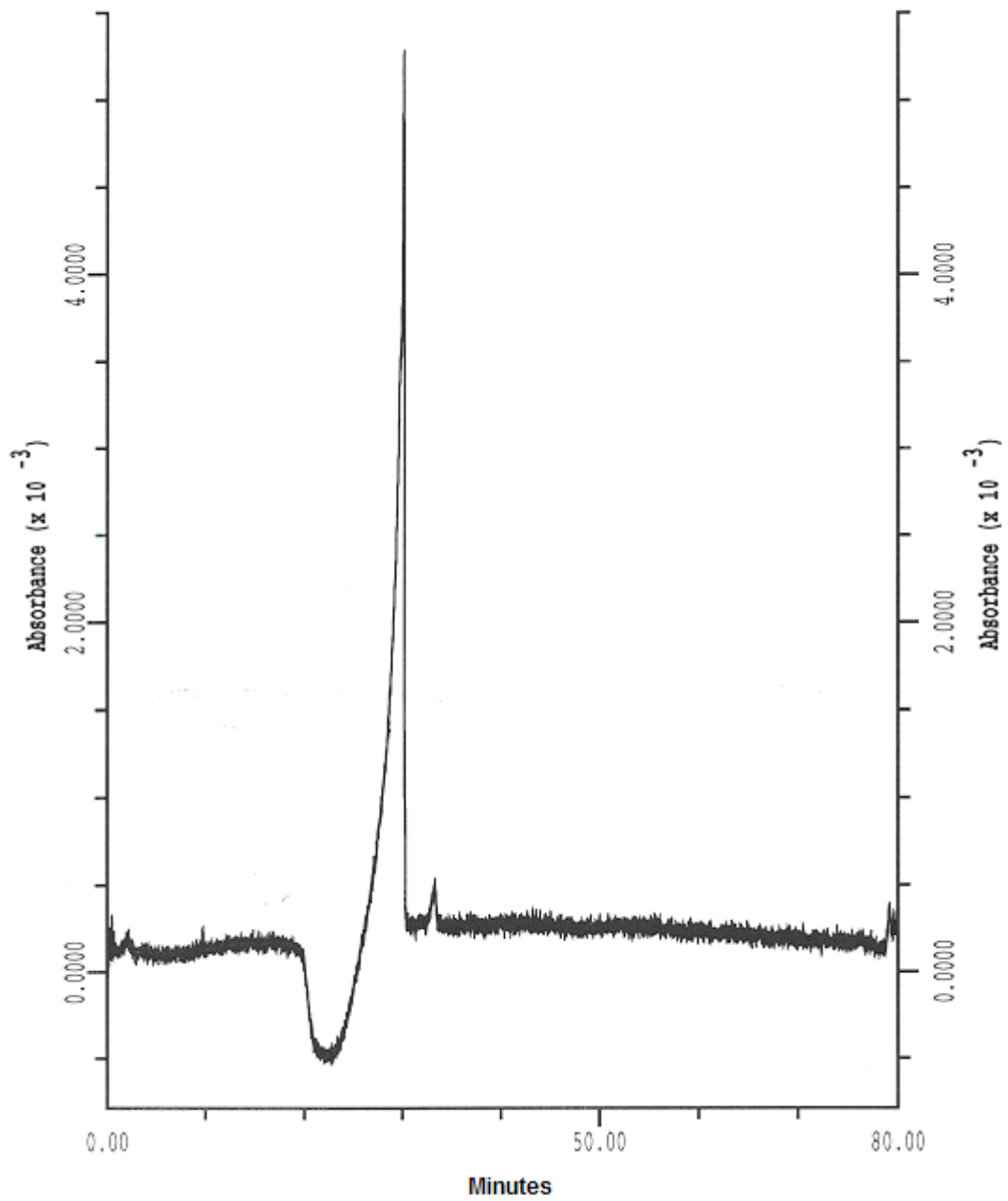


Fig. 83 CE of ibuprofen with 30  $\mu\text{M}$   $\beta$ -cyclodextrin. Conditions: run buffer, 30  $\mu\text{M}$  BSA, 67 mM phosphate (pH7.4), 30  $\mu\text{M}$   $\beta$ -cyclodextrin; capillary, CElect P150, 37 cm (30 cm to detector)  $\times$  50  $\mu\text{m}$  i.d.; instrument, PACE 2050; temperature, 25  $^{\circ}\text{C}$ ; voltage 8 kV; detection wavelength, 254 nm.

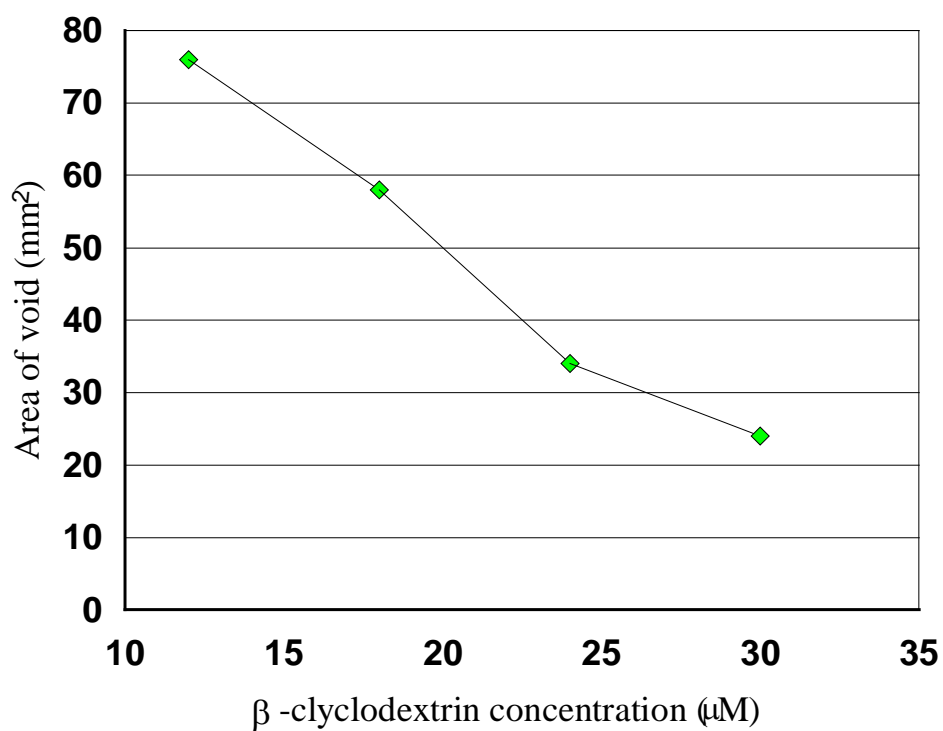


Fig. 84 Area of the ibuprofen-BSA void. Conditions: run buffer, 30 μM BSA, 67 mM phosphate (pH7.4), x μM β-cyclodextrin; capillary, CElect P150, 37 cm (30 cm to detector) × 50 μm i.d.; instrument, PACE 2050; temperature, 25 °C; voltage 8 kV; detection wavelength, 254 nm.

## 5.4 Allosteric interactions

### 5.4.1 Introduction

There has been extensive research into the binding of ligands to proteins and a binding site theory has been developed to explain drug-ligand binding, displacement and allosteric effects [Fehske 1981]. Three major binding sites have been proposed for HSA based on the affinities of drug molecules to the different sites on HSA. The three sites exhibit affinity for digitoxin, warfarin and indole-diazepam. A summary of molecules that bind to the sites is summarised in Table 85.

Table 85 Summary of molecules which bind to specific sites on HSA

Binding site	Indole-diazepam	Warfarin	Digitoxin
Molecules which have a high affinity to the site	Benzodiazepines  Tryptophan  Ibuprofen	Warfarin  Dicoumorol	Digitoxin

As already demonstrated, protein affinity CE can be utilised to probe the effects of different modifiers, e.g. organic solvents, on the chiral selectivity of proteins. Protein affinity CE should, therefore, be a good model for studying ligand-protein binding. This is of interest in itself but also it might be possible to induce enhanced chiral resolution e.g. as observed by Noctor and co-workers [Noctor 1993] by allosteric interactions. The protein will be in free solution so any conformational changes will be from ligand-protein interactions. This is in contrast to immobilised protein in

HPLC where the protein conformation may be changed by chemically bonding it to a silica support. It has been possible to produce albumin phases for which the tertiary structure has not been greatly altered so that the CSP can be used to study binding [Ashton 1996, Thaud 1983, Shibukawa 1996 & He 1997]. However for AGP CSP the structure is often greatly distorted through cross-linking to produce better stability and enantioselectivity (TAG Noctor, personal communication).

#### 5.4.2 Discussion

The results for the addition of competing ligands on the resolution of tryptophan enantiomers are shown in Table 86 and the corresponding electropherograms in Figures 87 to 90.

Table 86 Selectivity of tryptophan enantiomers with the addition of competing ligands

Competing Ligand	Tryptophan Migration Time 1	Tryptophan Migration Time 2	Resolution
Lorazepam	11.8	12.4	0.25
Digitoxin	10.5	10.6	0.2
Warfarin	8.5	-	-
Ibuprofen	8.4	-	-

It has already been reported that the addition of small amounts of competing ligands can have dramatic effects on chiral selectivity [Aubry 1994]. Consequently a competing ligand concentration less than the protein in the buffer ought to have a significant effects on the test anayte. Therefore any effects should be observed using a ratio of 10:1 for protein to competing ligand. This did have, and in some cases, had



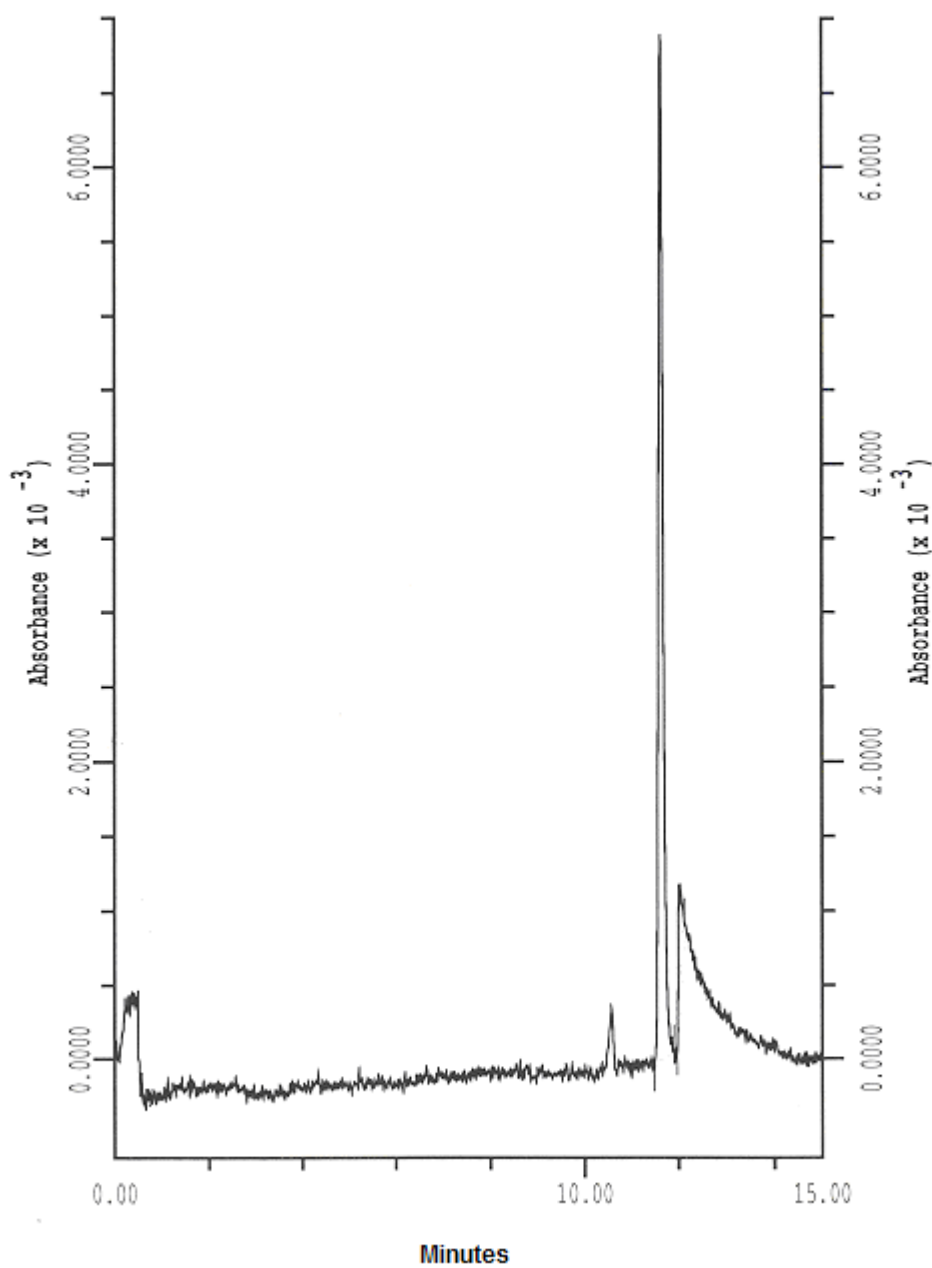


Fig. 87 Resolution of tryptophan enantiomers with addition of lorazepam. Conditions: run buffer, 30  $\mu\text{M}$  HSA, 67 mM phosphate (pH7.4), 3  $\mu\text{M}$  lorazepam; capillary, CElect P150, 37 cm (30 cm to detector)  $\times$  50  $\mu\text{m}$  i.d.; instrument, PACE 2050; temperature, 25  $^{\circ}\text{C}$ ; voltage 8 kV; detection wavelength, 280 nm.

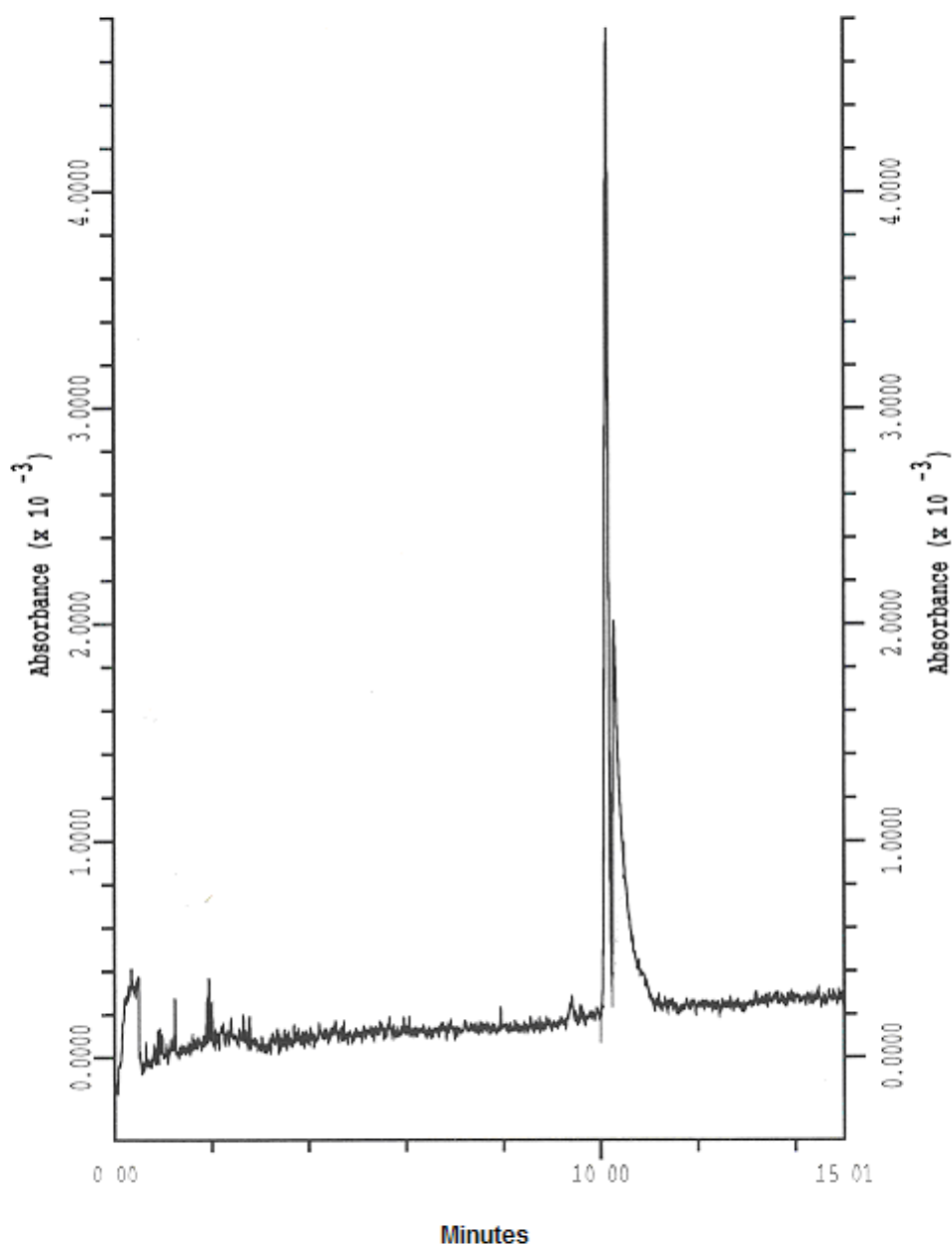


Fig. 88 Resolution of tryptophan enantiomers with addition of digitoxin. Conditions: run buffer, 30  $\mu$ M HSA, 67 mM phosphate (pH7.4), 3  $\mu$ M digitoxin; capillary, CElect P150, 37 cm (30 cm to detector)  $\times$  50  $\mu$ m i.d.; instrument, PACE 2050; temperature, 25  $^{\circ}$ C; voltage 8 kV; detection wavelength, 280 nm.

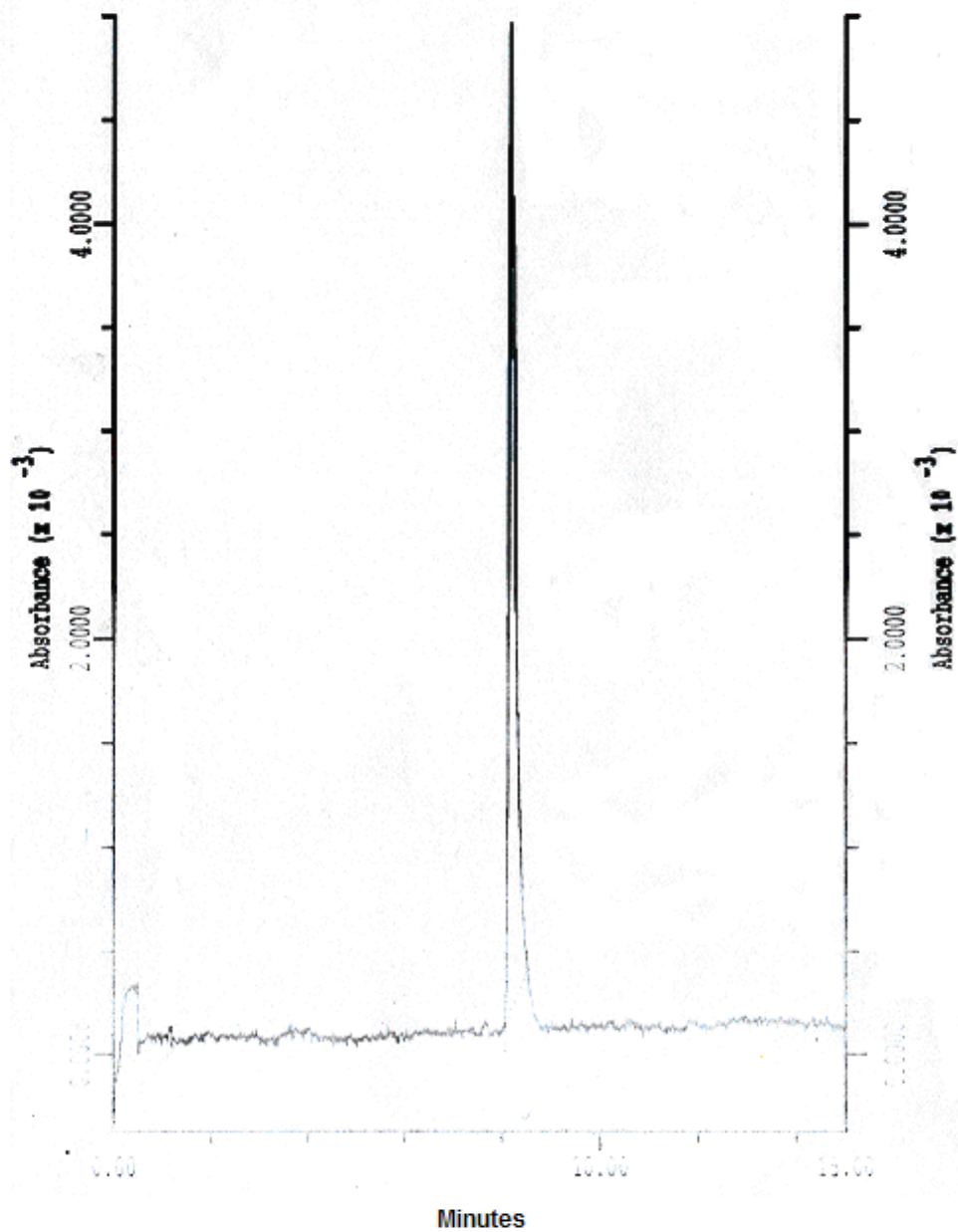


Fig. 89 Resolution of tryptophan enantiomers with addition of warfarin. Conditions: run buffer, 30  $\mu$ M HSA, 67 mM phosphate (pH7.4), 3  $\mu$ M warfarin; capillary, CElect P150, 37 cm (30 cm to detector)  $\times$  50  $\mu$ m i.d.; instrument, PACE 2050; temperature, 25  $^{\circ}$ C; voltage 8 kV; detection wavelength, 280 nm.

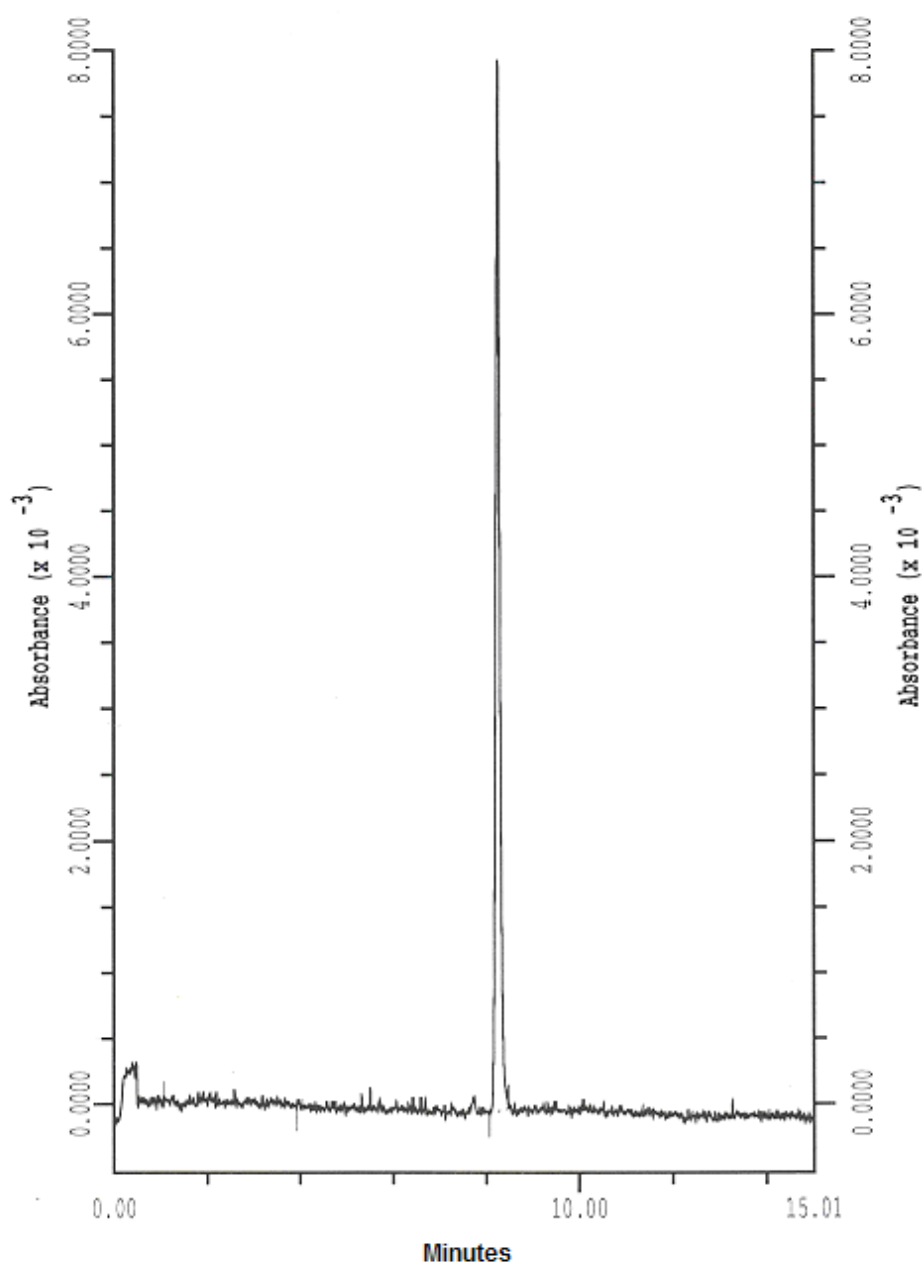


Fig. 90 Resolution of tryptophan enantiomers with addition of ibuprofen. Conditions: run buffer, 30  $\mu\text{M}$  HSA, 67 mM phosphate (pH7.4), 3  $\mu\text{M}$  ibuprofen; capillary, CElect P150, 37 cm (30 cm to detector)  $\times$  50  $\mu\text{m}$  i.d.; instrument, PACE 2050; temperature, 25  $^{\circ}\text{C}$ ; voltage 8 kV; detection wavelength, 280 nm.

a dramatic effect on the separation and overall migration times of tryptophan enantiomers. The most significant effects were noticed with ibuprofen and warfarin and in both cases the resolution of tryptophan enantiomers was decisively eliminated and there was a reduction in the retention times. Ibuprofen is known to bind to the same site as tryptophan so it is clear from Fig. 90 that ibuprofen binds more strongly and displaces tryptophan from HSA. However, from the site binding theory warfarin binds to a different site compared to tryptophan so clearly there was more going on than direct competition.

Therefore providing that there is no direct displacement of tryptophan then warfarin would alter the conformation of HSA when bound so preventing tryptophan binding to HSA and thus eliminating chiral selectivity and decreasing the migration times.

The addition of lorazepam and digitoxin to the run buffer had little effect on the resolution or migration times of tryptophan. The benzodiazepine binds to the same bind site as tryptophan but in this case it would appear that it is the tryptophan that was bound more strongly to HSA. The binding of digitoxin at a different site compared to tryptophan appeared not to change the conformation of HSA to prevent binding of tryptophan since there is still a baseline separation of enantiomers.

## **5.5 Conclusions**

Protein affinity CE had demonstrated the applicability of the technique to probe the effects of including additives in the run buffer. For the examples studied here there were no improvements in chiral selectivity and while only a limited range of examples were studied there was sufficient evidence to suggest that cases where there were improvements in enantioselectivity would be difficult to find and therefore that the approach of manipulating additives might not be the best one with respect to the primary aim of identifying systems that would give rise to good broad

spectrum enantioselectivity by protein affinity CE. However it seemed that the technique could easily be adapted to show the competitive effects of ligands and this may be a more promising application area for the future. Providing some technical difficulties can be overcome, then it may be useful as a tool to monitor the bio-availability of drugs *in vivo*, especially in cases where several drugs are taken at the same time. In particular the use of low concentrations of proteins in CE would seem to be an ideal solution to the immobilisation difficulties encountered by Wainer's group in working with transporter proteins in LC [Wainer 2003, Moaddel 2002 & 2005].

## **Chapter 6 Practical issues associated with protein affinity CE**

### **6.1 Artefacts associated with the Dionex CES I**

#### **6.1.1 Capillary fill method**

Before commencing the optimisation of chiral separations using CE, conditions quoted in the literature were tested [Kraak 1992 & Barker 1992] using the Dionex CES I instrument and associated AI-450 software. Tryptophan was chosen as the test compound as the enantiomers have been successfully separated using BSA as the chiral selector in CE [Birnbaum 1992] and HPLC [Krstulovic 1989]. Early experiments to resolve tryptophan were unsuccessful as shown by Fig. 91 which shows a single peak. A feature of the electropherograms was an increase in the absorbance towards the end of the run which can be seen between 35 and 40 min in Fig. 91. By modifying the method to flush the capillary with the phosphate buffer followed by a blank run with one end of the capillary in a vial containing BSA phosphate buffer, the UV absorbance attained a maximum and then remained constant forming a plateau, Fig. 92.

The experimental procedure to fill the capillary with the BSA containing run buffer was to rinse the capillary with 0.05 M sodium hydroxide, water and BSA free run buffer for three minutes each followed by a three minute pressure injection of the run buffer from a vial on the carousel. The capillary was not rinsed with the BSA containing run buffer because the capillary was easily blocked and the amount of BSA required was considered prohibitive. The amount of rinse solution required was approximately 100 ml and with a run buffer containing 30  $\mu$ M BSA this would use 200 mg of the protein. The samples were injected and the inlet was placed in a vial containing the BSA run buffer and the outlet placed in the fixed source vial, which contained phosphate run buffer.

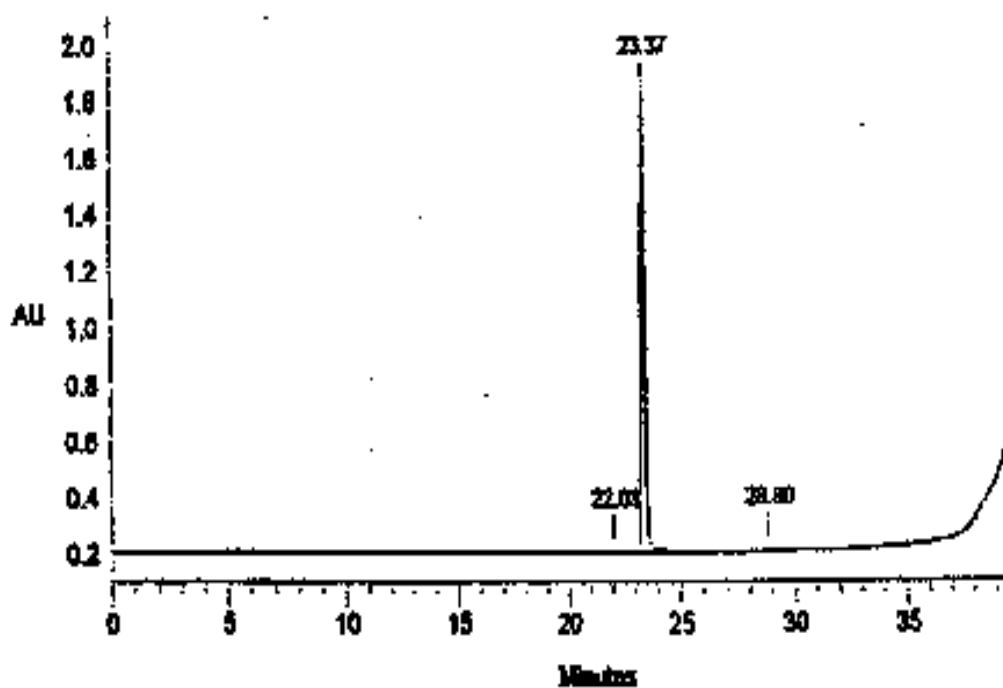


Fig. 91 CE of tryptophan using a three minute pressure injection to load BSA onto the capillary; Unresolved tryptophan enantiomers at 23 min with an increase in the baseline starting at 37 min due to the BSA passing the detector. Conditions: run buffer, 30  $\mu$ M BSA, 67mM phosphate (pH 7.4); capillary, CElect p150, 40 cm (35 cm to detector) x 50  $\mu$ m i.d.; instrument, CES I; temperature, ambient; voltage 10 kV; detection wavelength, 280nm.



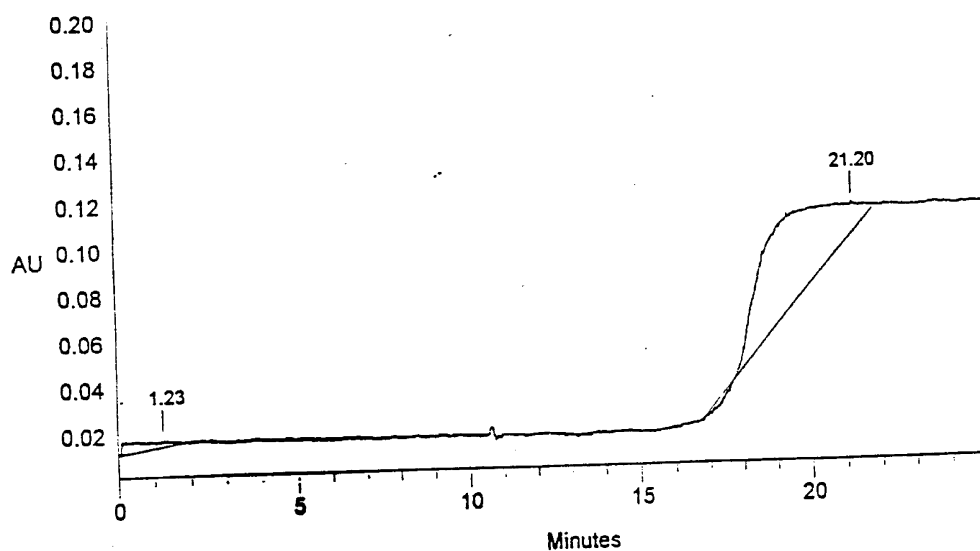


Fig. 92 The capillary fill method showing the BSA breakthrough starting at 17 min and plateauing out after 20 min. The capillary was rinsed with 0.05 M sodium hydroxide, water and 67 mM phosphate buffer. A blank run was performed from a vial containing BSA-phosphate buffer. Conditions: run buffer, 30  $\mu$ M BSA, 67 mM phosphate (pH 7.4); capillary, CElect p150, 40 cm (35 cm to detector) x 50  $\mu$ m i.d.; instrument, CES I; temperature, ambient; voltage 10kV; detection wavelength, 254 nm.

The sample mixture of enantiomers was then applied which resulted in unresolved enantiomers and an increase in UV absorbance after 20 to 25 min.

The increase in absorbance was thought to be BSA passing the detector given that it was the only UV absorbing species in the run buffer. The main question was whether there was a BSA breakthrough or an increase in the level of BSA. Experiments were undertaken to verify the presence of BSA passing the detector. The inlet vial was replaced with phosphate buffer and the procedure was repeated as before. There was no enantiomeric separation and there was an increase in UV absorbance after 25 min. It was concluded that BSA had not been injected into the capillary by the pressure injection method. BSA was only present in the capillary after a period of time when the inlet was placed in a vial with the BSA containing buffer. A sample of tryptophan was injected after the plateau had been established. This resulted in an enantiomeric separation, Fig. 93, and the baseline remained stable throughout the run. The experimental procedure was subsequently altered to include a 25 min run with the BSA-containing run buffer to ensure that the protein was present in the capillary prior to any sample injections. However, this revised procedure substantially increased the total analysis time, by 40 %, of the experiment. There were a number of reasons why the time required for the BSA to pass through the detector was relatively long. At the pH used, the electrophoretic mobility of the BSA was low, as discussed in Chapter 3. Also at the concentration used the BSA containing buffer had a high viscosity which would also lead to a decrease in the electrophoretic mobility of the BSA, Equation 18, [Camilleri 1983].

$$\bar{\mu} = \frac{\bar{v}}{E} = \frac{q}{6\pi\eta r}$$

Equation 18 Electrophoretic Mobility

where

$\bar{\mu}$	=	electrophoretic mobility
$\bar{v}$	=	electrophoretic velocity
$\bar{E}$	=	electric field strength
$q$	=	charge of the ion
$\eta$	=	viscosity of the buffer
$r$	=	radius of the molecules.

When these experiments were repeated using the PACE 2050 it was only necessary to rinse the capillary with the BSA containing buffer to achieve enantiomeric separations and no breakthrough of the BSA was observed. The time required to condition the capillary prior to injection was reduced from 34 min to 10 min.

The high pressure rinse of the PACE 2050 was 20 psi compared to the 10 - 15 psi of the CES I. The difference between 15 and 20 psi had not been expected to make too much difference but it made a very marked difference in that it significantly decreased the time to condition capillary by 24 min.

### **6.1.2 Reduction of the overall run time**

Performing a BSA run prior to injecting samples effectively doubled the time of analysis. Experiments were undertaken to ascertain the reproducibility between sample injections without rinsing the capillary. The capillary was filled with the BSA containing buffer as described previously. The test compound was tryptophan. The run time for each analysis was 40 min. The reproducibility of the system decreased rapidly after only three injections. The migration times of the enantiomers increased from 20 min to over 40 min and in one case the enantiomers were detected in a subsequent analysis. The increase in the migration times could have been due to protein building up on the surface of the capillary wall during the sequential analyses

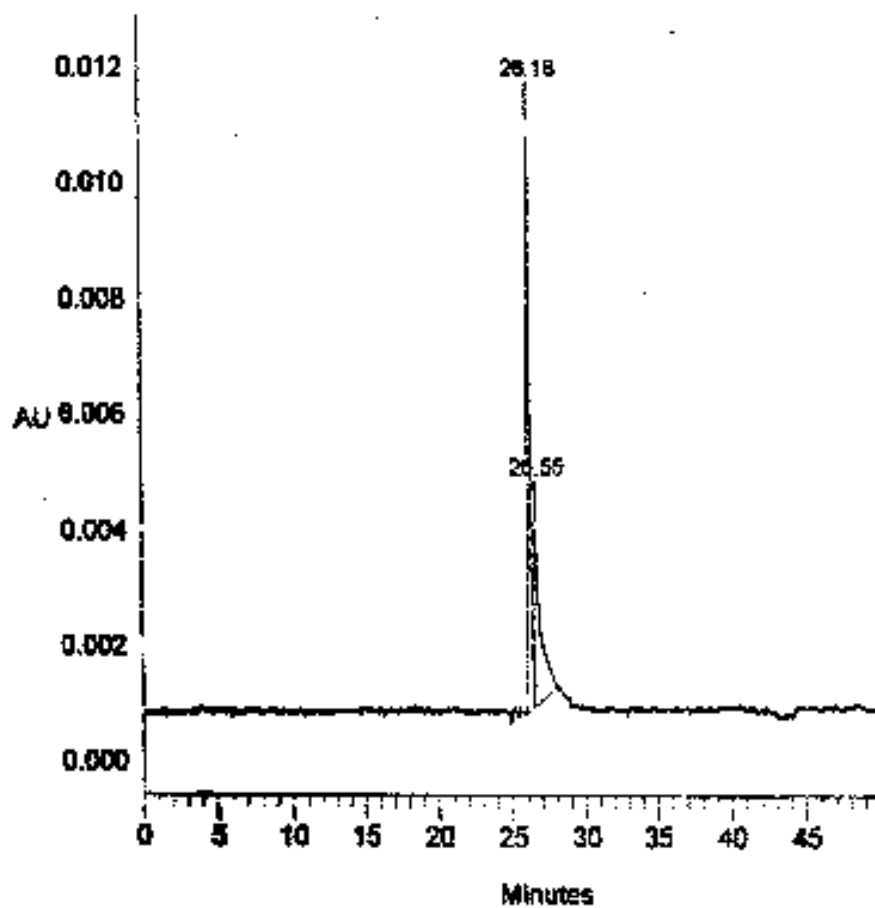


Fig. 93 CE of tryptophan enantiomers following the BSA breakthrough. Conditions: run buffer, 30  $\mu$ M BSA, 67 mM phosphate (pH 7.4); capillary, CElect

p150, 40 cm (35 cm to detector) x 50  $\mu\text{m}$  i.d.; instrument, CES I; temperature, ambient; voltage 10 kV; detection wavelength, 280 nm.

which could have resulted in the tryptophan interacting with relatively stationary BSA on the wall compared to BSA in solution which would have increased the migration times.

Clearly running samples without rinsing the capillary was unacceptable in terms of reproducibility so, despite the consequences for time and protein consumption, the capillary was rinsed with sodium hydroxide, water, phosphate buffer and the capillary fill method undertaken prior to any sample injection.

### **6.1.3 Baseline anomalies**

The technique of filling the capillary with the run buffer for the CES I prior to injection and then applying the voltage sometimes produced two distinct phenomena in the baselines. They were a spontaneous marker peak, Fig. 94, and a baseline shift, Fig. 95. The phenomena were random and occurred using the same capillary and the same injection procedure. This can be demonstrated by comparing Fig. 93, which does not exhibit any phenomena, and Figs. 94 and 95.

The phenomena were studied by Coyer *et al* [Colyer 1995]. They found that the phenomena depended on the physical geometries of the ends of the capillary. The appearance or disappearance of these phenomena could be observed using the same capillary. They demonstrated this by cutting small sections from the end of the capillary and running the same experimental conditions. They could not differentiate any features at the capillary tips between the active cut capillaries producing the phenomena or the passive cut capillaries which did not. They proposed that positive marker peaks and baseline shifts were caused by a slight increase in the buffer

concentration. Conversely negative marker peaks and baseline shifts were caused by a slight decrease in buffer concentration. These theories can explain the

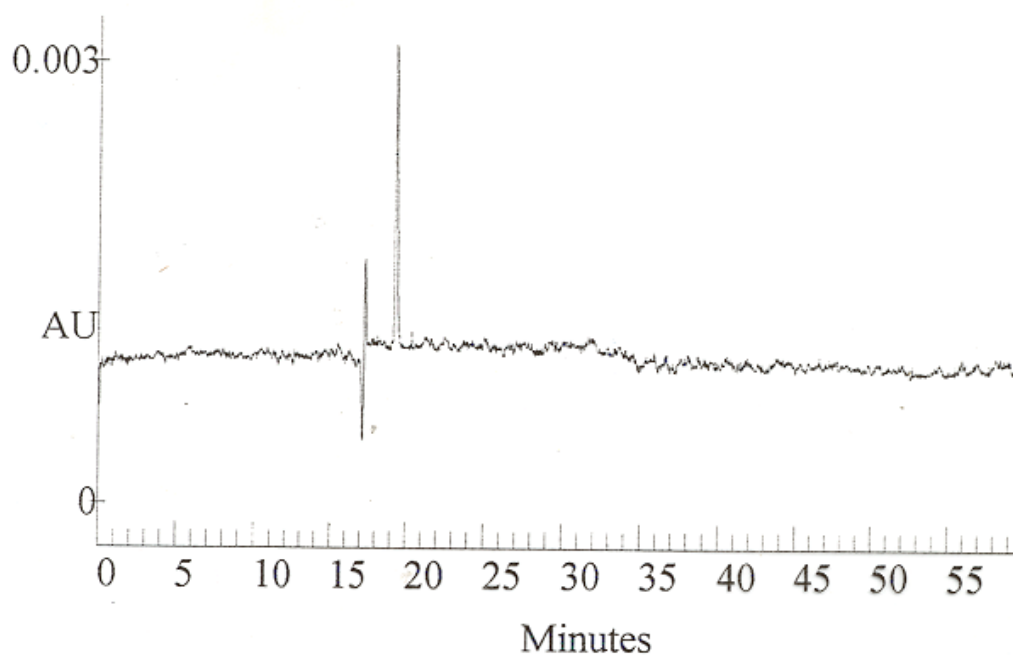


Fig. 94 CE of hexobarbitone enantiomers showing a spontaneous peak marker. The spontaneous peak marker occurs at 17 min. Conditions: run buffer, 30  $\mu$ M BSA, 67

mM phosphate (pH 7.4) – methanol (97.5 : 2.5, v/v); capillary, CElect p150, 40 cm (35 cm to detector) x 50  $\mu\text{m}$  i.d.; instrument, CES I; temperature, ambient; voltage 10 kV; detection wavelength, 254 nm.

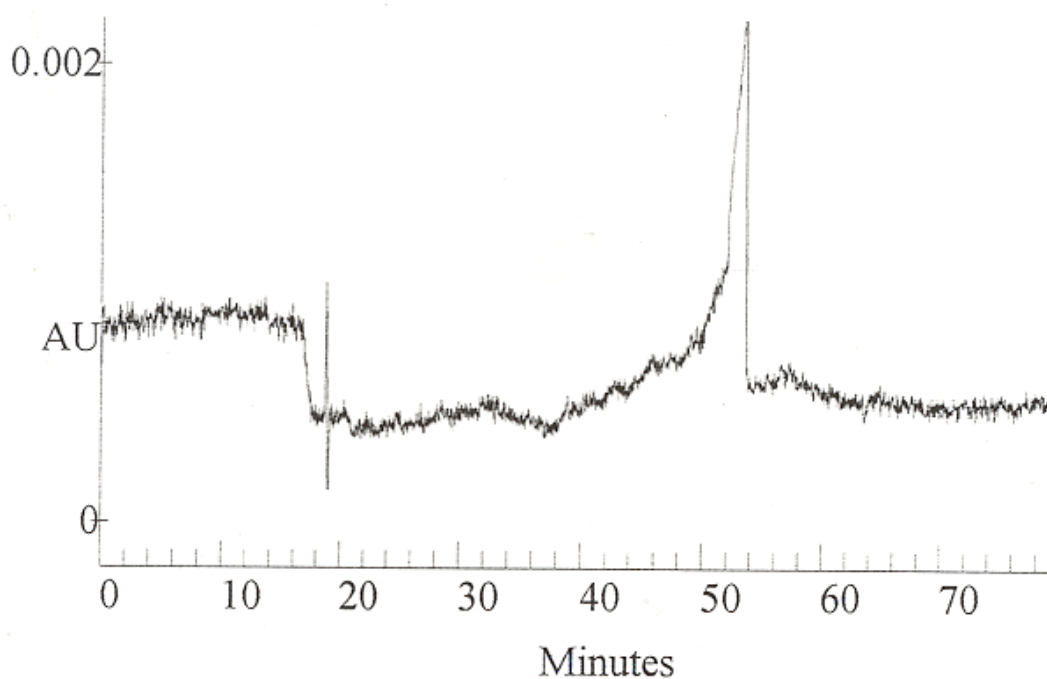


Fig. 95 CE of N-acetyl-DL-tryptophan enantiomers showing both a spontaneous peak marker and a baseline shift. The baseline shift occurs between 16 and 18 min. The

spontaneous peak marker occurs between 19 and 20 min. Conditions: run buffer, 30  $\mu$ M BSA, 67 mM phosphate (pH 7.4) – methanol (97.5 : 2.5, v/v); capillary, CElect p150, 40 cm (35 cm to detector) x 50  $\mu$ m i.d.; instrument, CES I; temperature, ambient; voltage 10 kV; detection wavelength, 254 nm.

spontaneous markers and the baseline shifts observed in some electropherograms of this study.

#### **6.1.4 Ibuprofen ghost peaks**

The electropherograms of ibuprofen were distinctive and unique compared to electropherograms of all the other compounds tested. A dip in the baseline was observed immediately before the main peaks. A typical example of an electropherogram of a partial separation of ibuprofen enantiomers is shown in Fig. 96.

The run buffer contained BSA which was a relatively high UV absorbing species so any local variations in the BSA concentration would cause a change in the detector output. When the ibuprofen is injected there is an equal concentration of the BSA run buffer in the zones immediately in front and behind the ibuprofen. From the electropherograms of ibuprofen and the BSA capillary fill method the migration time of ibuprofen was longer compared to BSA and the electrophoretic mobility of the ibuprofen was less than for BSA. Ibuprofen is known to bind strongly to BSA [Peters 1977] therefore assuming that the electrophoretic mobility of the ibuprofen-BSA complex was the same as BSA and the rate of association and dissociation of the ibuprofen and BSA was high compared to the length of the experiment then a void of BSA in the run buffer would develop. This can be graphically illustrated by Fig. 97. At the beginning of the analysis the concentration of the BSA is constant throughout the capillary and there is no separation of the ibuprofen enantiomers. As the analysis proceeds the concentration of BSA prior to the enantiomers decreases which is



shown by the lighter grey region in the illustration. Towards the end of the analysis the region of the lower BSA concentration prior to the ibuprofen enantiomers increases.

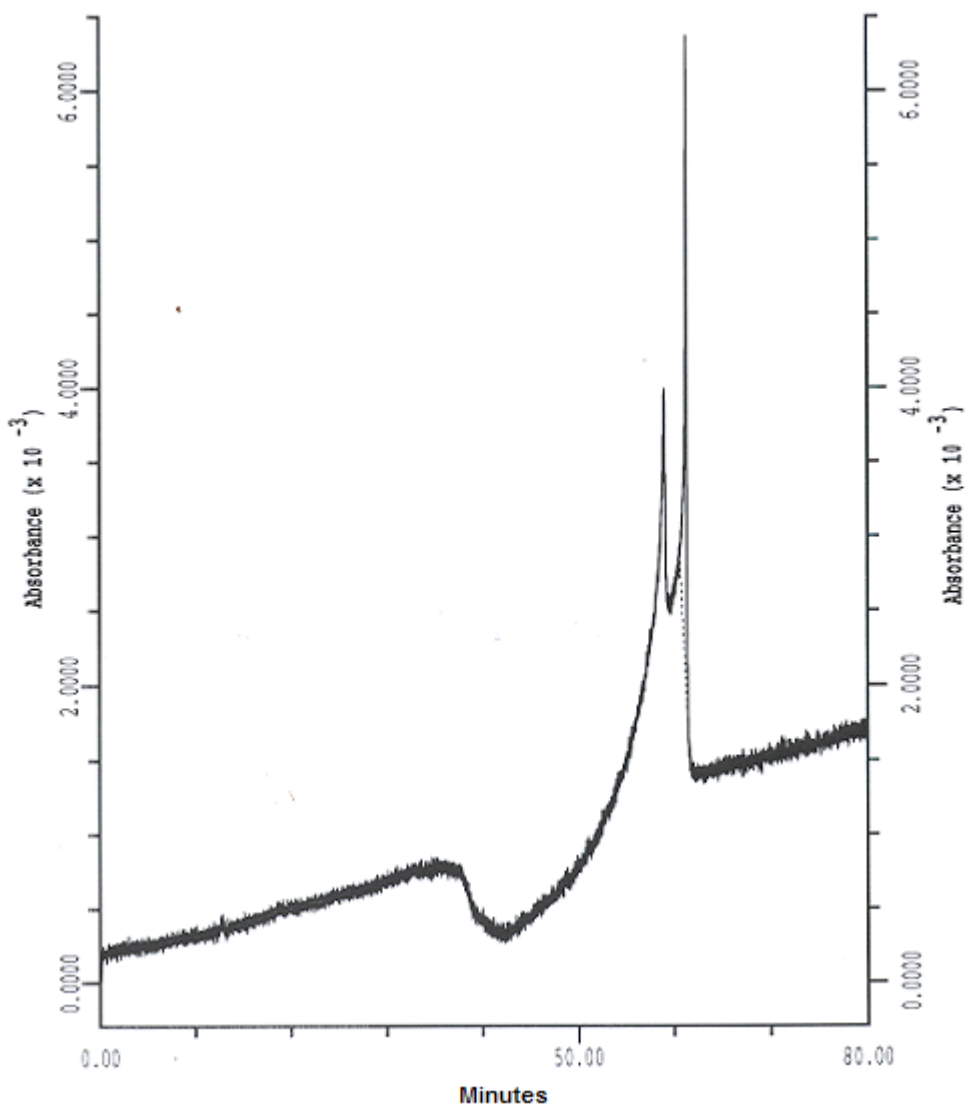


Fig. 96 CE of ibuprofen enantiomers showing the dip in the baseline. The dip in the baseline occurs between 40 and 50 min. Conditions: run buffer, 30  $\mu$ M BSA, 67 mM phosphate (pH 7.4) – methanol (97.5 : 2.5, v/v; capillary, CElect p150, 37 cm (30 cm to detector) x 50  $\mu$ m i.d.; instrument, PACE 2050; temperature, 25  $^{\circ}$ C; voltage 10 kV; detection wavelength, 254 nm.

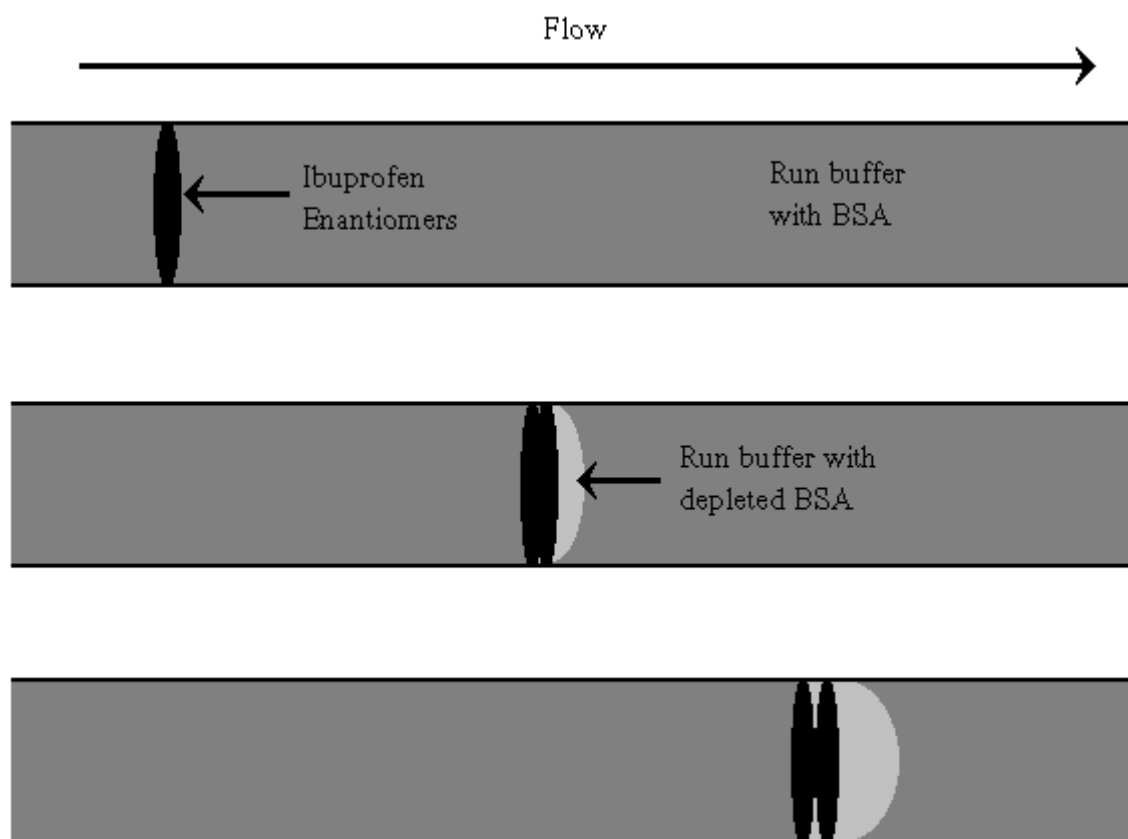


Fig. 97 The development of a region of low BSA concentration prior to the partial separation of ibuprofen enantiomers. At the beginning of the analysis the concentration of BSA was constant throughout the capillary. As the analysis proceeded a small region of low BSA concentration formed immediately before the ibuprofen enantiomers. Towards the end of the analysis the region of low BSA concentration had increased.

Two measures were undertaken which it was hypothesised might reduce the magnitude of the dip. The first was to increase the overall concentration of the BSA in the run buffer. This might minimise the magnitude by increasing the overall concentration of BSA compared to ibuprofen. The second measure was to increase the concentration of BSA in the injection vial. This measure would increase the concentration of free BSA in the injection vial compared to the BSA-ibuprofen complex concentration. The increased free BSA concentration would cause a decrease the observed dip in the baseline.

By increasing the overall BSA concentration from 30 to 60  $\mu\text{M}$  there were no obvious changes in the magnitude of the dip. The concentration of ibuprofen used was 1  $\text{mg ml}^{-1}$  in both experiments so the amount of the ibuprofen-BSA complex in both experiments would be approximately the same. Therefore the amount of BSA depleted from the zone prior to the ibuprofen enantiomers would be the same so the magnitude of the dip would also be the same and that was observed. Similarly the ibuprofen peak did not get larger, suggesting that there was no additional BSA complexing to the ibuprofen, so that the size of the peak relative to the dip was the same. The only change was that the background was at a higher level, albeit having been zeroed by the instrument.

By increasing the concentration of BSA in the injection phase compared to the run buffer it was hoped to increase the proportion of BSA-ibuprofen complexes prior to the introduction to the run buffer so there would be less free ibuprofen to complex

with BSA from the run buffer so that there would be a reduction in the magnitude of the dip. However, as is indicated in Fig. 98, there was little effect. The concentration of BSA in the injection phase was 60  $\mu\text{M}$  and the concentration of the ibuprofen was 5 mM so that this was in excess of the BSA to the extent that to fully complex all the ibuprofen the protein concentration would have had to be increased by two orders of magnitude and this was not practical to do.

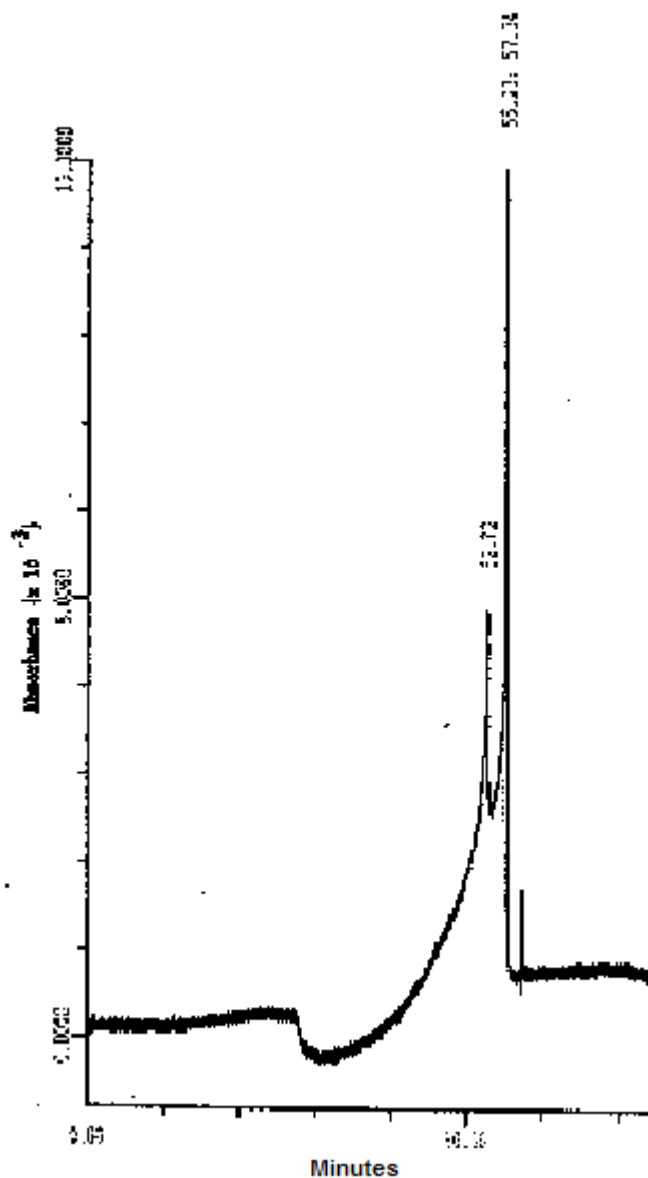


Fig. 98 CE of ibuprofen enantiomers injected with 60  $\mu$ M BSA showing the dip in the baseline between 30 and 40 min. Conditions: run buffer, 30  $\mu$ M BSA, 67 mM phosphate (pH 7.4) – methanol (97.5 : 2.5, v/v; capillary, CElect p150, 37 cm (30 cm to detector) x 50  $\mu$ m i.d.; instrument, PACE 2050; temperature, 25  $^{\circ}$ C; voltage 10 kV; detection wavelength, 254 nm.

There was also no corresponding increase in absorbance with the BSA where it was suspected that the overall volume of injected material was a fraction of the material in the section of capillary. The overall concentration of BSA at that point would tend towards the concentration of 30  $\mu\text{M}$  and so would have little effect on the observed dip prior to the ibuprofen enantiomers.

## **6.2 Artefacts associated with the PACE 2050**

### **6.2.1 The stepped baseline**

The pressure rinse of the PACE 2050 was sufficiently powerful to flush the capillary with the BSA-phosphate buffer. This eliminated the capillary fill method, which had to proceed a run using the Dionex CES I, and so the total analysis time had been decreased. The experimental procedure was subsequently altered to rinse the capillaries with 0.05 M NaOH, water, phosphate buffer and BSA-phosphate buffer prior to any injections. After injection both ends of the capillary were placed in vials containing the BSA-phosphate buffer and the separation voltage applied. After a period of time there was a decrease in absorbance followed by a lower constant absorbance; the electropherogram shown in Fig. 99 was a typical example. The effect was similar to the capillary fill method used for Dionex CES I only in reverse. Since BSA was the only UV absorbing species in the buffer then the BSA was being eliminated from the capillary. Experiments were undertaken to ascertain why the BSA was eliminated and steps were taken to prevent it.

### **6.2.2 Buffer depletion**

One possibility was that the source vial was being exhausted of BSA. After rinsing the capillary with the BSA-phosphate buffer, vials containing new phosphate buffer were used as the inlet and outlet vials while the separation voltage was applied.

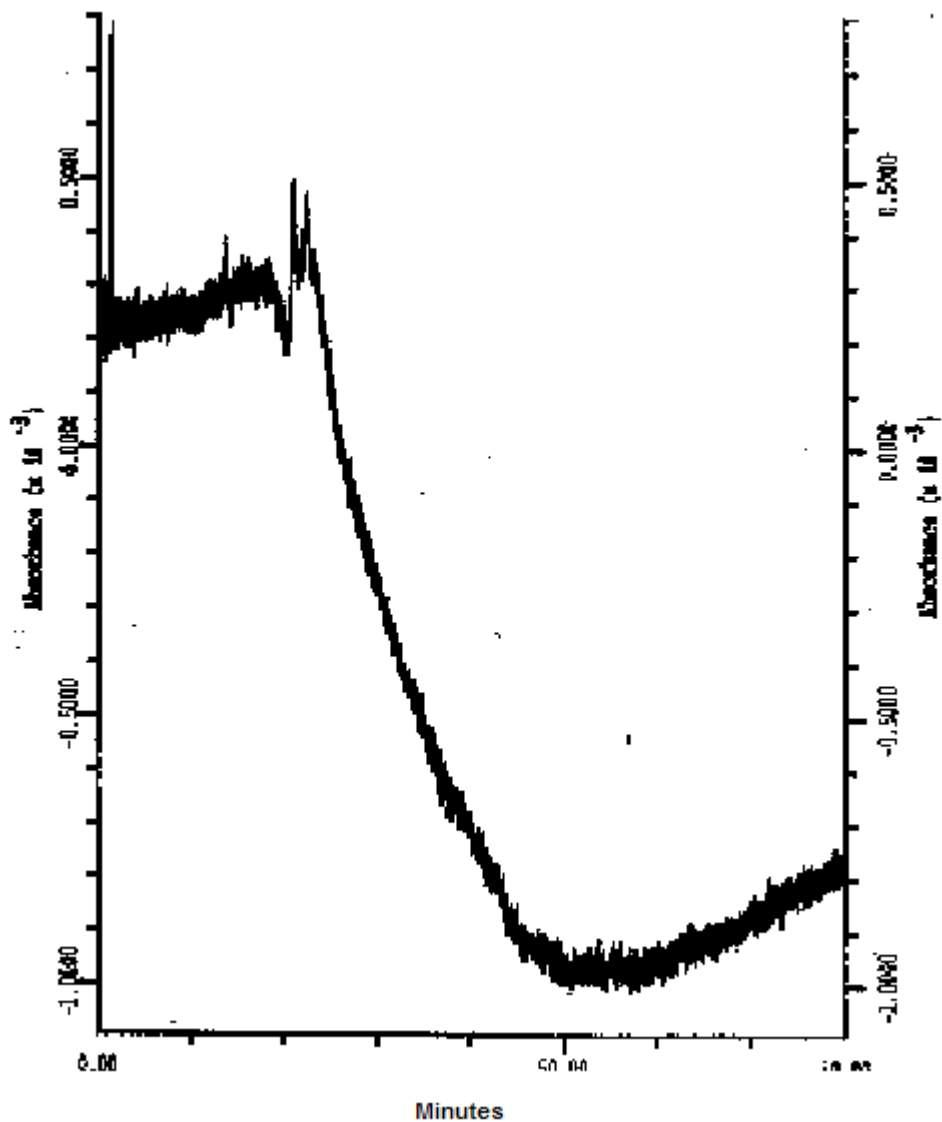


Fig. 99 CE of ibuprofen enantiomers showing the stepped baseline occurring about 25 min. Conditions: run buffer, 30  $\mu$ M BSA, 67 mM phosphate (pH 7.4) – methanol (97.5 : 2.5, v/v; capillary, CElect p150, 37 cm (30 cm to detector) x 50  $\mu$ m i.d.; instrument, PACE 2050; temperature, 25  $^{\circ}$ C; voltage 10 kV; detection wavelength, 254 nm.

However, the elimination of BSA still occurred. The UV absorbance of the buffers of the vials were measured before and after a run. There was no significant difference between the before and after measurements so there was still 30  $\mu\text{M}$  in both buffer vials.

The decrease in absorbance was not observed when using the Dionex CES I and the volume of the BSA-phosphate buffer vial was 0.6 ml compared to the 2.8 ml of the vials used in the Beckman PACE 2050 so buffer depletion was thought unlikely to be the cause.

### **6.2.3 Siphoning**

Another possibility was that there was sufficient difference in the levels of the buffers that siphoning was taking place, which could prevent BSA from being transported through the capillary. When the levels of the buffer vials were altered to give all the high and low buffer level combinations available there was the same decrease in absorbance in all cases. Therefore it was inferred that another mechanism was causing the effect.

### **6.2.4 Overload of BSA in the outlet vial**

The decrease in absorbance was never observed when using the methods for the Dionex CES I. The only major difference between the Dionex CES I and the Beckman PACE 2050 was the buffer in the outlet vial. The fixed outlet vial for the Dionex CES I contained phosphate buffer from the capillary rinse cycle. Experiments were undertaken to change the method so that the outlet vial contained only phosphate buffer. It was demonstrated that using the modified method the elimination of BSA from the capillary was prevented. This can be clearly shown by comparing electropherograms of ibuprofen. The stepped baseline was only observed



in Fig. 99 which had BSA-phosphate buffer in the outlet vial. The stepped baseline was not observed in Fig. 96 and Fig. 98 which had phosphate buffer in the outlet vial.

The elimination of BSA from the capillary could be due to a combination of concentration and electrical effects. Before the separation voltage is applied the concentration of BSA in the capillary and the inlet and outlet vials is the same. When the separation voltage was applied the EOF was sufficient for the BSA to migrate from the inlet vial, through the capillary and into the outlet vial. After a period of time an excess of BSA would be present in the outlet vial compared to the inlet vial. A concentration gradient of BSA would develop from the outlet vial to the inlet vial. The concentration gradient would then form an equilibrium with the BSA migrating through the capillary. The flow of BSA would effectively stop through the capillary and this was observed by the step in the baseline.

### **6.3 Conclusions**

As with any analytical technique there are some disadvantages of CE. These include apparent baseline irregularities for neutral markers [Kenndler-Blachkolm 1995] and adsorption of analytes to the capillary wall [Ermakov 1995]. On the whole on referencing more recent literature the mechanisms of these artefacts are generally well understood and even if they could not be eliminated then allowances could be made for them and accordingly using the CES I the capillary fill method was employed even though there was an increase in the overall analysis time and an outlet vial containing only phosphate buffer was employed with the PACE 2050.

## Chapter 7 BSA as a mobile phase additive in microbore HPLC

### 7.1 Introduction

There had been interest in the use of protein affinity CE to develop methodologies for enantiomer separations and, to a lesser extent, to study protein-ligand binding. In enantiomer differentiation using CE, very small amounts of chiral selector are required. Accordingly, a much wider range of biomacromolecules may be used. Also it may be possible for chiral discrimination to take place in free solution. The biomacromolecular structure should therefore not be grossly distorted and the behaviour of the molecule should be similar to how it behaves *in vivo*. CE with biomacromolecules ought to be a better model of the pharmacological behaviour of drugs than HPLC. Despite these seeming advantages and a few success stories, protein affinity CE was in general not living up to expectations [Lloyd 1995].

Shortcomings of protein affinity CE had included failure to resolve the complete range of chiral analytes that may be resolved by HPLC using immobilised albumin stationary phases, broad negative peaks arising from analytes with long run times [this study], difficulty in the interpretation of data [this study and Lloyd 1995], and baseline shifts at variable times during analytical runs [Colyer 1995].

Since protein affinity HPLC using miniaturised columns and the protein as a mobile phase additive might offer the nominal advantages of CE alluded to above, it was decided to evaluate it using BSA as the chiral selector.

## 7.2 Results and discussion

### 7.2.1 Mechanism of separation

Under normal circumstances, the method for chiral resolution depends on adsorption of the analyte to the stationary phase followed by desorption by the protein. This is graphically illustrated in Fig. 100.

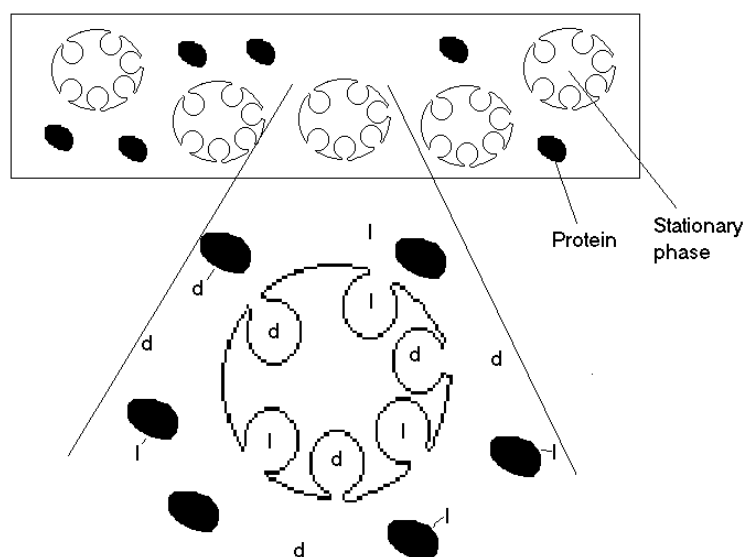


Fig. 100 Graphical representation between the stationary phase, the protein and the analytes showing that only the analytes, represented by d and l, can adsorb onto the stationary phase. When the analytes are desorbed from the stationary phase they can bind to the protein molecules in the stationary phase.

The pores of the stationary phase have a pore size of 60 Å and will be too small for the BSA protein, which being a prolate ellipsoid with dimensions 141 Å by 42 Å the

protein will not adsorb onto the stationary phase. However, the analytes are small enough to adsorb onto the stationary phase. Therefore the enantiomer which binds more strongly with the BSA will elute before the least bound enantiomer.

### 7.2.2 Enantioselectivity of the method

The selection of the stationary phase was critical for this method of using proteins as mobile phase additives. The functions of the stationary phase were twofold, the first was to reduce protein adsorption on the surface of the particles and the second was to allow the adsorption of the analytes. The stationary phase selected which closely matched the two required functions was Lichrosorb DIOL. The mobile phase was aqueous phosphate buffer which gave the best possibility to the analyte to adsorb onto the stationary phase.

Of the compounds tested, tryptophan, Fig. 102 and kynurenine, Fig. 103, were resolved into their individual enantiomers, Table 101. It was observed that the resolution of tryptophan occurred only when the concentration of BSA was raised to 60  $\mu\text{M}$ . This was in contrast with CE results where tryptophan was resolved with a BSA concentration of 30  $\mu\text{M}$  in the run buffer.

Warfarin had a low  $k$  value so this method was not appropriate. Temazepam had a moderate  $k$  value and therefore a greater concentration would probably be required for chiral resolution. No peaks were observed for benzoin and thioridazine which were highly retained on the stationary phase.

Table 101  $k$  values of analytes with BSA as a mobile phase additive

Analyte	30 $\mu$ M BSA	60 $\mu$ M BSA	
	$k_1$	$k_1$	$k_2$
Tryptophan	1.42	1.00	1.36
		$\alpha=1.36$	
Kynurenine	-	0.67	1.20
		$\alpha=1.80$	
Thioridazine	-	$\infty$	-
Benzoin	-	$\infty$	-
Temazepam	-	2.00	-
Warfarin	-	0.63	-

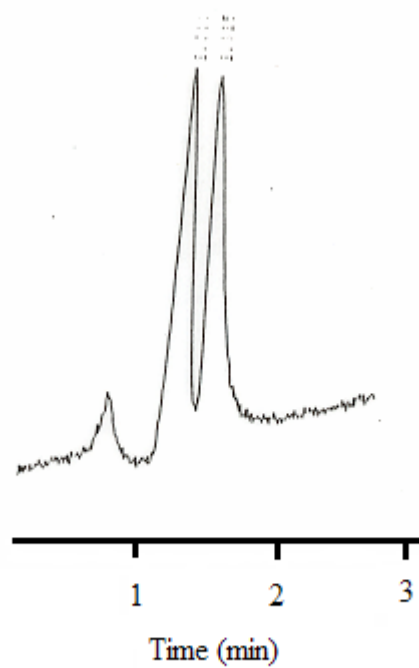


Fig. 102 Resolution of tryptophan using free-solution BSA and microbore HPLC. Conditions: mobile phase, 67 mM phosphate (pH 7.4), 60  $\mu$ M BSA; column, Lichrosorb DIOL, 5  $\mu$ M particle diameter, 60 Å pore size 15 cm x 1 mm i.d.; flow rate, 50  $\mu$ l  $\text{min}^{-1}$ .

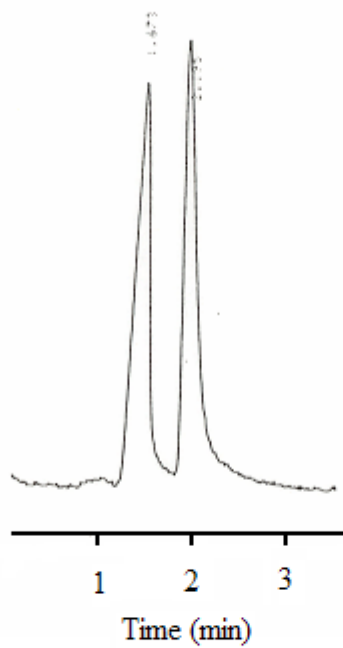


Fig. 103 Resolution of kynurenine using free-solution BSA and microbore HPLC. Conditions: mobile phase, 67 mM phosphate (pH 7.4), 60  $\mu$ M BSA; column, Lichrosorb DIOL, 5  $\mu$ M particle diameter, 60  $\text{\AA}$  pore size 15 cm x 1 mm i.d.; flow rate, 50  $\mu$ l  $\text{min}^{-1}$ .

### 7.2.3 Method practicalities

Although this method provided chiral resolutions and, given the nature of the retention mechanism, had potential as a viable alternative for exploring potential drug-protein interactions, there were a few challenges which made the method difficult to use. For example, over a period of time it was observed that the enantioselectivity for the tryptophan separation deteriorated, Fig. 104.

With the column being pumped with buffer / protein mobile phase it was possible that some of the protein would adsorb onto the stationary phase, at least outside of the pores including at the entrances to the pores. This would have the effect of blocking the pores and decrease the overall number of sites where the tryptophan could adsorb onto the stationary phase. Overall the tryptophan enantiomers would remain more in the mobile phase and as the mechanism for enantioselectivity was for the least bound enantiomer to adsorb onto the stationary phase then the enantioselectivity decreased.

This method also suffered the same inherent problems relating to UV detection as was found for the corresponding CE method. This was more pronounced as the overall concentration of BSA was 60  $\mu\text{M}$  compared to 30  $\mu\text{M}$  of the CE method. With the mobile phase used and using a column of 1 mm i.d. there was always the possibility of some precipitation with the chromatographic system. Indeed this problem did manifest itself on several occasions, which was indicated by a general increase in the backpressure of the system.



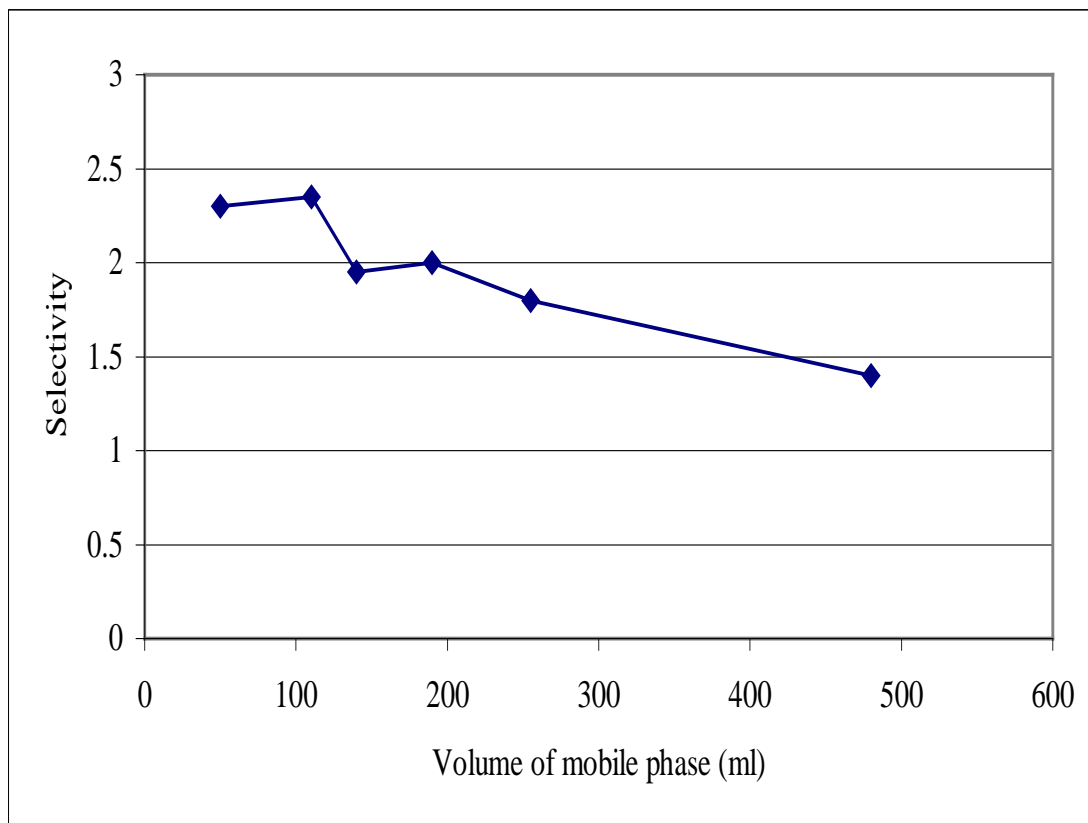


Fig. 104 Selectivity of tryptophan enantiomers with the amount of mobile phase pumped through the column. Conditions: mobile phase, 67 mM phosphate (pH 7.4), 60  $\mu$ M BSA; column, Lichrosorb DIOL, 5  $\mu$ m particle diameter, 60  $\text{\AA}$  pore size 15 cm x 1 mm i.d.; flow rate, 50  $\mu$ l  $\text{min}^{-1}$ .

Fortunately it was discovered that the principal sites of the adsorption were the column frits and so the life of the column was extended by replacing the frits when the system backpressure limit was exceeded.

### **7.3 BSA as a mobile phase additive in capillary LC**

Following the success of using BSA as a mobile phase additive in microbore LC it was an obvious choice to use the same methodology in capillary LC. This would have offered a greater saving in protein consumption. To perform a similar amount of analysis using a 0.3 mm i.d. capillary column compared to a 1 mm i.d. microbore column with equivalent flow rate would require approximately 10 % of the corresponding mobile phase. Unfortunately the method practicalities detailed earlier were such that no analysis was performed. The major issue was the ease by which the column became blocked with only a small amount of the mobile phase being pumped through the column. Unlike the microbore columns it was impractical to clean the frits to perform any analysis.

### **7.4 Conclusions**

Despite the practical problems, which were an inconvenience rather than a major limitation, this method offered the opportunity of studying enantioselectivity of proteins in free solution HPLC, i.e. with the *in vivo* tertiary structure preserved and without having to deal with the problems posed by the need to find suitable chemistry for bonding to the stationary phase. Importantly, with respect to proteins which might not be readily accessible, the amount of protein required was relatively small and when using a concentration of 60  $\mu\text{M}$  of BSA and a flow rate of

50  $\mu\text{l min}^{-1}$  the amount of BSA consumed during a 20 min run would be approximately 4 mg. Therefore, 2 g of BSA allowed a total analysis time of several days which would be more than adequate to study a range of compounds with this system.

Provided the practical difficulties of using proteins as mobile phase additives in capillary LC could be overcome then the consumption of protein could be decreased further. For example, using the same mobile phase running at 3  $\mu\text{l min}^{-1}$  would consume the equivalent of 0.25 mg BSA. Another development which could further reduce the amount of protein required is nanoscale high-performance liquid chromatography (nano-LC) [Chervet 1996 & Heron 2000]. Using columns of 0.1 mm i.d. and a flowrate of 0.15  $\text{ml min}^{-1}$  the amount of protein consumed in an equivalent 20 min run would be approximately 13  $\mu\text{g}$ . Healy [Healy 2001] has reported a 1000 fold reduction in reagent consumption when using methyl- $\beta$ -cyclodextrin as a mobile phase additive to separate naproxen enantiomers using nano-LC compared to conventional LC. Therefore, with such technologies it would allow the use of rare and expensive biomacromolecules to study enantioselectivity and protein-ligand binding.

## **Chapter 8    BSA as a pseudo stationary phase in microbore HPLC**

### **8.1    Introduction**

While the first priority had been to study the use of BSA present in its free form in the mobile phase, there was still some merit in studying systems in which the BSA was incorporated into the stationary phase. These types of systems would offer two key advantages over using the protein as a mobile phase additive. Once the protein had loosely adsorbed onto the stationary phase then the mobile phase used for the analysis would be protein free thereby decreasing the amount of protein required significantly. Also when using a protein free mobile phase, practical issues such as high UV detector background and possible frit blockage would not arise. The aim therefore of this part of the research programme was to develop a reduced dimensions system where the BSA was adsorbed onto the stationary phase in such a way that the BSA did not bleed off the column after the BSA was removed from the mobile phase.

A protocol for coating a stationary phase with protein had been reported for a conventional scale LC system using the 'bare' silica material, Nucleosil [Erlandsson 1986]. However, since the protein was thought to be adsorbed through interaction of the amino-groups with the weakly acidic silica, it was decided to first investigate the use of a less polar material stationary phase in order to reduce the chance of distortion of the protein tertiary structure occurring.

## 8.2 Results and discussion

### 8.2.1 Mechanism of separation

In protein affinity LC using large pore sizes, the protein molecules are in the pores therefore the mode of chiral resolution is more typical of using a typical protein-immobilised chiral stationary phase. There is generally little or no interaction with the stationary phase support and the interaction is with the protein. The enantiomer which binds more strongly to the protein will reside more on the stationary phase and will therefore elute after the least bound analyte which will proportionately reside more in the mobile phase. This is graphically represented in Fig. 105 where the l-enantiomer is bound to the protein and the d-enantiomer is essentially in the mobile phase.

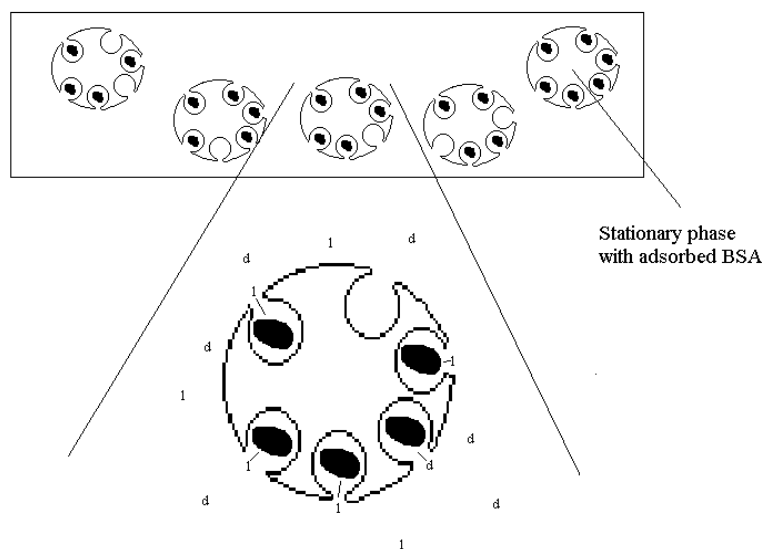


Fig. 105 Simplified graphical representation of the equilibrium of the pseudo protein stationary phase and the analytes showing the protein adsorbed onto the stationary phase.

### 8.2.2 BSA as a pseudo stationary phase on a C<sub>8</sub> stationary phase

Using a very similar protocol to that which had been reported in the literature for Nucleosil, BSA was strongly adsorbed onto the wide pore C<sub>8</sub> stationary phase, Fig. 106. In order to improve the forming of the pseudo stationary phase the BSA was pumped through the column at pH 5.0. This was approximately at the pI of BSA and as the BSA would be neutral at this pH it would more easily adsorb into the hydrophobic pores.

After adsorption at pH 5.0, the mobile phase pH was switched to 7.4 and there was no evidence, e.g. elevation of baseline, of significant desorption for some time. This made it possible to undertake more than enough HPLC than would be needed to evaluate it if it had been an unusual protein only available in small quantities.

From earlier work using BSA as a chiral selector in CE a wide range of test analytes had been accumulated so it was therefore possible to screen a large number of these analytes using the LC protocol. Separations of the enantiomers of tryptophan and kynurenine were achieved on the BSA pseudo stationary phase, Fig. 107 and 108 showing very good selectivity in both cases without the limitation of the previous method of background UV absorbance from the protein in the mobile phase. Particularly for kynurenine there was peak tailing of the more strongly bound enantiomer but this did not compromise the degree of resolution. However, a number of test analytes were retained with very high *k* even when some methanol was added to the mobile phase.

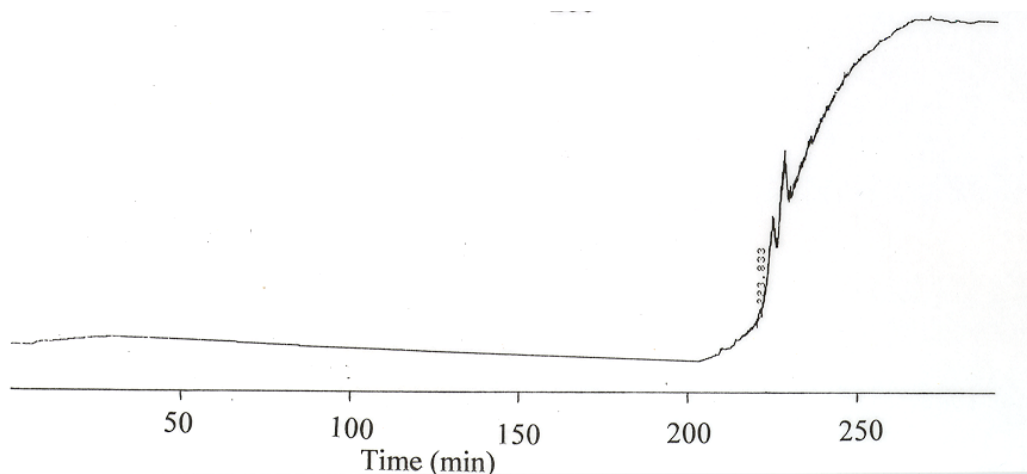


Fig. 106 Absorption of BSA onto the wide pore C<sub>8</sub> stationary phase showing the breakthrough of surplus BSA after about 210 min. The volume of the BSA mobile phase required for the breakthrough was 10.5 ml. The concentration of the BSA in the mobile phase was 2 mg ml<sup>-1</sup>, therefore the amount of BSA adsorbed onto the column was 21 mg. Conditions: mobile phase, 67 mM phosphate (pH 5.0), 30 μM BSA; column, Nucleosil C<sub>8</sub>, 5 μM particle diameter, 300 Å pore size 15 cm x 1 mm i.d.; flow rate, 50 μl min<sup>-1</sup>.

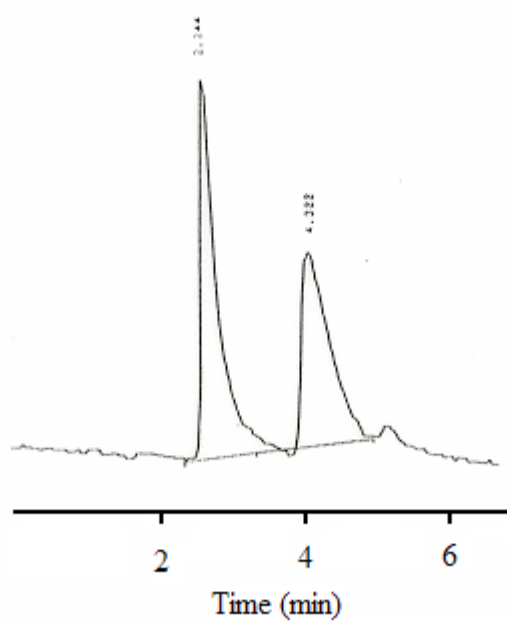


Fig. 107 Resolution of tryptophan enantiomers with a BSA pseudo stationary phase, selectivity 3.0. Conditions: mobile phase, 67 mM phosphate (pH 7.4); column, Nucleosil C<sub>8</sub>, 5 μM particle diameter, 300 Å pore size 15 cm x 1 mm i.d.; flow rate, 50 μl min<sup>-1</sup>.



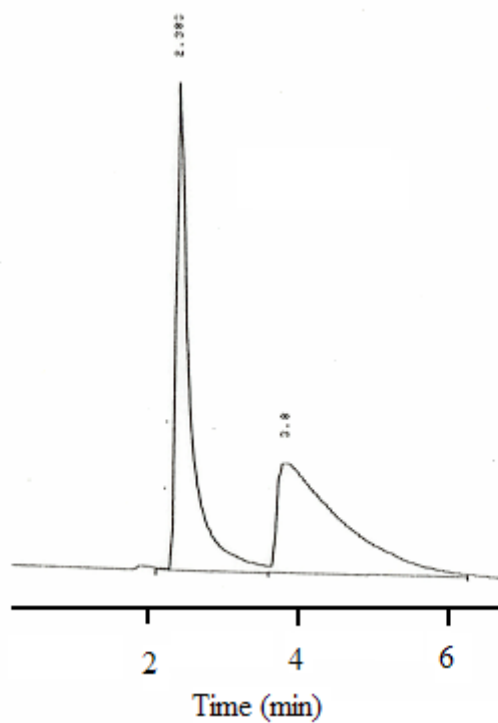


Fig. 108 Resolution of kynurenine enantiomers with a BSA pseudo stationary phase, selectivity 2.8. Conditions: mobile phase, 67mM phosphate (pH 7.4); column, Nucleosil C<sub>8</sub>, 5  $\mu$ M particle diameter, 300 Å pore size 15 cm x 1 mm i.d.; flow rate, 50  $\mu$ l min<sup>-1</sup>.

This would not be expected on, for example, a high density BSA-immobilised chiral stationary phase [Allenmark 1986 & Zhan 2000]. The logical conclusion then was that there was still a significant area of exposed C<sub>8</sub> surface and that it was this that was giving rise to the excessive retention.

### **8.3.3 BSA as a pseudo stationary phase on a DIOL stationary phase**

Since the C<sub>8</sub> stationary phase appeared to be too hydrophobic, attempts were therefore made to use a more hydrophilic wide pore DIOL phase but very little, 4 mg BSA was retained in the pores, Fig. 109. This small amount of adsorbed BSA was insufficient to give either a chiral separation or even significant retention for either tryptophan or kynurenine.

### **8.3.4 BSA as a pseudo stationary phase on Nucleosil silica**

Given that neither using wide pore C<sub>8</sub> nor DIOL stationary phases had proved to be satisfactory supports for BSA, it was decided to revert to investigating the use of wide pore Nucleosil, Fig. 110, despite the aforementioned problem of the interaction of the amino-groups with the weakly acidic silica. More compounds were eluted than had been the case with C<sub>8</sub> and, as had been observed when a similar system had been used on a conventional scale column [Erlandsson 1986]. Some chiral separation was achieved for the majority of the analytes in the test set, Table 111.

The amount of BSA retained by the pores was 70 mg. This was greater than the BSA retained on the DIOL column, 4 mg, and the C<sub>8</sub> column, 21 mg. However, this was

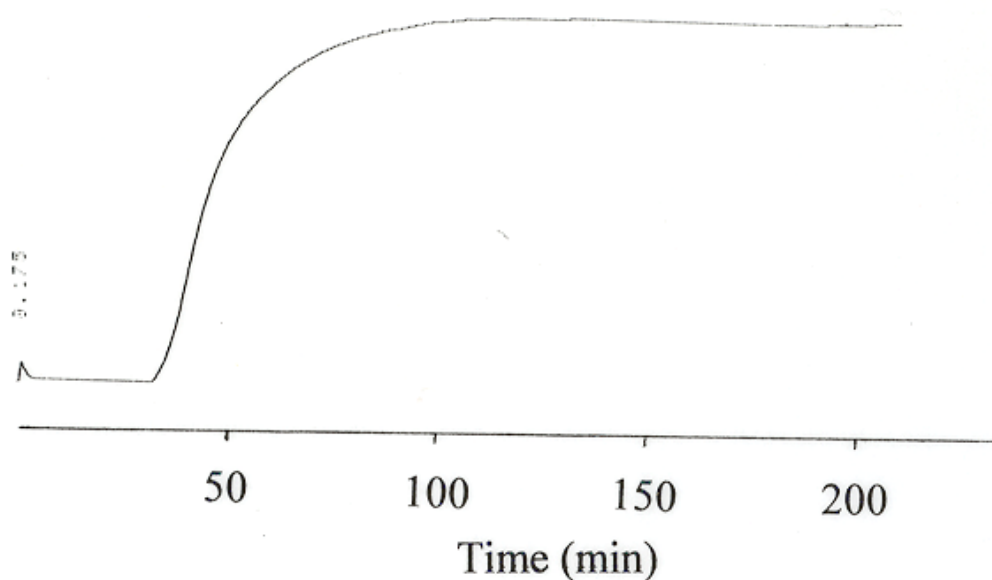


Fig. 109 Absorption of BSA onto the wide pore Lichrosorb DIOL stationary phase showing the breakthrough of surplus BSA after about 40 min. The volume of the BSA mobile phase required for the breakthrough was 2 ml. The concentration of the BSA in the mobile phase was  $2 \text{ mg ml}^{-1}$ , therefore the amount of BSA adsorbed onto the column was 4 mg. Conditions: mobile phase, 67 mM phosphate (pH 5.0),  $30 \text{ }\mu\text{M}$  BSA; column, Lichrosorb DIOL,  $5 \text{ }\mu\text{m}$  particle diameter,  $300 \text{ \AA}$  pore size  $15 \text{ cm} \times 1 \text{ mm}$  i.d.; flow rate,  $50 \text{ }\mu\text{l min}^{-1}$ .

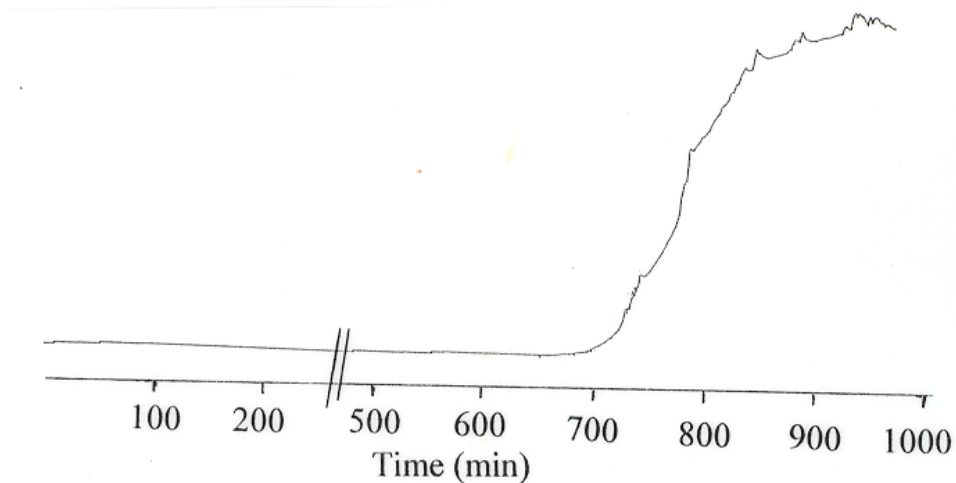


Fig. 110 Absorption of BSA onto the wide pore Nucleosil silica stationary phase showing the breakthrough of surplus BSA after about 700 min. The volume of the BSA mobile phase required for the breakthrough was 35 ml. The concentration of the BSA in the mobile phase was  $2 \text{ mg ml}^{-1}$ , therefore the amount of BSA adsorbed onto the column was 70 mg. Conditions: mobile phase, 67 mM phosphate (pH 5.0), 30  $\mu\text{M}$  BSA; column, Nucleosil silica, 5  $\mu\text{M}$  particle diameter, 300  $\text{\AA}$  pore size 15 cm x 1 mm i.d.; flow rate,  $50 \mu\text{l min}^{-1}$ .

significantly less than using BSA as a mobile phase additive where approximately 100 mg of BSA was required to perform similar analyses.

Unfortunately the stability of this system was such that it proved very difficult to remove BSA from the stationary phase. This clearly would be a problem in terms of developing a system for rapidly screening a large number of different proteins. Also, while the system proved suitable for exhibiting the enantioselectivity of the protein, it remains to be seen whether or not this was the same enantioselectivity as would be exhibited by the protein *in vivo* or whether it arose at least in part from distortion of the protein caused by its adsorption onto the acidic silica.

Table 111  $k$  values of analytes with BSA adsorbed on the Nucleosil silica

Compound	$k_1$	$k_2$	$\alpha$	Chromatogram
Tryptophan	0.8	2.7	3.6	112
Kynurenine	0.7	2.8	4.0	113
Benzoin	3.7	5.1	1.4	114
Warfarin	7.0	8.5	1.2	115

Conditions: mobile phase, 67 mM phosphate (pH 7.4); flow rate, 50  $\mu\text{l min}^{-1}$ ; column, Nucleosil C<sub>8</sub>, 5  $\mu\text{m}$  particle diameter, 300 Å pore size, coated with BSA, 15 cm x 1 mm i.d.

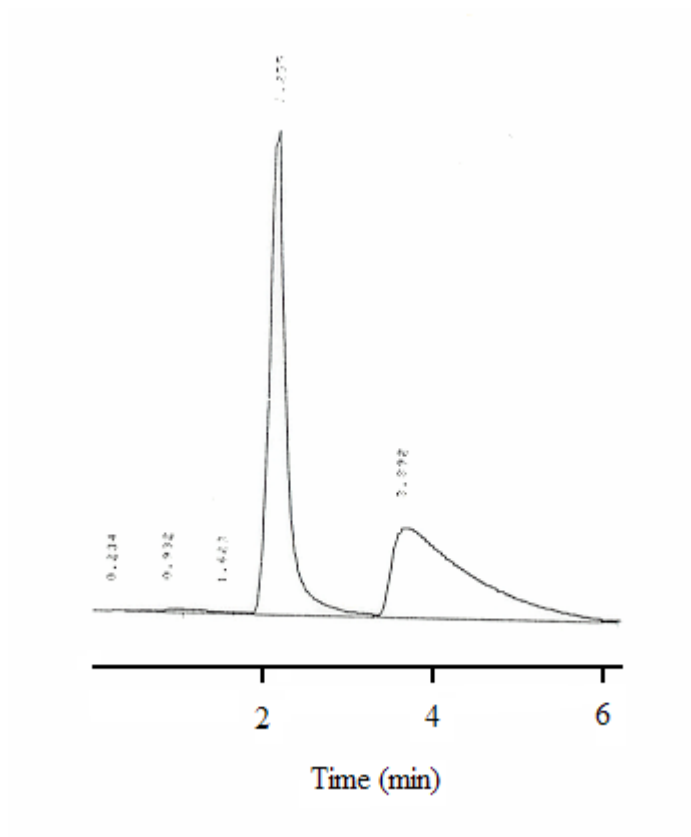


Fig. 112 Resolution of tryptophan enantiomers with a BSA pseudo stationary phase, selectivity 3.6. Conditions: mobile phase, 67 mM phosphate (pH 7.4); column, Nucleosil silica, 5  $\mu\text{M}$  particle diameter, 300  $\text{\AA}$  pore size 15 cm x 1 mm i.d.; flow rate, 50  $\mu\text{l min}^{-1}$ .

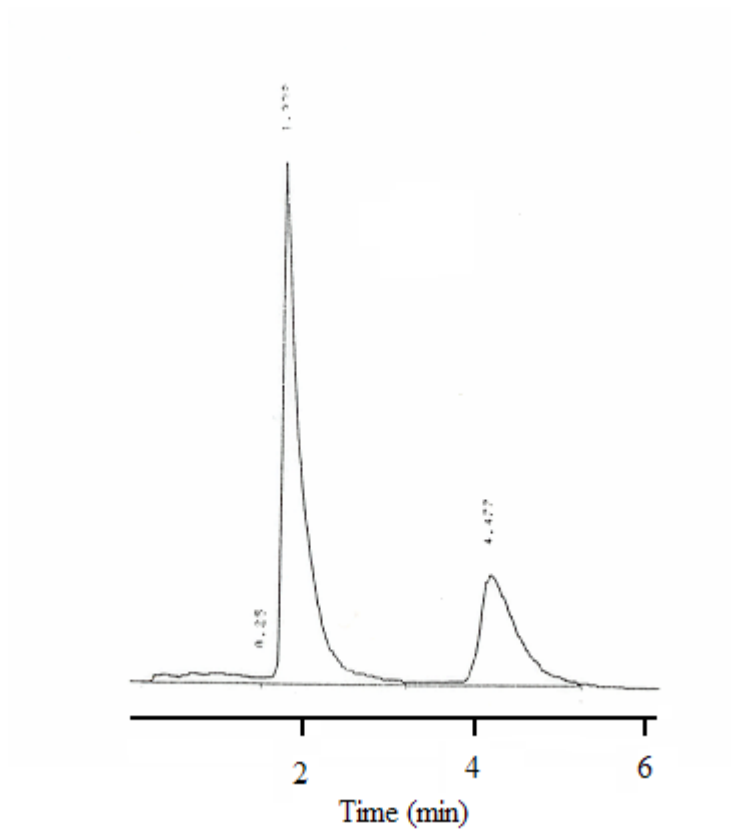


Fig. 113 Resolution of kynurenine enantiomers with a BSA pseudo stationary phase selectivity 4.0. Conditions: mobile phase, 67 mM phosphate (pH 7.4); column, Nucleosil silica, 5  $\mu\text{m}$  particle diameter, 300  $\text{\AA}$  pore size 15 cm x 1 mm i.d.; flow rate, 50  $\mu\text{l min}^{-1}$ .

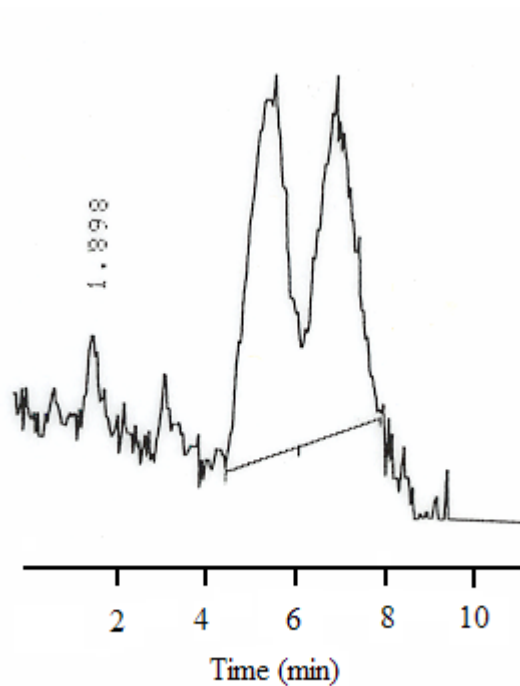


Fig. 114 Resolution of benzoin enantiomers with a BSA pseudo stationary phase, selectivity 1.4. The baseline noise is more apparent in this chromatogram because of poor efficiency and the weak chromophore of benzoin. Therefore, there is only a partial resolution despite good selectivity. Conditions: mobile phase, 67 mM phosphate (pH 7.4); column, Nucleosil silica, 5  $\mu\text{M}$  particle diameter, 300  $\text{\AA}$  pore size 15 cm x 1 mm i.d.; flow rate, 50  $\mu\text{l min}^{-1}$ .



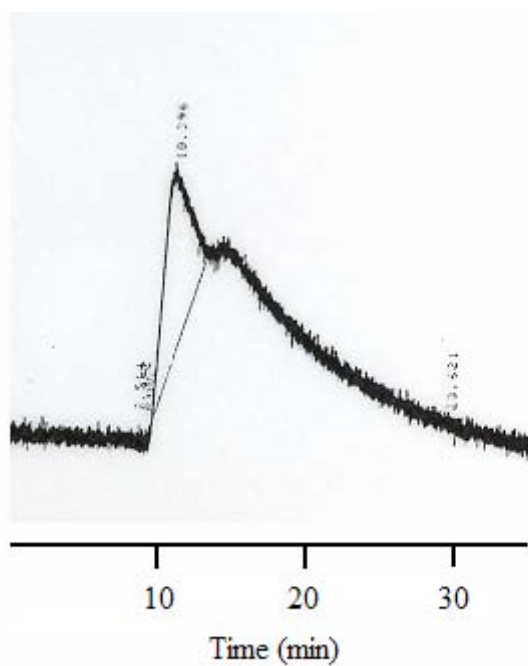


Fig. 115 Marginal resolution of warfarin enantiomers with a BSA pseudo stationary phase as evidenced by the shoulder at 16 min on the tailing peak. The selectivity was 1.2. Conditions: mobile phase, 67 mM phosphate (pH 7.4); column, Nucleosil silica, 5  $\mu$ M particle diameter, 300 Å pore size 15 cm x 1 mm i.d.; flow rate, 50  $\mu$ l  $\text{min}^{-1}$ .

## 8.4 Conclusions

Given the problems with the narrow pore DIOL and wide-pore C<sub>8</sub> systems and the fact that the use of the Hummel-Dreyer method with a number of matrix experiments [Oravcova<sup>1</sup> 1996 & Oravcova<sup>2</sup> 1996] and the complexity of immobilised artificial membrane (IAM) phases [Ong 1996] had already been discounted, the Nucleosil system looked to have the most potential, certainly for generating good chiral resolution without consuming too much protein. However, in terms of being used as a model for studying drug-protein interactions, it would need to be evaluated with HSA and a large set of common drugs to determine whether the LC retention reflected known drug-HSA binding properties and some way would have to be found to quickly remove adsorbed protein before moving on to the study of another. Alternatively the C<sub>8</sub> phase could be used if the set of test analytes could be restricted to polar compounds. Another perspective, bearing in mind the increasing more recent importance of screening for drug-protein interactions in drug candidate pre-development screening [Moaddel 2002] is that the use of one column per protein need not necessarily be considered as extravagant.

## Chapter 9 Conclusions

The outcome of the research programme was that, happily, it was demonstrated that all of the systems studied could be set up, with greater or lesser degrees of difficulty, so that they could be used to screen biomacromolecules as chiral selectors or evaluate ligand-biomacromolecule interactions while consuming low amounts of biomacromolecule. Unfortunately though none of the systems constituted the ideal vehicle for such work, as each had their difficulties or disadvantages, Fig. 116.

On balance, however, the system involving the coating of Nucleosil with the biomacromolecule appeared to have the most potential for progressing this work to further study unusual biomacromolecules that are only available in low amounts. Its ease of use and minimal consumption of biomacromolecule outweigh the possible (a) distortion of the tertiary structure, (b) interactions with the base silica, and (c) restriction of access to the biomacromolecule, all of which are an issue with respect to modelling *in vivo* drug-protein interactions but need not be a problem at all when it comes to use as a chiral selector. The latter point on restriction of access is an issue with HSA which is freely accessible in plasma but need not be a problem with, for example, membrane proteins so long as access was restricted in the same way as *in vivo*.

Fig. 116 Advantages and disadvantages of each system

System	Advantages	Disadvantages
BSA as a mobile phase additive in capillary electrophoresis	<ul style="list-style-type: none"> <li>• Successful resolution of a range of enantiomers</li> <li>• Straightforward protocol to allow the rapid study of other biomacromolecules for chiral discrimination</li> </ul>	<ul style="list-style-type: none"> <li>• UV detection of analytes is difficult due to the high UV absorbance of the biomacromolecule in the buffer</li> <li>• very difficult to establish whether or not there is any the effect of the electric field on the biomacromolecule-analyte interaction</li> </ul>
BSA coated capillary in capillary electrophoresis	<ul style="list-style-type: none"> <li>• no biomacromolecule in the buffer therefore analytes can be detected at lower levels compared to using the biomacromolecule in free solution</li> </ul>	<ul style="list-style-type: none"> <li>• chiral separations not obtainable.</li> </ul>

System	Advantages	Disadvantages
BSA as a mobile phase additive in microbore LC using a Lichrosorb DIOL stationary phase	<ul style="list-style-type: none"> <li>• successful resolution of a small range of enantiomers</li> <li>• would act as a suitable model for <i>in vivo</i> interactions</li> </ul>	<ul style="list-style-type: none"> <li>• UV detection of analytes is difficult due to the high UV absorbance of the biomacromolecule in the mobile phase</li> <li>• practical difficulties mainly due to blockages of the column frits, using this mobile phase</li> </ul>
BSA as a pseudo stationary phase in microbore LC using a Nucleosil C <sub>8</sub> column	<ul style="list-style-type: none"> <li>• successful resolution of a small range of enantiomers</li> <li>• detection of analytes is easier due to the virtual elimination of the biomacromolecule from the mobile phase</li> </ul>	<ul style="list-style-type: none"> <li>• very difficult to remove the biomacromolecule from stationary phase, therefore it prevents the use of the column with other biomacromolecules</li> <li>• not suitable for use as a model for <i>in vivo</i> interactions</li> </ul>

System	Advantages	Disadvantages
BSA as a pseudo- stationary phase in microbore LC using a Lichrosorb DIOL column	<ul style="list-style-type: none"> <li>• does not adsorb biomacromolecules to the same extent as the Nucleosil C<sub>8</sub> column</li> </ul>	<ul style="list-style-type: none"> <li>• chiral separations not obtainable</li> </ul>
BSA as a pseudo stationary phase in microbore LC using a Nucleosil silica column	<ul style="list-style-type: none"> <li>• successful resolution a greater range of enantiomers when compared to the Nucleosil C<sub>8</sub> column</li> <li>• detection of analytes easier due to the virtual elimination of the biomacromolecule from the mobile phase</li> </ul>	<ul style="list-style-type: none"> <li>• Difficult to analyse <i>in vivo</i> interactions</li> </ul>

As alluded to earlier the issue of biomacromolecule consumption, this could be reduced further by a factor of 100 by scaling down to capillary LC by using columns with 100  $\mu\text{m}$  i.d. In the not too distant past (*ca* 2003) very specialised equipment such as a flow splitter and a capillary Z-cell for the detector would be required to do this but a 10 fold reduction using 0.3 – 0.5 mm i.d. columns, might just be possible without too many experimental modifications. However, such specialised equipment tended to be difficult to manufacture or expensive to purchase. A novel approach would be to have two injection loops on the HPLC system (W.J.Lough, Exploitation of miniaturisation in Chiral Separations, 8<sup>th</sup> International Symposium on Chiral Discrimination, Edinburgh, 1996). For example, in Fig. 117 loop A could inject the exotic chiral selector while normal injections would be done through loop B. For a capillary column of 0.3 mm i.d., typical flow rates would be 3 to 6  $\mu\text{l min}^{-1}$ . Therefore, loop A of volume 1 ml would allow an analytical time of between 30 min and 1 h in which to inject test analytes from loop B.

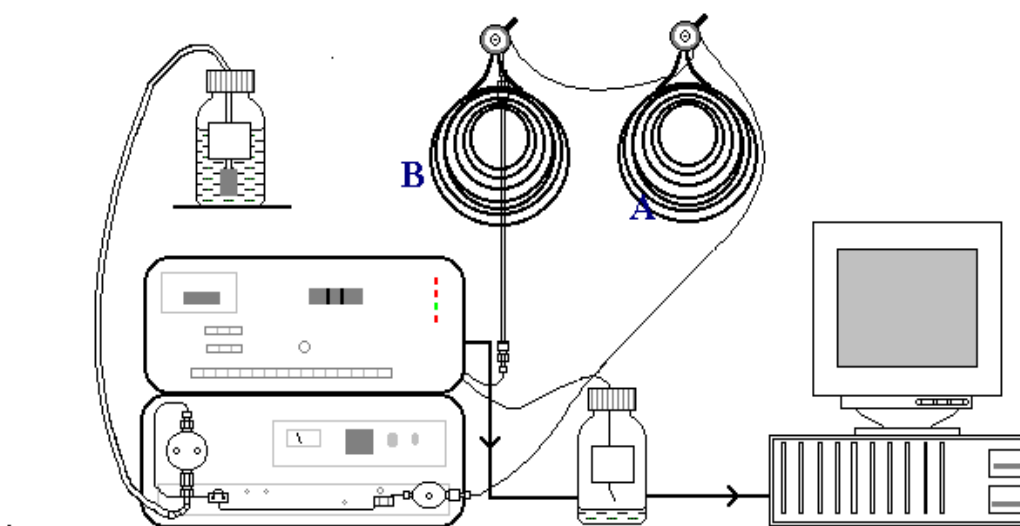


Fig. 117 A double loop HPLC system

Now in 2005, further miniaturisation than the scale employed in the studies reported here would be much easier because of the ready availability of a range of nano-LC systems such as those marketed in the UK by Dionex and Presearch. These systems come with appropriate fittings for work at nano-scale and options for obtaining focussing effects.

The work carried out on the individual systems in this research programme suggested further directions that could be taken and some of these have already been mentioned:

- prevention of the biomacromolecule masking the detection of analytes when used in free solution.
- probe the allosteric interactions of different analytes with a range of different biomacromolecules which could be achieved, for example, by the immobilisation of the biomacromolecule within the capillary or by ensuring the analytes migrate through the detector before the biomacromolecule.
- probe drug-protein binding properties on the most suitable system.
- use the most suitable system for modelling *in vivo* interactions, for example, a widely used drug and the major blood proteins.

Much progress is still being made into the field of drug-protein binding since the practical work was completed. Andre has reported the effects of salt modifiers on the displacement of progesterone by beta-estradiol on human serum albumin by biochromatography [ Andre 2003]. The stereoselective binding of 2,3-substituted 3-hydroxypropionic acids was studied by HPLC and an immobilised human stationary phase [Andrisano 2000]. HPLC and an immobilised human serum albumin stationary phase also used to measure the reversible binding of valprolate [Bertucci 2002]. HPLC was also used to study the stereoselective binding of benzodiazepine and coumarin drugs to serum albumins of human and six other mammalian species [Fitos 2002]. Immobilised-biomembrane affinity chromatography was used to study the binding properties of human facilitative glucose transporter GLUT 1 [Gottschalk



2002]. Review articles have also been published on the uses of HPLC and CE to study drug-protein / biopolymer interactions [Bertucci 2003], the use of the Hummel and Dreyer method to measure binding parameters of ligand-macromolecule interactions [Berger 2003] and the use of high-performance affinity chromatography as a powerful tool to study serum protein binding [Hage 2002].

However, essentially, on the LC side it would now be possible to proceed to use the systems, as mentioned the 'biomacromolecule-coated-on-Nucleosil' system in particular, for a diverse range of applications.

It is a different matter on the CE side. Since the last practical work in this research programme, much progress has been made in developing 'partial filling' protocols for CE. Tanaka has used the partial filling technique to separate enantiomers with proteins as chiral selectors [Tanaka 1995] and the separation of basic drugs using  $\alpha_1$ -acid glycoprotein [Tanaka 1997]. Brown used the same technique to study the binding of D-Ala-D-Ala terminus peptides to vancomycin [Brown 2004]. A review article has been written [Tanaka 2002] on the estimation of binding constants by capillary electrophoresis and this included the use of the partial filling technique.

The partial filling protocol involves carefully filling the capillary with a biomacromolecule containing buffer to just short of the detection window. The analytical conditions are such that the analytes are able to migrate through the biomacromolecules and to the detector while the biomacromolecules remain stationary or migrate away from the detector, Fig. 26.

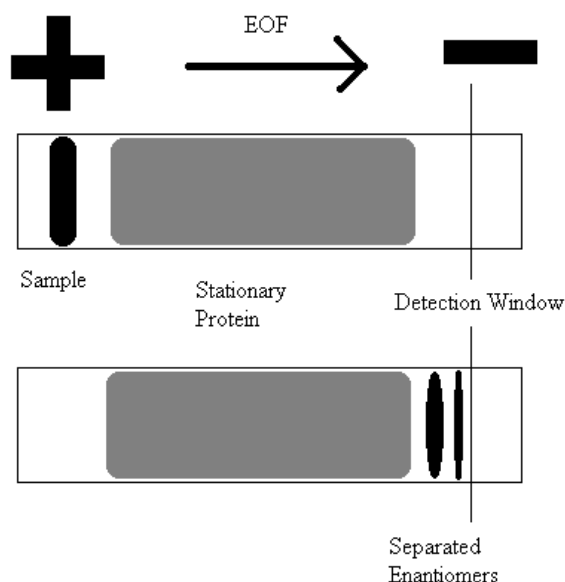


Fig. 26 A representation of protein pseudo-stationary phases with the capillary almost “complete filled” with protein; also a higher protein concentration may be used in a narrower band.

Using partial filling, much greater concentration of biomacromolecule can be used as the biomacromolecule does not pass the detector flow cell and therefore, for any given biomacromolecule it would be possible to obtain more chiral separations than for conventional protein affinity CE as used in this research programme. Clearly there would be a need to assess whether using a lower volume of a higher concentration solution as in partial filling resulted in greater or lesser protein consumption. This aside it must also be noted that in partial filling it is not straightforward to develop a protocol such the protein remains in the capillary as far up to the detection window as possible without encroaching on it.

In this context perhaps a more ‘user-friendly’ protocol that could be studied might be one involving a ‘pulse’ of protein solution. Preliminary work on such ‘pulse’ filling methods has been carried out at the University of Sunderland (BSc Chemical and

Pharmaceutical Science final year project, L.Williams, P Conjoyce and P.Wallis). Unlike the partial-filling protocol, this protocol involves injecting a concentrated plug of biomacromolecule into the capillary prior to the injection of the analytes. The experimental conditions are such that the analytes migrate through the plug of protein before UV detection. Unlike the partial filling protocol the biomacromolecule only fills a fraction of the capillary so the experimental conditions do not have to be as exact to prevent the biomacromolecule from being detected at the detector at the same time as the analyte of interest. In this way ligand-biomacromolecule studies could be carried out in a very rapid and simple manner. Again the only caveat would be that checks would need to be made that excessively long or concentrated 'plugs' were not needed in order to bring about a chiral separation or (for ligand-biomacromolecule interaction studies) a measurable shift in migration.

More recent developments such as this 'pulse' filling method would seem to supersede the work carried out in the research programme described in this thesis. However, it must be noted that quite a few variables need to be kept in check to perfect these newer methodologies so that they are far less reliable and reproducible than 'complete' or conventional capillary filling techniques. Therefore the CE protocol developed here could still be used advantageously compared to the more recent developments provided, for chiral resolution, the enantioselectivity was large enough to give resolution when using a dilute selector solution and, for studying ligand-protein interactions, the interactions are strong enough to bring about a change in migration time when using very dilute protein solutions as the buffer. Happily these provisos are not a restriction at all when screening for very good protein chiral selectors or for studying many types of drug-biomacromolecule interaction such as binding to DNA or receptor protein binding.

Last but not least with respect to CE, it should be noted that for all these systems a fundamental question remains unanswered, i.e. "Does the application of an electric

field disturb the ligand-biomacromolecule interaction?" There is no evidence that it does. Further it would be futile to assess this by an exhaustive comparison of *in vivo* data with 'in-CE' as there would always be other possible reasons to explain away any discrepancies. It would be only too easy to ignore this possibility of perturbation by the electric field. Indeed no mention of this has been made in the literature.

One day someone will have to do a definitive experiment. Applying an electric field along an NMR flow cell would certainly be a technological challenge. The best bet therefore might be to carry out molecular modelling and to attempt to model an electric field.

Having hopefully demonstrated that the methods established in the research programme still offer some advantages when compared to more recent developments, the other important question that must be addressed when considering how the work sits in the context of current developments is whether or not there is still a need for chiral separations employing protein chiral selectors or for the study of drug – biomacromolecule interactions. The former was very much the main focus of the research programme with the latter being very much a side issue. However there is now a much greater need for the latter than the former.

The field of chiral separations has advanced considerably since the mid-90's to the point where most enantiomer separation problems may easily be solved and chiral method development in the pharmaceutical industry is dominated by automated screening systems employing primarily derivatised polysaccharide chiral stationary phases for LC [Anderson 2003]. However, proteins are still used when chiral LC separations are needed with a high proportion of aqueous buffer in the mobile phase e.g. for compatibility with other coupled systems. Chiral CE using proteins is still used [Tanaka 2001] but cyclodextrins are more popular. Despite the speed with which method development may be carried out, and other advantages, chiral CE has

not supplanted chiral LC. CE though still offers better possibilities if it were wished to carry out an enantiomeric impurity assay and a related substances assay in one system and protein chiral selectors could have a role in this.

With respect to drug – biomolecule interactions there is definitely now a much greater need for studies of these (e.g. [Hage 2002] and the work of Wainer [Wainer 1993 & 2003]) especially that much more screening is being carried out in the Discovery phase of pharmaceutical R&D rather than in Development in order to prevent expensive late stage failures of drug candidates. It is in this sphere that the protocols developed in this programme are now more likely to find application. The use of the microbore LC system adapted to nano-LC has much to commend it over the immobilisation and frontal analysis strategies employed by Wainer [Moaddel 2005] in his studies of transporter proteins.

## References

Ahmed, A. & D.K.Lloyd (1997) *J. Chromatogr. A*, **766**, 237, "Effect of organic modifiers on retention and enantiomeric separations by capillary electrophoresis with human serum albumin as a chiral selector in solution".

Agranat, I., H.Caner & A.Caldwell (2002) *Nature Reviews Drug Discovery*, **1**, 753. "Putting chirality to work: The strategy of chiral switches".

Allenmark, S. (1986) *J. Liq. Chromatogr.*, **9**, 425, "Optical resolution by liquid-chromatography on immobilized bovine serum-albumin".

Allenmark, S., B.Bomgren & H.Boren (1982) *J. Chromatogr.*, **237**, 473, "Direct resolution of enantiomers by liquid affinity chromatography on albumin-agarose under isocratic conditions".

Anderson, M.E., D.Aslan, A.Clarke, J.Roeraade & G.Hagman (2003) *J. Chromatogr. A*, **1005**, 83, "Evaluation of generic chiral liquid chromatography screens for pharmaceutical analysis".

Andre, C., Y.Jacquot, T.T.Truong, M.Thomassin, J.F.Robert & Y.C.Guillaume (2003) *J. Chromatogr. B*, **796**, 267, "Analysis of the progesterone displacement of its human serum albumin binding site by  $\beta$ -estradiol using biochromatographic approaches: effect of two salt modifiers".

Andrisano, V., C.Bertucci, V.Cavrini, M.Recanatini, A.Cavalli, L.Varoli, G.Felix & I.W.Wainer (2000) *J. Chromatogr. A*, **876**, 75, "Stereoselective binding of 2,3-substituted 3-hydroxypropionic acids on an immobilised human serum albumin

chiral stationary phase: stereochemical characterisation and quantitative structure-retention relationship study”.

Amini, A., C.Pettersson & D.Westerlund (1997) *Electrophoresis*, **18**, 950, “Enantioresolution of disopyramide by capillary affinity electrokinetic chromatography with human  $\alpha_1$ -acid glycoprotein (AGP) as chiral selector applying a partial filling technique”.

Arai, T., M.Ichinose, H.Kuroda, N.Nimura & T.Kinoshita (1994) *Anal. Biochem.*, **217**,7, “Chiral separation by capillary affinity zone electrophoresis using an albumin-containing support electrolyte”.

Armstrong, D.W., K.L.Rundlett & J-R.Chen (1994) *Chirality*, **6**, 496, “Evaluation of the macrocyclic antibiotic vancomycin as chiral selector for capillary electrophoresis”.

Armstrong, D.W., M.P.Gasper & K.L.Rundlett (1995) *J. Chromatogr.*, **689**, 285, “Highly enantioselective capillary electrophoretic separations with dilute solutions of the macrocyclic antibiotic ristocetin A”.

Ashton, D.S., C.R.Beddell, G.S.Cockerill, K.Gohil, C.Gowrie, J.E.Robinson, M.J.Slater & K.Valko (1996) *J. Chromatogr. B.*, **677**, 194, “Binding measurements of indolocarbazole derivatives to immobilised human serum albumin by high-performance liquid chromatography”.

Aubry, A-F. & A.McGann (1994) *LC-GC Int.*, **7**, 389, “Applications of biochromatography to the determination of drug-protein binding interactions”.

Aumatell, A., R.J.Wells & D.K.Y.Wong (1994) *J. Chromatogr. A.*, **686**, 293, "Enantiomeric differentiation of a wide-range of pharmacologically active substances by capillary electrophoresis using modified  $\beta$ -cyclodextrins".

Baba, Y., N. Ishimaru, K. Samata & M. Tshako (1993) *J. Chromatogr. A*, **653**, 329, "High-resolution separation of DNA restriction fragments by capillary electrophoresis in cellulose derivative solutions".

Barker, G.E., P.Russo & R.A.Hartwick (1992) *Anal. Chem.*, **64**, 3024, "Chiral separation of leucovorin with bovine serum albumin using affinity capillary electrophoresis".

Beck, G.M. & S.N.Neau (1996) *Chirality*, **8**, 503, "Lambda-Carrageenan: A novel chiral selector for capillary electrophoresis".

Berger, G. & G.Girault (2003) *J. Chromatogr. B*, **797**, 51, "Macromolecule-ligand binding studied by the Hummel and Dreyer method: Current state of the methodology".

Bertucci, C., V.Andrisano, R.Gotti & V.Cavrini (2002) *J. Chromatogr. B*, **768**, 147, "Use of an immobilised human serum albumin HPLC column as a probe of drug-protein interactions: the reversible binding of valporate".

Bertucci, C., M.Bartolini, R.Gotti & V.Andrisano (2003) *J. Chromatogr. B*, **797**, 111, "Drug affinity to immobilized target bio-polymers by high-performance liquid chromatography and capillary electrophoresis".

Bijvoet, J.M., (1955) *Endeavor*, **14**, 71, "Determination of the absolute configuration of optical antipodes".



Bijvoet, J.M., A.F.Peerdeman & A.J.Van Bommel (1951) *Nature*, **168**, 271.

Birnbaum, S. & S.Nilsson (1992) *Anal. Chem.* **64**, 2872, "Protein-based capillary affinity gel electrophoresis for the separation of optical isomers".

Brown, A., I.Silva, D.Chinchilla, L.Hernandez & F.Gomez (2004) *LC.GC Europe*, **January**, 32, "Partial-filling techniques for affinity capillary electrophoresis to probe receptor-ligand interactions".

Brumley, W.C., (1992) *J. Chromatogr.*, 603, 267, "Qualitative-analysis of environmental-samples for aromatic sulfonic-acids by high-performance capillary electrophoresis".

Busch, M.H.A., L.B.Carels, H.F.M.Boelens, J.C.Kraak & H.Poppe (1997) *J. Chromatogr. A*, **777**, 311, "Comparison of five methods for the study of drug-protein binding in affinity capillary electrophoresis".

Cahn, R.S., C.K.Ingold & V.Prelog (1966) *Angew. Chem. Int. Ed.*, **5**, 385, "Specification of molecular chirality".

Camilleri, P. (1983) "Capillary Electrophoresis: Theory and Practice", CRC Press.

Carey, F.A. (1992) "Organic Chemistry" McGraw-Hill, inc.

Chervet, J.P., M.Ursem & J.B.Salzmann (1996) *Anal. Chem.*, **68**, 1507, "Instrumental requirements for nanoscale liquid chromatography".

Chilmonczyk, Z., H.Ksycinska & I.Polec (1998) *J. Chromatogr. B*, **720**, 65, "Application of chiral chromatographic parameters in quantitative structure-activity relationship analysis of homologous malathion derivatives".

Christians, T. & U.Holzgrabe (2000) *Electrophoresis*, **21**, 3609, "Enantioseparation of dihydropyridine derivatives by means of neutral and negatively charged  $\beta$ -cyclodextrin derivatives using capillary electrophoresis".

Clark, B.J., & A.M.Abushoffa (1995) *J. Chromatogr.*, **700**, 51, "Resolution of enantiomers of oxamniquine by capillary electrophoresis and high-performance liquid-chromatography with cyclodextrin and heparin as chiral selectors".

Colyer, C.L., K.B.Oldham & A.V.Sokirko (1995) *Anal. Chem.*, **67**, 3234, "Electroosmotically transported baseline perturbations in capillary electrophoresis".

Dalgliesh, C.E. (1952) *J.Chem. Soc.*, **137**, 3940,"The optical resolution of aromatic amino-acids on paper chromatograms".

Dickerson, R.E. & I.Geis (1969) "The structure and action of proteins", Harper & Rowe.

Deiderio, C., C.M. Polcaro, P. Padiglioni & S. Fanali (1997) *J. Chromatogr. A*, **781**, 503, "Enantiomeric separation of acidic herbicides by capillary electrophoresis using vancomycin as chiral selector".

Ellington, J.J., J.J. Evans, K.B. Prickett & W.L. Champion (2001) *J. Chromatogr. A*, **928**, 145, "High-performance liquid chromatographic separation of the enantiomers of organophosphorus pesticides on polysaccharide chiral stationary phases".

Erlandsson, P., P.Hanson & R.Iisaksson (1986) *J. Chromatogr.*, **370**, 475, "Direct analytical and preparative resolution of enantiomers using albumin adsorbed to silica as a stationary phase".

Ermakov, S.V., M.Y.Zhukov, L.Capelli & P.G.Righetti (1995) *J.Chromatogr. A*, **699**, 297, "Wall adsorption in capillary electrophoresis – experimental study and computer simulation".

Fanali, S., (1991) *J. Chromatogr.*, **545**, 437, "Use of cyclodextrins in capillary zone electrophoresis - Resolution of terbutaline and propranolol enantiomers".

Ferguson, P.D., D.M.Goodall & D.K.Lloyd (1998) *Trends in Analytical Chemistry*, **17**, 148, "Quantitative relationships between retention in HPLC and CE via binding constants and selector concentrations".

Fehske, K.J., W.E.Muller & U.Wollert (1981) *Biochemical Pharmacology*, **30** 687, "The location of drug binding sites in human serum albumin".

Fischer, E. (1891) *Ber. Dtsch. Chem. Ges.*, **47**, 3181.

Fitos, I., J.Visy & M.Simonyi (2002) *J. Biochem. Biophys. Methods*, **54**, 71, "Species-dependency in chiral-drug recognition of serum albumin studied by chromatographic methods".

Gottschalk, I., C.Lagerquist, S-S Zuo, A.Lundqvist & P.Lindahl (2002) *J. Chromatogr. B*, **768**, 31, "Immobilized-biomembrane affinity chromatography for binding studies of membrane proteins".

Gozel, P., E.Gassman, H.Michelsen & R.N.Zare (1987) *Anal. Chem.*, **59**, 44, “Electrokinetic resolution of amino-acid enantiomers with copper (II) aspartame support electrolyte”.

Grossman, P.D. & J.C Colburn (1992) “Capillary Electrophoresis: Theory and Practice”, Academic Press, Inc.

Hage, D.S., T.A.G.Noctor & I.W.Wainer (1995) *J. Chromatogr. A*, **693**, 23, “Characterization of the protein-binding of chiral drugs by high-performance affinity-chromatography – interactions of R-ibuprofen and S-ibuprofen with human serum albumin”.

Hage, D.S. (2002) *J. Chromatogr. B*, **768**, 3, “High-performance affinity chromatography: a powerful tool for studying serum protein binding”.

He, T-Y., S.Akimasa, S.Tokunaga & T.Nakagawa (1997) *Journal of Pharmaceutical Sciences*, 86, 120, “Protein-binding high-performance frontal analysis of (R)- and (S)-warfarin with and without phenylbutazone”.

Healy, L.O., J.P.Murrihy, A.Tan, D.Cocker, M.McEnery & J.D.Glennon (2001) *J. Chromatogr. A*, **924**, 459, “Enantiomeric separation of R,S-naproxen by conventional and nano-liquid chromatography with methyl- $\beta$ -cyclodextrin as a mobile phase additive”.

Hermansson, J. & A.Grahn (1995) *J. Chromatogr.*, **694**, 57, “Optimization of the separation of enantiomers of basic drugs Retention mechanisms and dynamic modification of the chiral bonding properties on the  $\alpha_1$ -acid glycoprotein column”.

Heron, S., A.Tchapla & J.P.Chervet (2000) *Chromatographia*, **51**, 495, “Influence of injection parameters on column performance in nanoscale high-performance liquid chromatography”.

Ishihama, Y., Y.Oda, N.Asakawa, Y.Yoshida & T.Sato (1994) *J. Chromatogr.*, **666**, 193, “Optical resolution by electrokinetic chromatography using ovomucoid as pseudo-stationary phase”.

Iwata, Y.T., A.Garcia, T.Kanamori, H.Inoue, T.Kishi & T.S.Lurie (2002) *Electrophoresis*, **23**, 1328, “The use of a highly sulfated cyclodextrin for the simultaneous chiral separation of amphetamine-type stimulants by capillary electrophoresis”.

Jorgenson, J.W. & K.D.Lukacs (1981), *J. Chromatogr.*, **218**, 209, “High-Resolution Separations based on electrophoresis and electroosmosis”.

Kaliiszan, R. (1992), *Anal. Chem.*, **64**, 619, “Quantitative structure-retention relationships”.

Kano, K., K.Minami, K.Horiguchi, T.Ishimura & M.Kodera (1995) *J. Chromatogr. A*, **694**, 307, “Ability of non-cyclic oligosaccharides to form molecular-complexes and its use for chiral separation by capillary zone electrophoresis”.

Kenndler-Blachkolm, K., S.Popelka, B.Gas & E.Kenndler (1995) *J. Chromatogr. A*, **734**, 96, “Apparent baseline irregularities for neutral markers in capillary zone electrophoresis with electroosmotic flow”.

Kilar, F. & S.Fanali (1995) *Electrophoresis*, **16**, 1510, "Separation of tryptophan-derivative enantiomers with iron-free human serum transferrin by capillary zone electrophoresis".

Knoche<sup>1</sup>, B. & G.Blaschke (1994) *Chirality*, **6**, 221, "Stereoselectivity of the in-vitro metabolism of thalidomide".

Knoche<sup>2</sup>, B. & G.Blaschke (1994) *J. Chromatogr. A*, **666**, 235, "Investigations on the in-vitro racemization of thalidomide by high-performance liquid-chromatography".

Kraak, J.C., S.Busch & H.Poppe (1992) *J. Chromatogr.*, **608**, 257, "Study of protein-drug binding using capillary zone electrophoresis".

Krstulovic, A.M. (1989) "Chiral Separations by HPLC: Applications to pharmaceutical compounds" John Wiley and Sons

Kuhn, R., C.Steinmetz, T.Bereuter, P.Hass & F.Erni (1994) *J. Chromatogr.*, **666**, 367, "Enantiomeric separations in capillary zone electrophoresis using a chiral crown ether".

Landers, J.P. (1994) "Handbook of Capillary Electrophoresis", CRC Press.

Lloyd, D.K., A.Ahmed & F.Pastore (1997) *Electrophoresis*, **18**, 958, "A quantitative relationship between capacity factor and selector concentration in capillary electrophoresis and high performance liquid chromatography: Evidence from the enantioselective resolution of benzoin using human serum albumin as a chiral selector".

Lloyd, D.K., S.Li & P.Ryan (1995) *J. Chromatogr.*, **694**, 285, "Protein chiral selectros in free-solution capillary electrophoresis and packed-capillary electrochromatography".

Lough, W.J. (1989) "Chiral Liquid Chromatography", Blackie and Son Ltd.

Loun, B. & D.S.Hage (1994) *Anal.Chem.*, **66**, 3814, "Chiral separation mechanisms in protein-based HPLC columns. 1. Thermodynamic studies of (R)- and (S)-warfarin binding to immobilized human serum albumin".

MacDermott, A.J. (2002) *Chirality in Natural and Applied Science* (Editors W.J Lough and I.W Wainer), Blackwell Science Ltd., ISBN 0-632-0543502, Chapter 2, "The Origin of Biomolecular Chirality".

Mason S.F. (2002) *Chirality in Natural and Applied Science* (Editors W.J Lough and I.W Wainer), Blackwell Science Ltd., ISBN 0-632-0543502, Chapter 1, "Pasteur on Molecular Handedness – and the sequel"

Massey, P.R. & M.J.Tandy (1994) *Chirality*, **6**, 63, "Challenges and frustrations in the separation and analysis of chiral agrochemicals".

Massolini, G., E. De Lorenzi, D.K.Lloyd, A.M.McGann & G.Caccialanza (1998) *J. Chromatogr. B.*, **712**, 83, "Evaluation of  $\beta$ -lactoglobulin as a stationary phase in high-performance liquid chromatography and as a buffer additive in capillary electrophoresis: observation of a surprising lack of stereoselectivity".

McMenamy, R.H. & J.L. Oncley (1958) *J. Biol. Chem.*, **233**, 1436, "The specific binding of L-tryptophan to serum albumin".

Michotte, Y., S.Boonkerd, M.R.Dataevernier & J.Vindevogel (1995) J. Chromatogr. A, **704**, 238, "Suppression of chiral recognition of 3-hydroxy-1,4-benzodiazepines during micellar electrokinetic capillary chromatography with bile salts".

Moaddel, R., L.L.Lu, M.Baynham & I.W. Wainer (2002) J. Chromatogr. B., 768, 41, "Immobilized receptor- and transporter-based liquid chromatographic phases for on-line pharmacological and biochemical studies: a mini-review".

Moaddel, R., R.Yamaguchi R, P.C.Ho, S.Patel, Hsu C.P., V.Subrahmanyam & I.W.Wainer (2005) J. Chromatogr. B., **818**, 263, "Development and characterization of an immobilized human organic cation transporter based liquid chromatographic stationary phase".

Muijselaar, P.G., K.Otsuka & S.Terabe (1998) J. Chromatogr. A, **802**, 3, "On-line coupling of partial-filling micellar electrokinetic chromatography with mass spectrometry".

Nishi, H & S.Terabe (1995) J. Chromatogr. A, **694**, 245, "Optical resolution of drugs by capillary electrophoretic techniques".

Noctor, T.A.G. & I.W.Wainer (1993) J. Liq. Chromatogr., **16**, 783, "The use of displacement chromatography to alter retention and enantioselectivity of a human serum albumin-based HPLC chiral stationary phase – a mini-review".

Novotny, M., H.Soini & M.Stefansson (1994) Anal. Chem., **66**, 646, "Malto-oligo saccharides as chiral selectors for the separation of pharmaceuticals by capillary electrophoresis".



Novotny, M.V., H.Soini, M.Stefansson & M-L.Riekkola (1994) *Anal. Chem.*, **66**, 3477, "Chiral separation through capillary electromigration methods".

Ohara, T., A.Shibukawa & T.Nakagawa (1995) *Anal. Chem.*, **67**, 3520, "Capillary electrophoresis / frontal analysis for microanalysis of enantioselective protein binding of a basic drug".

Ong, S., H.Liu & C.Pidgeon (1996) *J. Chromatogr. A*, **728**, 113, "Immobilized-artificial-membrane chromatography: measurements of membrane partition coefficient and predicting drug membrane permeability".

Oravcova<sup>1</sup>, J., D.Sojkova & W.Lindner (1996) *J. Chromatogr. B*, **682**, 349, "Comparison of the Hummel-Dreyer method in high-performance liquid chromatography and capillary electrophoresis conditions for study of the interaction of (RS)-, (R)- and (S)-carvedilol with isolated plasma proteins".

Oravcova<sup>2</sup>, J., B.Bohs & W.Lindner (1996) *J. Chromatogr. B*, **677**, 1, "Drug-protein binding studies New trends in analytical and experimental methodology".

Peters, T. & I.Sjoholm, (1977) "Albumin: Structure, Biosynthesis, Function", Pergamon Press.

Rauws, A.G. & K.Groen (1994) *Chirality*, **6**, 72, "Current regulatory (draft) guidance on chiral medicinal products: Canada, EEC, Japan, United States".

Schmitz, O., & S.Gab (1997) *J. Chromatogr. A*, **781**, 215, "Separation of unsaturated fatty acids and related isomeric hydroperoxides by micellar electrokinetic chromatography".

Shibukawa, A. & T.Nakagawa (1996) *Anal. Chem.*, **68**, 447, “Theoretical study of High-Performance Frontal Analysis: A chromatographic method for the determination of drug-protein interaction”.

Riering, H. & M.Sieber (1996) *J. Chromatogr. A*, **728**, 171, “Covalently bonded permethylated cyclodextrins, new selectors for enantiomeric separations by liquid chromatography”.

Snopek, J., I.Jelinek & E.Smolkova-Keulemansova (1992) *J. Chromatogr.*, **609**, 1, “Chiral separation by analytical electromigration methods”.

Spitzer, T., E.Yashima & Y.Okamoto (1999) *Chirality*, **11**, 195, “Enantiomer separation of fungicidal triazolyl alcohols by normal phase HPLC on polysaccharide-based chiral stationary phases”.

Stalcup, A.M. & N.M.Agyei (1994) *Anal. Chem.*, **66**, 3054, “Heparin: A chiral mobile-phase additive for capillary zone electrophoresis”.

Tait, R.J., D.O.Thompson, V.J.Stella & J.F.Stobaugh (1994) *Anal. Chem.*, **66**, 4013, “Sulfobutyl ether  $\beta$ -cyclodextrin as a chiral discriminator for use with capillary electrophoresis”.

Takaka, Y., K. Otsuka & S.Terabe (2000) *J. Chromatogr. A*, **875**, 323, “Separation of enantiomers by capillary electrophoresis-mass spectrometry employing a partial filling technique with a chiral crown ether”.

Tanaka, Y. & S.Terabe (1995) *J. Chromatogr. A*, **694**, 277, “Partial separation zone technique for the separation of enantiomers by affinity electrokinetic chromatography”.

with proteins by affinity electrokinetic chromatography with proteins as chiral pseudo-stationary phases”.

Tanaka, Y. & S.Terabe (2001) *J. Biochem. And Biophys. Methods*, **48**, 103, “Recent advances in enantiomer separations by affinity capillary electrophoresis using proteins and peptides”.

Tanaka, Y. & S.Terabe (2002) *J. Chromatogr. B*, **768**, 81, “Estimation of binding constants by capillary electrophoresis”.

Tanaka, Y., N.Matsubara & S.Terabe (1994) *Electrophoresis*, **15**, 848, “Separation of enantiomers by affinity electrokinetic chromatography using avidin”.

Tanaka, Y. & S.Terabe (1997) *Chromatographia*, **44**, 119, “Separation of enantiomers of basic drugs by affinity capillary electrophoresis using a partial filling technique and  $\alpha_1$ -acid glycoprotein as chiral selector”.

Tanaka, Y., Y.Kishimoto & S.Terabe (1998) *J. Chromatogr. A*, **802**, 83, “Separation of acidic enantiomers by capillary electrophoresis mass spectrometry employing a partial filling technique”.

Thuaud, N., B.Sebille, M.H.Livertoux & J.Bessiere (1983) *J. Chromatogr.*, **282**, 509, “Determination of diazepam-human serum albumin binding by polarography and high-performance liquid chromatography at different protein concentrations”.

The Insight Team (1979) “Suffer the children: The story of thalidomide”, Andrew Deutsch.

Valko, I.E., H.A.H.Billiet, J.Frank & K.Ch.A.M.Luyben (1994) *Chromatographia*, **38**, 730, "Factors affecting the separation of mandelic acid enantiomers by capillary electrophoresis".

Valtcheva, L., J.Mohammad, G.Pettersson & S.Hjerten (1993) *J. Chromatogr.*, **638**, 263, "Chiral separation of  $\beta$ -blockers by high-performance capillary electrophoresis based on non-immobilized cellulase as enantioselective protein".

Verbeke, N & A.D'Hulst (1994) *Chirality*, **6**, 225, "Separation of the enantiomers of coumarinic anticoagulant drugs by capillary electrophoresis using maltodextrins as chiral modifiers".

Vespalec, R., V.Sustacek & P.Bocek (1993) *J. Chromatogr.*, **638**, 255, "Prospects of dissolved albumin as a chiral selector in capillary zone electrophoresis".

Wainer, I.W. & F.Beigi (2003) *Anal. Chem.*, **75**, 4480, "Syntheses of immobilized G protein-coupled receptor chromatographic stationary phases: Characterization of immobilized mu and kappa opioid receptors".

Wainer, I.W., R.Kaliszan & T.A.G. Noctor (1993) *J. Pharm. Pharmacol.*, **45**, 367, "Mobile phase additives as probes of solute binding to protein based high-performance liquid-chromatographic chiral stationary phases".

Wainer, I.W., & R.M.Stiffen (1988) *J. Chromatogr.*, **424**, 158, "Direct resolution of the stereoisomers of leucovorin and 5-methyltetrahydrofolate using a bovine serum albumin high-performance liquid chromatographic chiral stationary phase coupled to an achiral phenyl column".

Ward, T.J. (1994) *Anal. Chem.*, **66**, 632, “Chiral media for capillary electrophoresis”.

Wren, S.A.C. & R.C.Rowe (1992) *J. Chromatogr.*, **603**, 235, “Theoretical aspects of chiral separation in capillary electrophoresis, I. Initial evaluation of a model”.

Zhan, Q., H.F.Zou, H.L.Wang & J.Y.Ni (2000) *J. Chromatogr. A.*, **866**, 173, “Synthesis of a silica-bonded bovine serum albumin s-triazine chiral stationary phase for high-performance liquid chromatographic resolution of enantiomers”.